The role of brain endothelial MAP kinases in ICAM-1-mediated lymphocyte transmigration

Natalie Hudson

Thesis submitted in fulfilment of the requirements for the degree of

Doctor of Philosophy

University College London

Institute of Ophthalmology

Supervisor: Dr Patric Turowski

Declaration

I, Natalie Amanda Hudson, confirm that the work presented in this thesis is my own. Where information has been derived from other sources, I confirm that this has been indicated in the thesis.

Acknowledgements

I would like to thank my supervisor Patric Turowski for his support, guidance, patience and encouragement during my entire studies. I also wish to thank my second supervisor, John Greenwood for his assistance and advice.

I am hugely grateful to all past and present lab and office members that have helped make it a great place to work, especially to Mike and Charlie for helping keep me sane and the provision of snacks. Thanks to others within Cell Biology for being an amazing group of people and for the coffee/breakfast/lunch breaks and general happy, fun out of work things that have taken place. Fellow 'library club/weekend' members- you helped make coming in at weekends that much easier and bearable.

Thank you to the British Heart Foundation for funding my studies.

To my friends- for always being there and knowing what to say.

And finally, a massive thank you to my family for believing in me when I didn't think I could do it and for their continued love and support.

Abstract

Leukocyte migration from the blood vessel, across the vascular wall and into the tissue underneath occurs in both an inflammatory response as well as immunosurveillance. During this process multiple adhesive interactions occur between leukocytes and vascular endothelial cells (ECs). The EC itself is rendered compliant to transmigration following inside-out signalling in response to leukocyte adhesion altering the activity of a number of different cellular components including the actin cytoskeleton, Rho GTPases and various protein kinases. For this, adhesion to endothelial intercellular adhesion molecule-1 (ICAM-1/CD54) is particularly important and the focus of this study. Indeed, previous work in our lab has shown that endothelial ICAM-1 signalling controls lymphocyte diapedesis by modulating interendothelial VE-cadherin (VEC) junction phosphorylation via a pathway involving calcium, AMP kinase and nitric oxide synthase (eNOS).

In this study, I have investigated if ICAM-1-mediated endothelial mitogen-activated protein (MAP) kinases activation played a role during lymphocyte transmigration across brain microvascular ECs. All three MAP kinases, namely ERK, JNK and p38, were found to be activated in response to ICAM-1 engagement, however only JNK was important for lymphocyte transmigration. Significantly, specific neutralisation experiments using small-molecule inhibitors or dominant-negative plasmids inhibiting JNK resulted in inhibition of transmigration. Activation of JNK required Src, Rho GTPase, MKK7 and protein kinase C (PKC), with all these components also found to be important for lymphocyte transmigration. I further demonstrate that this novel pathway led to the phosphorylation of the actin-associated protein paxillin and its association with VEC. Ultimately this triggered VEC internalisation, suggesting that adherens junction modulation is an important element during transendothelial leukocyte migration. Furthermore, this also suggests that at least two endothelial signalling pathways (JNK-paxillin and eNOS-VEC) converge and cooperate to regulate ICAM-1-mediated lymphocyte transmigration.

Contents

List of Figures

List of Tables

Abbreviations

AEBSF	4-(2-Aminoethyl)-benzenesulfonyl fluoride hydrochloride
ADIP	Afadin DIL domain interacting protein
AJ	Adherens junction
ALCAM	Activated leukocyte cell adhesion molecule
AMPK	5'adenosine monophosphate–activated protein kinase
AP-1	Activator protein-1
APC	Antigen presenting cell
APS	Ammonium persulphate
Arp	Actin related protein
ATP	Adenosine tri-phosphate
BBB	Blood Brain Barrier
bFGF	Basic fibroblast growth factor
BMVEC	Brain microvascular endothelial cell
BRB	Blood retinal barrier
BSA	Bovine serum albumin
Ca^{2+}	Calcium
CAM	Cell adhesion molecule
CaMKK	Calmodulin kinase kinase
CCL	CC-chemokine ligand

CO_2	Carbon dioxide
CNS	Central Nervous System
cSMAC	Central supramolecular activation cluster
CXCL	CXC chemokine ligand
Cyto D	Cytochalasin D
DAG	Diacylglycerol
DEP	Density enhanced PTP-1
DMSO	Dimethyl sulfoxide
DNA	Deoxyribonucleic acid
DOC	Sodium deoxycholate
DTT	Dithiothreitol
EAE	Experimental autoimmune encephalomyelitis
EC	Endothelial Cell
ECL	Enhanced chemiliminescence
ECM	Extracellular matrix
E.Coli	*Escherichia coli*
EDTA	Ethylenediaminetetraacetic acid
EGF	Epidermal growth factor
eNOS	Endothelial nitric oxidase
ERK	Extracellular signal-regulated kinase
ERM	Ezrin/radixin/moesin
ESAM	Endothelial cell selective adhesion molecule

FAK	Focal Adhesion Kinase
FCS	Foetal calf serum
FGF	Fibroblast growth factor
GA-1000	Gentamicin, Amphotericin-B
GAM	Goat anti-mouse
GAPs	GTPase activating proteins
GDIs	Guanine nucleotide dissociation inhibitors
GDP	Guanosine diphosphate
GEFs	Guanine nucleotide exchange factors
GFP	Green fluorescent protein
GlyCAM-1	Glycosylation-dependent adhesion molecule
GPCRs	G-protein coupled receptors
GPNT	GP8 newly transformed (Immortalised rat brain microvascular endothelial cells)
GTP	Guanosine triphosphate
GTPase	Guanosine triphosphatase
HBSS	Hanks' Buffered Saline Solution
HC	Hydrocortisone
HCl	Hydrochloric acid
HCE	Human corneal epithelial
hCMEC/D3	Human cerebral microvascular endothelial cell
hEGF	Human epidermal growth factor

HEPES	4-(2-Hydroxyethyl)piperazine-1-ethanesulfonic acid
HEV	High endothelial venules
hFGF	Human fibroblast growth factor
HMW	High molecular weight
HPAEC	Human pulmonary artery endothelial cell
HRP	Horseradish peroxidase
Hsp	Heat shock protein
HUVECs	Human umbilical vein endothelial cells
ICAM	Intracellular adhesion molecule
IF	Immunofluorescence
IFN	Interferon
IGF	Insulin growth factor
IgG	Immunoglobulin G
IL	Interleukin
ILPs	Invadasome-like protrusions
IP	Immunoprecipitation
IS	Immunological synapse
JAM	Junctional adhesion molecule
JNK	c-Jun N-terminal Kinase
kDa	kilodaltons
LB	Luria Broth
LD domains	Leucine- and aspartate-rich domains

LERs	Low expression regions
LFA-1	Leukocyte functional antigen-1
LMW	Low molecular weight
LPA	Lysophosphatidic acid
LPS	Lipopolysaccharide
LRBC	Lateral recycling border compartment
Mac-1	Macrophage antigen -1
MAdCAM	Mucosal addressin cell adhesion molecule
MAGUK	Membrane associate guanylate kinases
MAP kinase	Mitogen-activated protein kinase
MBP	Myelin basic protein
MCAM	Melanoma cell adhesion molecule
MCP-1	Monocyte chemoattractant protein-1
MEM alpha	Minimum essentials medium alpha
Mg^{2+}	Magnesium
$MgCl_2$	Magnesium chloride
MHC	Major histocompatibility complex
MK	MAP kinase-activated protein kinases
MKK	Mitogen- activated protein kinase kinase
MLC	Myosin light chain
MLCK	Myosin light chain kinase
MMPs	Matrix metalloproteinases

MS	Multiple Sclerosis
MTOC	Microtubule organising centre
mTORC2	Mammalian target of rapamycin 2
MVEC	Microvascular EC
NaCl	Sodium chloride
NADPH oxidase	Nicotinamide adenine dinucleotide phosphate oxidase
NaF	Sodium fluoride
$NaHCO_3$	Sodium biocarbonate
NK cells	Natural killer cells
NO	Nitric oxide
NP40	Nonidet® P40 Substitute
NRK cells	Normal rat kidney cells
PAF	Platelet activating factor
Par	Partitioning defective
PAS	IL-2 activated, antigen-specific T-cells
PB1 domain	Phox/Bem 1 domain
PBS	Phosphate buffered saline
PCR	Polymerase chain reaction
PDK1	Phosphoinositide-dependent kinase 1
PECAM-1	Platelet endothelial cell adhesion molecule
P-gp	P-glycoprotein
PH domain	Plekstrin homology domain

PI3K	Phosphatidylinositol 3-kinases
PICK-1	Protein interacting with C-kinase-1
PKA	cAMP-dependent protein kinase 1
PKC	Protein Kinase C
PKG	cGMP-dependent protein kinase
PLC	Phospholipase C
PLN	Peripheral Lymph Node
PMSF	Phenylmethanesulfonyl fluoride
PNAd	Peripheral node addressin
Prox1	Prospero-related homeobox gene 1
PSGL-1	P-selectin glycoprotein ligand 1
PTPases	Protein tyrosine phosphatases
PVM	Perivascular macrophages
Pyk2	Proline -rich tyrosine kinase 2
R^3-IGF-1	Insulin growth factor
RACKs	Receptors for activated C kinase
Rho	Ras homology gene family member
RNA	Ribonucleic acid
ROCK	Rho kinase
ROI	Regions of interest
ROS	Reactive oxygen species
SAPK	Stress-activated protein kinase

SDS	Sodium dodecyl sulphate
SDS-PAGE	Sodium dodecyl sulphate–polyacrylamide gel electrophoresis
SEM	Standard error mean
SH2	SRC-homology 2
sICAM-1	Soluble intracellular adhesion molecule
siRNA	Small interfering RNA
SLOs	Secondary lymphoid organs
Src	Sarcoma tyrosine kinase
TAE	Tris.acetate-EDTA
TBS	Tris buffered saline
TCR	T-cell receptor
TEM	Transendothelial migration
TEMED	N,N,N'-tetramethylethylene diamine
TEER	Transendothelial electrical resistance
TJ	Tight junction
TLCK	N_{α}-Tosyl-L-lysine chloromethyl ketone hydrochloride
TNF	Tumour necrosis factor
TPA/PMA	12-O-Tetradecanoylphorbol-13-acetate
TPCK	Tosyl phenyalanyl chloromethyl ketone
TRH	Thyrotropin releasing hormone
UTR	Untranslated region
VCAM-1	Vascular cell adhesion molecule-1

VEC	Vascular endothelial cadherin
VEGF	Vascular endothelial growth factor
VLA-4	Very late antigen-4
VVOs	Vesicular-vacuolar organelles
WASp	Wiskott - Aldrich syndrome proteins
XL	Cross-linking
ZO	Zonula occludens
ZONAB	ZO-1-associated nucleic acid binding

Chapter 1: General Introduction

1.1 The vasculature

1.1.1 Vascular endothelium

Two complementary vascular networks facilitate the transport of oxygen, nutrients and cells through tissues (Oliver and Alitalo, 2005), namely the blood and lymphatic vasculature. Blood vessels form a circulatory system starting and ending at the same organ, the heart, facilitating the transport of nutrients and oxygen throughout the whole body (Lee et al., 2010). Lymphatic vessels are unidirectional in returning tissue fluid, cells and macromolecules (collectively termed lymph) from capillaries to the thoracic duct where the lymph can drain into the vena cava for recirculation (Pepper and Skobe, 2003; Oliver and Alitalo, 2005; Lee et al., 2010).

The endothelium forms the inner lining of both the blood and lymphatic vasculature and displays great heterogeneity and plasticity (Aird, 2003). Heterogeneity does not just occur between blood vessels and lymphatic vessels but also between different organs, within the vascular loop and also between neighbouring endothelial cells (ECs) (Aird, 2003; Tse and Stan, 2010). The health of the organism is maintained by the communication that is established between the endothelium and the underlying tissue in every organ (Aird, 2004). The importance of the endothelium is shown by its involvement in most disease states, either as a primary cause or affected as a secondary response (Aird, 2008). Vascular diseases only affect particular regions of the vascular tree rather than altering every blood vessel type (Aird, 2003). For example, in diabetes the small arterioles of the retina and kidney are affected whilst it is the liver sinusoids in veno-occlusive disease.

ECs differ in their shape across the vascular tree. They are generally flat but at high endothelial venules (HEVs) they are plump and tall with a thick basal lamina (Miyasaka and Tanaka, 2004). ECs also differ in thickness ranging from less than 0.1µm to 1µm for capillaries and aorta respectively (Aird, 2007b). The orientation of the cell nucleus also varies across the vascular tree (Aird, 2003) aligning with the direction of blood flow in straight sections but not in regions where branching occurs (Aird, 2007a). The organisation and function of interendothelial junctions

varies in response to the requirement of the organ (Bazzoni and Dejana, 2004). Adherens junctions (AJs) are expressed in both blood and lymphatic vessels with ubiquitous distribution along the vascular tree. Tight junction (TJ) expression varies and depends on the requirement of the vascular bed.

The endothelium of the lymphatic system is highly adapted to its functions. The larger, collecting lymphatic vessels are found to have basement membrane and pericyte coverage along with the presence of valves to prevent retrograde flow (Oliver and Alitalo, 2005; Lee et al., 2010). Intercellular junctions of collecting lymphatic vessel ECs resemble those found in blood vessel endothelia with a conventional zipper-like structure. In contrast, lymphatic capillaries are blind-ended structures that lack basal lamina and pericyte coverage, and have overlapping intercellular junctions acting as primary valves to aid unidirectional flow of fluid (Pepper and Skobe, 2003; Oliver and Alitalo, 2005; Lee et al., 2010). These characteristics ensure that capillaries, also known as initial lymphatics, are highly permeable to large macromolecules, pathogens and migrating cells. ECs of initial lymphatics are equipped with specialised junctions where AJs and TJs are concentrated at the borders of overlapping flaps. Button- rather than zipper-like arrangement allows fluid entry without disruption to the integrity of the junction (Baluk et al., 2007; Dejana et al., 2009). These differences show that in distinct regions of the same vasculature junctions vary to mediate the specific functions carried out.

Gross morphological differences can be seen between blood vessels from arteries, veins and capillaries. Arteries have thick walls, surrounded by smooth muscle cells, which pulsate to carry oxygenated blood around the body (Aird, 2003; Aird, 2007b; Dyer and Patterson, 2010). The smooth muscle cells provide extra support to the vessel as they experience high shear stress. Veins in comparison have no pulsatile motion, are equipped with thin walls and require valves to help carry the deoxygenated blood back to the heart (Aird, 2007b; Dyer and Patterson, 2010). Capillaries form the majority of the circulatory surface area; they are extremely thin which aids in the function of being the major exchange vessels (Aird, 2007b). The blood flow at the level of capillaries is extremely slow to allow maximal diffusion. As observed with lymphatic vessels interendothelial junction organisation reflects the specific vessel function. Arterioles have a complex TJ and AJ protein network whilst in venules junctions are rather loose (Aird, 2003). The disorganisation of junctions at postcapillary venules reflects the role they play in inflammation-induced migration of leukocyte and plasma constituents (Aird, 2007b). However, the ‘tightness’ of

junctions can vary between organs. For instance, at the blood-brain barrier (BBB), the TJs are highly enriched and tight in most, if not all, parts of the vasculature (Hickey, 2001; Aird, 2007a; Dejana et al., 2009).

Endothelium lining the blood vessels can either be continuous, fenestrated or discontinuous (Aird, 2007a). In organs such as the brain and heart the endothelium is continuous due to the presence of a continuous basement membrane while in capillaries of exocrine and endocrine glands and the kidney the endothelium is fenestrated. Fenestrae are transcellular pores that extend the cell thickness and are associated with increased local permeability and transendothelial transport (Aird, 2007a; Rocha and Adams, 2009). Discontinuous endothelium is found in sinusoidal vascular beds including the liver where larger fenestrations and a poorly formed basement membrane is found (Aird, 2007a).

Functions of specific blood vessel types or vascular sub-regions are primarily characterised by the EC they are made up by (Aird, 2003; Aird, 2007a). Therefore, in first approximation, vascular function can be interrogated *in vitro* by studying the respective EC behaviour. For instance, capillaries primarily undertake the function of permeability and only in states of inflammation, be it acute or chronic, can postcapillary venules carry out the task (Aird, 2007a). Postcapillary venules are the key site where leukocyte trafficking occurs although in other areas of the vascular tree different regions mediate this function. In the pulmonary circulation, alveolar capillaries sequester leukocytes whilst in the liver leukocyte adhesion primarily takes place at the sinusoidal endothelium. HEVs support recirculation of lymphocytes from blood and lymph due to the expression of a unique adhesion molecule repertoire (Miyasaka and Tanaka, 2004). Arteriolar EC are involved in vasomotor tone (Aird, 2008). Biochemical and biomechanical signals received by the ECs from the microenvironment, including soluble mediators, temperature and pH, aid the functions carried out (Aird, 2004). Dysfunction of the endothelium is specific to the vascular tree location. For instance, in the brain dysfunction occurs when there is a loss of TJs at the BBB whilst the normally fenestrated liver sinusoids become dysfunctional following the formation of a tight barrier (Aird, 2004).

1.1.2 The blood brain and blood retinal barrier

Vasculature heterogeneity is important for the many different functions and roles that arise throughout the whole vascular tree. Of particular interest in our laboratory is the BBB.

The vast majority of the central nervous system (CNS) is separated from the blood circulatory system by the BBB which regulates the entry of immune cells, molecules and blood-borne ions (Hawkins and Davis, 2005). The discovery of the BBB was first shown in 1885 by Paul Ehrlich's observation that water soluble dye, when injected into the blood, is taken up by all organs with the exception of the brain and spinal cord (reviewed by: Engelhardt, 2003; Hawkins and Davis, 2005). The separation of the brain parenchyma from the circulatory system was further demonstrated by Ehrlich's colleague Edwin E Goldmann who showed that injection of trypan blue dye in to the cerebral spinal fluid stained all cells in the brain but not cells of other organs (reviewed by: Engelhardt, 2003; Hawkins and Davis, 2005).

The BBB has specialised fortified barrier properties resulting in the separation of the CNS from the blood circulation. A similar specialised barrier is seen in the retina due to the presence of the blood-retinal barrier (BRB). The BRB is maintained at two sites: the vasculature of the inner BRB is similar to that of the vascular BBB and is thought to have equivalent functions. The outer BRB, which is anatomically similar to the blood-cerebrospinal fluid barrier, is maintained by the retinal pigment epithelial cells on Bruch's membrane (Crane and Liversidge, 2008)

Both the BBB and BRB are selective barriers which permit the entry of nutrients, such as glucose, into the tissue whilst excluding harmful, toxic compounds (Abbott et al., 2006). The brain and retinal microenvironment is stringently controlled to mediate efficient signalling and maintain homeostatic conditions. The BBB has an increased concentration of mitochondria due to the high metabolic need of the tissue, and has low permeability due to the presence of TJs and lack of fenestrae (Hawkins and Davis, 2005). The brain vasculature has limited transcellular transport due to fewer vesicles present (Engelhardt and Sorokin, 2009; Daneman and Rescigno, 2009).

Small gases, such as oxygen and carbon dioxide, and small lipophilic molecules can diffuse freely through the lipid membrane of the BBB (Abbott et al., 2006). Trafficking of small hydrophilic molecules is regulated by the presence of specific transport systems on the luminal and abluminal membrane (Abbott et al., 2006; Daneman and Rescigno, 2009). GLUT1 transporter supplies the

brain with glucose which is its main energy source (Abbott et al., 2006; Zlokovic, 2008). The P-glycoprotein (P-gp) efflux pump is also found at high concentrations in BBB ECs and is important in removing toxic lipophilic metabolites (Rubin and Staddon, 1999; Zlokovic, 2008). Mice lacking P-gp have an enhanced sensitivity to drugs and toxins which accumulate in high levels in the brain. Peptides and proteins, such as insulin, are generally excluded from the brain unless they enter by receptor-mediated transcytosis (Abbott et al., 2006; Zlokovic, 2008). The BBB is also a metabolic barrier due to the presence of intracellular and extracellular enzymes present in the EC membrane (Zlokovic, 2008).

1.1.2.1 Neurovascular unit

It is now accepted that the basic building block of the BBB is the neurovascular unit which consists of ECs, pericytes, astrocytes and microglia (Abbott et al., 2006). The BBB is formed of a single EC that surrounds the capillary circumference with the pericytes and EC covered by the basal lamina which is continuous with the astrocyte end-feet (Hawkins and Davis, 2005). Each cell type associated with the neurovascular unit contributes to the barrier properties of the BBB aiding in homeostasis, signalling or stability (Abbott et al., 2006). The blood vessel is innervated by neurones which also regulate the barrier function (Hawkins and Davis, 2005). The close proximity of these different cell types allows paracrine regulation which is important for both CNS function and disease pathology (Zlokovic, 2008). Gliovascular units, formed of the astrocytes and neurones, are also present which mediates communication between different segments of the vasculature (Abbott et al., 2006).

1.1.2.1.1 Pericytes

In the CNS pericytes contribute to the stability of microvessels (Guillemin and Brew, 2004; Hawkins and Davis, 2005) as they promote matrix deposition and EC differentiation (Zlokovic, 2008). Blood flow is regulated in response to contraction and relaxation of pericytes surrounding the blood vessels (Peppiatt et al., 2006; Hamilton et al., 2010). In the CNS and retina pericyte-to-EC

ratios are considerably higher than in other tissues, with a greater pericyte-to-EC ratio observed in the BRB (Frank et al., 1990). In addition, close functional relationship is further guaranteed by the presence of TJs, AJs and gap junctions at pericyte-EC contact sites (Allt and Lawrenson, 2001; Zlokovic, 2008).

1.1.2.1.2 Astrocytes

Astrocytes are important for the association of pericytes with the endothelium (Abbott et al., 2006). Many characteristics of the BBB have been attributed to astrocytes including communication (Zlokovic, 2008), high transendothelial electrical resistance (TEER) (Daneman and Rescigno, 2009) and its development and maintenance (Hawkins and Davis, 2005). Calcium (Ca^{2+}) signalling between the astrocytes and endothelium regulates microvascular permeability. Astrocytes also lead to development of tighter junctions and a role in the expression and location of transporters found in the membranes which mediate uptake or removal of nutrients and toxins (Abbott et al., 2006). Electrolyte metabolism and a role in detecting salt concentrations are also contributed to astrocytes (Zlokovic, 2008).

1.1.2.1.3 Microglia and macrophages

Microglia are derived from monocytes and mesenchymal progenitor cells that enter the brain during embryogenesis and remain present for a long period of time (Guillemin and Brew, 2004; Perry et al., 2010). Microglia are the CNS tissue-resident macrophages that continually survey the microenvironment becoming activated in response to homeostatic changes due to their sensitivity (Ransohoff and Perry, 2009; Perry et al., 2010). Microglia are highly sensitive to brain injury and disease and their main function is immune surveillance (Perry et al., 2010). Microglia have been shown to have a role in experimental autoimmune encephalomyelitis (EAE) contributing to autoimmune reactions targeting CNS antigens (Ransohoff and Perry, 2009).

Perivascular macrophages (PVMs) are a population of migratory macrophages (Guillemin and Brew, 2004) continually entering the CNS as part of normal physiology (Hickey, 1999). PVMs are the principal antigen-presenting cell (APCs) in the CNS which have a phagocytic role ingesting and accumulating materials from the microenvironment to present antigens to T-lymphocytes (Hickey, 1999; Ransohoff and Perry, 2009). They are also thought to have a role in maintenance and function of the BBB (Ransohoff and Perry, 2009).

1.1.2.1.4 Basement membrane and extracellular matrix

The basement membrane maintains BBB integrity with contribution from the pericytes, astrocytes and the ECs (Zlokovic, 2008). Extracellular matrix (ECM) normally provides high tensile strength to the tissue. Since this is not required in the brain ECM levels at the BBB are low (Engelhardt and Sorokin, 2009). ECM proteins influence TJ protein expression and consequently play an important role in EC junction integrity and vessel permeability (Hawkins and Davis, 2005). BBB integrity is also maintained by matrix adhesion receptors (Zlokovic, 2008).

1.1.2.2 Intercellular Junctions at the BBB

Cell-cell junction adhesion is mediated by homophilic interactions of transmembrane proteins which also interact with intracellular proteins and most importantly the actin cytoskeleton (Bazzoni and Dejana, 2004). The junctions of the brain EC are comprised of TJs, AJs and gap junctions which are important for adhesion, stability and communication. The presence of sophisticated TJs at BBB and BRB is unique within the vascular tree and the main reason (the other being low to absent vesicular transport) for the elaborate barrier properties at these sites. Endothelial distribution of TJs and AJs is not as defined as that seen in epithelial cells where TJs are found apically and AJs basolaterally. In contrast, in EC both junction types are found intermingled (Dejana, 2004). Each junction type is formed of transmembrane components, which mediate homophilic interactions and define adhesiveness, and of associated proteins, which are important in regulating junction properties and communication with the remainder of the cell (Bazzoni and

Dejana, 2004; Dejana, 2004). Dysfunction of junction components plays a major role in many brain and retinal pathogenesis (Abbott et al., 2006).

Gap junctions, which are involved in cell communication, are formed of connexins (Imhof and Aurrand-Lions, 2004) and the vascular endothelium constitutively expresses connexins 37, 40 and 43 (Bazzoni and Dejana, 2004; Abbott et al., 2006). Since little is known about gap junctions at the BBB and in particular their role in barrier function (Zlokovic, 2008) they will not be discussed further.

1.1.2.2.1 Tight junctions

TJs form a paracellular diffusion barrier restricting the movement of molecules including small ions across the cell monolayer (Tsukita et al., 2001; Matter and Balda, 2003). The TJs have a 'gate' (paracellular permeability) and a 'fence' (apical/basolateral polarity barrier) function (Balda and Matter, 2008) which are both important in keeping permeability low whilst providing a high TEER. Individual cells can regulate the 'tightness' of the junction depending on the physiological and pathological requirements of the cell (Tsukita et al., 2001). TJs are formed of a number of protein that interact in a heteropolymer complex (reviewed by: Tsukita et al., 2001; Matter and Balda, 2003; Balda and Matter, 2008). The main transmembrane proteins, occludin, claudins and junctional adhesion molecules (JAMs), are linked to the actin cytoskeleton by a cytoplasmic plaque consisting of adaptor, scaffold and signalling proteins (Matter and Balda, 2003; Balda and Matter, 2008).

Proteins of TJs are subject to changes in their location, expression and protein-protein interactions which can be mediated by Ca^{2+} concentrations, phosphorylation and G-coupled proteins (Wolburg and Lippoldt, 2002; Hawkins and Davis, 2005). TJ proteins can alter a number of signalling pathways, including protein kinase A (PKA), protein kinase C (PKC) and Rho GTPases, which influence TJ assembly, function and polarity (Wolburg and Lippoldt, 2002; Matter and Balda, 2003). Gene expression can also be regulated by TJ proteins (Balda and Matter, 2000a; Balda and Matter, 2003; Balda and Matter, 2009).

Occludin was the first integral membrane protein to be identified that localised to TJs (Furuse et al., 1993; reviewed in: Tsukita et al., 2001). The expression of occludin correlates with low endothelial permeability and- due to its high expression in BBB EC- in part explains their low permeability (Hawkins and Davis, 2005). However, mice lacking occludin do not have a deficient BBB (Saitou et al., 2000; Tsukita et al., 2001) suggesting that occludin may have more of a regulatory role in paracellular permeability, which can be compensated. Multiple domains, including cytoplasmic and transmembrane domains of occludin have been implicated in paracellular permeability regulation (Balda and Matter, 2000a). Anchorage of occludin to the junction can occur via either the C- or N-terminus (Wolburg and Lippoldt, 2002; Balda and Matter, 2008) with each termini having a different functional role. The C-terminus of occludin associates with the cytoskeleton via accessory proteins, such as zonula occluden (ZO)-1 (Furuse et al., 1994; reviewed by: Balda and Matter, 2000b) and is important for paracellular permeability (Balda et al., 1996). The N-terminus, on the other hand, is important for neutrophil transmigration (Huber et al., 2000).

The phosphorylation status of occludin is important in the ability to associate with the cell plasma membrane (Hawkins and Davis, 2005). Phosphorylation of occludin is important for TJ formation (Sakakibara et al., 1997), increased barrier permeability (Antonetti et al., 1999; Harhaj et al., 2006) and TJ trafficking (Murakami et al., 2009). Numerous signalling cascades can also be regulated by occludin including those involving RhoA and mitogen activated protein (MAP) kinases (Balda and Matter, 2008).

Claudins are another important transcellular component of TJs and thought to be the main structural components of intramembrane strands (Furuse et al., 1998; Tsukita et al., 2001; Furuse and Tsukita, 2006). They comprise a family of more than 20 proteins which through homophilic or heterophilic interactions form the primary seal in the junction (Tsukita et al., 2001; Krause et al., 2008). Claudins establish barrier properties, restrict permeability to solutes and form charge specific pores which permit ion diffusion (Tsukita et al., 2001; Wolburg and Lippoldt, 2002; Balda and Matter, 2008; Krause et al., 2008). The function of the claudins is assumed to be specified by the extracellular loop; with the first loop involved in the tightness and ion selectivity whilst the second loop is important for interaction and adhesion of the two opposing membranes (Krause et al., 2008).

Claudins are expressed in a tissue-specific manner, with most cell types expressing more than one family member (Tsukita et al., 2001; Wolburg and Lippoldt, 2002; Balda and Matter, 2008). It is thought that the combination and ratio of TJ claudin composition determines both the 'tightness' and ion selectivity of the junction (Liebner et al., 2000; Tsukita et al., 2001; Balda and Matter, 2008). In BBB ECs, claudin- 3, -5 and -12 are found and they collectively contribute to the very high TEER observed (Morita et al., 1999; Nitta et al., 2003; Wolburg et al., 2003; Krause et al., 2008). Claudin-1 expression in the BBB varies among different species and it is debated whether it is required for TJ in the BBB (Wolburg and Lippoldt, 2002). Claudin-5 is expressed only on EC (Morita et al., 1999). Mice lacking claudin-5 show a size-selective increase (for small molecules up to 800 Da) in BBB permeability (Nitta et al., 2003). In fact, each claudin regulates the ion selectivity of a particular molecule across the junction barrier. A decrease in permeability can occur in response to overexpression of some claudins (McCarthy et al., 2000).

ZO proteins are one of the cytoplasmic plaque proteins that form the structural link to the actin cytoskeleton (Wolburg and Lippoldt, 2002; Balda and Matter, 2008) with ZO-1 being the first TJ protein to be discovered in both epithelial cells and EC (Stevenson et al., 1986; Tsukita et al., 2001). ZO-2 and ZO-3 were later discovered to localise to TJs with similar sequence homology to ZO-1 (Tsukita et al, 2001), although ZO-3 is not expressed in the TJs of the BBB (Hawkins and Davis, 2005). ZO-1 is found in two isoforms with the α^- form expressed in EC (Balda and Anderson, 1993).

All three ZO proteins are members of the membrane associate guanylate kinases (MAGUK) family sharing three defined core regions: SH3 domain, guanylate cyclase and PDZ domains, allowing a number of protein-protein interactions to arise (Wolburg and Lippoldt, 2002; Balda and Matter, 2008; Balda and Matter, 2009). ZO-1 interacts with ZO-2, ZO-3 and carboxyl termini of claudins via PDZ domains and to occludin via the guanylate cyclase domain (Tsukita et al., 2001; Balda and Matter, 2008). ZO-1 and ZO-2 can bind to a number of actin binding proteins including α-catenin and cortactin (Pachter et al., 2003).

ZO-1 and ZO-2 have a role in gene transcription regulating transcription factors (Balda and Matter, 2009). ZO-1 binds to the Y-box transcription factor ZO-1-associated nucleic acid binding (ZONAB) via its SH3 domain (Balda and Matter, 2000a). ZONAB can localise to both the nucleus, where it regulates gene expression and intercellular junctions where it binds to ZO-1 (Balda and Matter, 2000a; Balda and Matter, 2003; Balda and Matter, 2009). Cell density determines ZONAB

distribution: cells at high density results in ZO-1-ZONAB interactions at the junctions whilst low cell density leads to accumulation of ZONAB in the nucleus (Balda and Matter, 2003; Balda et al., 2003; Balda and Matter, 2009). ZONAB can interact with CDK4 controlling the expression of cell cycle regulators including cyclin D1, therefore sequestration of ZONAB by ZO-1 regulates cell proliferation (Balda and Matter, 2003; Balda et al., 2003; Balda and Matter, 2009). A role of ZO-2 in gene expression has been proposed in light of its capability of binding to the DNA scaffolding factor SAF-B and the transcription factors Fos, Jun, C/EBP and *c-myc* (Balda and Matter, 2009).

Junctional adhesion molecules (JAMs) are important for formation of TJs (Ebnet et al., 2004), as well as regulating changes in permeability (Aurrand-Lions et al., 2001). JAM-A has been implicated in leukocyte trafficking as well as junction integrity (Woodfin et al., 2007; reviewed by: Zlokovic, 2008). Endothelial selective cell adhesion molecule (ESAM) localisation is supported by its interaction with ZO-1 in the brain capillaries (Nasdala et al., 2002).

1.1.2.2.2 Adherens junctions

The AJs stabilise cell-cell interactions and regulate paracellular permeability and contact inhibition (Rudini and Dejana, 2008). Cadherins are the transmembrane proteins that organise AJ protein complexes at the cell border (Bazzoni and Dejana, 2004). Vascular endothelial cadherin (VEC) is expressed specifically by all EC found in vessels (Dejana, 2004; Dejana et al., 2009) and is important for the integrity of the endothelium (Zlokovic, 2008). N-cadherin is found at comparable levels to VEC but is diffuse in the cell membrane (Dejana et al., 2008). N-cadherin does not localise to the AJs and is mainly found at the basolateral membrane in contact with pericytes and astrocytes (Bazzoni and Dejana, 2004; Dejana et al., 2009).

VEC is found to associate via its intracellular C-terminus distal part with β-catenin and plakoglobin (γ-catenin) (Bazzoni and Dejana, 2004). The complex is further anchored to actin through the binding of α-catenin to β-catenin or plakoglobin. The complex is further stabilised by the ability of α-catenin to bind vinculin and α-actinin (Dejana et al., 2008). The juxta-membrane region of the intracellular domain of VEC can bind to p120-catenin and this association can be altered in response to phosphorylation of VEC (Potter et al., 2005; Allingham et al., 2007). When

dissociated from cadherin, all three catenins can also be found in the nucleus where they can modulate gene transcription (Bazzoni and Dejana, 2004). For instance, claudin-3 expression can be induced by β-catenin acting as a transcription factor which mediates BBB maturation and stabilisation (Liebner et al., 2008).

1.1.2.2.3 Nectin-based junctions

Nectin, in association with afadin, forms cellular adhesion sites that regulate the velocity and formation of AJs and TJs (Fukuhara et al., 2002a; Takai and Nakanishi, 2003; Honda et al., 2003a). Nectins are calcium-independent immunoglobulin-like intercellular adhesion molecules which were first described as virus receptors closely related to the poliovirus receptor (Morrison and Racaniello, 1992; Lopez et al., 1995; Eberle et al., 1995; Lopez et al., 1998). At least four family members comprise the nectin family with all, but nectin-4, expressed as at least two splice variants (Takahashi et al., 1999a; Satoh-Horikawa et al., 2000; Reymond et al., 2001; Takai and Nakanishi, 2003). Nectin-4 is found in ECs of the placenta whilst nectin-1, -2 and -3 are ubiquitously expressed (Satoh-Horikawa et al., 2000; Reymond et al., 2001; Takai and Nakanishi, 2003).

Afadin links nectin to the actin cytoskeleton and is found in two splice variants which vary in their ability to bind F-actin along with their expression profile (Mandai et al., 1997; Takai and Nakanishi, 2003). The ubiquitously expressed l-afadin variant has the ability to bind both nectin and F-actin whilst s-afadin is expressed in neural tissue and lacks the appropriate F-actin binding domain. Nectin binds to the PDZ domain within the cytoplasmic tail of afadin via a conserved four residue motif (Takahashi et al., 1999a). The interaction of afadin with nectin is important for the complex to cluster at sites of cell-cell contact (Miyahara et al., 2000).

An initial ‘spot-like’ cell-cell junction is formed by nectins which lead to the recruitment of cadherins to sites of cell-cell contact to form AJs (Tachibana et al., 2000; Fukuhara et al., 2002a; Fukuhara et al., 2002b). The association occurring between nectin and cadherin is mediated by their associated proteins l-afadin and α-catenin, respectively, (Tachibana et al., 2000). Subsequently, JAMs, claudins and occludin accumulate at the apical side of AJs to form TJs (Fukuhara et al., 2002b; Takai and Nakanishi, 2003) requiring afadin, ZO’s and the actin

cytoskeleton (Kuramitsu et al., 2008). ZO-1 can bind afadin and is recruited to nectin-based adhesion sites in an α-catenin and ponsin- independent manner (Yokoyama et al., 2001).

A number of structural proteins can interact and co-localise with nectin-afadin at AJs including ponsin (Mandai et al., 1999), vinculin (Mandai et al., 1999), afadin DIL domain interacting protein (ADIP) (Asada et al., 2003) and protein interacting with C-kinase-1 (PICK-1) (Reymond et al., 2005). It is still not yet certain the roles these proteins play in nectin-based junctions.

Src activity can be induced by *trans*-interaction of nectins which leads to the phosphorylation of Vav2 (Kawakatsu et al., 2005; Takai et al., 2008). The small Rho GTPases Rac and Cdc42 have also been shown to be activated (Kawakatsu et al., 2002; Fukuhara et al., 2004) prior to MAP kinase activation (Honda et al., 2003b). Nectins have also been implicated in cell polarity due to their ability to interact with the partitioning defective (Par) proteins and cell migration (Takai et al., 2003; Takai et al., 2008).

1.1.2.3 Disruption of BBB and BRB and inflammatory pathologies

The CNS and retina although considered immune privileged are routinely surveyed by immune inflammatory cells (Hickey, 2001). Activated T-lymphocytes are able to cross non-inflamed BBB and BRB endothelium (Engelhardt and Ransohoff, 2005) regardless of their antigen specificity (Hickey, 1999). Immune surveillance is aided by the drainage of lymphocytes, and thus potential antigenic material, into the cerebral spinal fluid circulatory system (Hickey, 2001; Engelhardt and Ransohoff, 2005). There are a number of routes which can be utilised by leukocytes to enter the CNS and retina and the route used is determined by both the inflammatory stimulus and CNS compartment affected (reviewed in: Engelhardt and Ransohoff, 2005; Zlokovic, 2008).

In the brain and retina leukocyte trafficking occurs at lower levels than that observed in other organs (Hickey, 1999) as excessive infiltration of leukocytes can be detrimental rather than beneficial (Hawkins and Davis, 2005; Zlokovic, 2008). Diseases such as Multiple Sclerosis (MS) and Alzheimer's Disease can occur following BBB disruption (Zlokovic, 2008) whilst damage to the retinal barrier can lead to development of diabetic retinopathy and the auto-immune disease

endogenous posterior uveoretinitis (Crane and Liversidge, 2008). In MS, autoaggressive T-lymphocytes traverse the BBB accumulating in the brain where they induce an autoimmune response targeting the myelin white matter leading to tissue destruction and neural damage (Engelhardt and Ransohoff, 2005; Abbott et al., 2006; Frohman et al., 2006; Zlokovic, 2008).

Disruption of the BBB and BRB occurs in response to TJ disruption, inflammatory responses or altered molecule transport across the barriers (Zlokovic, 2008). Inflamed endothelium upregulates its adhesion molecule expression and induction of chemokines which recruit leukocytes to the area (discussed in further detail in Section 1.2.2) (Hickey, 2001; Engelhardt and Ransohoff, 2005). In MS and diabetic retinopathy a loss of integral TJ proteins has been described including claudin-3 (Wolburg et al., 2003), occludin (Antonetti et al., 1998; Zlokovic, 2008) and ZO-1 (Hawkins and Davis, 2005). Actin cytoskeletal alterations reducing association with TJ proteins (Zlokovic, 2008) and loss of basement membrane (Abbott et al., 2006) can also contribute to barrier disruption. These responses increase both permeability and leukocyte infiltration facilitating immune response initiation.

The specialisation of the brain and retinal vascular beds makes investigating leukocyte trafficking relevant due to the limited immune surveillance and vesicular transport that occurs in these regions. The mechanisms of leukocyte migration at the BBB, or BRB, are likely to be important at non-BBB EC beds as well. Therefore these studies are important to understand BBB inflammatory immune functions, as inflammation has catastrophic effects in both acute and chronic neuropathologies, and provide a paradigm for leukocyte migration elsewhere.

1.2 Leukocyte transmigration

In response to infectious pathogens and tissue damage, leukocytes are recruited from the blood at postcapillary venules to the underlying tissue to initiate an immune response (Wittchen, 2009). Leukocytes begin life in the bone marrow before they migrate into the bloodstream (Friedl and Weigelin, 2008; Carman, 2009). Lymphocytes then mature in the thymus before they enter the vascular circulation and continually enter and exit secondary lymphoid organs (SLOs) such as the spleen, Peyer's Patch and peripheral lymph nodes (PLNs) (Miyasaka and Tanaka, 2004;

Carman, 2009). Lymphocytes continually recirculate between the blood and lymphoid tissue to seek out antigens and pathogens in the process of immune surveillance, also known as lymphocyte homing (Vestweber, 2007; Ward and Marelli-Berg, 2009). Naïve lymphocytes migrate into draining PLNs at HEVs where they are activated on encountering antigens presented by APCs (Cook-Mills and Deem, 2005). Lymphocytes are activated and differentiate into different effector or memory subsets prior to migrating to sites of inflammation or other tissue effector sites (Vestweber, 2007; Friedl and Weigelin, 2008; Ward and Marelli-Berg, 2009).

The process of transendothelial migration (TEM) of leukocytes is evolutionary conserved. It is highly adapted to the specific needs of the underlying tissue through the properties of the EC. In fact, ECs induce specific expression of adhesion molecules in response to priming by a specific antigen in a particular environment (Springer, 1994). The endothelial adhesion molecules then signal to the appropriate subset of leukocyte. Each leukocyte subset functions in a different way; e.g. neutrophils internalise and degrade pathogens whilst B-lymphocytes produce antibodies neutralising bacteria and viruses (Luster et al., 2005). TEM can be separated into several key steps as shown in Figure 1.1. The leukocytes need to be captured initially from the blood flow. Following that, the leukocyte rolls along the blood vessel, slows its momentum before adhering firmly to the EC (reviewed by: Springer, 1994; Luster et al., 2005; Ley et al., 2007; Wittchen, 2009). Leukocytes then crawl along the blood vessel to the site of the endothelium where they are required. Once the leukocyte reaches the site of transmigration it undergoes diapedesis, i.e. the process of passing through the vasculature into the underlying tissue. This final step of TEM can occur in two ways, via a paracellular route where the leukocyte passes between the endothelial junctions or a transcellular route where it squeezes through the cell body of a single EC (Ley et al., 2007; Carman and Springer, 2008; Carman, 2009; Muller, 2010). Once the leukocyte has undergone TEM it can either carry out its response directly within the tissue or return to the lymph for recruitment of other leukocytes, particularly the B- and T-lymphocytes.

Each of these steps of TEM involves different interactions between the endothelium and the leukocyte, which are mediated by adhesion molecules of the selectin, integrin and cell adhesion molecule (CAM) families (Table 1.1) (Luster et al., 2005; Ley et al., 2007).

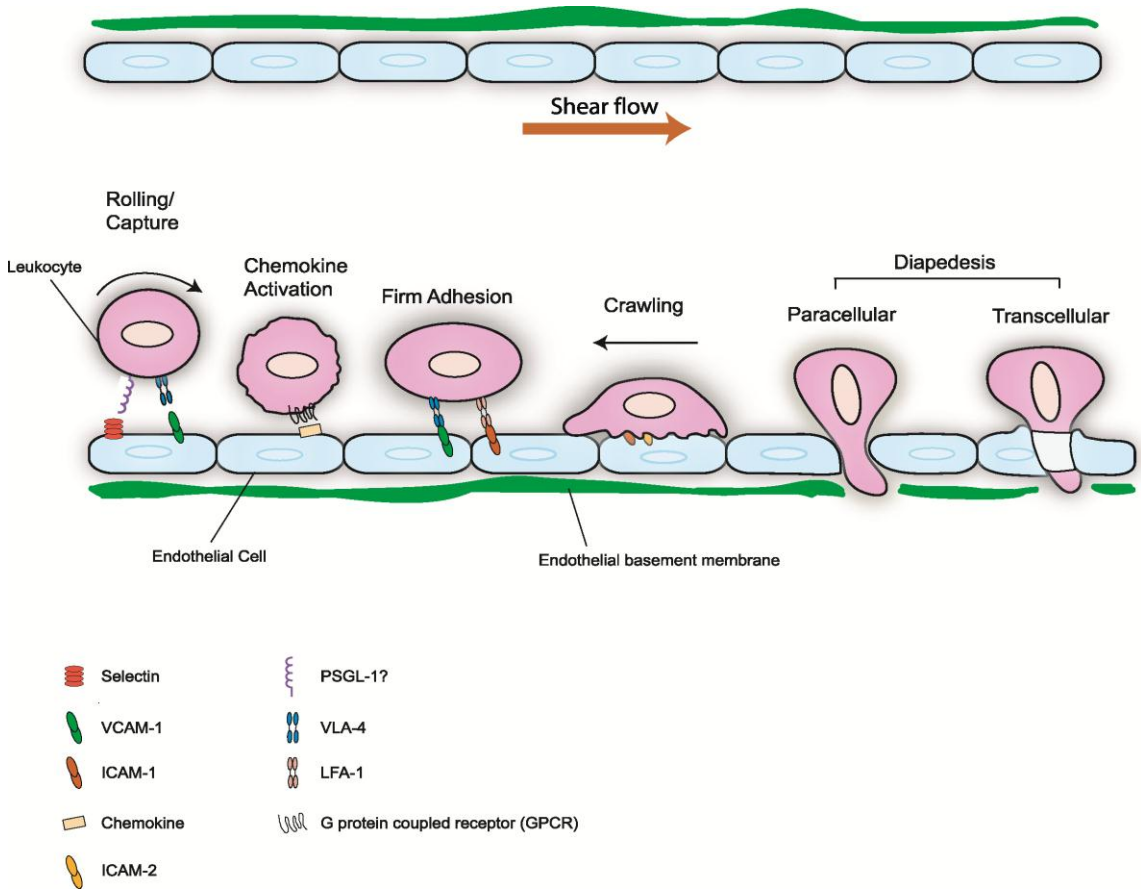

Figure 1.1 Mechanism of leukocyte transmigration at the BBB

Leukocyte transmigration is a multi-step process involving a number of interactions between the endothelium and the leukocyte mediated by selectins, integrins and cell adhesion molecules.

Table 1.1: Adhesion molecules used during leukocyte transmigration

Transendothelial migration step	Leukocyte	Endothelium
Rolling/Capture	PSGL-1 L-selectin $\alpha_4\beta_7$ VLA-4($\alpha_4\beta_1$)	P-selectin/ E-selectin E-selectin/CD34/GlyCAM-1/MadCAM-1/ PNAd MAdCAM-1/VCAM-1 VCAM-1
Chemokine activation	G-protein coupled receptors (GPCRs)	Chemokines
Firm adhesion/arrest	Activated VLA-4 ($\alpha_4\beta_1$) LFA-1 ($\alpha_L\beta_2$) Mac-1 ($\alpha_M\beta_2$) Activated $\alpha_4\beta_7$	VCAM-1 ICAM-1 (CD54)/ICAM-2 ICAM-1 MAdCAM-1/VCAM-1
Crawling		ICAM-1/ICAM-2/Mac1
Diapedesis: Paracellular Transcellular	 PECAM-1	 PECAM-1/CD99/JAMs/ESAM ICAM-1/PECAM-1

Trafficking of immune cells and metastatic cells appear to use similar migration pathways. Metastatic cancer cells use the circulatory system to migrate to other organs to form secondary tumours (Kobayashi et al., 2007). In a similar manner to leukocytes, cancer cells need to migrate across the vascular endothelium and the basement membrane to reach the underlying tissues. Cancer cells extravasate by binding to the activated/inflamed endothelium through CAMs and then migrate into the underlying tissue. Endothelial E-selectin has also been shown to bind to the siayl Lewis (a/x) antigens expressed on cancer cells. In fact, findings from leukocyte TEM have frequently been adapted to study and describe cancer cell TEM.

1.2.1 Capture and Rolling

First, weak, transient interactions mediated by selectins tether the leukocyte to the endothelium. This slows its movement allowing exposure to the local environment until stronger interactions can occur to facilitate firm arrest. This process is primarily mediated by multiple members of the selectin family that differ in their expression profile and their counter receptors. In the EC, both vascular platelet (P)- and endothelial (E)-selectin are the most important rolling molecules during the recruitment of neutrophils, monocytes, NK cells, eosinophils and lymphocyte subsets (Luster et al., 2005; Ley et al., 2007). P-selectin is often involved in early leukocyte recruitment (Patel et al., 2002) whilst E-selectin is responsible for stabilisation of leukocyte rolling and slowing the leukocytes momentum within the blood vessel (Vestweber, 2007).

P-selectin is constitutively expressed in the α-granules of platelets and the Weibel-Palade bodies of the EC (Springer, 1994; Patel et al., 2002). P-selectin is mobilised from its pre-formed stores fusing with the plasma membrane within minutes in response to acute inflammatory mediators, such as thrombin and histamine. Expression of P-selectin at the plasma membrane mediates the initial capture of monocytes and neutrophils in response to the interaction with P-selectin glycoprotein ligand (PSGL-1) (Springer, 1994; Ley et al., 2007; Vestweber, 2007).

E-selectin expression on EC is transcriptionally regulated in response to cytokines, such as interleukin (IL)-1, tumour necrosis factor (TNF)-α or lipopolysaccharide (LPS) (Springer, 1994; Patel et al., 2002). E-selectin also binds to PSGL-1, as well as glycosylated CD44 and E-selectin ligand 1 (Ley et al., 2007).

Leukocyte (L)-selectin is expressed on most leukocytes, with an exception of a small population of memory lymphocytes (Springer, 1994). Rolling of the leukocyte is in part mediated by L-selectin presenting carbohydrates to the vascular P- and E-selectins (Butcher, 1991). Lymphocytes expressing L-selectin recognise peripheral node addressin (PNAd) on HEVs allowing migration to occur at the PLNs (Miyasaka and Tanaka, 2004). Although all leukocytes express L-selectin and can roll on the HEV endothelium, only lymphocytes are capable of adhering and migrating. L-selectin is also capable of recognising the secreted glycosylation-dependent cell adhesion molecule (GlyCAM-1), Mucosal addressin cell adhesion molecule (MAdCAM-1) and CD34 found on the cell surface of HEV in SLOs (Springer, 1994; Patel et al., 2002; Ley et al., 2007). L-selectin also binds to PSGL-1 which is shown to be an important interaction for support neutrophil rolling (Patel et al., 2002; Luster et al., 2005). L- and P-selectins require shear stress to support leukocyte adhesion as in the absence of blood flow the cells detach (Ley et al., 2007).

1.2.2 Chemokine activation

Following the initial capture, rolling leukocyte 'sense' chemokines presented on the luminal side of the endothelium. They bind to and activate leukocyte G-protein coupled receptors (GPCRs) (Vestweber, 2007). During inflammation, cytokine-stimulated endothelium is activated to synthesise and secrete chemokines, such as platelet activating factor and leukotriene B_4 (Imhof and Aurrand-Lions, 2004; Ward and Marelli-Berg, 2009). Leukocyte GPCRs can also bind lipid chemoattractants, such as sphingosine- 1-phosphate and eicosanoids for activation (Ley et al., 2007). Chemokines can be derived from the underlying tissue and expressed following transcytosis (Ley et al., 2007; Ward and Marelli-Berg, 2009) whilst others are generated in response to proteolytic cleavage by mast cells and platelets (Ley et al., 2007).

The chemokine interaction with GPCRs triggers the arrest of leukocytes on the endothelium (Cook-Mills and Deem, 2005; Ley et al., 2007) before directing the leukocytes migration in response to increasing chemokine concentration (Springer, 1994). GPCR-mediated signalling leads to a conformational change in β_1 and β_2 integrins on the leukocyte leading to their activation and an increased affinity for their counter EC CAMs (Springer, 1994; Imhof and Aurrand-Lions, 2004; Vestweber, 2007). Outside-in signalling can be induced within milliseconds through different

second messengers depending on the specific chemokine and GPCRs (Imhof and Aurrand-Lions, 2004; Ley et al., 2007).

Chemokines are defined according to the pattern of cysteine residues, or function and pattern of expression (Ward and Marelli-Berg, 2009). Specific leukocyte subfamilies are recruited in response to activation by distinct chemokines (Springer, 1994). CXC chemokines tend to attract neutrophils whilst CC chemokines act on monocytes, and in certain situations eosinophils and lymphocyte subsets. For example, monocyte rolling is arrested in response to platelets depositing CC-chemokine ligand (CCL)-5 and CXC chemokine ligand (CXCL)-5 onto inflamed endothelium (Ley et al., 2007). Organ specific trafficking is shown to be dependent on the expression of certain chemokine receptors. Lymphocyte migration into lymph nodes at HEVs depends on the expression of CCL21 and CCL19 which aids lymphocyte trafficking (Miyasaka and Tanaka, 2004). Chemokines involved in developmental processes are constitutively expressed whilst inducible chemokines are generated in response to inflammation to control recruitment of cells (Ward and Marelli-Berg, 2009).

1.2.3 Firm adhesion

The local production of cytokines not only initiates a positive feedback loop to produce more cytokines but also upregulates the expression of CAMs on the EC surface. The expression of CAMs, specifically vascular cell adhesion molecule (VCAM-1) and intercellular adhesion molecule (ICAM-1), are required for binding leukocyte integrins thus facilitating firm adhesion (Muller, 2009). ICAM-1 binds to β_2 integrins: leukocyte-functional antigen-1 (LFA-1, $\alpha_L\beta_2$) and monocyte antigen-1 (Mac-1, $\alpha_M\beta_2$) by a distinct site in its third immunoglobulin domain (Hubbard and Rothlein, 2000; Ley et al., 2007; Vestweber, 2007). VCAM-1 is an endothelial ligand for very late antigen-4 (VLA-4, $\alpha_4\beta_1$) and $\alpha_4\beta_7$ (Ley et al., 2007; Vestweber, 2007).

Selectins and CAMs have overlapping functions when recruiting leukocytes to the tissue (Steeber et al., 1999). Migration at inflammatory sites is greatly inhibited when both L-selectin and ICAM-1 are lost. Adhesion molecules expression is upregulated in response to inflammation and on resting brain microvascular EC (BMVEC) it is lower than other organs (Hickey, 2001; Engelhardt and Ransohoff, 2005). Initial capture and rolling at the BBB may be mediated by different CAMs

compared to other vascular beds, although subsequent steps are thought to use the same CAMs. VCAM-1 mediates leukocyte adhesion at the BBB rather than selectins (Engelhardt, 2008; Daneman and Rescigno, 2009) and VLA-4 supports rolling (Engelhardt and Ransohoff, 2005; Ley et al., 2007). VLA-4-VCAM-1 interaction is critical for leukocyte recruitment to the CNS (Yednock et al., 1992) and different mechanisms are used for recruitment of distinct lymphocyte subsets across the BBB and BRB (Engelhardt and Ransohoff, 2005). The key interaction required for recruitment of leukocytes across the BRB into inflamed retina is that of PSGL-1 with P- or E-selectin.

1.2.4 Crawling and diapedesis

The interaction of integrins with their respective adhesion molecule can lead to clustering on the EC surface and initiate signals within the cell to mediate the final step of the cascade-diapedesis, also known as TEM. The clustering of integrins is important for the leukocyte to crawl along the blood vessel lumen as well as diapedesis.

Before diapedesis and following firm capture, the leukocyte starts to crawl to the site of transmigration. In response to binding to the endothelium the leukocyte alters its appearance with notable actin polymerisation and actin cytoskeletal rearrangements (Springer, 1994; Nourshargh et al., 2010). The leukocyte becomes polarised forming a protrusive leading edge and a contractile uropod. The polarised leukocyte migrates laterally along the luminal surface of the vessels searching for sites that are permissive to transmigration (reviewed in: Carman, 2009; Nourshargh et al., 2010). At the BBB T-lymphocytes preferentially crawl against the blood flow to the site of recruitment (Matharu et al., 2008; Steiner et al., 2010).

Lymphocytes and monocytes protrude and retract a number of ‘invadasome-like projections’ (ILPs) on the surface of the endothelium (Carman et al., 2007). The ILPs are thought to ‘probe’ the endothelium, forming podoprints, for regions that have low endothelial resistance and therefore might allow for easier transmigration (Carman, 2009). ILPs are formed with a rich inner core formed of F-actin and an outer core containing LFA-1 and talin-1 (Carman et al., 2007). Neutrophil protrusions can form in response to shear stress developing invaginations that aid TEM across the endothelium (Nourshargh et al., 2010).

Lymphocytes are capable of migrating within minutes across the endothelium in the presence or absence of flow *in vitro*; therefore including flow when interrogating lymphocyte TEM *in vitro* makes little difference (McGettrick et al., 2009). Flow conditions improve the specificity of lymphocyte adhesion in response to cytokines but do not influence initial migration.

A transmigratory cup forms with ICAM-1 enriched projections rapidly surrounding the leukocyte following adhesion to the endothelium (Carman et al., 2003; Carman and Springer, 2004). The projections have become synonymous for both transcellular and paracellular diapedesis, since they surround the leukocyte for the entire process and successful TEM does not occur in their absence.

The TEM steps of adhesion, capture and rolling are all reversible. The leukocyte is not committed at this stage to undergo transmigration and interactions with the endothelium can be broken (Muller, 2010). In contrast, once the leukocyte has committed itself to diapedesis, TEM becomes an irreversible process (Muller, 2009).

1.2.5 Targeting TEM for therapeutic intervention

The interaction of leukocytes with ECs has been exploited for anti-inflammatory therapies. Extravasation of leukocytes is a key characteristic in several inflammatory pathologies, and in the case of neurological diseases such as MS it is vital to avoid leukocyte penetration and a strong inflammatory response (Turowski et al., 2005). Many of these therapies target the interaction of integrins with the appropriate CAMs, either targeting part of the integrin structure or the active conformation (Simmons, 2005). EAE was shown to be successfully attenuated following the targeting of the interaction of VLA-4 and VCAM-1 (Yednock et al., 1992) which prompted the development of therapies for MS, including natalizumab (Miller et al., 2003). Natalizumab, which binds to and neutralises interactions of VLA-4 and $\alpha_4\beta_7$ (Mackay, 2008), limits T-lymphocyte migration into inflamed tissue in MS and Chron's disease patients. Efulizumab specifically recognises the α-chain of LFA-1 preventing the activation, trafficking and reactivation of T-lymphocytes for treatment of chronic plaque psoriasis (Simmons, 2005).

Both natalizumab and efulizumab were removed from the market due to serious side effects and occurrence of the rare neurological disease progressive multifocal leukoencephalopathy. Although natalizumab has in the meantime been reintroduced albeit in a restricted manner, these cases have illustrated that anti-adhesion therapy despite being extremely effective in restricting leukocyte recruitment are often associated with severe side-effects presumably because house-keeping immunological functions will be altered as well. This also underscores the importance of clinical developments in targeting other aspects of the leukocyte migration cascade. The chemoattractant receptor inhibitor, FTY-720, was shown to successfully inhibit leukocyte migration to inflammatory sites by regulating retention within SLOs (Mackay, 2008). The tyrosine kinase inhibitors, Tyrphostin AG490, prevented development of EAE as both lymphocyte adhesion and accumulation were attenuated (Constantin et al., 1999). Statins have been shown to attenuate EAE by inhibiting T-lymphocyte migration (Greenwood et al., 2003b).

A number of groups, including our own, have focused their attention on endothelial events downstream of leukocyte adhesion. It is hoped that by understanding specific processes drugable targets will be identified which are specific to a specific leukocyte subset and a particular vascular bed (reflecting the underlying tissue and disease state). Targeting such processes would exploit the demonstratable effectiveness of inhibiting TEM but presumably have less general immunological side effects since the target would be highly disease and tissue-specific.

1.3 The role of EC in leukocyte transmigration

Leukocytes undergoing TEM execute many steps of the transmigration process on their own. These include integrin activation (Ley et al., 2007), podosome probing (Carman et al., 2007), lateral migration on the endothelium towards sites of TEM or even endothelial junction breakdown in the case of neutrophils (Moll et al., 1998; Ionescu et al., 2003). At the same time it has become clear that TEM depends on the activity of the vascular EC: they regulate expression of adhesion molecules which not only selectivity recruit leukocytes adapted to the particular tissue inflammatory signal but also can initiate EC outside-in signalling. Such signalling has been shown to regulate a number of important steps of TEM, namely guiding leukocytes to sites of transmigration, opening a passageway and finally dispatching the leukocyte to the underlying

tissue (see below and Figure 1.2). Thus, numerous findings during the last decade have unequivocally shown that endothelial activity is important to leukocyte TEM and that the vascular endothelium should be viewed as a key part of the immune system and function.

1.3.1 Endothelial Adhesion molecules

Leukocyte interaction with endothelial adhesion molecules triggers signals within the EC. This paradigm is best demonstrated by endothelial ICAM-1 interaction with LFA-1 on leukocytes and many groups have contributed to our understanding of endothelial compliance TEM by focusing on the intraendothelial events following the engagement of ICAM-1. Other adhesion molecules such as selectins, VCAM-1 or platelet/endothelial cell adhesion molecule-1 (PECAM-1) also convey signals (Matheny et al., 2000; van Wetering et al., 2003; Deem and Cook-Mills, 2004; Couty et al., 2007) but this has been less studied.

1.3.1.1 Intracellular adhesion molecule (ICAM)

ICAM is a member of the immunoglobulin- like superfamily and can be found in five different forms. Each form varies in cell and/or tissue expression and the number of immunoglobulin-like domains it contains. Generally, ICAMs span the cell membrane once and contain a short cytoplasmic tail. ICAMs vary in molecular weight, from 80-114 kilodaltons (kDa) dependent upon tissue specific glycosylation (Lawson and Wolf, 2009; Rahman and Fazal, 2009).

1.3.1.1.1 ICAM-1

ICAM-1 is formed of 5 immunoglobulin-like domains and a cytoplasmic tail consisting of 29 amino acids in human (Turowski et al., 2005; Lawson and Wolf, 2009). It is constitutively expressed at low levels on vascular EC, as well as some lymphocytes and monocytes (Cook-Mills and Deem, 2005; Lawson and Wolf, 2009). Expression of ICAM-1 is upregulated in response to

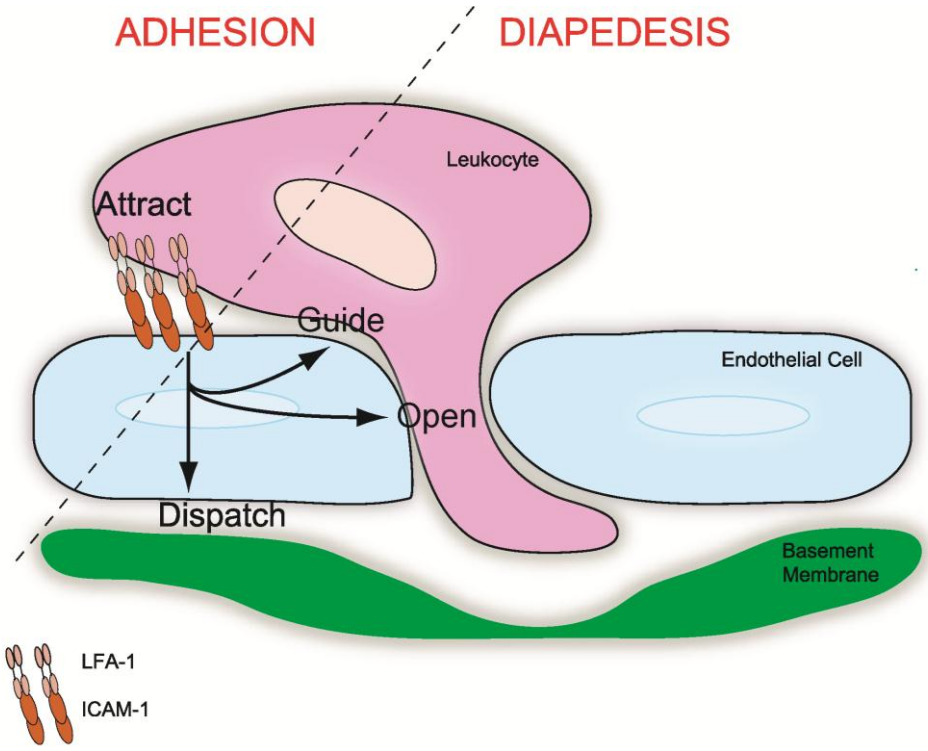

Figure 1.2 Endothelial compliance in leukocyte transmigration

The involvement of the EC in leukocyte transmigration can be separated into a role in either adhesion or diapedesis. The process of diapedesis can be further separated into a role in guiding, opening or dispatching the leukocyte to the underlying tissue.

pro-inflammatory cytokines, including TNF-α, interferon (IFN) -γ and IL-1β, as well as LPS, phorbol esters, vascular endothelial growth factor (VEGF) and shear stress (Rahman and Fazal, 2009). Pro-inflammatory cytokines also upregulate ICAM-1 expression in a concentration- and time-dependent manner in BMVEC (Wong and Dorovini-Zis, 1992; Dietrich, 2002). Maximal expression was shown in response to LPS and a combination of IFN-γ and TNF-α, whilst IFN-γ on its own led to a minimal increase in expression (Wong and Dorovini-Zis, 1992). ICAM-1 expression requires NFκB binding to the ICAM-1 promoter and activity of the transcription factor activator protein 1 (AP-1) is also important in some cases (Rahman and Fazal, 2009). Inflammatory lesions in MS and EAE show both early and focal ICAM-1 upregulation correlating with adhesion and extravasation of leukocytes across the BBB (Sobel et al., 1990; Dietrich, 2002).

The first and third immunoglobulin-like domain of ICAM-1 binds to leukocyte LFA-1 or Mac-1, respectively. ICAM-1 can also bind to fibrinogen, rhinoviruses and *Plasmodium falciparum*-infected erythrocytes (Cook-Mills and Deem, 2005; Lawson and Wolf, 2009). ICAM-1 has numerous functions depending on the cell type it is expressed in (Hubbard and Rothlein, 2000). These roles include trafficking of inflammatory cells, cell-cell interactions during antigen presentation, microbial pathogenesis and signal transduction through outside-in signalling events. The role of ICAM-1 in inflammatory cell trafficking and signalling events will be described in Section 1.4. Leukocytes are capable of migrating on a surface coated with ICAM-1 showing that ICAM-1 on its own is sufficient to direct migration (Smith et al., 2003).

1.3.1.1.2 Soluble ICAM-1 (sICAM-1)

A soluble form of ICAM-1 (sICAM-1) has been described which is produced by a variety of different cell types including human umbilical vein EC (HUVEC) and hematopoietic cell line (Lawson and Wolf, 2009). The 5 immunoglobulin-like domains of ICAM-1 are present in sICAM-1 but the transmembrane and cytoplasmic domain is lacking. It has been detected in various body fluids, with elevated levels being observed in patients with atherosclerosis, autoimmune disease and heart failure. Increased levels of sICAM-1 have been shown in HIV-infected children, MS relapsing patients and correlated with BBB breakdown in meningitis (Dietrich, 2002). sICAM-1 could potentially act as a decoy binding to ICAM-1 ligands in a competitive manner (Lawson and Wolf,

2009). Signalling appears to be induced by sICAM-1 in astrocytes and BMVEC (Otto et al., 2000b; Otto et al., 2002) but how this is mediated is unclear as the receptor to which it binds has not yet been determined.

1.3.1.1.3 ICAM-2

ICAM-2 has 2 immunoglobulin-like domains and is constitutively expressed on ECs. ICAM-2 is found concentrated at EC borders and on mononuclear leukocytes (Hubbard and Rothlein, 2000; Muller, 2010). ICAM-2 is not involved in lymphocyte adhesion (Reiss et al., 1998) but is important for T-lymphocyte polarisation and crawling to permissive TEM sites (Steiner et al., 2010). In the absence of ICAM-1, ICAM-2 may contribute to adhesion to the BBB *in vitro* (Steiner et al., 2010). Leukocyte recirculation across lymph nodes is, in part, mediated by ICAM-2 due to its constitutive expression contributing to leukocyte TEM under non-inflammatory conditions (Lehmann et al., 2003; van Buul et al., 2007b). Neutrophil transmigration across EC monolayers is mediated by ICAM-2 (Issekutz et al., 1999) in a stimulus-dependent manner (Huang et al., 2006; Woodfin et al., 2009). ICAM-2 deficient mice show large numbers of arrested neutrophils at the interface between the lumen and EC junctions along with a delay in eosinophil airway infiltration (Woodfin et al., 2009). Attachment of leukocytes to junctional and luminal ICAM-2 could potentially mediate their movement from the lumenal wall to the junctions.

1.3.1.1.4 ICAM-3, -4 and -5

ICAM-3, ICAM-4 and ICAM-5 have more restricted profiles with expression on mononuclear and polymorphonuclear leukocytes, erythrocytes and erythroid precursors and strong expression in brain grey matter (Hubbard and Rothlein, 2000). These forms have not been shown to contribute to leukocyte TEM and therefore will not be discussed any further in this thesis.

1.3.1.2 Vascular cell adhesion molecule-1 (VCAM-1)

Resting vascular endothelium generally does not express VCAM-1; its expression is regulated by inflammatory cytokine stimulation and adapted to needs of the underlying tissue (Springer, 1994; Vestweber, 2007; van Buul et al., 2007b). The role of VCAM-1 in leukocyte TEM has not been studied as much as that of ICAM-1. However, VCAM-1 upregulation in response to inflammatory stimuli points to an important in leukocyte TEM. VCAM-1 has been shown to be important in several disease states and it is likely that it has a similar role as ICAM-1. VCAM-1 is recruited to sites of ICAM-1 clustering, independent of VLA-4 binding (van Buul et al., 2010). VCAM-1 mediates firm adhesion to monocytes and lymphocytes expressing VLA-4 and clustering of VCAM-1 is observed in the steps prior to diapedesis (Muller, 2010). VCAM-1 also plays a minor role in lymphocyte homing into primary lymphatic organs (Vestweber, 2007).

VCAM-1 supports migration of lymphocytes on a solid support (Chan and Aruffo, 1993) and migration is inhibited when VCAM-1, α_4-integrins or β_1-integrins are targeted (Chan and Aruffo, 1993; Matheny et al., 2000). Both adhesion and migration of lymphocytes is therefore dependent on VCAM-1 engagement.

VCAM-1 engagement, following lymphocyte binding or use of anti-VCAM-1-beads, stimulates activation of endothelial nicotinamide adenine dinucleotide phosphate (NADPH) oxidase (Matheny et al., 2000). Activation of NADPH oxidase only occurs in response to VCAM-1 engagement and not in response to ICAM-1 or PECAM-1 engagement. VCAM-1 induced NADPH oxidase activation generates reactive oxygen species (ROS) which is important for lymphocyte transmigration. ROS production reduces cadherin cell-cell adhesion thus affecting EC function (van Wetering et al., 2003). VCAM-1 expression on ECs is not altered by inhibition of endothelial NADPH oxidase and ROS. NADPH oxidase activation is dependent on GTPase Rac1 and the influx of Ca^{2+} (Cook-Mills and Deem, 2005; Muller, 2010). VCAM-1 signalling via Rac1 requires p38 MAP kinase to mediate endothelial ROS generation (van Wetering et al., 2003). VCAM-1 stimulated ROS production activates PKCα which is required for TEM, but not adhesion, and transient weakening of cell-cell contacts (reviewed in: van Buul et al., 2007b).

VCAM-1 engagement can activate intracellular tyrosine phosphatase PTP1B following serine phosphorylation (reviewed in: van Buul et al., 2007b; Wittchen, 2009). This response is mediated by the ROS-PKCα pathway although how this promotes TEM is still unclear.

Actin stress fibre formation occurs in the region surrounding the attached lymphocyte or anti-VCAM-1 beads in response to VCAM-1 binding (Matheny et al., 2000). Stress fibre formation leads to changes in the shape of the EC causing the EC to contract and intercellular gaps to form within the junction (van Wetering et al., 2003; Cook-Mills and Deem, 2005). These gaps provide a pore that could help aid migration across the endothelium.

Endothelial associated matrix metalloproteinases (MMPs) can be activated by low concentrations of hydrogen peroxide generated in response to lymphocytes binding to VCAM-1 (Deem and Cook-Mills, 2004). Endothelial associated MMPs, particularly MMP-2 and MMP-9, require NADPH oxidase for their activation. It is thought MMP-2 and MMP-9 degrade the cell matrix and EC junctions at sites of TEM making it easier for transmigration to occur (Cook-Mills and Deem, 2005). VCAM-1 binding leads to a delay in activation of lymphocyte-associated MMP with this delay being prevented in response to ROS inhibition (Deem and Cook-Mills, 2004).

1.3.1.3 Platelet/endothelial cell adhesion molecule-1 (PECAM-1)

Another member of the immunoglobulin superfamily is PECAM-1 (CD31). It is expressed on EC concentrated at the cell borders along with leukocytes and platelets (Garrido-Urbani et al., 2008; Muller, 2010). Interruption of homophilic PECAM-1 interactions between the leukocyte and the EC by using anti-PECAM-1 antibodies results in the arrest of leukocytes on the apical surface of cytokine-stimulated EC (Cook-Mills and Deem, 2005; Muller, 2010). Homophilic interactions also arise between lateral borders of adjacent non-activated EC which form part of AJs (Cook-Mills and Deem, 2005). PECAM-1 can act as a scaffold recruiting signalling molecules and other junctional proteins which bind to the intracellular domain of PECAM-1 (Ilan and Madri, 2003). Association of phosphorylated β-catenin and γ-catenin with PECAM-1 can lead to relocalisation to cell junctions.

Work carried out by William Muller's group show that PECAM-1 recycles locally between the cell membrane and cytoplasmic compartment in a complex named the lateral border recycling

compartment (LBRC) (Mamdouh et al., 2003; Muller, 2009; Muller, 2010). The LBRC is enriched in phosphorylated PECAM-1 when compared to PECAM-1 residing on the cell surface (Dasgupta and Muller, 2008). Around 30% of EC PECAM-1 resides in the tubulovesicular structures found underneath the plasma membrane and the membrane is redirected to the cell border at sites of TEM when leukocytes are transmigrating (Mamdouh et al., 2003; Muller, 2010). The LBRC could provide the extra membrane needed to increase the surface area for the pore formation seen during paracellular and transcellular migration whilst providing molecules that the leukocyte needs to interact with on its passage (Mamdouh et al., 2003). The increased contact site induced by the LBRC is important in sealing the gap that forms as well as initiating responses required to propel migration of the leukocyte across the endothelium (Ager, 2003). The mobilisation of the LBRC to the plasma membrane is important for both paracellular (Mamdouh et al., 2008) and transcellular diapedesis (Mamdouh et al., 2009) of lymphocytes, monocytes and neutrophils. Importantly, both paracellular and transcellular leukocyte migration rely on LBRC activity.

PECAM-1 engagement on BMVEC surface appears to have an inhibitory effect on multiple ICAM-1 signalling pathways (described in Section 1.4), counteracting ICAM-1-induced tyrosine phosphorylation of cortactin and actin rearrangements (Couty et al., 2007). PECAM-1 can associate with SHP-2 which is required for ICAM-1 signalling suggesting the two pathways may co-operate to regulate the ECs response to leukocyte adhesion.

1.3.1.4 CD99

CD99 is an O-glycosylated protein expressed by most leukocytes, red blood cells and ECs (Garrido-Urbani et al., 2008). Homophilic interactions arise between CD99 on the endothelium and on monocytes or neutrophils. CD99 is important for TEM but believed to act at a later stage than PECAM-1 interactions (Muller, 2009; Muller, 2010). Antibody-mediated neutralisation of CD99 causes monocyte to arrest between the EC junctions and an additive effect on the inhibition of TEM is observed following antibody blocking of both PECAM-1 and CD99 (Schenkel et al., 2002). CD99 has a role in monocyte and neutrophils migration at EC junctions (Schenkel et al., 2002; Lou et al., 2007) and also lymphocyte migration (Bixel et al., 2004). The functional relationship between PECAM-1 and CD99 also appears to be important in the LBRC (Mamdouh et al., 2008).

CD99 has been shown to activate MAP kinases in Jurkat cells and could potentially have the same function in EC, although this has not yet been clarified (Cook-Mills and Deem, 2005).

A distant relative to CD99 is CD99L2 which is expressed on leukocytes and ECs (Bixel et al., 2007). CD99L2 is involved in neutrophil TEM and recruitment into inflamed tissue but is not important for lymphocyte extravasation.

1.3.1.5 Junctional adhesion molecule (JAM) and endothelial cell selective adhesion molecule (ESAM)

JAMs are components of the TJ. JAM-A and JAM-C are concentrated at all EC cell borders (Muller, 2009) while JAM-B is highly expressed at intercellular junctions of HEVs (Garrido-Urbani et al., 2008). Brain ECs have a high level of JAM-A expression (Aurrand-Lions et al., 2001). JAM-A engages in homophilic interactions, although heterophilic engagement with LFA-1 occurs in response to inflammation (Muller, 2009). Inflammation and TEM is decreased greatly when JAM-A is blocked. JAM-A deficiency in mice leads to transmigrating neutrophils being trapped within EC junctions (Woodfin et al., 2009). JAM-A can interact with other TJ proteins and also binds to calcium/calmodulin-dependent protein kinase (CaMKK) and indirectly to PKC via Par3 (Cook-Mills and Deem, 2005).

JAM-B interacts with VLA-4 on lymphocytes, monocytes and eosinophils (Garrido-Urbani et al., 2008) which is important for leukocyte rolling and adhesion (Ludwig et al., 2009). Inhibition of JAM-B inhibits cutaneous inflammation due to impaired leukocyte extravasation (Ludwig et al., 2009). JAM-B is specifically expressed in HEV and lymphatic EC, with no expression in brain EC (Aurrand-Lions et al., 2001).

JAM-C can form heterophilic interactions with JAM-B and Mac-1 (Muller, 2009). Interaction of JAM-C and Mac-1 has been implicated during leukocyte TEM. Lymphocyte TEM is increased in response to overexpression of JAM-C. Reverse transmigration is thought to involve JAM-C and this is an important mechanism for tissue clearance and subsequent inflammation resolution (Bradfield et al., 2007; Garrido-Urbani et al., 2008).

ESAM is closely related to JAM family members although it has a longer cytoplasmic domain (Muller, 2009). ESAM, like the JAMs, is mainly localised to endothelial junctions where it binds in a homophilic manner. Evidence suggests that ESAM is important for neutrophil migration but not lymphocyte extravasation (Wegmann et al., 2006).

1.3.1.6 Other adhesion molecules

Other endothelial CAMs that have recently been shown to be important in leukocyte transmigration are activated leukocyte cell adhesion molecule-1 (ALCAM-1) (Cayrol et al., 2008) and melanoma cell adhesion molecule (MCAM/CD146) (Guezguez et al., 2007; Bardin et al., 2009) but their role in TEM is still completely unclear.

1.3.2 Role of the endothelium

1.3.2.1 Guiding leukocytes to sites of TEM

Leukocytes appear to have preferred sites of transmigration which occurs often near tri-cellular junctions (Burns et al., 1997; Sumagin and Sarelius, 2010). During TEM, ICAM-1 is found enriched in these areas and this is thought to signal to leukocytes the location of an active portal. Blocking of the ICAM-1 extracellular domain significantly reduces the leukocytes ability to migrate to these portals. Tri-cellular junctions are regions of the cells were the junction proteins, including occludin and ZO-1, are found to be discontinuous (Burns et al., 1997) and therefore may allow easier transmigration. The observation that ICAM-1 redistributes from the luminal EC surface to juxta-junctional areas following antibody-mediated engagement and activation (Turowski et al., 2008) (Figure 1.3), suggests that EC may contribute to leukocytes 'sensing' their way to TEM portals. Actin stress fibres guide ICAM-1 towards areas of the cell with a reinforced actin cytoskeleton (Millan et al., 2006). This is similarly seen with VCAM-1 but not E-selectin, which localises to the perinuclear region throughout TEM consistent with it role during crawling.

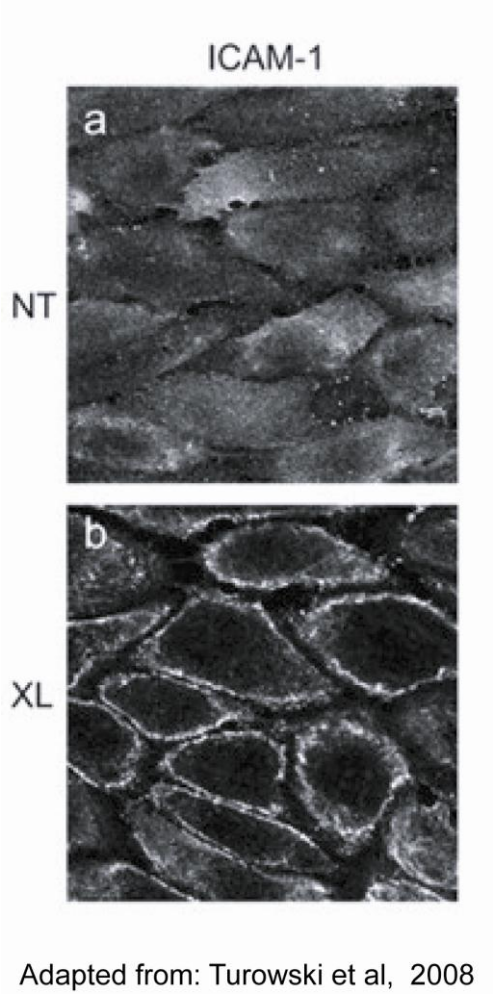

Figure 1.3 ICAM-1 receptors cluster in lateral areas following antibody engagement
ICAM-1 is uniformly distributed on the EC surface and, following its cross-linking, is found clustered and translocated to lateral areas.

1.3.2.2 Opening a passageway

Increasing evidence shows that the endothelium participates in formation of a channel used by the leukocyte for paracellular or transcellular diapedesis. The adherent leukocyte's arrival to cell junctions leads to the formation of endothelial pores (Figure 1.4) (Shaw et al., 2001; Carman and Springer, 2004; Woodfin et al., 2011). The interaction of the leukocyte with the EC induces the formation of a small pore at the centre, of around 0.5-2μm in diameter which is devoid of ICAM-1 (Carman and Springer, 2004). The pore is surrounded by endothelial ICAM-1 and enlarges in size as TEM progresses. The endothelium also has pre-existing gaps which are found to mediate diapedesis (Shaw et al., 2001). Pore formation is also seen *in vivo* in murine cremasteric venules as neutrophils migrate across the endothelium (Woodfin et al., 2011). The pore formed at cellular junctions reseals itself within minutes of the leukocyte completing TEM, demonstrating that the pore formation is a transient response (Shaw et al., 2001; Woodfin et al., 2011).

These pores form in both paracellular and transcellular migration and during TEM of many leukocyte subfamilies including lymphocytes, monocytes and neutrophils (Carman and Springer, 2004; Woodfin et al., 2011). Multiple leukocytes can use the same pore in the endothelium to migrate, with the second leukocyte following the first leukocyte before the junction reseals itself (Shaw et al., 2001). The pores that form as leukocyte migrate via a transcellular route appear in close proximity to EC junctions (Carman and Springer, 2004; Woodfin et al., 2011) consistent with the LBRC playing an important role for all routes of TEM (Mamdouh et al., 2008; Mamdouh et al., 2009).

ICAM-1 enriched endothelial projections form a cup-like structure upon engagement of leukocyte LFA-1 (Carman et al., 2003) and surround the site of diapedesis (Carman and Springer, 2004). The projections are 'microvilli-like' and extend up around the adherent leukocyte, curving over the top of the cell forming a cup-like structure (Carman et al., 2003). Enrichment of ICAM-1, VCAM-1 and ezrin is observed around the cup-like projections (Carman et al., 2003) but not of ICAM-2, PECAM-1 or VEC (Carman and Springer, 2004). The interaction of ICAM-1 and LFA-1 promotes the formation of the projections surrounding the leukocyte which has adhered (Carman et al., 2003). The ICAM-1 projections remain attached to the LFA-1 uropod of monocytes,

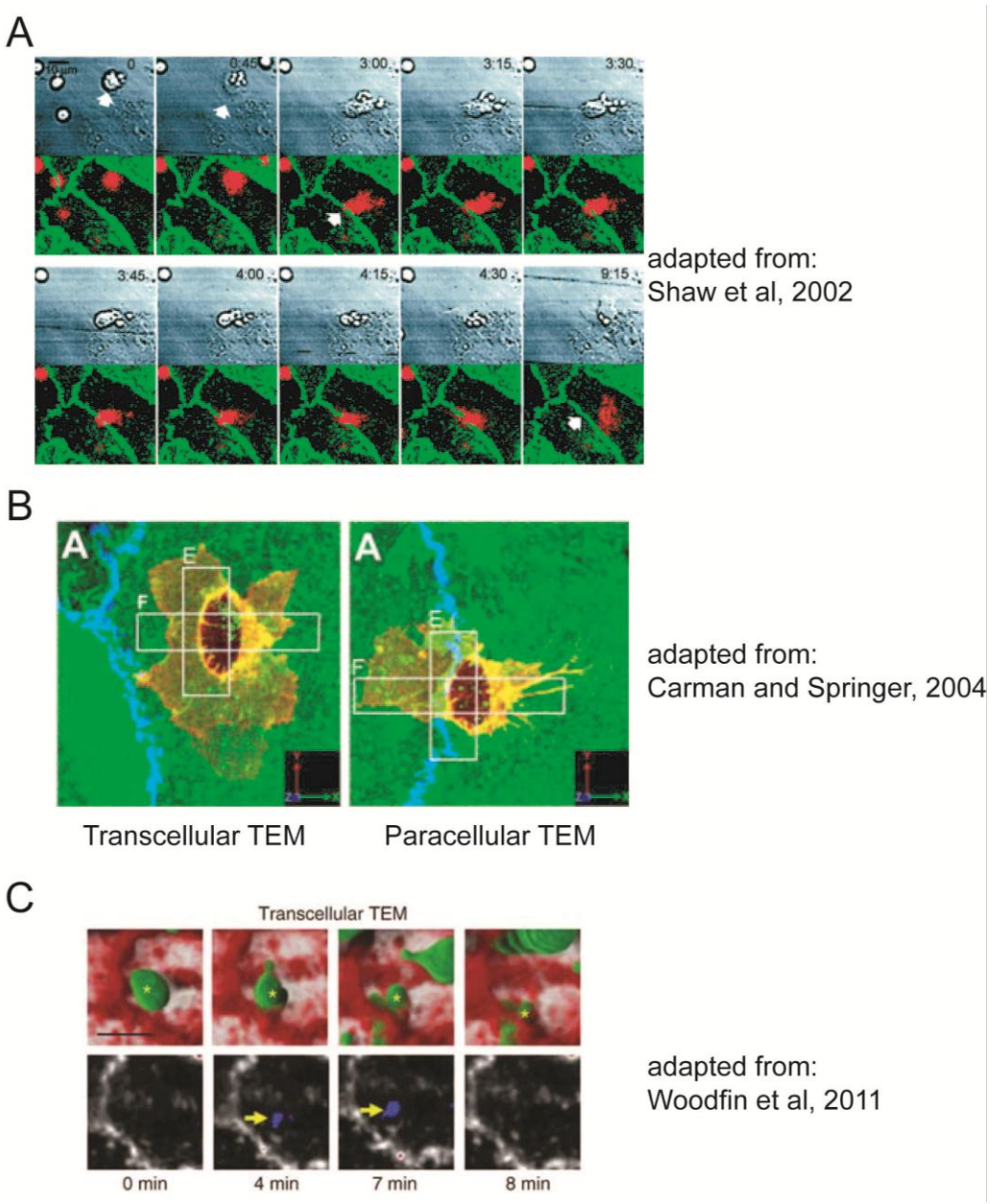

Figure 1.4 Channel opening in endothelium to facilitate leukocyte migration

(A-C) Examples of leukocyte migration across the EC either via a paracellular or transcellular route. (A) Endothelial pore formation in the VEC junction (green) facilitates the paracellular transmigration of a monocyte (red). (B) Transcellular monocyte migration occurs via the formation of a pore in response to the interaction of ICAM-1 (green) and LFA-1 (red) in close proximity to EC junctions (VEC-blue). (C) Neutrophils (green) migrate *in vivo* across murine cremasteric venules through pores. The junction area is visualised by staining for PECAM-1 (red).

neutrophils and lymphocytes found in the subendothelial space (Carman and Springer, 2004) and are therefore found associated with all steps of transmigration.

Several components of the EC are important for the formation of the projections following pharmaceutical disruption. The projections are enriched in actin, require intact microtubules, microfilaments, Ca^{2+} and the small GTPases Rac and Cdc42 (Carman et al., 2003; Carman and Springer, 2004). Disruption of the endothelial projections leads to less efficient leukocyte diapedesis, whilst adhesion is not altered showing the projections are important for diapedesis but not firm adhesion.

ICAM-1-mediated VEC phosphorylation is required for successful leukocyte transmigration (Allingham et al., 2007; Turowski et al., 2008). Since phosphorylation of VEC also results in an increase in transendothelial permeability it is assumed that junctional disruption occurs. Thus AJ modulation appears to be a molecular end point of ICAM-1 signalling in response to leukocyte adhesion.

VEC phosphorylation in response to ICAM-1 activation occurs in the binding areas for β-catenin and p120-catenin (Potter et al., 2005; Allingham et al., 2007; Turowski et al., 2008), suggesting that VEC-catenin interaction may be compromised. In agreement, high expression of p120-catenin prevents the gap formation seen following VEC displacement and inhibits neutrophil TEM (Alcaide et al., 2008). Since dissociation of p120-catenin can lead to VEC internalisation via an endocytic pathway (Xiao et al., 2003), it is possible that junction internalisation is the driving force in gap/pore formation.

Caveolae are membrane domains found in various cell types which may also be involved in TEM (Stan, 2002; Gratton et al., 2004). It is thought that they may control signalling in membrane microdomains of the endothelium (Gratton et al., 2004). It has been proposed that caveolae could fuse to form a transendothelial channel which could be utilised by leukocytes to cross ECs (Stan, 2002). However, the role of caveolae in aiding transmigration is controversial. Millan *et al.* show ICAM-1 within caveolae can translocate across the endothelium potentially assisting in pore formation (Millan et al., 2006). In other cases caveolae are found to only be partially important (Carman and Springer, 2004) or not at all (Carman et al., 2007).

1.3.2.3 Dispatching leukocytes to the underlying tissue

As well as aiding in the attraction, directing and channelling of leukocytes, the EC is also involved in dispatching the leukocyte across the basement membrane to the underlying tissue. This process is not as clearly understood. Work by Sussan Nourshargh's group shows that the ECs appear to participate to this step by providing key signals early in TEM indicating areas of lower expression of basement components, including laminin 8 and laminin 10 (Wang et al., 2006). These low expression regions (LERs) are often found near tri-cellular or bi-cellular junctions, close to regions where pericyte coverage is low or absent. Significantly, neutrophils preferentially migrate within a distance of 0 to 3µm of LERs. LERs act as gates for migrating leukocytes in many tissues in a range of inflammatory reactions (Nourshargh et al., 2010). Adhesive interactions between the neutrophils and basement membrane may play a role in guiding the cell to the site of LERs. The pattern of LER expression is directly associated with the number of gaps per unit area in pericyte sheath in different vascular beds (Voisin et al., 2010). PECAM-1 also has a role in dispatching leukocytes passing through the basement membrane as use of anti-PECAM-1 antibodies inhibited the accumulation of leukocytes to inflammatory sites. The leukocytes are able to pass the EC barrier but became stuck within the vessel walls as they are unable to pass through the basement membrane (Wakelin et al., 1996). Domain 6 of PECAM-1 is important for traversing the basement membrane (Thompson et al., 2000).

There are suggestions that additional signals are required for progression of lymphocytes from the EC subendothelial space (McGettrick et al., 2009). Lymphocytes are retained in the endothelium basement membrane but are able to migrate into tissue more effectively when stromal chemokines, such as CXCL10, are present. Neutrophils, on the other hand, do not appear to require additional signals for their migration into underlying tissue. As there is tissue heterogeneity it is likely that numerous chemokines are required to allow lymphocytes to migrate from the subendothelial space to the tissue.

1.4 Endothelial ICAM-1 signalling contributes to TEM

Although ICAM-1 has classically been considered an adhesion molecule, experimental evidence points to a prevalent role during diapedesis (i.e. during the guiding, opening or dispatch steps). Work by Oppenheimer-Marks *et al.* has shown that antibodies targeting ICAM-1, or its counter-receptor LFA-1, results in inhibition of lymphocyte migration across HUVECs even when ICAM-1 was not involved in the initial adhesion step (Oppenheimer-Marks et al., 1991). Significantly, VCAM-1 did not play a role in T-lymphocyte transmigration under any condition tested. Similar results have been found for lymphocyte transmigration across BBB ECs. Activated T-lymphocytes primarily use LFA-1 to adhere to BMVEC, however not via endothelial ICAM-1 (Male et al., 1994). In contrast, both anti-LFA-1 and anti-ICAM-1 blockage abrogate lymphocyte diapedesis indicating that whilst LFA-1 is important for adhesion and migration throughout TEM the main function of ICAM-1 is during the actual phase of transmigration (Greenwood et al., 1995; Pryce et al., 1997). In agreement, lymphocyte migration across BMVEC deficient for ICAM-1 is greatly attenuated (Lyck et al., 2003).

Endothelial ICAM-1 is also important for diapedesis of leukocytes other than T-lymphocytes. Carman *et al.* show that ICAM-1 rich projections, which are synonymous for TEM, are rapidly formed in response to adhesion of monocytes to ECs (Carman et al., 2003; Carman and Springer, 2004). This response occurs independently of VLA-4 and VCAM-1. Neutrophil diapedesis is also dependent on endothelial ICAM-1 activity similar to that seen during T-lymphocyte TEM (Allingham et al., 2007; Turowski et al., 2008).

Taken together, available evidence clearly points towards an important contribution to TEM which goes beyond a role of providing an adhesion platform for leukocytes. In fact, these observations predict that EC signalling is triggered. Indeed, the intracellular domain and cytoplasmic tail of ICAM-1 are both important for leukocyte TEM and signalling responses (Sans et al., 2001; Lyck et al., 2003; Greenwood et al., 2003a).

1.4.1 Recruitment of other molecules

Receptor multimerisation triggers ICAM-1 signalling (Martinelli et al., 2009). Activation and subsequent clustering of surface ICAM-1 receptor molecules can be modelled in a number of ways. These include using anti-ICAM-1-coated beads or using anti-ICAM-1 antibodies in solution (ligation) on their own or followed by the addition of a second antibody which cross-links the surface ICAM-1 molecules. However, unlike other cell surface receptors, it is not understood how ICAM-1 induces signalling. ICAM-1 has only a short cytoplasmic tail which lacks any known intrinsic enzyme activity or identifiable protein-protein interactions domains (Lawson and Wolf, 2009). It is therefore unknown what downstream molecules are recruited to the ICAM-1 cytoplasmic domain for signalling.

The cytoplasmic tail of ICAM-1 associates with the actin cytoskeleton and this association is important for its localisation in microvilli (Carpen et al., 1992). Indeed, the majority of ICAM-1 associated proteins identified by *in vitro* binding assays can also associate with actin, namely α-actinin (Carpen et al., 1992), ezrin, radixin and moesin (ERM) proteins (Heiska et al., 1998), cortactin (Tilghman and Hoover, 2002) or filamin B (Kanters et al., 2008). ERM proteins form a structural link between transmembrane proteins and the cortical cytoskeleton regulating signalling pathways and cytoskeletal dynamics (Bretscher et al., 2002; Fehon et al., 2010). ERM proteins function as protein scaffolds interacting and associating with a number of proteins including several adhesion molecules such as VCAM-1 (Barreiro et al., 2002), ICAM-2 (Thompson et al., 2002) and ICAM-1 along with F-actin (Romero et al., 2002). These interactions all play a role in cell adhesion, direction, cell spreading or TEM. Filamin B recruits ICAM-1 to the leukocyte docking structure, thereby having a role in leukocyte adhesion and TEM and lateral movement of ICAM-1 in the plasma membrane (Kanters et al., 2008). Significantly, many of these actin interactors/regulators have also been found within the transmigration cup (Barreiro et al., 2002; Carman and Springer, 2004). Thus, available biochemical evidence points to a predominant role of the ICAM-1 cytoplasmic domain in organising the EC cortical actin. Furthermore, one of the primary responses of clustering ICAM-1 would be rearrangements of the actin cytoskeleton, and this has been described by many groups in many EC systems (see below Section 1.4.3).

A 5 amino acid motif, ^{507}RKIKK^{511}, has been found in the N-terminal region of ICAM-1 intracellular domain that regulates ICAM-1 surface distribution and association with F-actin, ezrin

and moesin (Oh et al., 2007). Deletion of this 5 amino acid motif decreases leukocyte adhesion and TEM along with a delay in formation of LFA-1 dependent membrane projections. The cytoplasmic tail also has one conserved tyrosine residue, Y512, which has been proposed to have a role in signalling. Indeed, its phosphorylation by Src increases ICAM-1 clustering and binding avidity (Liu et al., 2011). Furthermore, the expression of phosphorylation deficient mutants decreased ICAM-1 association with the actin cytoskeleton and appeared to reduce TEM. It has been proposed that the protein tyrosine phosphatase (PTPase) SHP2 associates via one of its SRC-homology 2 (SH2) domains with phosphorylated ICAM-1 and thus initiates intracellular signalling (Pluskota et al., 2000). In contrast, Lyck *et al.* show that the expression of ICAM-1 mutants in BMVEC lacking the phosphotyrosine site are still capable of triggering many signalling events and of facilitating TEM of T-lymphocytes to levels similar to wild-type cells (Lyck et al., 2003), suggesting that tyrosine phosphorylation of ICAM-1 was not required during TEM. Clearly, further work is required to understand how the immediate early events of ICAM-1 signalling work.

1.4.2 Phosphorylation events

1.4.2.1 Mitogen activated protein kinases (MAP kinase)

Signalling induced by ICAM-1 receptor multimerisation utilises a number of different molecules and proteins. Many of these lead to protein phosphorylation events. The MAP kinase family has been implicated in mediating endothelial ICAM-1 signalling. The MAP kinase family include extracellular signal-regulated kinase (ERK), p38 and stress-activated kinase /c-Jun N-terminal kinase (SAPK, JNK) (Chang and Karin, 2001; Roux and Blenis, 2004).

MAP kinases are activated in response to different stimuli in a three-tiered cascade (Chang and Karin, 2001). Growth factors and phorbol esters generally activate ERK while JNK and p38 respond to stress stimuli such as osmotic stress and cytokine stimulation (Roux and Blenis, 2004). MAP kinases regulate a number of cellular processes including gene expression, cell survival and motility linking receptors to downstream targets to induce signalling (Chang and Karin, 2001; Roux and Blenis, 2004). ERK is primarily involved in growth and cytoprotective functions whilst JNK and p38 are important in inflammatory and stress functions (Hoefen and Berk, 2002). Downstream

targets include transcription factors, enzymes and other kinases. MAP kinases can mediate gene expression on various levels, and play an important role in mediating the nuclear response of transcription factors such as AP-1, CREB and NFκB in ECs (Roux and Blenis, 2004). Most MAP kinases phosphorylate Ets transcription factors involved in Fos gene expression (Treisman, 1996; Chang and Karin, 2001). A further role of p38 has been described in post-transcriptional regulation of messages carrying AU-rich regions in their 3' untranslated region (UTR) such as TNF-α and cyclooxygenase 2 (Clark et al., 2003). The AU-rich regions are thought to control mRNA degradation and translational arrest which can be overcome by p38 and its substrate MAPKAPK-2.

A distinctive difference between the MAP kinases is the ability of ERK and p38, but not JNK, to phosphorylate and activate downstream MAP kinase activated protein kinase (MKs), further amplifying the signalling pathway (Roux and Blenis, 2004; Gaestel, 2006). Subfamilies of MKs include RSK, MNK and MK2/3 which are all important for all levels of gene expression, including regulation of transcription factors Jun, Fos and NFκB and stability and translation of proteins. In contrast, JNK regulates nuclear targets directly by phosphorylation. Localisation of the MAP kinase family members augments specificities in the induced signalling. The inflammatory state of the endothelium is thought to be determined by the balance of MAP kinase activation (Hoefen and Berk, 2002).

1.4.2.1.1 ERK

In HUVECs ERK is activated within 30 minutes of ICAM-1 cross-linking (Lawson et al., 1999). ICAM-1 cross-linking induces an increase in VCAM-1 expression which is also inhibited by PD98059, an inhibitor of ERK activation, suggesting that ERK regulates ICAM-1-induced gene expression in EC. ERK has been shown to be important in neutrophil TEM (Stein et al., 2003).

1.4.2.1.2 p38

Phosphorylation and activation of p38 occur within a few minutes of ICAM-1 cross-linking in TNF-α treated pulmonary microvascular EC (MVEC) (Wang and Doerschuk, 2001). Activation is prevented when the EC are pre-treated with a xanthine oxidase inhibitor or the p38 inhibitor SB203580. Xanthine oxidase-generated oxidant production precedes p38 activation as SB203580 has no effect on oxidant production. Further studies by Wang *et al.* show that activation of Src tyrosine kinase occurs in response to ICAM-1 cross-linking which leads to the activation of p38 (Wang et al., 2003). Inhibition of Src prevents p38 activation indicating that Src is an upstream mediator of p38 MAP kinase activity. ICAM-1 cross-linking induces phosphorylation of heat shock protein (Hsp)-27 that could have a role in changes of the actin cytoskeleton (Wang and Doerschuk, 2001). Hsp-27, in response to oxidative stress, enhances and stabilises the F-actin network. Neutrophil migration and hsp-27 phosphorylation are dependent upon ICAM-1-mediated p38 activation since both were inhibited by SB203580.

1.4.2.1.3 JNK

Etienne and colleagues show JNK activation in two different rat BMVEC lines, GP8 and RBE4s, following ICAM-1 cross-linking (Etienne et al., 1998). In view of its usual role in regulating gene expression through phosphorylation of transcription factors (Treisman, 1996), JNK may regulate genes encoding inflammatory molecules such as cytokines and adhesion molecules (Manning and Davis, 2003). For example, JNK can bind and phosphorylate c-Jun, a component of the AP-1 complex on serine residues 63 and 73, increasing transcription activity (Davis, 2000). JNK deficient cells are defective in IL-2 production and proliferation as it is important in RNA stabilization in activated T-lymphocytes (Chang and Karin, 2001).

1.4.2.2 Src and cortactin

ICAM-1 cross-linking leads to the activation of Src (Etienne-Manneville et al., 2000; Pluskota et al., 2000; Tilghman and Hoover, 2002; Yang et al., 2006b; Allingham et al., 2007; Dasgupta and Muller, 2008; Liu et al., 2011). In BMVEC this has been shown to occur via a pathway involving phospholipase C (PLC), PKC and intracellular Ca^{2+} transients (Etienne-Manneville et al., 2000). Src activation clearly occurs very early in response to ICAM-1 activation since it has been shown that Src can phosphorylate endothelial ICAM-1 which promotes both ICAM-1 clustering and neutrophil adhesion (Liu et al., 2011). Also, the association of SHP-2 with ICAM-1 appears to be dependent on prior Src phosphorylation (Pluskota et al., 2000). Neutrophil TEM is inhibited when HUVECs are pre-treated with different Src inhibitors (Yang et al., 2006b; Allingham et al., 2007). Src inhibition blocks diapedesis of peripheral blood mononuclear cells across HUVEC as well as membrane recycling to TEM sites, suggesting the LBRC requires Src activity (Dasgupta and Muller, 2008).

Cortactin is a prominent Src substrate and has been implicated in ICAM-1-mediated TEM. It re-distributes to regions where active neutrophil migration occurs (Yang et al., 2006b). ICAM-1 cross-linking or addition of syngenic encephalitogenic T-lymphocytes in rat BMVEC induces Src-dependent cortactin phosphorylation (Durieu-Trautmann et al., 1994). Similar observations have also been made in HUVECs, where Src and phosphorylated cortactin were also found to directly associate with E-selectin and ICAM-1 in response to leukocyte binding (Tilghman and Hoover, 2002). Knock-down of cortactin in HUVEC inhibits both TEM and ICAM-1-mediated cytoskeletal reorganisation (Yang et al., 2006a; Yang et al., 2006b). Significantly, this absence of cortactin cannot be rescued by re-expression of Src mutated on three major Src phosphorylation sites, suggesting that Src phosphorylation of cortactin is indeed essential for endothelial compliance to TEM. *In vivo*, the absence of cortactin leads to reduced neutrophil extravasation (Schnoor et al., 2011). Defects in TEM appear to occur on the level of ICAM-1 clustering. Taken together it appears that Src phosphorylation has an important role in ICAM-1 clustering and associated cytoskeletal remodelling, possible cup formation and TEM.

1.4.2.3 Vascular endothelial cadherin (VEC)

VEC is the main constituent of endothelial AJs. VEC forms a complex with α-catenin, β-catenin, and plakoglobin through the cytoplasmic tail connecting to the actin cytoskeleton whilst p120-catenin binds to a juxtamembrane domain of VEC (reviewed by: Bazzoni and Dejana, 2004; Dejana et al., 2008). This complex is required for barrier function with p120-catenin regulating stability rather than coupling the complex to actin (Xiao et al., 2003). *In vitro* the transient removal of VEC from junctions is thought to facilitate TEM (Shaw et al., 2001), presumably due to tyrosine phosphorylation of key residues of VEC that also correlate with the disassembly of junctions (Potter et al., 2005; Allingham et al., 2007; Turowski et al., 2008; Alcaide et al., 2008).

A number of different phosphorylation sites and signalling pathways have been described in ICAM-1-dependent VEC phosphorylation. So far, all studies agree that phosphorylation occurs on Y731, a site which is found in the β-catenin binding domain (Allingham et al., 2007; Turowski et al., 2008; Alcaide et al., 2008). Potter *et al.* have proposed that phosphorylation of Y731 abolishes the association of VEC with β-catenin (Potter et al., 2005). However, in BMVEC the amount of β-catenin associated with VEC does not change in response to ICAM-1 cross-linking (Turowski et al., 2008), suggesting that dissociation may not be an inevitable consequence of Y731 phosphorylation. In HUVEC, but not BMVEC, Y658 has been shown to be phosphorylated in response to ICAM-1 cross activation or leukocyte adhesion (Allingham et al., 2007; Alcaide et al., 2008) and this has been proposed to abolish binding to p120-catenin (Potter et al., 2005). Phosphorylation on either Y658 or Y731 inhibits endothelial barrier function, suggesting that this directly affects junction integrity (Potter et al., 2005). In BMVEC, the expression of Y to F VEC mutants at position 645, 731 and 733 leads to reduced lymphocyte TEM (Turowski et al., 2008). However, Y645 and Y733 may not be phosphorylated directly but their mutations could alter the overall phosphorylation pattern of VEC. In HUVEC, ICAM-1-dependent VEC phosphorylation is dependent on Src and proline-rich tyrosine kinase 2 (Pyk2) (Allingham et al., 2007) whilst in BMVEC, Rho GTPase, actin, Ca^{2+} (Turowski et al., 2008), CaMKKII, AMP-activated protein kinase (AMPK) and endothelial nitric oxide synthase (eNOS) (Martinelli et al., 2009) are involved (Figure 1.5). These observations raise the possibility that different signalling pathways can mediate VEC phosphorylation during TEM and this may depend on the vascular bed and the leukocyte subset. However, more careful analysis will be required to confirm such a conclusion.

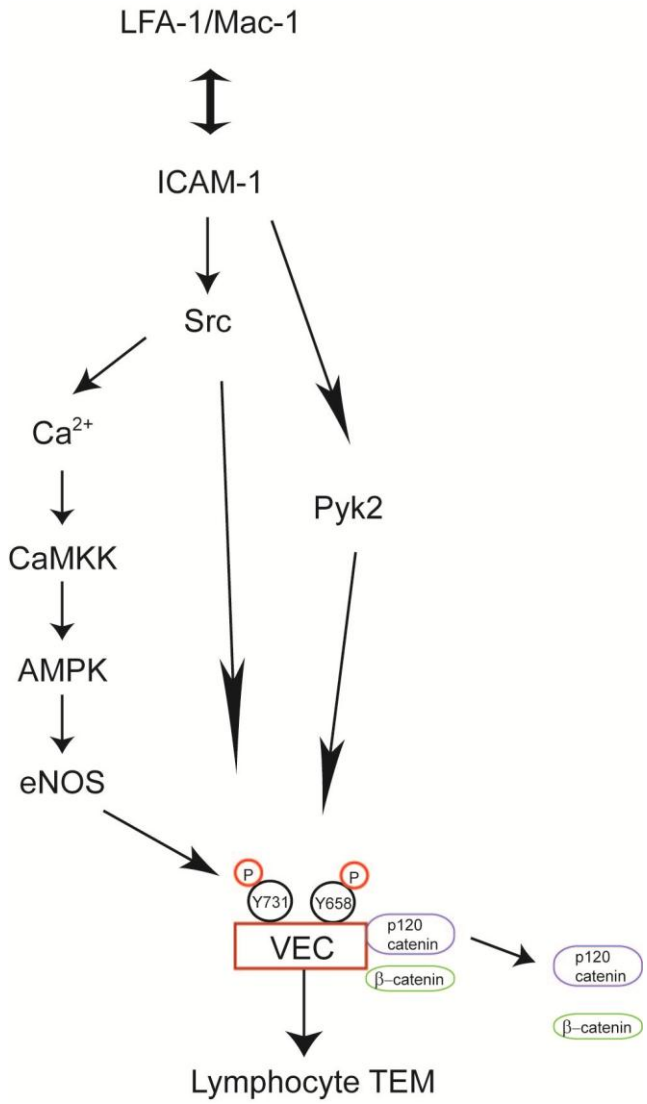

Figure 1.5 ICAM-1-mediated signalling leads to VEC phosphorylation.

Schematic representation of events leading to phosphorylation of VEC at residues Y658 and Y731 and the proposed dissociation of the AJs complex, which is thought to facilitate lymphocyte TEM.

Displacement of VEC from the cell junctions is regulated by p120-catenin which controls VEC surface expression through VEC internalisation and degradation (Xiao et al., 2003). Overexpression of p120-catenin in HUVEC increases VEC expression at cell-cell junctions, prevents VEC displacement from the junctions and inhibits neutrophil or mononuclear leukocyte TEM (Alcaide et al., 2008). p120-catenin overexpression is also linked to reduced tyrosine phosphorylation of VEC Y658 and Y731, suggesting that leukocyte passage at cell-cell junctions is dependent on the phosphorylation status of VEC and its association with p120-catenin.

In BMVEC, a key regulator linking ICAM-1 engagement to VEC phosphorylation is eNOS (Martinelli et al., 2009). A variety of agonists, including VEGF, thrombin, insulin and shear stress, can modulate eNOS activity by inducing phosphorylation at serine or threonine residues (Dimmeler et al., 1999). Phosphorylation of eNOS on S1177 can occur in response to ICAM-1 (Martinelli et al., 2009), insulin (Montagnani et al., 2001) and thrombin (Stahmann et al., 2006). ICAM-1 and thrombin activate eNOS in a signalling pathway requiring Ca^{2+}, CaMKK and AMPK (Stahmann et al., 2006; Martinelli et al., 2009) whilst insulin activates eNOS via phosphatidylinositol 3-kinase (PI3K) and Akt (Montagnani et al., 2001). ICAM-1 activation or thrombin have clear pro-inflammatory roles whereas insulin acts as an EC survival factor. Since compartmentalisation is important for eNOS activation and nitric oxide (NO) production (Fulton et al., 1999), differences in eNOS subcellular location may explain how eNOS activation via different signalling pathways can lead to significantly different cellular responses.

1.4.3 Rho GTPases and the actin cytoskeleton

As described above the actin cytoskeleton appears to mediate important endothelial TEM functions, downstream and in conjunction with ICAM-1 clustering. Many actin regulators have been found to interact with ICAM-1. The actin cytoskeleton is also a major structural component of the transmigration cup which visually reflects successful TEM. Small Rho GTPases are major regulators of the actin cytoskeleton and unsurprisingly have been implicated in ICAM-1-mediated signalling and leukocyte TEM (Etienne et al., 1998; Adamson et al., 1999; Carman et al., 2003; Carman and Springer, 2004; Millan et al., 2006; Kanters et al., 2008).

Rho GTPases have been implicated in a number of EC processes including gene expression, junction integrity, permeability and cell migration (reviewed by: Wojciak-Stothard and Ridley, 2002). The best characterised Rho GTPase family members RhoA, Rac-1 and Cdc42 influence the actin cytoskeleton by inducing the formation of stress fibres, lamellipodia and filopodia, respectively (reviewed by: Wojciak-Stothard and Ridley, 2002; Cernuda-Morollon and Ridley, 2006). Rho GTPases are found in an active, guanosine triphosphate (GTP)-bound, and inactive, guanosine diphosphate (GDP)-bound form. Transition between the two forms is regulated by guanine nucleotide exchange factors (GEFs) and GTPase activating proteins (GAPs) (Millan and Ridley, 2005). GEFs promote the exchange of GDP for GTP whilst GAPs enhance transition back to GDP by stimulating intrinsic GTPase activity. In addition, guanine nucleotide dissociation inhibitors (GDIs) can directly influence the nucleotide state of the GTP-binding proteins as well as their cellular location. Rho GTPases act at cell membranes and this localisation is regulated by post-translational prenylation which anchors Rho to the membrane (Wojciak-Stothard and Ridley, 2002; Cernuda-Morollon and Ridley, 2006).

Stress fibre formation in response to Rho activation induces changes to cell junction integrity, cell contraction and increases in cell permeability (Millan and Ridley, 2005; Cernuda-Morollon and Ridley, 2006). Stress fibres are linked to focal adhesions where integrins are found to cluster and often appear at discontinuous AJs (Pellegrin and Mellor, 2007). Adhesion of leukocytes or antibody engagement of endothelial adhesion molecules induces stress fibre formation (Wojciak-Stothard et al., 1999; Wang and Doerschuk, 2001). In fact, ICAM-1 cross-linking activates Rho (A and/or B) (Etienne et al., 1998; Adamson et al., 1999) and this is dependent on the cytoplasmic tail of ICAM-1 (Greenwood et al., 2003a). This leads to stress fibre induction along which ICAM-1 appears to be moved towards EC lateral areas and possibly sites of TEM (Millan et al., 2006). ERM protein may mediate the activation of Rho downstream of ICAM-1 by sequestration of RhoGDI (Bretscher et al., 2002). Clustering of E-selectin, ICAM-1 and VCAM-1 is dependent on Rho activity and actin integrity (Wojciak-Stothard et al., 1999). Both are involved in the formation of the TEM docking structure (Barreiro et al., 2002; Carman et al., 2003; Carman and Springer, 2004; van Buul et al., 2007a). Furthermore, RhoG, which colocalises with ICAM-1 at sites of adhesion, has also been shown to be required for docking structure formation downstream of RhoA (van Buul et al., 2007a). Inhibition of Rho (ABC, using C3 transferase) or actin rearrangements inhibit leukocyte

TEM without altering leukocyte adhesion and endothelial integrity (Adamson et al., 1999; Turowski et al., 2008).

ICAM-1-mediated Rho activation also controls tyrosine phosphorylation of the cytoskeletal proteins focal adhesion kinase (FAK), paxillin and p130cas (Etienne et al., 1998), further underlining the interdependence of Rho, the actin cytoskeleton and cell adhesion. JNK activation is also dependent on Rho activation; however, the function of this is unclear. Along with exerting direct effects in ICAM-1-mediated signalling and TEM, Rho GTPases play a role in adhesion molecule gene expression, in particular ICAM-1, VCAM-1 and E-selectin (Cernuda-Morollon and Ridley, 2006).

1.5 Aims

A number of components of the EC have been identified in mediating leukocyte transmigration including Rho GTPases, actin and several protein kinases such as the MAP kinases and Src. However, it is not yet known how these components work and interlink to facilitate leukocyte transmigration. Using the model system of rat BMVEC co-cultured with antigen-specific lymphocytes this thesis aims to identify a major EC protein kinase signalling pathway involved in ICAM-1-mediated leukocyte transmigration and to determine how any of the previously described components may be involved. Furthermore, it is expected that additional insight can be gathered into the functional consequence and mechanism of this pathway's involvement in facilitating lymphocyte TEM across the EC barrier.

Chapter 2: Material and Methods

2.1 Reagents

2.1.1 General reagents

Chemicals were purchased from Sigma (Poole, UK) unless otherwise stated. The 30% (w/v) acrylamide, 0.8% (w/v) bis-acrylamide stock solution was purchased from National Diagnostics (Fisher Scientific, Leicestershire, UK) along with Tris.acetate-EDTA (TAE) buffer. Calcein-AM and Dynabeads® Protein G were obtained from Invitrogen (Paisley, UK). The following reagents were purchased from GE Healthcare (Buckinghamshire, UK): Whatman Protran nitrocellulose membrane, high and low molecular weight maker and protein A/G Sepharose beads. Lumi-light western blot substrate and protease inhibitor pill were provided by Roche (Burgess Hill, West Sussex). Agarose was purchased from Bioline (London, UK) whilst Fluoresbrite YG Polystyrene microspheres were obtained from Polysciences Inc (Worthington, PA, USA). The Nucleofector™ Solution V was provided by Amaxa (Amaxa, Germany). Mowiol® 4-88 reagent was supplied by Merck (Nottingham, UK).

2.1.2 Tissue Culture

The following reagents were obtained from Invitrogen: Foetal Calf Serum (FCS: heat inactivated, European origin), Hanks' Buffered Saline Solution (HBSS), Dulbecco's Phosphate Buffered Saline (PBS) without Ca^{2+} and magnesium (Mg^{2+}), F-10 with Glutamax™-1, RPMI with Glutamax™-1 and 25mM Hepes, 4-(2-hydroxyethyl)-1-piperazineethanesulfonic acid) (HEPES), sodium pyruvate, gentamicin and Penicillin/Streptomycin. EMB®2 and EGM®2 MV Single Quots® were purchased from Lonza-Biowhittaker/Cambrex (Slough, UK). DNase I, concanavalin-A, puromycin, basic fibroblast growth factor (bFGF), trypsin (from porcine pancreas), collagen IV and fibronectin were purchased from Sigma. 22% bovine serum albumin (BSA) was obtained from First Link (Birmingham, UK), Collagen I from BD Biosciences (Oxford, UK) and Percoll from GE

Healthcare. Collagenase (CLS2) and Dispase (Neutral Protease, NPRO2) were provided by Lorne Laboratories (Reading, UK).

Plastic tissue cultureware was supplied by Nunc (Rokslide, Denmark).

2.1.3 Molecular Cell Biology

All kits used were purchased from Qiagen (Crawley, UK) unless otherwise stated. The GenElute™ Plasmid Miniprep kit was provided by Sigma. XL1-Blue® Supercompetent cells were obtained from Stratagene (Cheshire, UK). The following reagents were purchased from Invitrogen: Reverse transcription kit containing Superscript ®III Reverse Transcriptase, RNase OUT recombinant ribonuclease inhibitor, oligo(dT) primer, TOPO TA cloning kit and 1Kb DNA ladder. The dNTP set was obtained from GE Healthcare whilst Taq DNA polymerase was purchased from Roche. Primers were supplied by Eurofins MWG Operon (Ebersberg, Germany). For gene cleaning, genCLEAN 96 well spin plates were provided by Genetix (Hampshire, UK). Restriction enzymes from either Roche (*Eco*R1) or New England Biolabs (Hertfordshire, UK) (*Ava*II, *Bg1*II, *Pst*1, *Sac*1) were used.

During this study a number of different plasmids were used. The pEGFP C1 paxillin-β and pEGFP C1 paxillin-β S178A plasmids were kindly provided by Ken Jacobson, University of North Carolina, USA. The pRK5 FLAG-hCNK1 and pRK5 FLAG hCNK1 W493A plasmids were kindly provided by Alan Hall, Sloan-Kettering Institute, New York, USA. The pEGFP paxillin and pEGFP Y31F/Y118F plasmids were kindly provided by Alan Horowitz, University of Virginia, USA. The pcDNA3 FLAG MKK7 WT, pcDNA3 FLAG MKK7 (Ala) DN, pCMV-FLAG JNK1 and pcDNA3 JNK1 APF plasmids were all kindly provided by Roger Davis, University of Massachusetts Medical School, USA. The pEGFP N' VEC and pEGFP N' VEC Y731F plasmids were kindly provided by Patric Turowski, UCL- Institute of Ophthalmology, London, UK.

2.1.4 Antibodies

Antibodies for phospho-ERK, -p38, -JNK and -tyrosine 118 paxillin were purchased from Cell Signaling Technology (Hertfordshire, UK). The anti-phosphotyrosine antibody 4G10 was purchased from Upstate (Millipore, Watford, UK). Antibodies against VEC, PKCβ_I, PKCβ_{II}, PKCδ, PKCε, PKCθ, PKCη, PKCμ and horseradish-peroxidase linked donkey-anti-goat secondary antibody were purchased from Santa Cruz (Insight Biotechnology, Middlesex, UK). Anti-tubulin antibody (clone DM1A) was from Sigma as was the anti-mouse IgG (whole molecule- GAM). Anti-phospho-S178 paxillin was purchased from Abcam (Cambridge, UK). Anti-paxillin and -PKCι were obtained from BD Transduction Laboratories (Oxford, UK). Mouse anti-rat CD54 (ICAM-1, clone 1A29) was either purchased from AbD Serotec or purified from hybridoma cultures. Mouse anti-human CD54 (ICAM-1), rabbit anti-human CD144 (VEC), CD18 (clone WT3), CD11α (clone WT1) and CD49 were purchased from AbD Serotec (Kidlington, UK). Alexa Fluor® 488 and rhodamine phalloidin were supplied by Molecular Probes, Invitrogen. Horseradish-peroxidase linked donkey-anti-rabbit and sheep-anti-mouse secondary antibodies were purchased from GE Healthcare. Cy™3-conjugated affinipure donkey anti-rabbit IgG, goat anti-mouse IgG and goat anti-rabbit IgG were purchased from Jackson ImmunoResearch Laboratories (Suffolk, UK). Fluorescein-conjugated goat affinity purified antibodies to rabbit IgG (whole molecule) was supplied by Cappel Laboratories (Malvern, PA, USA).

Antibodies against PKCα (MC5a,) PKCγ (369G) and PKCζ/ι (524/i) were kindly provided by Peter Parker, Cancer Research UK, London, UK. Affinity purified VEC antibody was kindly provided by Patric Turowski, UCL-Institute of Ophthalmology, London, UK.

2.1.5 Cell permeable small molecule inhibitors

Gö6976, Gö6083, Calyculin A, PP2, SB202130 and SP600125 were purchased from Merck. GF109203X was supplied by Sigma, Cell permeable C3 transferase was obtained from Universal Biologicals (Cambridge, UK), UO126 was from Promega (Southampton, UK) whilst PF573228 and FAK inhibitor 14 were obtained from Tocris (Bristol, UK).

2.2 Methods

2.2.1 Cell culture

2.2.1.1 Immortalised rat brain microvascular endothelial cells

Growth medium: F-10 supplemented with 10% FCS, 2µg/ml bFGF, 80µg/ml heparin, 100 i.u/ml penicillin, 100µg/ml streptomycin

Immortalised rat BMVECs, GPNT, (Regina et al., 1999) were maintained in growth medium at 37°C and 5% carbon dioxide (CO_2). GPNTs were grown on collagen I coated plastic tissue culture flasks and dishes. Briefly, 0.1mM acetic acid was added to 22.5ml filtered water before addition of 25mg/ml collagen I and added to a 500ml bottle of HBSS. The collagen was used to coat the appropriate tissue culture dishes and flasks and left for at least 30 min. The collagen was then aspirated off and the remaining film of collagen polymerised by alkalisation in a box containing ammonia vapour. Subsequently tissue culture plastic was washed twice with HBSS. The dishes and flasks are then ready for plating GPNT cells.

GPNTs were passaged at confluency (usually every seven days) by trypsinisation: cells were washed twice with PBS before the addition of trypsin with excess solution being removed so that only a thin layer coated the bottom of the dish. These were placed back in the incubator until all the cells had detached from the bottom of the flask. The flasks were then washed twice with 10ml of growth medium and syringed three times through a 23G needle to produce a single cell suspension. The cells were plated at a density of 31250 ECs/cm^2 onto collagen I-coated dishes.

Stocks of cells were suspended in ice-cold relevant medium containing 10% dimethyl sulfoxide (DMSO) and frozen in cryotubes (usually at 1-5 X 10^6/ml). The cells were then stored long-term in liquid nitrogen following slow freezing at -20°C for 3 h and -80°C overnight.

2.2.1.2 hCMEC/D3 human brain microvascular endothelial cells

Immortalised hCMEC/D3 human BMVECs were cultured and passaged as described for GPNT (Section 2.2.1.1) with the exception that the growth medium used was EGM®-2 MV growth medium: EBM®-2 MV supplemented with 5% FBS, gentamicin sulphate/ amphotericin-B (GA-1000) and growth factors (human fibroblast growth factor (hFGF), VEGF, ascorbic acid, human epidermal growth factor (hEGF), insulin growth factor (R^3-IGF-1) and hydrocortisone) at 25% of the volume suggested by the manufacturers.

2.2.1.3 Primary rat brain microvascular endothelial cell isolation

Working Buffer: Ca^{2+}/Mg^{2+}- free HBSS, 10mM HEPES, 100 i.u/ml penicillin, 100µg/ml streptomycin, 0.5% (w/v) BSA

Digest Medium: Ca^{2+}/Mg^{2+}- free HBSS containing 1mg/ml collagenase/dispase, 10mM HEPES, 100 i.u. penicillin, 100µg/ml streptomycin, 20 U/ml DNase I, 0.147µg/ml N_{α}-Tosyl-L-lysine chloromethyl ketone hydrochloride (TLCK)

EGM®-2MV growth medium: EBM®2 MV supplemented with 5% FBS, hFGF, VEGF, ascorbic acid, hEGF, R^3-IGF-1, hydrocortisone and GA-1000 according to manufacturer's instructions

Percoll Density Gradient: 50ml Percoll, 5ml 10X HBSS with Ca^{2+}/Mg^{2+}, 45ml HBSS with Ca^{2+}/Mg^{2+}

The protocol was adapted from the method of Abbott and colleagues (Abbott et al., 1992). Female Lewis rats up to six weeks of age were killed by CO_2 asphyxiation, sprayed with ethanol and the head removed by severing the neck. The skin on the skull was pulled back and incisions of 3-5mm were made in the skull at the centre and on either side of the cerebellum. Using coarse forceps, the cut parts were removed to reveal the entire brain. Using a spatula the brain was carefully removed, placed into working buffer and kept on ice.

All dissection instruments were sterilised in alcohol. Dissections were performed on a piece of sterile lint, placed in a petri dish and moistened with working buffer. Using a scalpel the cerebellum was removed and the remaining brain cut in half to separate the two hemispheres.

One hemisphere was processed at a time whilst all others were in working buffer on ice. Using fine forceps the meninges, pia and choroid plexus were removed until the surface appeared featureless and free of surface vessels. The white matter from the hind- and mid-brain was carefully removed before the brain was transferred to a dry piece of lint and rolled to remove any remaining leptomeningial cells. The brain was transferred back to the moist lint to re-wet it before the white matter and striatum was removed. The remaining grey matter was then transferred to a sterile new universal tube containing 10ml working buffer and chopped up into small pieces using a scalpel. This was placed back on ice and the same procedure carried out for all other brain hemispheres.

The chopped brains were triturated through a 5 ml pipette and then centrifuged at 600x*g* at 4°C for 5 min. The medium was aspirated off and the tissue resuspended in 15ml of digest medium (per three brains). The tissue digest was incubated for 1 h at 37°C in a water bath, with agitation every 15 min by vigorous tapping of tubes. Subsequently, the tissue digests were further mechanically disrupted by two 5 min triturations: first through a Pasteur pipette, then through a Pasteur pipette which had been narrowed to about 1/3 in a flame. The suspension was transferred into a new universal tube and then centrifuged at 600x*g* at 4°C for 5 min. The supernatant was removed and the pellet resuspended in 20ml of 22% (w/v) BSA in PBS before centrifugation at 1,000x*g* at 4°C for 20 min. The myelin plug which formed on top of the BSA gradient was carefully rolled away from the tube walls, retriturated and passed through a BSA gradient to recover extra microvessels. Tubes containing the vessel pellets were left inverted to prevent contamination by any myelin. Pellets were resuspended in 1ml of working buffer, transferred to a fresh universal containing 4ml of working buffer and centrifuged at 600x*g* at 4°C for 5 min. After centrifugation the supernatant was removed and the pellets resuspended in 5ml of digest medium (per three brains of starting material) and incubated at 37°C for 3 h with occasional agitation.

During the second digestion culture plasticware was coated by incubation with 100µg/ml collagen IV and 50µg/ml fibronectin in tissue-culture water. They were left to coat for at least 2 h in a humidified incubator at 37°C. Just before use the tissue cultureware was washed twice with PBS for 15 min.

Percoll gradients were prepared in 10ml Du Pont centrifuge tubes. 7ml of 50% Percoll gradient solution was centrifuged at 25,000x*g* at 4°C for 1 h. Tissue digests were centrifuged at 600x*g* for 5 min and the supernatant discarded. The pellet was resuspended in 1ml of working

buffer before being layered onto the Percoll gradients and centrifuged at 1,000x*g* at 4°C for 20 min. Capillary fragments formed a hazy band above a pronounced layer of single cells consisting mainly of blood cells. They were removed using a Pasteur pipette, washed in 20ml working buffer and centrifuged at 600x*g* for 5 min. Each pellet (from 3 brains) was then resuspended in 10ml of EGM®-2 MV growth medium and this vessel fragments solution plated at 1ml/5 cm^2 (or more concentrated if required) and left to adhere and spread at 37°C/5% CO_2 overnight.

The next day medium was changed into growth medium containing 5µg/ml puromycin which is toxic to any residual contaminants and vessel-associated cells but not the BMVECs (Perriere et al., 2005). After three days the puromycin was removed, the cells were washed twice with PBS and normal EGM®-2 MV growth medium added.

Primary BMVEC normally reached confluency 6 days after isolation and could be passaged up to three times as described for GPNT cells (Section 2.2.1.1).

2.2.1.4 Production of anti-ICAM-1 antibody

Growth Medium: RPMI with Glutamax™-1 and 25mM HEPES, supplemented with 10% FCS, 50µg/ml gentamycin

Mouse anti-rat ICAM-1 antibody was purified from the clone 1A29 hybridoma which was kindly provided by Dr M. Miyasaka (Osaka University, Osaka, Japan). 1 vial of 1A29 (1 X 10^7/ml) was thawed, cells placed into 50ml of growth medium and then cultured at 37°C/5% CO_2 until they reached a density of 1 X 10^6/ml. At this point they were either diluted 1:10 and further amplified in growth medium or left to produce antibody. For this, the cells were resuspended in Opti-MEM 1 X 10^6/ml. After around 5 days, when cells were clearly apoptotic, they were pelleted by centrifugation at 600x*g* at room temperature for 5 min. The supernatant was retained for further antibody purification (see Section 2.2.5).

2.2.1.5 Preparation and culture of Peripheral Lymph Nodes (PLN) lymphocytes

Working Buffer: Ca^{2+}/Mg^{2+}- free HBSS containing 10mM HEPES, 100 i.u/ml penicillin, 100µg/ml streptomycin, 0.5% (w/v) BSA

Growth medium: RPMI-1640 containing 2mM L-glutamine supplemented with 10% FCS and 100 i.u/ml penicillin, 100µg/ml streptomycin

Female Lewis rats up to the age of 3 months were asphyxiated by CO_2 and peripheral lymph nodes removed and placed into working buffer on ice. The lymph nodes were disrupted by passing them through a cell strainer (70µm). The volume was made up to 20ml and then centrifuged at 1500*xg* for 5 min. The supernatant was discarded and the pellet resuspended in 25ml of growth medium before a further 5 min centrifugation at 1500*x*g. The supernatant was removed and the cells dispersed by tapping the tube before the addition of 50ml of fresh medium. The cells were filtered once more through a 70µm cell strainer to remove any aggregates (mostly fat), counted and diluted to a density of 1 X 10^6/ml in growth media. Concanavalin-A (5µg/ml) was added to cells for stimulation and activation 24 h after isolation.

2.2.1.6 MBP antigen specific T-lymphocytes (PAS)

Growth medium: RPMI-1640 containing 2mM L-glutamine supplemented with 10% FCS, 1mM sodium pyruvate, 1mM nonessential amino acids, 100 i.u/ml penicillin, 100µg/ml streptomycin, 25µM β-mercaptoethanol.

1 vial of PAS (Beraud et al., 1993) (1.5 X 10^6/ml) were thawed and resuspended in RMPI before being centrifuged at 1800x*g* for 5 min at room temperature. The pellet was resuspended in growth medium and supplemented with addition of 50 U/ml IL-2 for at least 24 h to activate the cells. PAS were resuspended to a density of 2 X 10^5/ml prior to use.

2.2.2 Nucleofection of BMVECs

GPNT cells were grown to 75-80% confluency, trypsinised and pelleted at a density of 3 X 10^6 GPNT cells per nucleofection. The supernatant was discarded and the cell pellet resuspended in 100µl of Amaxa's Nucleofector™ solution V. To the resuspended cells, 10µg (at a maximal volume of 5µl) of the required plasmid was added and the solution transferred immediately into electrocuvettes and nucleofected using programme U13 of the Nucleofector Device. The nucleofected EC were immediately resuspended in 2ml of pre-warmed GPNT medium using a sterile plastic pipette and mixed thoroughly. Transfected ECs were plated into appropriate dishes (at a density of 3 X $10^5/cm^2$) and kept at 37°C/5% CO_2 before experimental analysis was carried out 48 h later.

2.2.3 T-lymphocyte endothelial transmigration

ECs were passaged into wells of 96-well plates and grown to confluence. Cells were washed twice with HBSS prior to the addition of 100µl of IL-2 activated PAS (as prepared in Section 2.2.1.6). PAS lymphocytes were then left to adhere to and transmigrate across EC monolayers at 37°C/5% CO_2. After 1 h lymphocyte-EC co-cultures were mounted on a phase contrast microscope (Zeiss 200 M- equipped with a humidified CO_2/temperature chamber) and analysed by time-lapse microscope: images of an 672µm x 512µm area were taken every 10 sec for 5 min. Playback of such recordings at accelerated speed revealed adherent, non-migrated lymphocytes as phase-bright and transmigrated lymphocytes as phase-dark and significantly flattened. Transmigration rates were determined by tracking adherent T-lymphocytes above and below the EC monolayers and expressed as number of transmigrated per total number of adherent cells. Mean migration rates and standard mean errors (SEM) were calculated from at least three independent experiments (each consisting of data from 6 wells). Statistical analysis was performed by Student's t-test.

Pathway analysis was performed by either pre-treating EC monolayers with small molecule inhibitors as detailed elsewhere (Section 2.1.5) followed by extensive washing to avoid any effects on T-lymphocytes or by using monolayers of transiently transfected EC (see Section 2.2.2).

2.2.2.3 PLN lymphocyte Adhesion assay

Concanavalin-A stimulated PLNs were fluorescently labelled: PLN lymphocytes (as prepared in Section 2.2.1.5) were suspended at a density of 5 X 10^6/ml in growth medium containing 1µM calcein-AM and incubated for 30 min at 37°C. The cells were harvested by centrifugation at 1800x*g* and washed in growth medium. Labelled PLNs were counted under fluorescent light and resuspended to a final concentration of 1 X 10^6/ml.

Calcein-labelled PLN lymphocytes were added to EC, grown to confluency in a 96-well plate at 1 X 10^5 per well and left to adhere for 90 min at 37°C/5% CO_2. At this point non-adhered PLN lymphocytes were washed off by washing each well 6 times with 200µl warmed Ca^{2+}/Mg^{2+}-free HBSS. Subsequently, 200µl of Ca^{2+}/Mg^{2+}-free HBSS was added to each well and fluorescence in each well determined by recording the light emission at 517 nm following excitation at 494 nm in a Saphire fluorescent multiwell plate reader.

Pathway analysis was performed by either pre-treating EC monolayers with small molecule inhibitors as detailed elsewhere (Section 2.1.5) or by using monolayers of transiently transfected EC (see Section 2.2.2).

Data analysis: average fluorescent values from 12 wells of identical conditions were used. Fluorescent values were corrected by subtracting average background (derived from wells incubated with medium alone). Values were then divided by the total fluorescence of the added PLN lymphocytes (derived from wells that had not been washed) to generate adhesion rates. Mean adhesion rates and SEM were calculated from at least three independent experiments (each consisting of data from 12 wells) and expressed as percent of control. Statistical analysis was performed by Student's t-test.

2.2.4 Functional blocking antibody experiment

3 X 10^5/cm^2 Concanavalin-A activated PLNs (prepared as detailed in Section 2.2.1.5) were resuspended in 500µl of ice-cold HBSS containing 20µg/ml of appropriate functional blocking antibody (CD11α and CD18 for LFA-1 and CD49 for VLA-4). PLNs were incubated on ice for 1 h with

gentle agitation to prevent internalisation. 4.5ml of pre-conditioned GPNT growth medium without FCS was added to the PLNs and incubated with serum-starved GPNT for 30 min. Adherent PLNs were extensively washed off with ice-cold PBS before dishes were lysed in an appropriate volume of lysis buffer.

2.2.5 1A29 monoclonal antibody purification

Protein G Sepharose beads were washed twice in 0.1M Tris/Cl (pH 8.0) in a 15ml polycarbonate tube and centrifuged at 600x*g* for 5 min. The supernatant was discarded and the beads resuspended 1:1 in 0.1M Tris/Cl (pH 8.0), placed into a fresh column and allowed to settle by gravity. The antibody to be purified (as described in Section 2.2.1.4) was equilibrated to 0.1M Tris (pH 8.0), added to the column and left to flow-through the column. The column was washed with 10 volumes of 0.1M Tris, 10 volumes of 0.01M Tris and 10 volumes of water. The antibody was eluted with 920µl 0.2M glycine/HCl, pH 1.9 into microfuge tubes containing 80µl of 2M Tris to neutralise the eluate immediately. 50µl of eluted antibody fractions were then taken and added to 1ml of Bradford reagent to determine which fractions contained the antibody. Protein-containing fractions were pooled and dialysed against PBS overnight. Exact protein concentrations were determined by comparing the purified antibody against increasing amounts of a commercial IgG standard on Coomassie Blue stained SDS-PAGEs.

2.2.6 ICAM-1 ligation and cross-linking

Confluent GPNT cells were starved overnight in culture medium without FCS. Conditioned medium was removed, filtered and used to dilute antibodies; 5µg/ml of either antibody produced and purified in the laboratory or commercially bought anti-ICAM-1 antibody, 1A29, for different lengths of time. For cells to be subjected to cross-linking two washes with HBSS were carried out prior to addition of 10µg/ml of GAM for variable lengths of time. Once the cells had been stimulated the dishes were washed twice with HBSS before lysed in a buffer appropriate for subsequent processing.

2.2.7 Immunoprecipitation (IP)

Ripa buffer: 1X TBS, 0.2% SDS, 1% Triton X-100, 1% (w/v) sodium deoxycholate (DOC), 1mM vanadate, 5µM E64, 1µM pepstatin A, 200µM tosyl phenyalanyl chloromethyl ketone (TPCK), 0.3µM aprotinin, 4µM leupeptin, 1mM benzamidine, 100µM TLCK, 1mM 4-(2-Aminoethyl)-benzenesulfonyl fluoride hydrochloride (AEBSF), 5mM ethylenediaminetetraacetic acid (EDTA)

Cells, once stimulated and treated, were washed twice in ice-cold HBSS containing 10mM vanadate. Cells were lysed immediately on ice in 1ml of Ripa buffer and syringed through a 26G needle 5 times. The lysed samples were left on ice for 10 min with occasional gentle agitation before centrifugation at 20,000x*g* at 4°C for 10 min. Supernatant was transferred to new microfuge tube containing 2µg/ml of specific antibody and left on ice for 3 h. 50µl of protein A/G Sepharose beads were added and mixtures incubated with end over end rotation at 4°C for 1 h. Immunocomplexes were collected by centrifugation for 10 sec, and washed three times in 1ml of Ripa buffer before 50µl of lysis buffer was added. The samples were boiled and SDS-PAGE, western blotting and immunodetection carried out.

2.2.8 Assessment of VEC internalisation by cell surface trypsinisation

Confluent monolayers of GPNTs were serum-starved overnight before stimulation with ICAM-1 primary antibody 1A29 or ICAM-1 cross-linking for appropriate lengths of time. Cells were washed twice in ice-cold PBS before the addition of 1.8ml of trypsin (1mg/ml). Cells were incubated on ice for 30 min before 100µl of soybean trypsin inhibitor (2.5mg/ml) was added to inhibit the trypsin. Cells were gently scraped off and centrifuged at 500x*g* at 4°C for 5 min. Dishes were washed in an additional 2ml of ice-cold PBS and combined with the cell pellet. The cells were subjected to centrifugation once again at 500x*g* at 4°C for 5 min. The supernatant was removed and the cell pellet re-suspended in 100µl PBS. Finally cells were lysed by the addition of 4X SDS-PAGE sample buffer.

2.2.9 Cell Fractionation

Wash Buffer: 1X TBS, 10% glycerol, 0.1mM EDTA

Hypotonic Buffer: 20mM Tris/Cl pH 7.4, 5mM EDTA, 1mM DTT, protease inhibitor pill, 100nM calyculin A, 1mM vanadate

Resuspension buffer: 20mM Tris/Cl pH 7.4, 1% Triton X-100, 5mM EDTA, 200mM NaCl, 1mM DTT, protease inhibitor pill, 100nM calyculin A, 1mM vanadate

Stimulated ECs were placed on ice and washed with ice-cold wash buffer before excess solution was removed. The ECs were scraped off in 1ml of hypotonic buffer and passed through a 25G needle 8 times. Centrifugation at 800x*g* at 4°C for 5 min was carried out to produce a pellet containing the nuclei (pellet 1). The supernatant was transferred into a new microcentrifuge tube and centrifuged at 15,000x*g* at 4°C for 10 min to produce the organelle fraction (pellet 2). The supernatant was further centrifuged at 100,000x*g* at 4°C for 30 min to produce the membrane fragment fraction (pellet 3). The remaining supernatant contained the cytosol fraction. Each of the three pellets was resuspended in 500µl of resuspension buffer and left on ice with occasional gentle vortex. The pellet fractions were clarified by centrifugation at 25,000x*g* at 4°C for 10 min and an appropriate volume of SDS-PAGE sample buffer added.

2.2.10 Sodium dodecyl sulphate–polyacrylamide gel electrophoresis (SDS-PAGE)

Running buffer: 25µM Tris, 0.1% SDS, 192mM glycine

The mini-gel system Protean II (Bio-Rad) was used for SDS-PAGE and set up according to the manufacturer's instructions. Seperating and stacking gel solutions were set up as described in Table 2.1 and gels left to polymerise for at least 1 h. For a 0.75mm slab gel, 3.5ml of seperating gel solution was used. 15µl-30µl of boiled lysate were loaded per well along with either a low (97, 66, 45, 30, 20.1 and 14.4 kDa) or high (220, 170, 116, 76 and 53 kDa) molecular weight marker. The gel tank chamber was filled with running buffer and the gel was run at constant amperage of 15mA for stacking gel and 30mA for seperating gel.

Table 2.1: Solutions used for SDS-PAGE			
Seperating gel			
	7.5%	10%	12.5%
Acrylamide: bis-acrylamide (37.5:1) (ml)	2.5	3.34	4
1.5M Tris pH 8.8 (ml)	2.5	2.5	2.5
Pure Water (ml)	4.85	4	3.35
10% SDS (µl)	100	100	100
10% APS (µl)	80	80	80
TEMED (µl)	4	4	4
5% Stacking gel			
Acrylamide: bis-acrylamide (ml)	0.75		
1M Tris pH 6.8 (ml)	0.63		
Pure Water (ml)	3.4		
10% SDS (µl)	50		
10% APS(µl)	75		
TEMED (µl)	10		

2.2.11 Western blotting

Transfer buffer: 25µM Tris, 192mM glycine, 20% methanol

Following SDS-PAGE proteins were transferred onto nitrocellulose membrane using a Bio-Rad Semi-dry transfer cell. Gels were equilibrated in transfer buffer for 10 to 20 min. Subsequently, sandwiches consisting of five sheets of filter paper, the nitrocellulose membrane, the gel and finally a further five sheets of filter paper were set up all soaked in transfer buffer. Protein transfer was performed at a constant 12V for between 30 to 85 min depending on the molecular weight of the protein of interest. Once the transfer was completed the membrane was stained with 0.1% (w/v) Ponceau red (in 5% acetic acid) to verify successful protein transfer and identify the position of the molecular markers.

2.2.12 Immunodecoration

Blocking solution: 1% (w/v) BSA, 1X TBS, 0.2% Triton X-100, 0.1% Tween-20

Secondary antibody solution: 1% (w/v) BSA, 1X PBS, 0.2% Triton X-100, 0.1% Tween-20

The nitrocellulose membrane was incubated in blocking solution for 2 h at room temperature (or overnight at 4°C) to block non-specific binding. Primary antibody was diluted as stated in Table 2.2 in blocking solution and added to the membrane for 1.5 h. The membrane was then washed twice for 10 min with blocking solution and once with secondary antibody solution. Subsequently membranes were incubated for 1 h with secondary antibody diluted in secondary antibody solution as stated in Table 2.2. The nitrocellulose membrane was then washed once again in secondary antibody solution, followed twice in 1X TBS,0.2% Triton X-100, 0.1% Tween-20 and once in 1X TBS.

Enhanced chemiliminescence (ECL) was used to detect the presence of the HRP-conjugated secondary antibody complexes. The membrane was placed in 10ml ECL mix/membrane (5ml of each lumi-light western blot substrate solution) for 5 min. Excess solution was removed and the membrane placed in Saran wrap and membranes exposed to film.

Table 2.2: Antibodies used for immunodecoration				
	Primary Antibody	Species raised in	Secondary Antibody	Species raised in
Phospho-JNK (Thr 183/Tyr 185)	1:2000	Rabbit	1:10000	Donkey anti-rabbit
Phospho-ERK (Thr 202/Tyr 204)	1:2000	Rabbit	1:5000	Donkey anti-rabbit
Phospho-p38 (Thr180/Tyr 182)	1:2000	Rabbit	1:5000	Donkey anti-rabbit
Tubulin	1:10000	Mouse	1:10000	Sheep anti-mouse
4G10	1:2000	Mouse	1:5000	Sheep anti-mouse
VEC (Santa Cruz)	1:500	Goat	1:5000	Donkey anti-goat
Anti-paxillin	1:2000	Mouse	1:10000	Sheep anti-mouse
Phospho-Paxillin (Tyr 118)	1:2000	Rabbit	1:10000	Donkey anti-rabbit
Phospho-Paxillin (Ser 178)	1:2000	Rabbit	1:10000	Donkey anti-rabbit
MC5A (PKCα)	1:2000	Mouse	1:5000	Sheep anti-mouse
$PKC\beta_I$	1:2000	Rabbit	1:5000	Donkey anti-rabbit
$PKC\beta_{II}$	1:2000	Rabbit	1:5000	Donkey anti-rabbit
369G (PKCγ)	1:2000	Mouse	1:5000	Sheep anti-mouse
PKCδ	1:2000	Rabbit	1:5000	Donkey anti-rabbit
PKCε	1:2000	Rabbit	1:5000	Donkey anti-rabbit
PKCθ	1:2000	Rabbit	1:5000	Donkey anti-rabbit
PKCη	1:2000	Rabbit	1:5000	Donkey anti-rabbit

PKCμ	1:2000	Rabbit	1:5000	Donkey anti-rabbit
524/i (PKCζ/ι)	1:2000	Mouse	1:5000	Sheep anti-mouse
PKCι	1:2000	Mouse	1:5000	Sheep anti-mouse
VEC (affinity purified)	1:2000	Rabbit	1:5000	Donkey anti-rabbit

2.2.13 Loading of ICAM-1 antibody to green fluorescent protein (GFP) protein G beads

20µl of Fluoresbrite YG Polystyrene Microspheres were washed in 1ml of PBS followed by centrifugation at 16,400x*g* at 4°C for 1 min. This was repeated twice. The beads were then incubated with 7.5mg/ml of 1A29 homemade ICAM-1 antibody at 4°C for 1 h with end over end rotation (25 rpm). The bead-antibody complexes were then washed three times in 1ml of PBS with centrifugation at 16,400x*g* at 4°C for 1 min. The pellet was resuspended in 1ml of tissue-culture PBS and a 1:10 dilution was counted to determine the concentration of the bead-antibody complex. Beads were used at a density of 0.36 X $10^6/cm^2$ for experimental analysis.

Dynabeads® Protein G were incubated and loaded with ICAM-1 antibody, 1A29, in a similar manner with the exception that beads were collected using a Dynal magnet. Experimental analysis was carried out in the same way as ICAM-1-coated GFP protein G beads.

2.2.14 Immunofluorescence (IF)

Formalin fix: 3.7% formaldehyde, 1X PBS

Methanol fix: 80% methanol, 3.2% formaldehyde, 50mM HEPES

Block solution: 0.2% BSA, 1X PBS

GPNT cells were grown to confluency in 35mm² Petri dishes, stimulated and washed once with PBS. Cells were then fixed with either 3.7% formaldehyde for 15 min or in methanol fix for 10 min before being replaced with block solution. Extraction was carried out using ice-cold acetone that was added to the dish with a residual amount of block solution remaining for 30 sec before being diluted out with 1X PBS. The acetone dilution was replaced with block solution and left for 10 min. During this time the staining solution for the primary antibody was prepared and centrifuged at 9,300*x*g for 5 min. The blocking solution was removed and a central circle formed to which 95µl staining solution was added to the appropriate dishes. The dishes were placed in a 37°C incubator for 1 h. The dishes were washed once with 1X PBS and excess solution removed before the addition of 95µl secondary antibody staining solution. Cells were incubated at 37°C for

45 min. Nuclei of cells were visualised by the addition of 1µg/ml Hoechst 33258 (bis-benzimide) in the secondary antibody staining solution. The dishes were washed once with block solution, once with 1X PBS and a final wash with water before a coverslip was mounted using a drop of 10% Mowiol® 4-88 reagent.

Table 2.3 shows the primary and secondary antibodies dilutions used for IF during the studies.

2.2.15 Visualisation of VEC internalisation

Confluent monolayers of GPNT were washed twice in ice-cold HBSS. The cells were incubated with 5µg/ml rabbit anti-human CD144 (VEC) antibody (or rabbit IgG for control) diluted in F10 medium containing 20mM HEPES and 3% BSA, on ice at 4°C for 1 h to prevent internalisation. Subsequently, the cells were washed again with ice-cold HBSS and stimulated with the 1A29, ICAM-1, antibody for appropriate lengths of time at 37°C for uptake of VEC to be internalised. The cells were then either fixed directly for 15 min in 3.7% formaldehyde in PBS or washed three times for 5 min with 25mM glycine, 3% BSA in PBS, pH 2.7 before fixation. Subsequently, cells were processed for IF (as detailed in Section 2.2.14).

2.2.16 Molecular Biology

2.2.16.1 Ribonucleic acid (RNA) isolation

RNeasy Mini Kit 250 was used for the isolation of RNA from confluent ECs. The cells were washed once with PBS, lysed by scraping into lysis buffer RLT supplemented with 1% β-mercaptoethanol. The lysate was further homogenised using QIA shredders. One volume of ethanol was mixed into the lysate and the mixture added to an RNeasy spin column (700µl at a time). The solution was centrifuged through for 15 sec and flow-through was discarded. 350µl of RWI wash buffer was centrifuged through the RNeasy spin column for 15 sec. 10µl of RNase-free DNase I stock solution was diluted in 70µl buffer RDD, added to RNeasy spin column and left at room temperature for 15 min. A further 350µl of RWI wash buffer was added, centrifuged through

Table 2.3: Antibody dilutions used for IF

	Primary Antibody	Species raised in	Secondary antibody	Secondary antibody used
VEC (affinity purified)	1:50	Rabbit	1:100	DAR Cy3
Phospho-paxillin (Tyr 118)	1:50	Rabbit	1:30	GAR FITC
Anti-paxillin	1:100	Mouse	1:100	GAM Cy3
PKCγ (369G)	1:100	Mouse	1:100	GAM Cy3
PKCζ/ι (524/i)	1:100	Mouse	1:100	GAM Cy3
PKCι	1:100	Mouse	1:100	GAM Cy3
$PKC\beta_I$	1:50	Rabbit	1:200	GAR Cy3
PKCε	1:50	Rabbit	1:200	GAR Cy3
PKCθ	1:50	Rabbit	1:200	GAR Cy3
Rhodamine or Alexa Fluor® 488 phalloidin	1:50		n/a	

and the flow-through discarded. The column was further washed using 2 times 500µl of buffer RPE. Centrifugation at 20,000x*g* for 2 min followed and a further 1 min to ensure complete elimination of buffer RPE and the ethanol it contains. Final RNA elution was performed by the addition of 30-50µl of RNase free water. RNA concentration was determined by UV spectroscopy at 260nm in a nano-drop spectrophotometer ND1000 (Labtech).

2.2.16.2 First Strand complementary deoxyribonucleic acid (cDNA) synthesis

Total RNA was reverse transcribed using a reverse transcription kit in reactions containing SuperScript® III Reverse Transcriptase. In a standard reaction 1µl of oligo(dT)$_{12\text{-}18,}$ 1µl of 10mM dNTP mix and 5µg total RNA was used in a final volume of 13µl. The reaction was then heated to 65°C for 5 min and quenched immediately on ice for at least 1 min. The mixture was briefly vortexed before the addition of 4µl of 5X first strand buffer, 1µl of 0.1M DTT, 1µl of RNaseOUT™ recombinant ribonuclease inhibitor (40 U/µl) and 1µl of SuperScript® III Reverse Transcriptase (200 U/µl). The reaction was mixed by gentle pipetting before incubation at 50°C for 60 min. The reaction was stopped by heat inactivation at 70°C for 15 min.

2.2.16.3 Polymerase Chain Reaction (PCR)

Amplification of DNA was carried out in standard reactions of 25µl that were formed of 12.5µl of mastermix 1 and mastermix 2 each.

Mastermix 1: 10µl cDNA (or 1µl of amplified PCR product)

1.25µl of each appropriate 12.5µM forward and reverse primer

To volume 12.5µl with distilled water

Mastermix 2: 2.5µl 10X PCR buffer + $MgCl_2$

0.5µl $MgCl_2$

0.64µl dNTP (10mM each)

0.64µl Taq DNA polymerase (0.625 U/25µl reaction)

To volume 12.5µl with distilled water

Table 2.4 shows the forward and reverse primers utilised to amplify DNA fragments. The primers were designed from the *Rattus norvegicus* sequences obtained via Blast. Some of the sequences used for the PKC isoforms were of a predicted sequence and hence not fully determined. The accession numbers of the sequences obtained from Blast are as follows: NM_001105713 (PKCα), NM_012713 (PKCβ_I), NM_012628 (PKCγ), NM_133307 (PKCδ), NM_017171 (PKCε), NM_022507 (PKCζ), XM_341553 (PKCθ variant 2) XM_234108 (PKCµ) and XM_342223 (PKCι). Predicted sequences were used for PKCι, PKCµ and PKCθ with the sequence for PKCι recently being replaced by NM_032059. ClustalW was used to align the 9 PKC isoforms to find regions of similarity and intron/exon boundaries determined (see Appendix 10.1). The accession number, NM_031085, for the sequence of PKCη was obtained from Blast. The sequence of PKCη was aligned with the sequences of PKCδ, PKCε and PKCθ using ClustalW as they all are from the same class of PKCs and therefore similar in sequence (see Appendix 10.2). The primers were designed within the coding sequence and designed to have roughly the same GC content and length.

Reactions were carried out in an Eppendorf Mastercycler Gradient. The DNA was initially denatured by heating for 5 min at 95°C; these samples were then subsequently heated at 95°C for 30 sec, 55°C for 60 sec and 72°C for 45 sec for 35 cycles. A final extension period was carried out at 72°C for 7 min to ensure that full length products were produced and to increase the amount of amplified DNA products.

Nested PCR was carried out to ensure specific DNA amplification had occurred. The same protocol as mentioned above for the mastermixes and programme for the denaturation, amplification and annealing temperatures was used to amplify the DNA using the new primers.

Table 2.4: Primers for PCR amplification

Name	Accession Number	Primer	Sequence	Start	End
PKCα	NM_001105713	forward	gagaagttggagaacagggag	1967	1987
		reverse	tcaggcctctgtgtggaacaa	2280	2300
PKCβ	NM_012713	forward	gaccggatgaaactgaccga	1687	1706
		reverse	ggagtgccacagaatgtctt	2179	2198
PKCγ	NM_012628	forward	gcagcggcgaaaactttgaca	2070	2090
		reverse	atgctggggaacagcgtctag	2508	2528
PKCδ	NM_133307	forward	gatcaccaaggagtccaagga	2066	2086
		reverse	aagtactgtgagcccagccaa	2524	2544
		nested for	ggagaagctcttcgagaggga	2093	2133
		nested rev	agccagactctccgaggaaga	2499	2519
PKCε	NM_017171	forward	ggggaagatgccatcaagcaa	2165	2185
		reverse	agacctagcactgcacacaga	2642	2662
PKCη	NM_031085	forward	gaatgaagatgacctttttga	1857	1878
		reverse	ggctccccgggacttgacaga	2387	2407
PKCθ	XM_341553	forward	agagattgacccacccttcag	2086	2106
		reverse	gatcgggaaccatctttcaag	2336	2557
		nested for	ggctatcgttcgctgacagag	2172	2192
		nested rev	gatgccattagtgaaggagac	2443	2463

PKCμ	XM_234108	forward	aagaccttgagtcacccctgg	2633	2653
		reverse	gagctggctctcaccaaaatg	3196	3216
PKCι	NM_032059	forward	gagcagaagcaagtggttccg	2494	2514
		reverse	agccttccatgccttaaccca	3011	3031
PKCζ	NM_022507	forward	aggcctcacacgtcttgaaag	1598	2018
		reverse	acaggaagtggttccttccag	2133	2152
M13 (-20)	Sequencing primer	forward	gtaaaacgacggccagt		
M13	Sequencing primer	reverse	ggaaacagctatgaccatg		

2.2.16.4 Agarose Gel Electrophoresis

DNA fragments were separated by agarose gel electrophoresis according to their molecular weight. Routinely, 2% (w/v) agarose gels were prepared by melting 2g agarose in 100ml TAE buffer (40mM Tris.acetate, 2mM Na_2 EDTA). Ethidium bromide (0.5µg/ml) was added and then poured into a gel tray support and comb. DNA samples were prepared by the addition of 2µl of 6X loading dye (30% (w/v) glycerol, 0.25% xylene cyanol) to 10µl of PCR product. The samples, along with 6µl of 1Kb DNA ladder (1µg/µl), were loaded and electrophoresed in TAE buffer at a constant voltage (usually at 80V) until DNA fragments were sufficiently resolved. The gel was visualised at 320nm under a UV illuminator (Gene Genius Bio Imagine System, Syngene).

2.2.16.5 Restriction Enzyme digest

DNA was digested with restriction enzymes in a final volume of 20µl. Reactions contained 5-10µl of PCR product, 2µl of appropriate 10X buffer, 0.5µl of restriction enzyme and BSA. The reactions were incubated at 37°C for 1.5 h. The reactions were then analysed on 2% agarose gels.

2.2.16.6 Cloning

The QIAquick gel extraction kit was used to isolate and purify PCR fragments from agarose gels. The DNA fragment was excised from the agarose gel using a clean sharp scalpel. 3 volumes of Buffer QG was added and the gel completely dissolved by incubation at 50°C for 10 min. One volume of isopropanol was mixed in to increase the DNA yield. The resulting mixture was added to a QIAquick spin column placed in a 2ml collection tube and centrifuged at 16000*xg* for 1 min. The flow-through was discarded and the column washed by spinning through 500µl of Buffer QG. The column was further washed with 750µl of Buffer PE, which contains ethanol, and the flow-through discarded. The column was centrifuged again at 16000x*g* for 1 min to remove any residual ethanol. The spin column was transferred to a new microcentrifuge tube and the DNA eluted by adding 50µl 10mM Tris.Cl pH 8.5 and centrifugation for 1 min.

2.2.16.7 Topo TA Cloning

The Topo TA cloning kit was used according to the manufacturer's instructions. Briefly, reactions were set up containing 4µl of DNA, 1µl of salt solution and 1µl of Topo vector. The reaction was gently mixed and left to incubate at room temperature for 30 min. Reactions were placed on ice until used for transformation

2.2.16.8 Transformation of XL1-Blue® Supercompetent Cells

2xYT medium: 1.6% (w/v) bacto-tryptone, 1% (w/v) bacto-yeast extract, 0.5% (w/v) NaCl, pH7.0, dissolved in 1l of deionised water.

One vial of XL1-Blue® Supercompetent cells was gently thawed on ice and for each reaction 50µl of the cells was aliquoted to a pre-chilled, sterile polycarbonate tube. 0.85µl of β-mercaptoethanol (provided with kit) was added to the bacteria and the mixture swirled gently before incubation for 10 min on ice. 5µl of plasmid DNA was added to the cells and incubated on ice for 30 min, with occasional agitation. The reaction was heat shocked at 42°C for 45 sec and immediately quenched on ice for 2 min. 900µl of pre-warmed 2xYT medium was added and the tubes incubated at 37°C for 1 h on a shaker at 230 rpm. The transformation reaction was centrifuged at 300*x*g for 10 min and around 850µl of supernatant was discarded. The remaining transformation reaction was plated onto a pre-warmed agar plate containing appropriate antibiotic (ampicillin or kanamycin) allowing recognition and selection. The plate was placed into an incubator at 37°C for 16 h for colonies to grow (afterwards the plates were placed at 4°C to prevent further growth).

2.2.16.9 Small Scale Preparation of plasmid DNA

In 3ml of LB medium containing 100µg/ml of ampicillin a single colony of XL1-Blue® Supercompetent cells was added and left to grow overnight in a shaking incubator at 37°C.

DNA was prepared using the GenElute™ plasmid miniprep kit according to the protocol provided. Briefly, 1.5ml of the overnight culture was pelleted by centrifugation at 12,000x*g* for 1 min with the supernatant being discarded. The pellet was completely resuspended in 200µl of resuspension solution containing RNase. 200µl of lysis solution was added and mixed by gentle inversion 6-8 times for a maximum of 5 min incubation. Cell debris was precipitated by the addition of 350µl of neutralization/binding solution with the tube once again being gently inverted 4-6 times. Cell debris was pelleted by centrifugation at 12,000x*g* for 10 min. During this time a Genelute miniprep binding column was prepared by insertion into a microcentrifuge tube with the addition of 500µl of column preparation solution and centrifuged at 12,000x*g* for 1 min with the flow-through being discarded. The cleared lysate was transferred to the prepared Genelute binding column and centrifuged at 12,000x*g* for 1 min. The flow-through was discarded prior to the addition of 750µl of wash solution (containing ethanol) and centrifuged at 12,000x*g* for 1 min. The flow-through was discarded and the column was centrifuged again at 12,000x*g* for a further 2 min to remove any excess ethanol that might be present. The column was transferred to a new collection tube to which 100µl of elution buffer was added to elute the DNA from the column by centrifugation at 12,000x*g* for 1 min. Plasmid minipreps were either used directly or stored at -20°C.

2.2.16.10 Maxi preparation using Qiagen Endo-free plasmid maxi-kit

A pre-culture of a single colony of XL1-Blue® Supercompetent cells was grown in 3ml of LB medium with appropriate antibiotic for 8 h in a shaking incubator at 37°C. The pre-culture was then added to a further 150ml of LB medium and antibiotic and left to grow overnight in a shaking incubator at 37°C.

DNA was prepared using the Endo-free plasmid maxi kit according to the protocol provided. Briefly, 150ml of the overnight culture was pelleted by centrifugation at 6,000x*g* at 4°C for 15 min. The pellet was completely resuspended in 10ml of Buffer P1 supplemented with RNase A. 10ml of Buffer P2 was added and mixed by inversion 4-6 times before 5 min incubation at room temperature. During this incubation period the QIAfilter cartridge was prepared. 10ml of chilled Buffer P3 was added to the lysate and mixed immediately by vigorous inversion 4-6 times. The

lysate was poured into the barrel of the QIAfilter cartridge where it was left to incubate for 10 min at room temperature. After the incubation period the cell lysate was filtered into a 50ml polycarbonate tube. 2.5ml of Buffer ER was added to the filtered lysate and mixed by inverting 10 times before 30 min incubation on ice. During this incubation period a QIAGEN-tip 500 was equilibrated with 10ml of Buffer QBT. The filtered lysate was passed through the QIAGEN-tip by gravity flow followed by two washes of 30ml Buffer QC. 15ml of Buffer QN was used for elution of DNA into endo-free polycarbonate tubes. The eluted DNA was split into 2 tubes and precipitated with 0.7 volumes of room temperature isopropanol. This was mixed and immediately subjected to centrifugation at 8,000x*g* at 4°C for 40 min. The supernatant was carefully decanted and each DNA pellet washed with 2.5ml of endotoxin-free room temperature 70% ethanol before further centrifugation at 8,000x*g* at 4°C for 20 min. The supernatant was carefully decanted and the pellet left to air-dry before the DNA was redissolved in a total volume of 200µl of Buffer TE. DNA concentration was measured using the spectrophotometer at wavelength 260nm. The maxi-preps were then used immediately or stored as 10µg aliquots, in 2.5 volumes of 100% ethanol and 0.1 volume of 3M sodium acetate, at 4°C.

2.2.16.11 Sequencing

PCR reactions containing 0.5µl big dye reaction mix, 2µl big dye buffer, 1µl DNA and 6.5µl of each M13 primer (0.25µM) (as stated in Table 2.4) were set up. The mixture was denatured at 96°C for 1 min, and then subsequently heated at 96°C for 10 sec, 50°C for 5 sec and 60°C for 4 min for 25 cycles. 10µl of water was added to each sample and reaction products purified using genCLEAN 96 well spin plates.

Reactions were cleaned up using gene cleaning. A gene clean plate was brought to room temperature and centrifuged at 910x*g* for 5 min with a wash plate underneath to remove the liquid from the wells. 100µl water was added to the wells being used and the plate was spun again at 910x*g* for 5 min. The collection plate was aligned underneath and 20µl of the sequencing PCR sample was added to the wells before centrifugation at 910x*g* for 5 min. Reactions were transferred to the sequencing plate ready to be run on a Hitachi 3730 DNA analyzer (Applied

Biosystems). Sequencing traces were analysed and edited using chroma (weblink) software. Subsequently, sequences were identified using Blast.

2.2.16.12 DNA precipitation

To concentrate DNA 0.1 volume of 3M sodium-acetate and 2.5 volumes of 100% ethanol were added. After 30 min incubation on ice, samples were centrifuged at 25,000x*g* at 4°C for 10 min. The supernatant was discarded and followed by a wash with 70% ethanol for 10 min before a further 10 min centrifugation. The supernatant was removed and pellets left to air dry before resuspension in a minimal volume of water. Samples were further heated at 55°C for 2 min to fully redissolve the DNA.

2.2.17 Statistics/densitometry/quantification

Phosphorylation of ERK, p38, JNK and paxillin was quantified from immunoblots by densitometry. The western blots were scanned, images inverted and the intensity set so that background was absolutely black (pixel intensity of zero). Subsequently, signal bands were encircled and the mean pixel intensity and area determined using ImageJ. The absolute intensity was determined as the product of mean intensity and the area of the band. In most cases accumulation of phospho-proteins/cell mass was determined and tubulin used as a loading control. Previous experiments in the laboratory have shown that levels of key proteins (ERK, JNK and p38) did not alter in response to any ICAM-1 stimulation when compared to tubulin. It is understood that these results do not shown the proportion of protein being phosphorylated. Values were set to fold-increase and normalised to the tubulin/ total paxillin loading control. Means and SEM from at least three independent immunoblots were calculated. Statistical analysis was by Student's t-test.

To determine the observed molecular weight of each of the PKC isoforms: the distance travelled by bromphenol blue and each molecular weight ladder marker was analysed and compared to the relative migration distance of the main band seen for each PKC isoform. These

values were then compared to those of the predicted molecular weight for each of the PKC isoforms for further verification.

Chapter 3: Activation of ECs following ICAM-1 engagement

3.1 Introduction

The process of diapedesis can be separated into three distinct steps: guidance of leukocyte to TEM sites, channel opening and dispatch to the tissue (as described in detail in Section 1.3.2). In this part of the studies, I was interested in the EC contribution to guiding leukocytes to sites of preferential transmigration. Adherent leukocytes bind to CAMs on the EC surface and later, immediately prior to diapedesis, find themselves in lateral EC areas, often near tri-cellular junctions (Burns et al., 1997). Since leukocytes can crawl on CAM substrates (Smith et al., 2003) it is commonly assumed that leukocyte find their own way to these TEM sites. However, it has been noted that antibody-activated ICAM-1 lateralises toward the EC junction area along actin stress fibres (Millan et al., 2006; Turowski et al., 2008), suggesting that the EC contributes to leukocyte lateralisation as well. Definitive proof of a role of EC is difficult to obtain since in leukocyte-EC co-cultures the contribution of the leukocyte cannot be eliminated. The use of antibody-coated beads may represent a satisfactory alternative: such anti-ICAM-1-coated beads have not only been shown to initiate EC signalling similar to that seen with soluble ICAM-1 (Allingham et al., 2007) but also to induce an adhesion structure which is reminiscent of a transmigration cup (Barreiro et al., 2002; Carman et al., 2003; Carman and Springer, 2004; Allingham et al., 2007; van Buul et al., 2007b). It therefore appears that such beads mimic TEM up to the moment when the process becomes irreversible (Muller, 2009) and could therefore also be used to study the endothelial role in lateralisation. Finally, antibody-coated beads are obviously more amenable to time-resolved microscopy.

3.2 Aim

The aim of this part of the study is to investigate whether anti-ICAM-1 antibody-coated beads are lateralised when they contact ECs. The time course and functional consequences will also be analysed.

3.3 Results

3.3.1 ICAM-1 engagement leads to its lateralisation to cell junctions

To investigate the involvement of ECs in directing leukocytes to preferential migration sites, anti-ICAM-1-coated fluorescent beads were added to GPNT BMVECs and left for various lengths of time before the cells were fixed and bead distribution analysed in relation to EC junctions. Figure 3.1A shows that increasing number of anti-ICAM-1 beads clustered and accumulated near AJs in a time-dependent fashion. Hardly any beads were observed to accumulate near the nuclei. To quantify possible lateralisation of beads, the number of beads found within one bead diameter (1µm) of the cell junctions within a set area was quantified (Figure 3.1B). In samples fixed 10 min after bead addition 45% of adherent beads were found in proximity of the cell junction. 38% of beads were engaged in clusters of 2 or more beads. At 30 min this increased by nearly 2-fold to 76% and 82% lateralisation and cluster formation, respectively. At 60 min, ca. 65% of beads were still found to be clustered and lateralised. Very few single beads were found near EC junctions, suggesting that beads do not lateralise unless they are found in clusters. The proportion of beads found to lateralise at tri-cellular junctions, sites of preferential transmigration, was also analysed from the same experimental series. A time-dependent increase in the number of beads found in the proximity of tri-cellular junctions was observed (Figure 3.1B). At 10 min after bead addition, 16% of them were found near at tri-cellular junctions. This nearly doubled to 31% after 60 min. Thus, combined across the 60 min observation period around a third of lateralised beads were found at tri-cellular junctions. Taken together, these observations suggested that ECs actively move clustered ICAM-1 towards the cell edge.

3.3.2 Anti-ICAM-1-coated beads induce luminal membrane ruffles

I next sought to investigate the dynamics of adhesion and lateralisation of anti-ICAM-1-coated beads on GPNT. For this, anti-ICAM-1 fluorescent beads were added to GPNT monolayers mounted on a fluorescent live imaging microscope. Beads were added and images taken every min for 1 h. Several areas of the cell monolayer were analysed simultaneously. During the entire

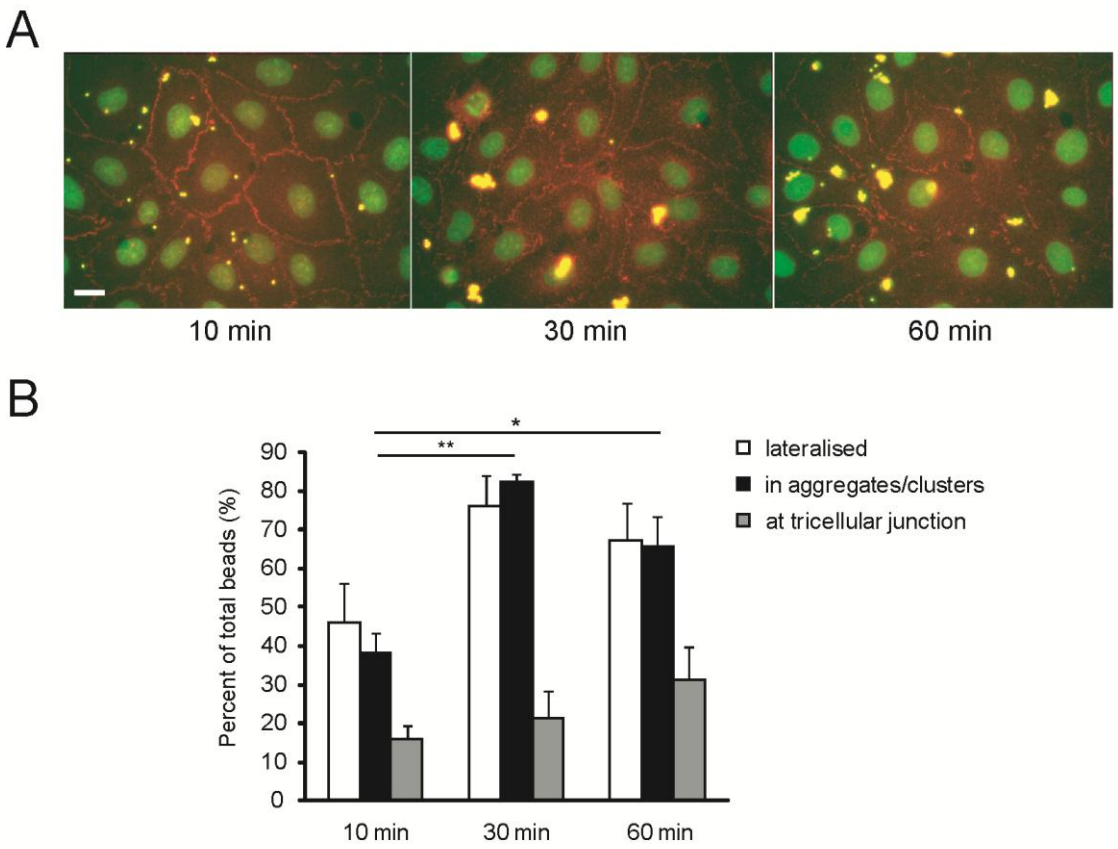

Figure 3.1 Anti-ICAM-1-coated beads lateralise and cluster at EC junctions in a time-dependent manner

Figure 3.1 figure legends

(A) Anti-ICAM-1 fluorescent GFP coated beads (3 beads/EC) were incubated with confluent GPNT monolayers for the indicated times before the cells were washed twice with PBS to remove any excess, unbound beads and methanol fixed. The dishes were stained for VEC (red) to reveal the cell edge and AJs and with Hoechst to identify nuclei (green). In these merged images the beads appear yellow. (Scale bar: 10µm)

(B) Quantification of bead localisation from experiments as in (A). Beads within 1 bead diameter (1µm) of VEC were counted as lateralised (open bars). If additionally they were found in tri-cellular areas they were recorded as such (grey bars). For bead clustering (black bars), at least two beads had to touch each other. Beads within 1 bead diameter (1µm) of VEC in tri-cellular areas were counted. Bead numbers per field (6 fields/experiment) were determined and expressed as percentage of the total number of adherent beads. Shown are means from 3 independent experiments +/- SEM.

course of the experiment I observed that the majority of beads were not adherent (Figures 3.2). It was also clear that the EC monolayer did not become activated in the absence of bead adhesion (Figure 3.2). Furthermore, immobilisation of a single bead did not lead to any apparent EC activation (Figure 3.3). In clear contrast, activation occurred in response to the immobilisation of a cluster of anti-ICAM-1 beads on the endothelial surface. As shown in a representative example in Figure 3.4 a clear change of cell shape associated with what appeared to be a wave of luminal membrane ruffles occurred in the single cell that contained an immobilised bead cluster. In this specific case, the bead cluster was recruited to regions of the cell junctions within 12 min (Figure 3.5), moved laterally to the site of immobilisation within 18 min. A change of cell morphology became apparent at around 22 to 24 min. Figure 3.6 clearly shows the activation period of EC from full immobilisation of the beads in more detail. The engagement of ICAM-1 on the endothelial surface with the anti-ICAM-1 beads induced membrane ruffling at the cellular junctions and the cell increased in size as time progressed. Noticeable differences also occurred in the cell nucleus from 28 min onwards as the nucleus became more defined in structure and appeared to shrink in size. Vesicular-like structures appear around the nucleus as time progresses and these appear to become denser in structure at around 46 min.

A delay in activation of the EC is observed following immobilisation of the bead cluster to the GPNT EC (Figure 3.4 and 3.5). The time between immobilisation and cell activation was determined from a number of experiments and analysed in more detail (Figure 3.7). Bead cluster immobilisation was defined as the time when adherent beads did not move any further. Start of EC activation was defined as the time when the first clear morphological change was observed in the EC whilst full activation was taken as the time when maximal morphological changes were observed. Not all beads will immobilise to the EC surface, therefore from all 3 independent experiments (and 4 fields imaged for each) all immobilised bead clusters were analysed. Some of the fields did not have any observed immobilised beads whilst others had more than 1 bead cluster immobilised on the EC surface leading to EC activation. Overall 13 bead clusters were analysed. Following the immobilisation of a bead cluster it took an average of 14 min for visible EC changes to occur. Full cell activation was reached 21 min after bead attachment. Taken together, these results indicate that clusters of anti-ICAM-1-coated beads can lead to EC activation once completely immobilised in lateral areas of the cell. These observations also gave us a time frame in which to investigate EC signalling in response to ICAM-1 activation.

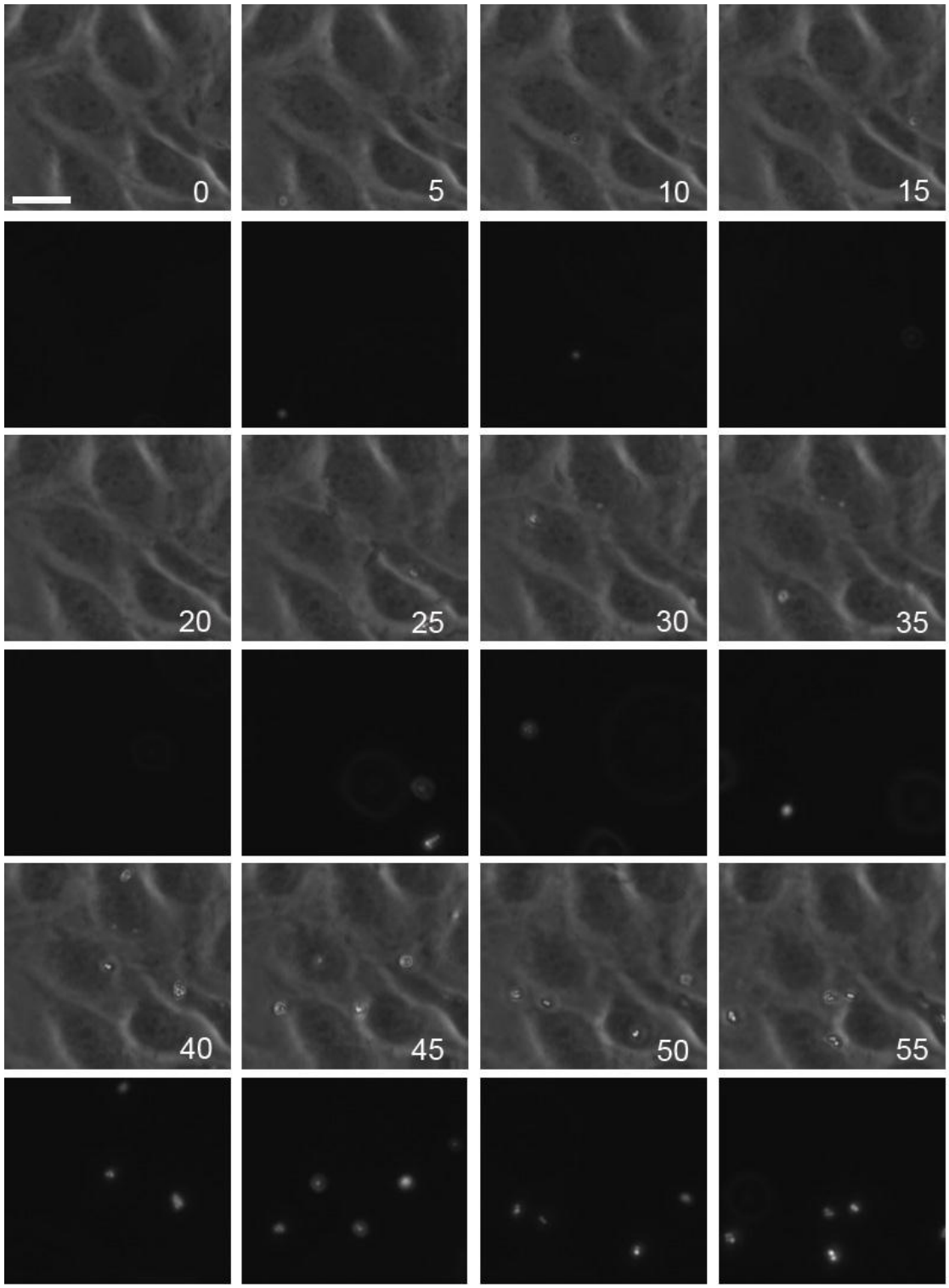

Figure 3.2 Activation of ECs does not occur when anti-ICAM-1-coated beads are not immobilised on the endothelial surface

Figure 3.2 figure legends

Anti-ICAM-1 fluorescent beads (3 beads/EC) were added to confluent GPNT monolayers and cells imaged every min for 1 h on an automated time-lapse fluorescent live imaging microscope. Videos were analysed to determine the time of bead immobilisation on the EC surface. The phase contrast and fluorescent images show the EC monolayer and anti-ICAM-1-coated beads movement, respectively. (Scale bar: 10µm)

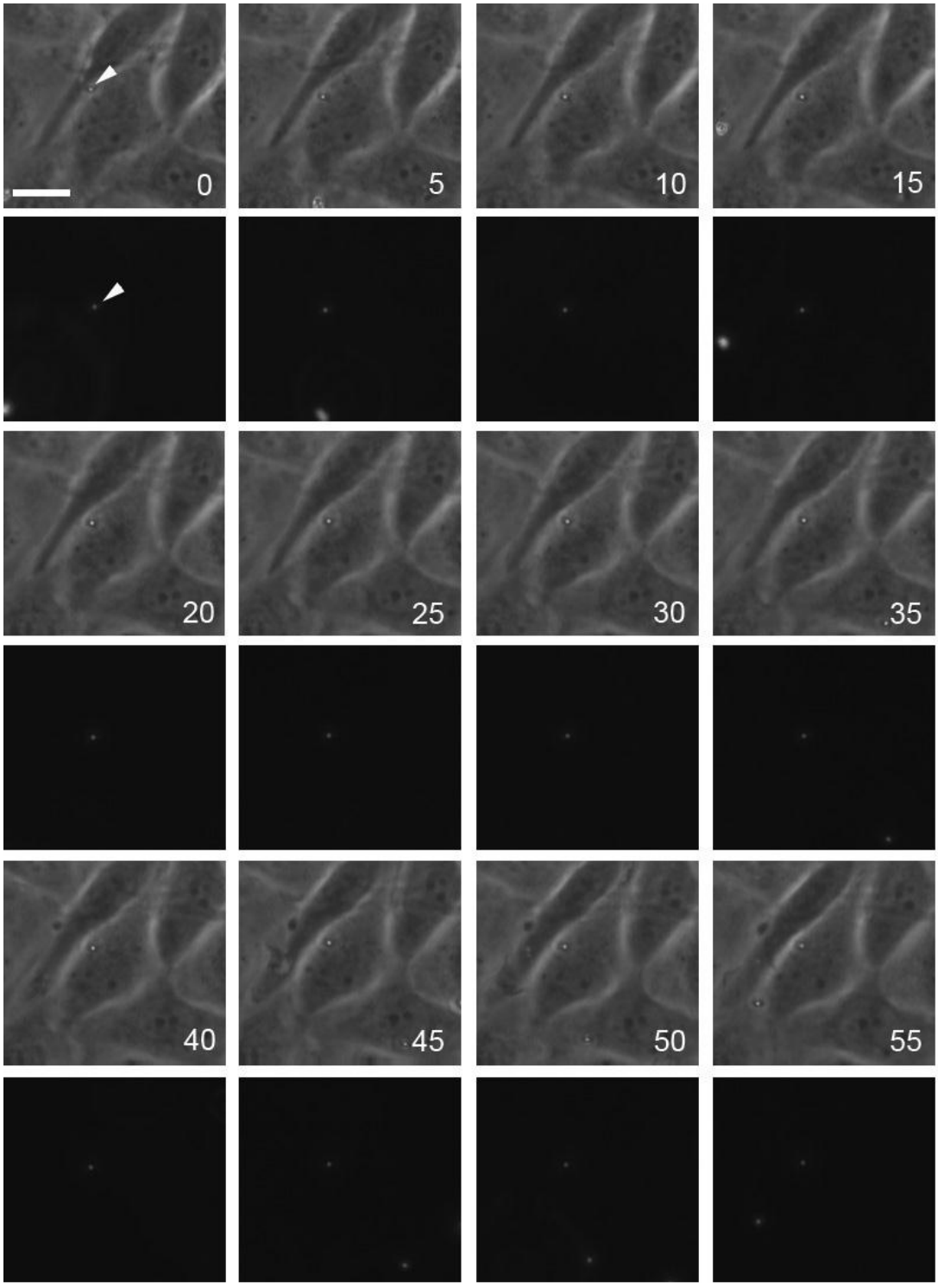

Figure 3.3 A single anti-ICAM-1-coated bead is insufficient in inducing EC activation

As described in Figure 3.2 with a single immobilised bead as indicated by arrows (Scale bar: 10µm)

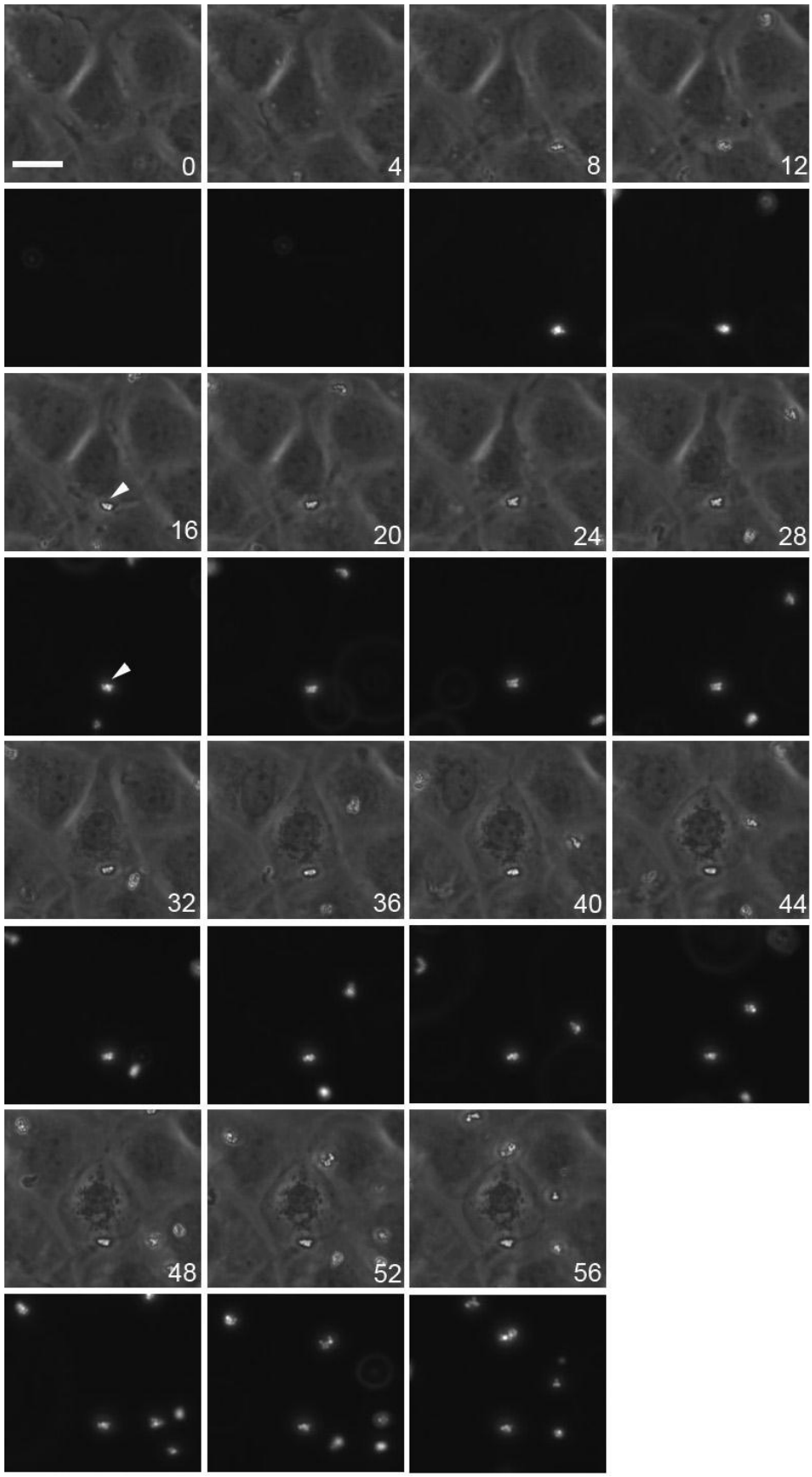
0
4
8
12
16
20
24
28
32
36
40
44
48
52
56

Figure 3.4 EC are activated following adhesion and immobilisation of an anti-ICAM-1 bead cluster on the endothelial surface

Experiment was carried out as described for Figure 3.2. The adherent cluster of anti-ICAM-1-coated beads is indicated by the arrow from the time of immobilisation. In preceding frames the beads were still moving on the EC surface (see Figure 3.5). (Scale bar: 10µm)

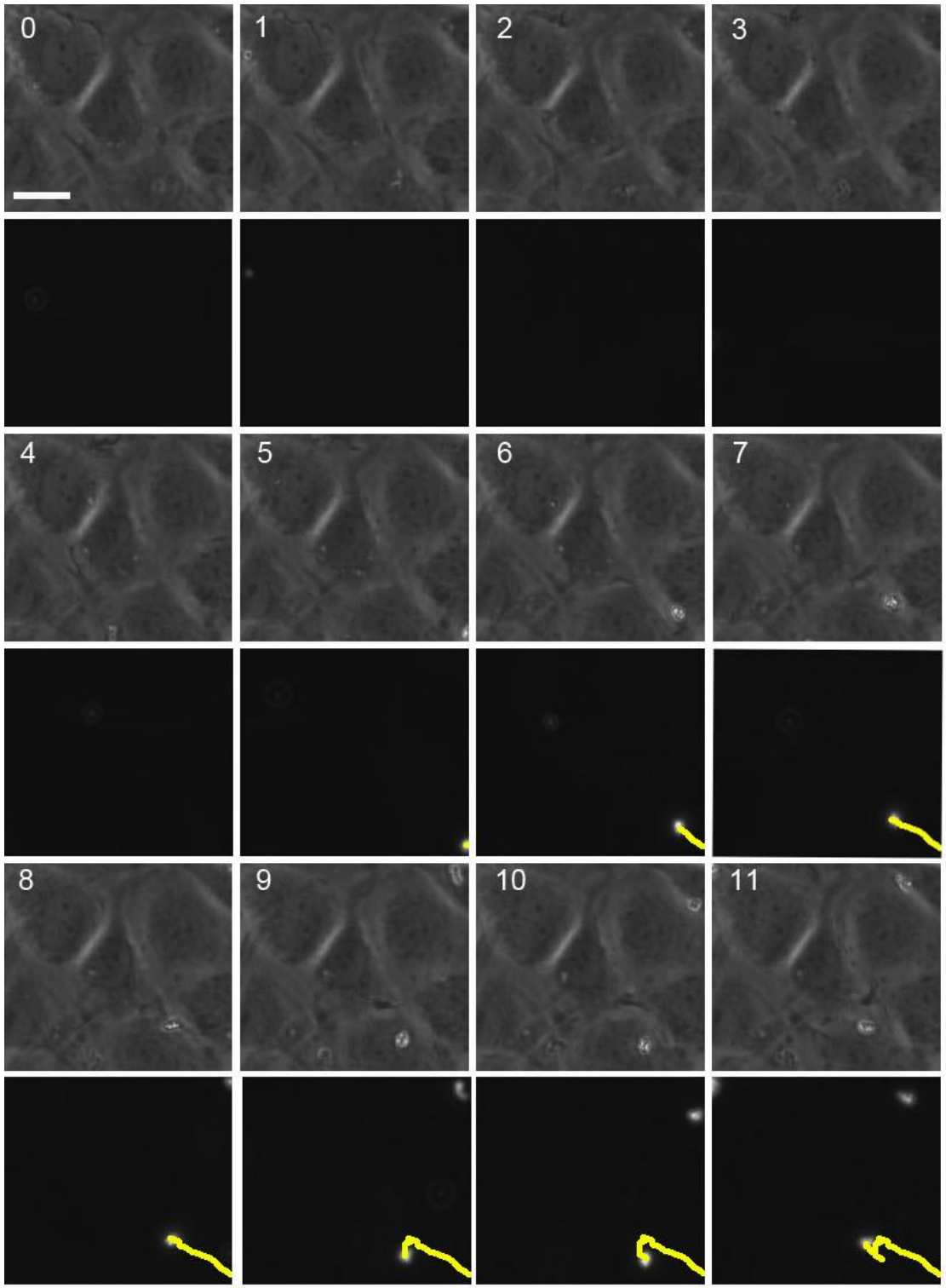
0
1
2
3
4
5
6
7
8
9
10
11

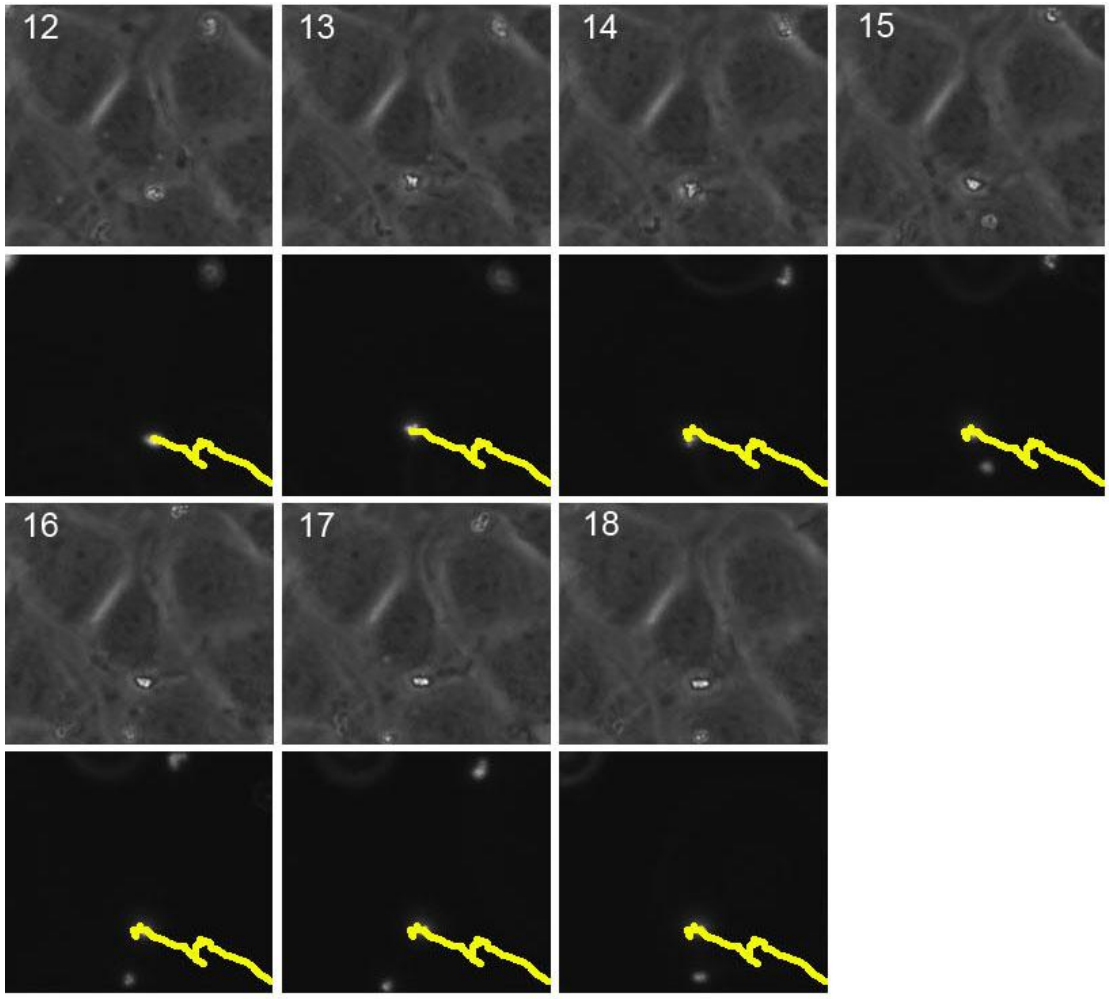

Figure 3.5 Lateralisation of beads to the cellular junctions

Experiment was carried out as described for Figure 3.2. The movement of the anti-ICAM-1-coated bead on the EC surface was tracked (yellow line) every min until the bead was recruited and immobilised. (Scale bar: 10µm)

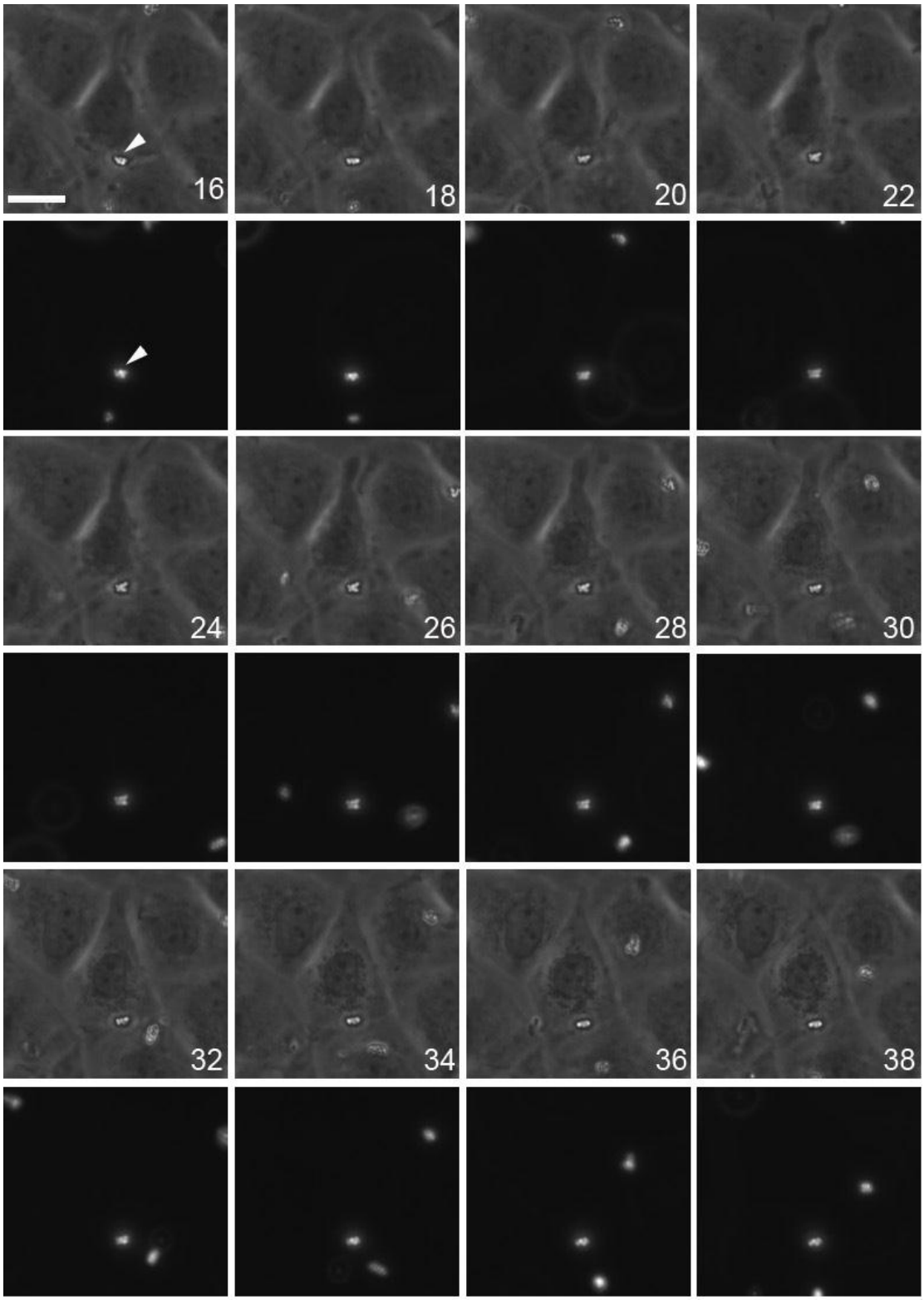
16
18
20
22
24
26
28
30
32
34
36
38

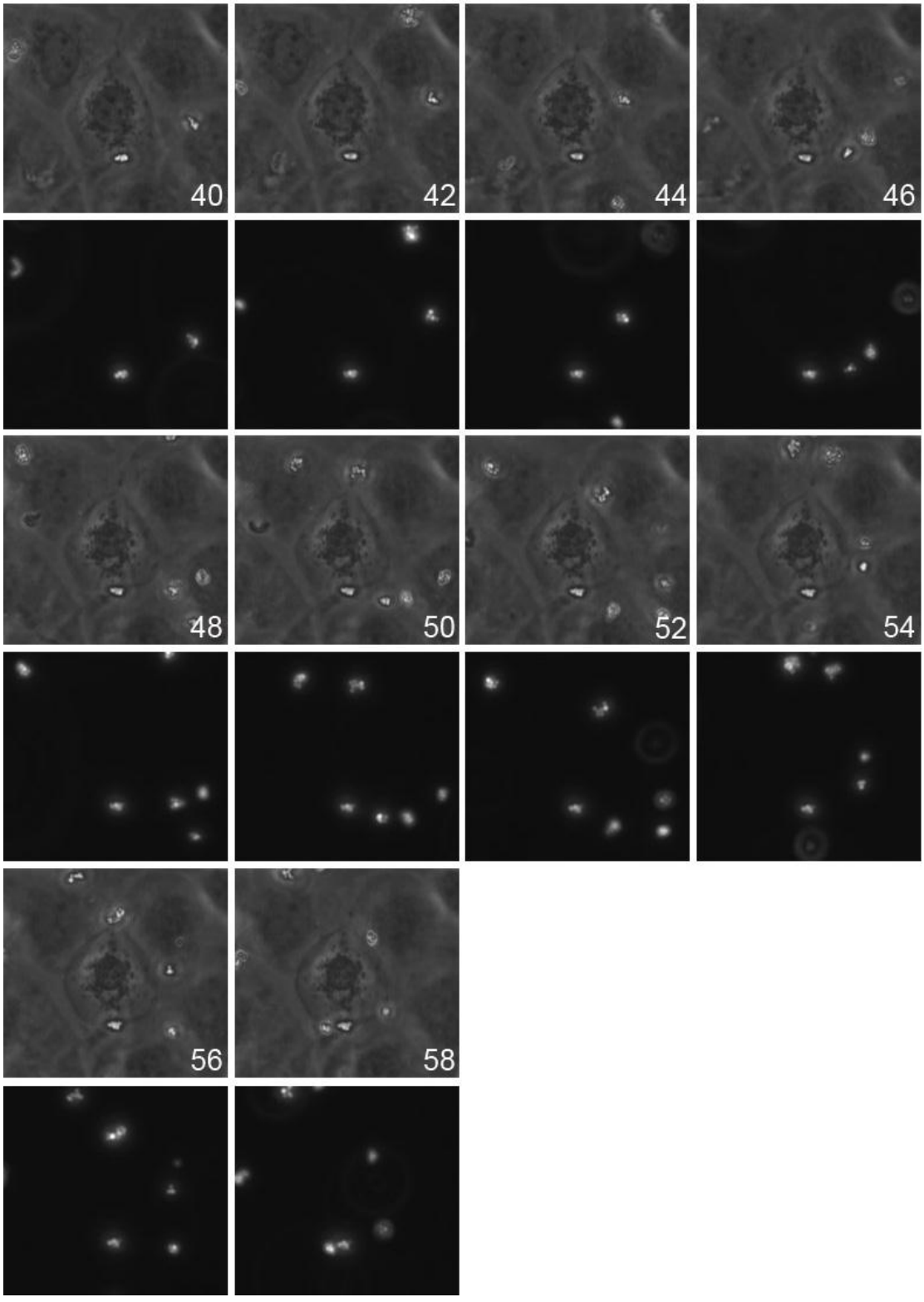

Figure 3.6 Activation of EC in response to immobilisation of anti-ICAM-1-coated beads on the endothelial surface

Figure 3.6 figure legends

The images shown are as described in Figure 3.4 with the exception that the image is every 2 min and shows only the activation period following immobilisation of the bead to the EC lateral junction (as indicated by the arrow). Clear morphological changes within the EC can be observed including membrane ruffling, increase in EC size and changes to the nucleus. (Scale bar: 10µm)

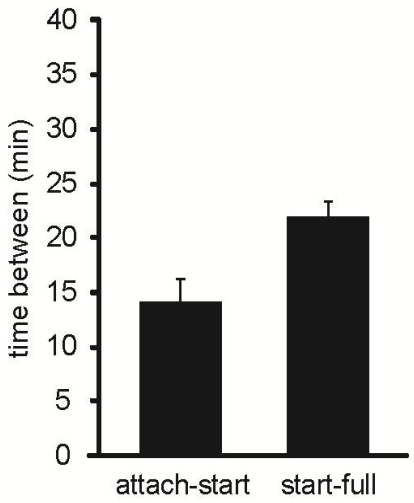

Figure 3.7 Immobilisation of anti-ICAM-1-coated beads to the EC surface leads to delayed EC activation

Experiments were carried out as described in Figure 3.2. All immobilised bead clusters leading to EC activation were analysed from 3 independent experiments (4 fields/experiment). Times were taken at bead immobilisation ('attach'), start of cytologically visible cell activation ('start') and full cell activation ('full') when cell expansion and nuclear shrinkage appeared maximal. 13 bead clusters were analysed for both attach-start and start-full. Shown are mean time intervals +/- SEM in min.

3.4 Discussion

Lymphocytes upon adhesion are directed to sites of transmigration, including tri-cellular junctions which are preferential sites used by leukocytes to cross into the underlying tissue (Burns et al., 1997). Previous work using anti-ICAM-1-coated beads shows that the EC responds and induces signalling cascades in response to CAM engagement on the cell surface (Allingham et al., 2007; van Buul et al., 2007b).

Lateralisation of antibody-coated beads to cellular junctions (Figure 3.1 and 3.5) occurs in agreement with antibody ligation cross-linking studies (Turowski et al., 2008) and with observations of preferential sites of TEM (Burns et al., 1997). Lateral localisation and clustering of the beads increases in a time-dependent manner. These observed results could be explained in two ways, either the antibody-coated beads could attach anywhere on the EC and then laterally be moved to the cellular junctions (lateralisation) or the beads direct attach to lateral areas of the EC. The latter idea is unlikely since the distribution of ICAM-1 on resting EC is ubiquitous across the entire luminal membrane (Figure 1.3 and Turowski et al., 2008) and as Figure 3.5 shows there is lateral movement of beads following attachment to the endothelium.

To fully elucidate and understand the movement of beads towards lateral EC areas and the clustering of beads, high resolution time-lapsed microscopy is required followed by bead tracking. As we are unable to predict where firm adhesion will occur in the approach used so far, large regions of interest (ROIs) are required to be imaged which are incompatible with high resolution microscopy. A potential way to resolve this issue may be to alter the bead concentration used or to record higher numbers of ROIs in neighbouring regions Therefore, optimisation of the microscope settings and protocol is needed to easily visualise the beads recruitment to the cell junctions.

Nevertheless, the observed results seem to imply that the EC is actively involved in lateralisation of beads. The EC activity is important for either moving the antibody-coated beads to the cellular junction regions of the cell or allows attachment only in these lateral areas.

ICAM-1 antibody-coated beads were found to form clusters and aggregates in a time-dependent manner (Figure 3.1), which is in agreement to ICAM-1 cross-linking studies (Martinelli et al., 2009). The EC is actively involved in inducing increased surface membrane area for the

adhesion of the anti-ICAM-1-coated beads. Cholesterol rich regions, also referred to as rafts, could be regions of the EC that are involved in the adhesion of anti-ICAM-1-coated beads (Dodelet-Devillers et al., 2009).

I observed noticeable EC activation in the model system used (Figure 3.4 and 3.6) and to my knowledge this is the first report of visual EC activation following ICAM-1 engagement. Previous experiments in the laboratory using soluble anti-ICAM-1 antibodies failed to visualise any such activation of GPNT (R. Martinelli and P. Turowski, unpublished observations).

EC activation following ICAM-1 engagement led to changes within the EC including increased EC size, the nucleus becoming more defined in structure and a vesicular appearance around the nucleus (Figure 3.6). The most pronounced morphological change is the induction of luminal membrane ruffles in response to bead adhesion. Cortical actin and Rac has been implicated in the induction of membrane ruffling and subsequent signalling that is initiated (Ridley, 1994). Rac activity has not yet been described downstream of ICAM-1. Leukocyte migration has been shown to require the activity of Rac (Gismondi et al., 2003) but this role has been attributed to VCAM-1 signalling (van Wetering et al., 2003). Interestingly our laboratory has recently found that ICAM-1 ligation and cross-linking led to activated Rac in a reciprocal manner to Rho activation (R. Martinelli and P. Turowski, unpublished observations). Future studies could focus on ICAM-1-induced Rac-mediated signalling during TEM, which could constitute a completely new and yet unexplored mechanism.

The data all seems to imply that the time frame of EC activation occurs within 15 to 35 min (Figure 3.7) although this needs to be verified by other means. It has been described in this study that the start of activation is when visible changes are seen such as membrane ruffling (Figure 3.4 and 3.6); however this could be in fact later than the actual activation start. It is highly possible that cell activation started immediately after beads adhesion but was not accompanied by microscopically visible changes. I did not look at recruitment of the antibody-coated beads to the tri-cellular regions in the video images. This could be of interest as around a third of beads that lateralise to EC junctions are found to accumulate at tri-cellular junctions (Figure 3.1B). More detailed analysis of bead recruitment could also determine if there are differences in recruitment of larger clusters in comparison to smaller clusters or single beads by the EC. The time frame of 1 h seems to be relevant for further investigation as beads were shown to adhere, lateralise, and

aggregate along with visible EC activation within this time frame. Therefore, future studies investigating ICAM-1-mediated signalling will focus at times frame between 0 and 60 min.

Anti-ICAM-1-coated beads mimic the adhesion of lymphocytes to the EC and hence it is reasonable to assume a similar response would be initiated upon lymphocyte adhesion to ECs. An advantage of using anti-ICAM-1-coated beads to lymphocytes means ICAM-1-mediated signalling can be specifically investigated rather than signalling induced by the interaction of the lymphocyte with other CAMs, including selectins and PECAM-1, on the EC surface. Therefore, antibody-coated beads are an appropriate way to study ICAM-1 signalling rather than classical methods of antibody ligation and cross-linking methods. Antibody-coated beads should certainly be used for many future studies. However, the use of antibodies in solution has the obvious advantage of inducing ICAM-1 activation more rapidly, thus producing crisper biochemical responses.

Chapter 4: PKC isoforms expression in BMVECs

4.1 Introduction

PKC is a family of serine/threonine kinases belonging to the AGC family, which represents two percent of the human kinome (Parker and Murray-Rust, 2004; Carmena and Sardini, 2007; Pearce et al., 2010; Rosse et al., 2010). Other AGC family members include PKA and cGMP-dependent protein kinase (PKG) (Pearce et al., 2010). PKC was originally identified by Nishizuka and colleagues in 1977 (Tan and Parker, 2003). PKC is found in all eukaryotes and has been found to have different functions in different cell types. Amongst other functions PKC has been shown to be involved in cell differentiation, cell proliferation, apoptosis, cell migration and cytoskeletal remodelling in response to different a wide variety of stimuli (reviewed in: Tan and Parker, 2003; Martelli et al., 2006).

There are 10 isoforms of PKC which have been classified into three classes depending on their activation mode and substrate preference, all of which is a result of differences in their primary structure (Figure 4.1) (reviewed by: Parker and Murray-Rust, 2004; Carmena and Sardini, 2007). The classical PKC (cPKC) isoforms, PKC alpha (α), beta (β) and gamma (γ) are activated by both diacylglycerol (DAG) and Ca^{2+} due to the presence of C1 and C2 domains that bind DAG and Ca^{2+}, respectively. PKCβ exists as two splice variants differing in their C-terminus (Kawakami et al., 2002). The novel PKCs (nPKC), delta (δ), epsilon (ε), eta (η) and theta (θ) lack a proper Ca^{2+} binding domain and are therefore Ca^{2+}-insensitive whilst still retaining the capability of binding DAG. PKC zeta (ζ) and PKC iota (ι) are atypical PKC (aPKC) family members that are both Ca^{2+}- and DAG-insensitive which reflects the absence of a C2 domain and the presence of a C1 domain incapable of DAG binding. Instead aPKCs are thought to be primarily regulated by protein-protein interactions in the N-terminal Phox and Bem 1p (PB1) domain (Parker and Murray-Rust, 2004; Corbalan-Garcia and Gomez-Fernandez, 2006; Sun and Alkon, 2009). Lastly, PKCμ/PKD contains a putative transmembrane domain and a pleckstrin homology (PH) domain and may be permanently anchored in the cell membrane (Rykx et al., 2003).

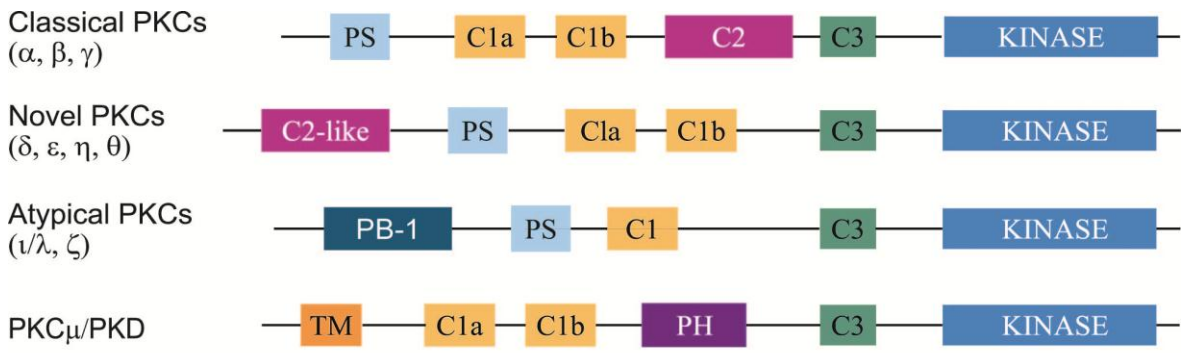

C1: DAG/ Phorbol ester binding domain

C2: Calcium binding domain

C3: ATP binding domain

Kinase (C4): substrate binding domain

PS: Pseudosubstrate domain

PH: Plekstrin homology domain

TM: Transmembrane domain

PB-1: phox and Bem 1p

Figure 4.1 PKC structure for the different family members

Inactive PKC is mostly cytoplasmic. Upon activation PKC translocates to various membrane compartments, such as the plasma membrane (Carmena and Sardini, 2007). Phosphorylation of particular residues in PKC ultimately controls the function and alters both its activity and location (Roffey et al., 2009). Most PKCs are catalytically inactive due to being in a conformation where the pseudosubstrate domain sits within the substrate binding domain (Tan and Parker, 2003). A conformational change in the structure of PKC is required to lead to its activation (Pearce et al., 2010). For cPKC and nPKC activation translocation to the plasma membrane is usually required where they allosterically bind DAG. Phosphoinositide-dependent kinase-1 (PDK1) phosphorylates the activation segment of PKC which triggers autophosphorylation on two further sites, the hydrophobic motif and turn motif (Carmena and Sardini, 2007; Pearce et al., 2010). The phosphorylation of the turn motif does not aid activation but helps to stabilise the active conformation of PKC and thus duration of activation (Carmena and Sardini, 2007). Evidence suggests that mammalian target of rapamycin complex 2 (mTORC2) is responsible for the phosphorylation of the hydrophobic motif (Parekh et al., 2000).

PKCs have also been shown to bind to molecular scaffolds named receptors for activated C kinase (RACKs) which bind to a region distinct from the substrate binding domain (Mochly-Rosen et al., 1991). RACKs are membrane associated anchoring proteins influencing the localisation of particular isoforms to distinct microdomains (Steinberg, 2008).

Although PKC isoform expression is mostly ubiquitous it can be restricted to certain tissues (as shown in Table 4.1). For example PKCθ is expressed only in skeletal muscle and T-lymphocytes (Altman and Villalba, 2003) whilst PKCγ is found predominantly in neuronal tissue (Martiny-Baron and Fabbro, 2007).

Soon after its discovery PKC had been shown to be an important regulator of tumourigenesis since phorbol esters, such as PMA, have been shown to induce tumours through PKC activation (Griner and Kazanietz, 2007). Furthermore, mutations in all isoforms have all been shown to occur in various tumours potentially acting as tumour promoters, leading to the enhancement of signalling pathways (Martiny-Baron and Fabbro, 2007). Thus, PKC is a much-studied target for therapeutic intervention. Its various functions are thought to be mediated by different isoforms and consequently many isoform-specific PKC inhibitors are sought and developed. Apart from roles in tumourigenesis, PKCα, $PKC\beta_I$, $PKC\beta_{II}$ and PKCδ have been shown to be chronically activated in response to hyperglycaemia caused by increased DAG concentrations (Geraldes and King, 2010).

Table 4.1: Tissue Expression of PKC isoforms		
Isoform	Expression	Reference
PKCα	Ubiquitous (including brain, pineal gland, retina and spleen)	Yoshida et al., 1988; Nakashima, 2002; Tan and Parker, 2003
PKCβ	Brain, pituitary and pineal gland, spleen, thymus, lung, intestine, pancreatic islets, human leukocytes, retina	Yoshida et al., 1988; Way et al., 2000; Tan and Parker, 2003; Lang, 2007; Martiny-Baron and Fabbro, 2007
PKCγ	Restricted mainly to CNS and spinal cord, specifically expressed in neuronal cells	Yoshida et al., 1988; Way et al., 2000; Shirai and Saito, 2002; Martiny-Baron and Fabbro, 2007; Verbeek et al., 2008
PKCδ	Ubiquitous, widely distributed among cells and tissues	Kikkawa et al., 2002; Tan and Parker, 2003
PKCε	Ubiquitous	Tan and Parker, 2003
PKCη	Highly expressed in lung and skin, slightly in brain, heart, spleen Predominantly expressed in epithelial tissue	Osada et al., 1990; Suzuki et al., 2009
PKCθ	Skeletal muscle and T-lymphocytes	Way et al., 2000; Tan and Parker, 2003; Altman and Villalba, 2003; Praveen et al., 2009; Rosse et al., 2010
PKCι	Ubiquitous- widely distributed	Fields and Regala, 2007
PKCζ	Ubiquitous	Tan and Parker, 2003
PKCμ	Ubiquitous	Johannes et al., 1994

This can lead to both micro- and macrovascular complications in diabetes. For instance, the role of endothelial PKCβ in diabetic retinopathy has been recognised and selective inhibitors of this kinase isoform are currently being tested (Lang, 2007). Ruboxistaurin, one such PKCβ inhibitor, has shown significant improvements for diabetic non-proliferative retinopathy and endothelial dysfunction (Meier and King, 2000; Geraldes and King, 2010). Ruboxistaurin has also been shown to inhibit glucose-induced adhesion of monocytes to EC (Kunt et al., 2007).

PKCs have been shown to mediate many diverse endothelial functions. PKCα appears to function in EC contraction and disassembly of VEC junctions along with having a role in the interaction and adhesion of leukocytes to the endothelium (Konopatskaya and Poole, 2010). The promotion of endothelial permeability is partly mediated by PKCα and PKCβ (Kumar et al., 2009). PKCα or PKCζ play a role in increasing endothelial permeability, in response to MCP-1 interaction with CCR2 or thrombin, leading to stress fibre formation and TJ protein redistribution (Stamatovic et al., 2006; Minshall et al., 2010).

A number of publications have shown that PKC activity is important during the establishment of cell-cell contacts. In the pituitary gland, stimulation with thyrotropin releasing hormone (TRH) or the PKC activating phorbol ester 12-O-tetradecanoylphorbol-13-acetate (TPA/PMA) regulates cell-cell contacts and AJ formation. This process is tightly regulated by a spatiotemporally coordinated cascade of PKC activation and translocation (Quittau-Prevostel et al., 2004; Collazos et al., 2006). Similar spatio-temporal co-ordinated PKC activation cascades have also been observed when cell-cell contacts form between different cell types. For instance, during the loose interaction of human fibroblast and cancer epithelial cells, PKCα and PKCε are recruited to the cell-cell contact region and again PKCδ does not show a significant relocalisation (Louis et al., 2005).

PKCθ also shows selective recruitment to cell-cell contacts. It is found to be recruited to the central supramolecular activation cluster (cSMAC) of the immunological synapse (IS) (Altman and Villalba, 2003; Yokosuka et al., 2008; Praveen et al., 2009). PKCθ regulates recognition of APC by T-lymphocytes due to a number of cell-cell interactions forming between the two cells helping to integrate the signals of the T-cell receptor (TCR)/CD28 which activates the T-lymphocytes (Rosse et al., 2010).

Importantly for this study, Etienne-Manneville and colleagues have shown that ubiquitous PKC inhibition in BMVEC significantly inhibited lymphocyte transmigration, suggesting that one or

several endothelial PKC isoforms are involved in ICAM-1-mediated TEM (Etienne-Manneville et al., 2000). Other studies have implicated PKCα in VCAM-1-mediated (inflammatory) lymphocyte migration (Deem et al., 2007) or PKCδ in neutrophil migration (Carpenter and Alexander, 2008), suggesting that endothelial PKC regulation of TEM is not only a prerogative of BMVEC.

4.2 Aim

Endothelial PKC constitute a key intracellular regulator which has been shown to play an important role during TEM. However, it is unknown which PKC isoforms are expressed in ECs. I therefore aim at establishing the expression profile of PKC isoforms in the GPNT and hCMEC/D3 cell lines. In addition, I aim to establish assays to test PKC isoform activation in EC.

4.3 Results

4.3.1 mRNA expression of PKC isoforms in BMVECs

To determine expression of PKC isoforms in BMVECs I first looked for their presence on mRNA level in the GPNT cell line. Primers were designed that were specific to each isoform of *Rattus norvegius* PKC. Transcript sequences were taken from NCBI database sets. If transcripts were not found predicted transcript sequences based on genomic sequence data were used (as described in Section 2.2.16.3). Forward and reverse primers were designed to span at least one intron/exon boundary to avoid genomic DNA being amplified (Appendix 10.1 and 10.2). I also used DNAse treated RNA and performed RT-PCR using oligo(dT). Analysis for PKCη has not yet been completed since no annotated appropriate sequence was initially found in public databases. Recently a transcript/genomic sequence NM_031085 was identified which is likely to represent rat PKCη as it showed high sequence identity with rat PKCδ, PKCε and PKCθ, 50%, 59% and 47% respectively, (Appendix 10.2). However, so far RT-PCR analysis based on NM_031085 have proven unsuccessful.

RT-PCR analysis of GPNT mRNA produced DNA fragments of the expected size for PKCα, PKCβ, PKCγ, PKCε and PKCθ (Figure 4.2A and Table 4.2). The fragments detected for PKCμ, PKCζ and PKCι were smaller than expected. PKCβ and PKCζ did produce additional DNA fragments suggesting that RT-PCR was not specific for these isoforms. A fragment of the expected size for PKCδ was only detected following nested PCR (Figure 4.2B).

The identity of PCR products was further verified by either restriction enzyme digest analysis (Figure 4.3) or sequence analysis (Figure 4.4). Restriction enzymes were chosen that were predicted to cut the expected product once and produce fragments of different noticeable sizes. Restriction enzyme analysis corroborated the identity of fragments for PKCα (Figure 4.3 and Table 4.3). The reaction for PKCε partially worked as at least one of the observed bands corresponded to that expected whilst the small observed fragment was slightly larger than expected. Digest products for PKCζ and PKCι varied by between 30 and 50 base pairs from those anticipated. Full-length PKCζ product could be seen alongside the digest fragments with the strongest band corresponding to the input material (as detected in Figure 4.2A). Thus, completely different size bands were produced although it could be considered that these bands closely resembled those expected following restriction digest analysis.

For all other PKC isoforms the predicted bands did not match those that were observed (Figure 4.3 and Table 4.3). Restriction enzyme digest analysis for PKCβ, PKCγ and PKCμ did not appear to work at all. Only the full-length PKCγ was observed suggesting that the restriction enzyme (*Ava*II) did not cut the fragment. For PKCβ the digest was unsuccessful as a band corresponding to the entire fragment (as seen in Figure 4.2A) was seen along with a second band of around 280 base pairs which was entirely unexpected. Only one digest fragment for PKCμ was identified which appears to be more compatible to the full-length product rather than that of the expected digest fragments implying that the reaction was inefficient. To this end, PKCδ was not included in any further analyses as results have been unreliable and PCR did not always produce an amplification product.

To find evidence of a transcript for PKCθ was unexpected since it has previously been reported to be only present in skeletal muscle and T-lymphocytes (Altman and Villalba, 2003). To verify that this fragment was indeed PKCθ, sequencing was carried out. The sequence of the putative PKCθ fragment was identical to the corresponding region of rat PKCθ in the NCBI databank (Figure 4.4), confirming that PKCθ was also expressed in GPNT ECs.

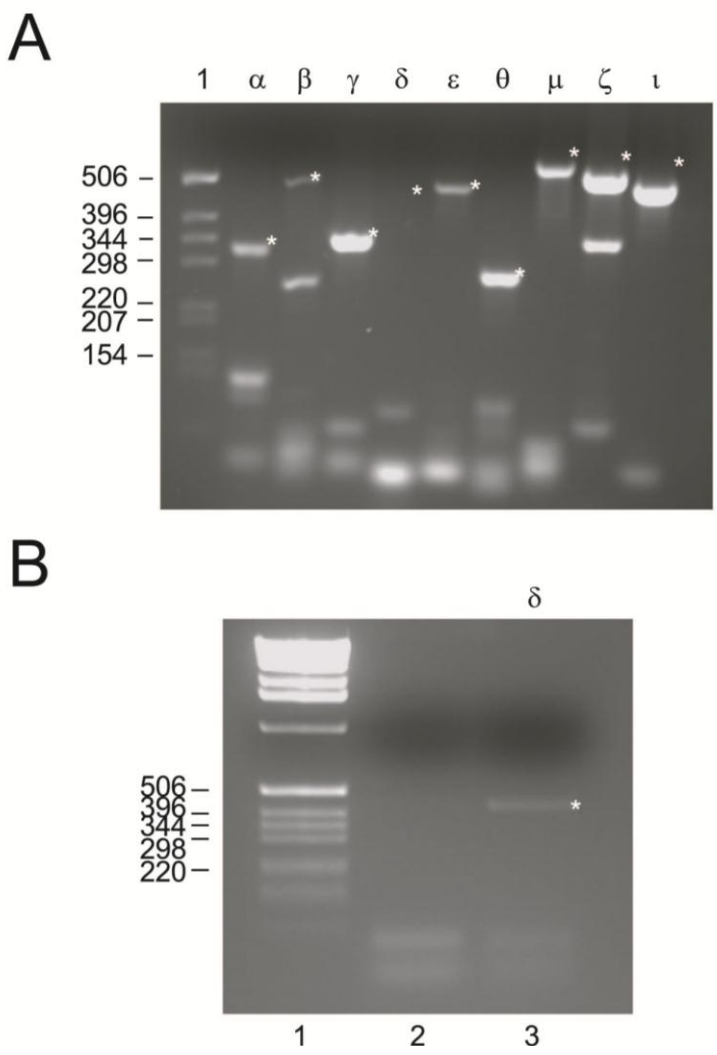

Figure 4.2 RT-PCR analysis of PKC isoform expression in rat GPNT EC

(A) RT-PCR analysis was performed using RNA isolated from GPNT and the primers specified in Chapter 2. PCR reactions were analysed by agarose gel electrophoresis. The size (in base pairs) of the fragments of the ladder run in lane 1 is indicated on the left. The asterisks indicate the relative migration position of the expected PCR product.

(B) As in (A), except that nested PCR was performed to detect PKCδ. Lane 1: sizing ladder (fragment size in base pairs indicated on the left), lane 2: RT-PCR using primer pair 1, lane 3: RT-PCR using primer pair 1 and the nested pair 2. The asterisk indicates the size of the predicted PKCδ amplification product.

Table 4.2: Amplified PKC product and verification method

Isoform	Expected fragment size (base pairs)	Observed fragment size (base pairs)	Verification
PKCα	333	333	Restriction enzyme (*Bg1*II)
PKCβ	512	506, 260	Restriction enzyme (*Eco*R1)
PKCγ	350	350	Restriction enzyme (*Ava*II)
PKCδ	427*	427	Nested PCR/ Restriction enzyme (*Sac*I)
PKCε	497	497	Restriction enzyme (*Eco*RI)
PKCθ	292*	292	Sequencing
PKCη	N/A	N/A	RT-PCR has not produced a product
PKCμ	563	515	Restriction enzyme (*Pst*1)
PKCζ	554	506, 344	Restriction enzyme (*Ava*II)
PKCι	537	497	Restriction enzyme (*Pst*I)

*nested PCR

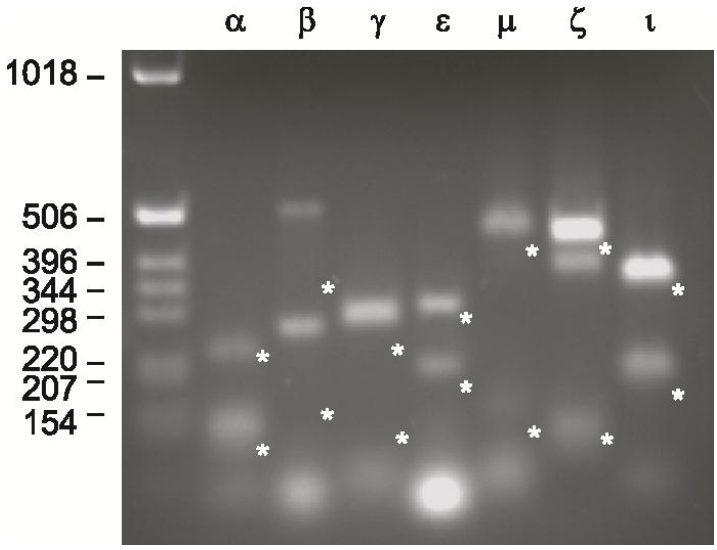

Figure 4.3 Restriction enzyme analysis of RT-PCR fragments

Restriction enzyme analysis of putative PKC fragments shown in Figure 4.2A. The asterisks indicate the relative migration position of the expected fragments after restriction enzyme digest.

Table 4.3: Restriction enzyme digest verification		
Isoform	Expected fragment size (base pair)	Observed fragment size (base pair)
PKCα	228, 105	228, 105
PKCβ	358, 158	506, 280
PKCγ	230, 138	320
PKCε	298, 199	298, 220
PKCμ	420, 143	506
PKCζ	435, 119	506, 400, 150
PKCι	348, 190	400, 228

A

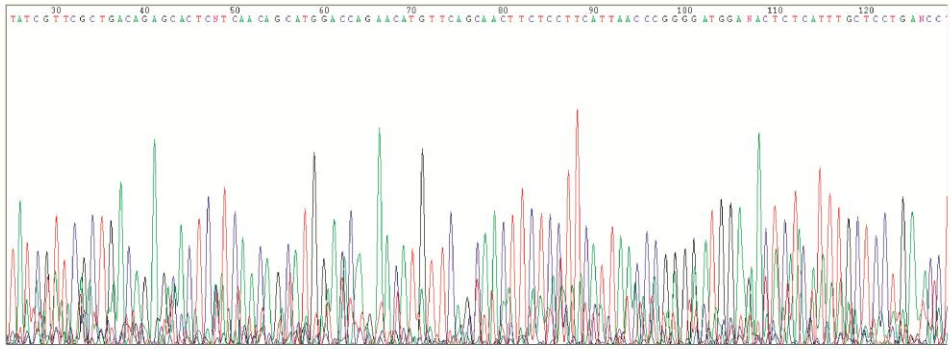

B

ref|XM_341553.4| PREDICTED: Rattus norvegicus protein kinase C, theta, transcript variant 2 (Prkcq), mRNA
Length=2124

GENE ID: 85420 Prkcq | protein kinase C, theta [Rattus norvegicus] (Over 10 PubMed links)

Score = 180 bits (97), Expect = 6e-44
Identities = 99/101 (99%), Gaps = 0/101 (0%)
Strand=Plus/Plus

```
Query  25    TATCGTTCGCTGACAGAGCACTCNTCAACAGCATGGACCAGAACATGTTCAGCAACTTCT  84
             ||||||||||||||||||||||| ||||||||||||||||||||||||||||||||||||
Sbjct  2024  TATCGTTCGCTGACAGAGCACTCATCAACAGCATGGACCAGAACATGTTCAGCAACTTCT  208


Query  85    CCTTCATTAACCCGGGGATGGANACTCTCATTTGCTCCTGA  125
             ||||||||||||||||||||| ||||||||||||||||||
Sbjct  2084  CCTTCATTAACCCGGGGATGGAGACTCTCATTTGCTCCTGA  2124
```

Figure 4.4 Sequencing analysis of the putative PKCθ fragment

(A) The putative PKCθ fragment amplified by RT-PCR (shown in Figure 4.2) was sub-cloned and subjected to DNA sequencing as detailed in Chapter 2. Shown is part of the sequence trace as analysed by Chromaslite.

(B) Sequence data from (A) was used to interrogate the NCBI database using the BLAST algorithm. Shown is a sequence alignment of our amplified fragment with rat PKCθ.

4.3.2 Protein expression of PKC isoforms in BMVECs

Next, I analysed the presence of PKC protein isoforms in GPNT cell lysates by immunoblotting. I had assembled a collection of PKC antibodies with demonstrated specificity to the respective isoforms (detailed in Chapter 2).

Extracts of proliferating GPNT ECs were subjected to SDS-PAGE and western blotting using all PKC isoform antibodies available within the laboratory. As documented in Figure 4.5 and Table 4.4 I observed bands of the predicted molecular weight for all PKC isoforms, apart from PKCγ, in GPNT extracts. Most of the antibodies produced a single clear band with the exception of the antibody against PKCη and PKCβ_I. PKCη in addition to the expected band also immunodecorated a band at ca. 70 kDa, possibly a degradation product. The antibody specific for PKCβ_I detected a strong band at the predicted molecular weight although a number of seemingly unspecific bands were also detected. A monoclonal antibody directed against a shared epitope of PKCζ and PKCι detected several bands, some of which were clearly unspecific. Nevertheless, three bands corresponded to the two forms of PKCι, which exists as a short and long form, and PKCζ. However, only the long form of PKCι was detected with an alternative antibody.

To validate the results seen in the GPNT cell line, expression of PKC isoforms in the human BMVEC cell line CMEC/D3 was also investigated. As shown in Figure 4.6 and Table 4.4 the majority of PKC isoforms was clearly detected. Antibodies against PKCα, PKCβ_I, PKCδ, PKCε, PKCθ and PKCι produced a single or predominant band(s) at the expected size(s). Blots for PKCβ_{II}, PKCγ and PKCμ showed many background bands. Nevertheless, a strong band at the expected size was detected for PKCμ. Due to numerous bands being immunodecorated for PKCβ_{II} and PKCγ it was difficult to confirm expression unambiguously. Similar to the results using GPNT, antibodies against PKCη and PKCζ/ι detected additional proteins which may represent shorter or degraded proteins. Unlike in GPNTs the antibody against PKCι detected two bands corresponding to the short and long form suggesting that short

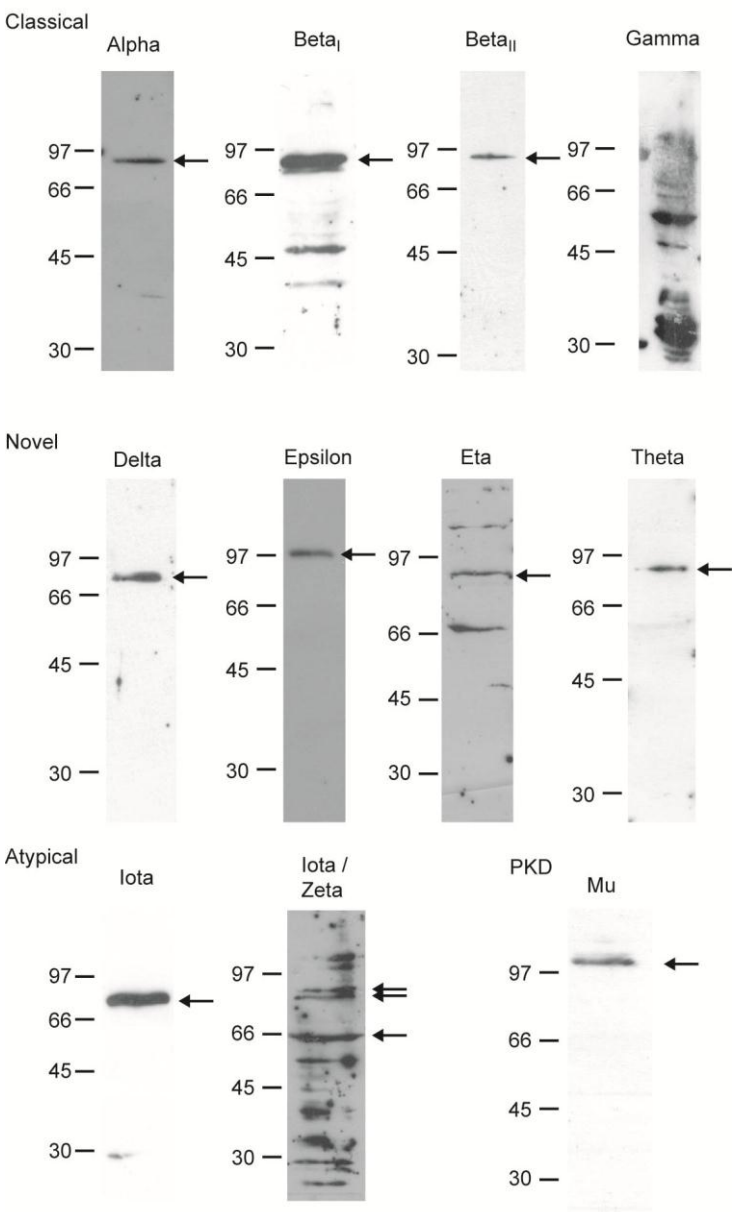

Figure 4.5 Expression of PKC protein isoforms in GPNT

Proliferating rat GPNT were lysed and subjected to SDS-PAGE, western blotting and immunodetection using anti-PKC antibodies specific to the isoforms indicated. Shown on the left of each immunoblot are the relative molecular mass (in kDa) of marker proteins run in parallel. Arrows indicate bands that match the predicted weight (as specified in Table 4.4) of the PKC in question.

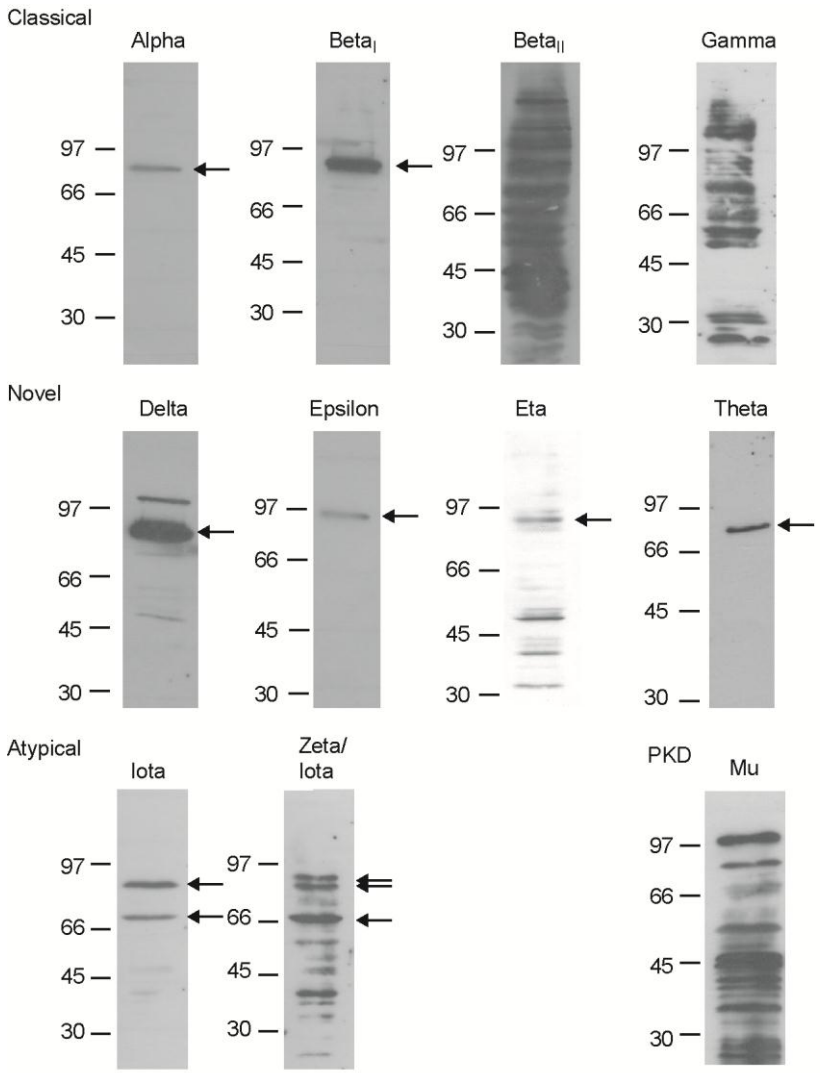

Figure 4.6 Expression of PKC protein isoforms in hCMEC/D3

Proliferating hCMEC/D3 were lysed and subjected to SDS-PAGE, western blotting and immunodetection using anti-PKC antibodies specific to the isoforms indicated. Shown on the left of each immunoblot are the relative molecular masses (in kDa) of marker proteins run in parallel. Arrows indicate bands that match the predicted weight (as specified in Table 4.4) of the PKC in question.

Table 4.4: Protein expression verification

Isoform	Predicted molecular weight (kDa)	Observed molecular weight (kDa)	
		GPNT	hCMEC/D3
PKCα	80	81	78
$PKC\beta_I$	79	84	88
$PKC\beta_{II}$	79	84	N/D
PKCγ	82	N/D	N/D
PKCδ	78	79	80
PKCε	82	87	88
PKCη	82	86	88
PKCθ	82	83	82
PKCι	65 (short) 74 (long)	63 78/ 80	74/72 85/87
PKCζ	86	83	89
PKCμ	115	95	94

(Underlined values are the relative migration rates for the PKCι antibody, N/D- not determined)

PKCι was expressed in human but not rat BMVEC. These two bands appeared to be at the same molecular weight as two observed using the PKCζ/ι antibody demonstrating that this antibody could distinguish between PKCι and PKCζ.

As illustrated in Table 4.4 there were also very little noticeable differences in the predicted and observed molecular weight as well as between the two cell lines. This is most probably due to inaccuracies that can occur when SDS-PAGE is performed on minigels (with total migration distances of ca. 6cm). A great difference between the predicted and observed molecular weight was observed for PKCμ in both cell lines. In fact, at ca. 95 kDa, the observed bands were significantly smaller than the predicted 115kDa. Degradation may have occurred during lysis. Alternatively, PKCμ may retain some folding during SDS-PAGE and thus appear smaller than predicted.

4.3.3 Translocation of PKC isoforms in response to cytokine, phorbol ester or antibody stimulation

It has been well documented that PKC activation coincides with its translocation to different membrane compartments of the cell (Quittau-Prevostel et al., 2004; Collazos et al., 2006). Thus translocation can be used to measure activation of PKC isoforms in response to a specific stimulus. To determine whether this method could be used in our cell systems I analysed PKC translocation following stimulation with classical PKC activators, namely the phorbol ester PMA and TNF-α, as well as with, more specifically to our research question, anti-ICAM-1 antibody 1A29.

Initially, I analysed PKC translocation by immunocytochemistry and fluorescent microscopy. All available antibodies were tested in GPNT. Good signals were obtained using the antibodies against PKCγ, PKCι and PKCζ/ι (Figure 4.7). All other isoform-specific antibodies failed to produce good signals (data not shown). Refinement of staining condition may lead to better result but this was not tried due to pursuit of other avenues. Sub-confluent GPNTs were stimulated with TNF-α or PMA and then stained for PKCγ, PKCι and PKCζ/ι. For these three isoforms, I was unable to investigate the response to ICAM-1 stimulation since the 1A29 antibody and the three anti-PKCs were derived from mouse and cross-reactivity would have been observed. PKCγ displayed diffuse

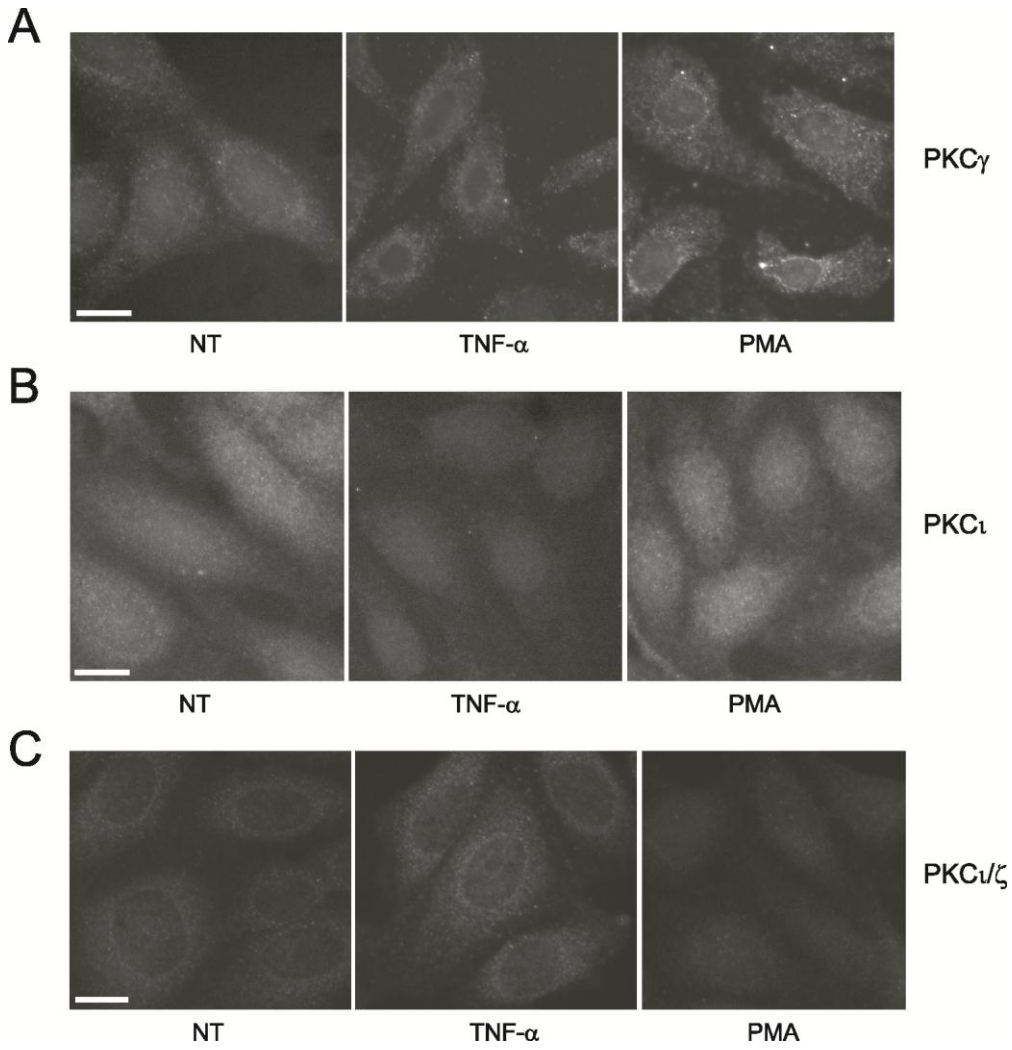

Figure 4.7 PKC distribution in GPNT

Sub-confluent GPNTs were either left untreated (NT) or stimulated with either 100 U/ml TNF-α or 160nM PMA for 10 min before being fixed using 3.7% formaldehyde. Following acetone extraction, dishes were stained for PKCγ (A), PKCι (B) or PKCι/ζ (C) as detailed in Chapter 2. Images were taken on Zeiss Axiophot light microscope. (Scale bar: 10µm)

(Images kindly provided by Keely Plewa, Masters Student under my supervision)

distribution throughout the cell and redistributed to the perinuclear region following both TNF-α and PMA stimulation (Figure 4.7A). PMA appeared to induce a more pronounced, vesicular distribution in the perinuclear region than TNF-α. PKCι was found diffuse throughout the GPNT cells. No clear change of localisation was seen following PMA or TNF-α stimulation (Figure 4.7B). When the anti-PKCζ/ι antibody was used I observed diffuse cytoplasmic staining which became more vesicular and more concentrated in perinuclear areas following TNF-α but not PMA, suggesting that PKCζ rather than PKCι was activated (Figure 4.7C).

I also analysed the distribution of PKCs in the hCMEC/D3 cell line. Again I tested all available antibodies and again only a few resulted in clear signals, with the others presumably requiring adjustments to the staining conditions. In hCMEC/D3 clear signals were found using antibodies against PKCβ_I, PKCε and PKCθ. Since all three antibodies were raised in rabbit, it was possible to study the response to ICAM-1 stimulation in addition to PMA or TNF-α (Figure 4.8). In unstimulated hCMEC/D3 cells PKCβ_I was mainly cytoplasmic with diffused staining. In response to PMA and anti-ICAM-1 the staining became more pronounced and more vesicular (Figure 4.8A). No clear change of distribution was seen in response to TNF-α. PKCε was also detected throughout the cytoplasm in a diffuse/punctate pattern with some concentrated on one side of the perinuclear region. Following stimulation with anti-ICAM-1 or TNF-α, this distribution did not change overtly but became much more pronounced in particular the perinuclear staining (Figure 4.8B). In contrast, PMA treatment did not produce a significant change in PKCε staining. PKCθ was cytoplasmic and strongly punctate (Figure 4.8C). This staining remained unchanged in response to TNF-α but became more diffuse following ICAM-1 ligation. The strongest redistribution was induced following PMA stimulation, which induced strong nuclear stain.

Another way to analyse PKC activation and translocation is by cell fractionation. In a series of pilot experiments, I used a sedimentation protocol which separated cytoplasm from three particulate fractions enriched in nuclei, organelles and membrane, respectively (see Section 2.2.10 for further details). hCMEC/D3 were grown to confluence, serum-starved and subjected to ICAM-1 stimulation. Lysates were fractionated and immunoblotted using anti-PKCα and anti-PKCβ_I antibodies (Figure 4.9). In non-treated cells, PKCα and PKCβ_I were mainly found in the cytoplasmic and organelle fraction (pellet 2). During ICAM-1 stimulation PKCα was increasingly found in the nuclear fraction (pellet 1) and the membrane fraction (pellet 3) with a concomitant reduction in the cytoplasm. At the same time, PKCβ_I primarily accumulated in the nuclear fraction but not the

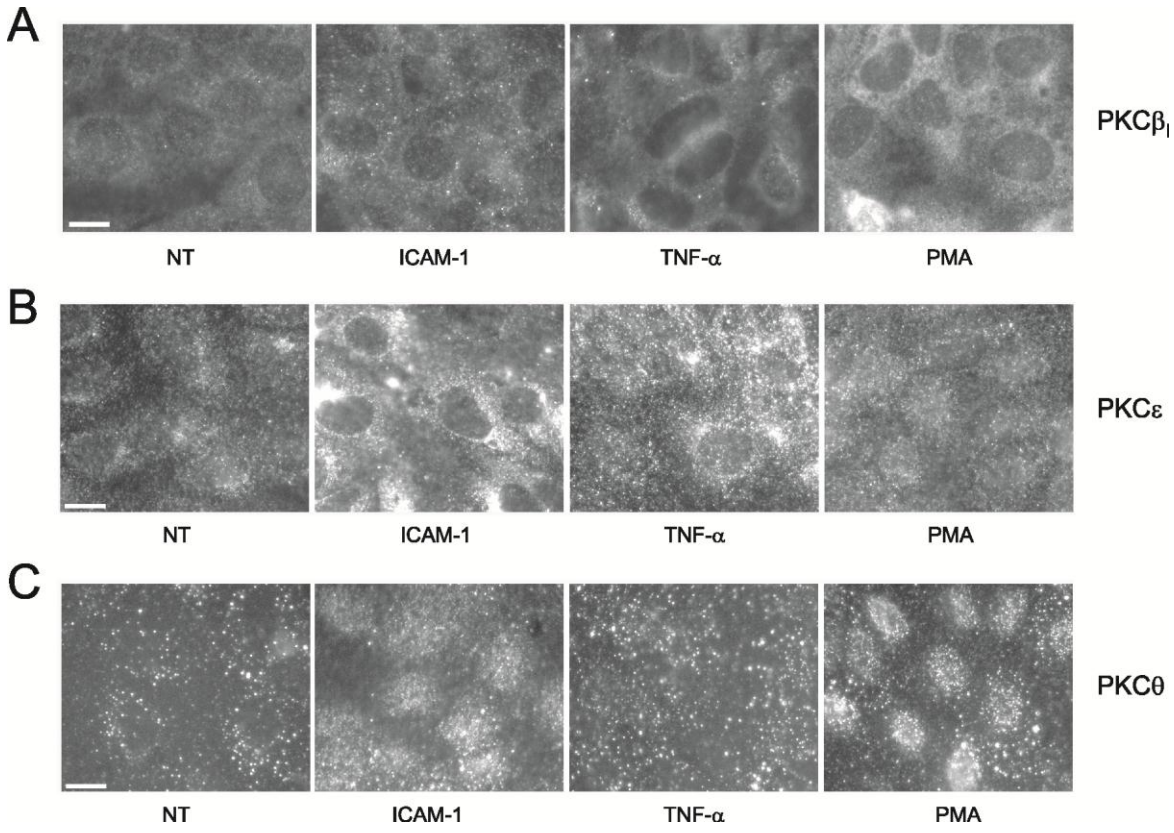

Figure 4.8 PKC distribution in hCMEC/D3

Sub-confluent hCMEC/D3 were either left untreated (NT) or stimulated with either 5µg/ml 1A29 anti-ICAM-1 antibody, 100 U/ml TNF-α or 160nM PMA for 10 min before being fixed using 3.7% formaldehyde. Following acetone extraction, dishes were then stained for (A) PKCβ_I, (B) PKCε or (C) PKCθ as detailed in Chapter 2. Images were taken on Zeiss Axiophot light microscope. (Scale bar: 10µm)

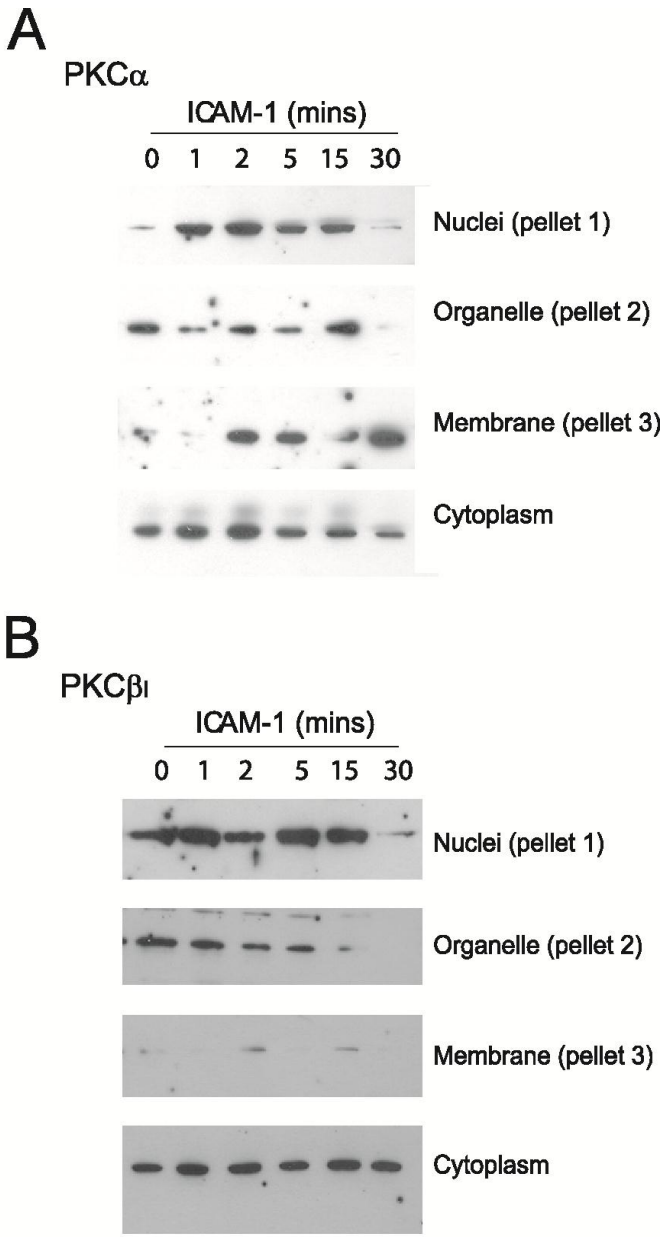

Figure 4.9 PKC translocation in response to ICAM-1 stimulation analysed by cell fractionation

Confluent hCMEC/D3 were serum-starved overnight before stimulation by ICAM-1 ligation for the times indicated. Fractionation and immunoblot analysis was carried out as described in Chapter 2. Shown are analyses of PKCα (A) and PKCβ_I (B).

membrane fraction. Taken together, PKC translocation occurred in response to ICAM-1 stimulation and this could be measured by both immunocytochemistry and immunoblotting.

4.4 Discussion

Based on pharmacological inhibition, endothelial PKC is involved in controlling TEM (Etienne-Manneville et al., 2000). However, so far the isoforms involved have not been identified. Before I looked further into the role of PKC in ICAM-1-mediated signalling and lymphocyte transmigration, the PKC expression repertoire of GPNT and hCMEC/D3 cells was analysed. Collectively, mRNA and protein analyses revealed that PKCα, PKCβ, PKCδ, PKCε, PKCθ, PKCι and PKCμ were expressed in GPNT and hCMEC/D3 cells. Restriction digest analysis was not always efficient and incurred problems for some PKC isoform analysis suggesting alternative restriction enzymes are required for use in the studies. Only PKCα, and to some extent PKCε transcripts were unambiguously identified. Restriction analysis of the other PKC isoforms often produced full-length fragments, suggesting that digests were incomplete and that there was either an issue with the restriction enzyme used, for example it may no longer have worked effectively or was not appropriate for that particular isoform in question or there may have been a problem with the DNA used in the reaction Alternatively, fragments were detected that varied by 30 to 50 base pairs from the predicted length, which were not too dissimilar from those expected. Variations in the bands may have arisen due to the agarose gel the digest was analysed on, for instance the bands may have migrated slighty faster or slower than anticipated or a problem with the gel may have been incurred. Another potential reason could be that for some of the PKC isoforms a predicted sequence was used from the NCBI database, thus potentially leading to miscalculations in the band sizes expected following the reaction with the restriction enzyme utilised.

In some cases, such as for PKCβ and PKCδ, RT-PCR analysis proved difficult but immunoblot analysis was unambiguous. I was unable to detect PKCη by PCR but in western blots a band close to the predicted weight was observed. However, since other low molecular weight proteins were detected in the same immunoblots it cannot be concluded unequivocally that PKCη is expressed in BMVEC. The expression of PKCι, PKCζ and PKCμ in BMVEC is likely since clear evidence was found by RT-PCR, albeit the observed fragments were slightly smaller in size than expected. PKCζ could

not be unambiguously identified in western blots since the antibody also recognised the PKCι isoform. PKCμ immunoblots revealed a band which migrated significantly faster than predicted. Alone the expression of PKCγ could not be verified appropriately: RT-PCR produced a fragment of the predicted size which, however, was resistant to restriction enzyme digests. DNA sequencing should probably have been performed. Furthermore, immunoblot analyses did not detect any protein in GPNT and in hCMEC/D3 a high background was observed making it difficult to verify its expression within the cell line. However, a clear PMA-sensitive signal was detected by immunocytochemistry. Taken together, it appeared that most, if not all, PKC isoforms are present in BMVEC, in particular GPNT, and that PKCγ and PKCη require further investigation. Our results are in agreement with studies by Kizbai and colleagues who studied the expression of PKCα, PKCβ, PKCγ, PKCδ, PKCε, PKCη and PKCζ in rat BMVEC and found them all to be present (Krizbai et al., 1995). Surprisingly clear evidence for PKCθ expression was found both on the mRNA and protein level. Its expression has so far been reported to be restricted to skeletal muscle and T-lymphocytes (Tan and Parker, 2003; Altman and Villalba, 2003; Quann et al., 2011). Clearly, the brain microvascular endothelium is another cell type that uses PKCθ.

Studies demonstrating that PKC is involved in lymphocyte transmigration used different PKC inhibitors which show broad specificity towards the different isoforms. One rationale to study the expression of PKC isoforms in BMVEC was to possibly be able to restrict future analyses due to a restricted isoform expression profile. However, our results have shown that this is not possible since most, if not all, known PKC isoforms are expressed in BMVECs. Further functional activation studies or analyses using isoform specific RNA interference will be required to identify the PKC isoforms involved in TEM.

Pilot experiments were performed to study PKC isoform activation through its intracellular localisation. For this, the translocation of PKC to cellular membranes during activation is exploited (Quittau-Prevostel et al., 2004; Louis et al., 2005; Collazos et al., 2006). These studies were initiated but not pursued to completion since other avenues (described in Chapters 5-8) took precedence. An important caveat for the following discussion is that none of the studies were performed systematically, i.e. only selected antibodies were used for each method of analysis.

Immunocytochemical analysis worked for some antibodies. PMA stimulation induced the translocation of PKCγ in GPNT and PKCβ_I and PKCθ in hCMEC/D3. TNF-α stimulation led to translocation of PKCζ in GPNT and PKCε in hCMEC/D3. ICAM-1 stimulation in hCMEC/D3 produced

clear translocation of PKCβ_I, PKCε and PKCθ. These results were in line with the known activation modes of PKC isoforms (see Section 4.1.), e.g. PKCζ was found to translocate in response to TNF-α but not PMA, as would be expected since aPKC lack the appropriate DAG/phorbol ester binding domain. Importantly, these results also showed that different PKC isoforms translocate to different regions of the cell in response to the same stimuli. For instance, PMA induced cytoplasmic (possibly membrane) localisation and nuclear translocation of PKCα and PKCθ, respectively.

Immunocytochemical analysis of PKC translocation was rapid, highly informative and required little starting material. However, since our objective was to study PKC activation during ICAM-1 stimulation which is brought about by ligating surface ICAM-1 using high concentrations of a mouse monoclonal antibody, this method could not be used when only mouse PKC isoform antibodies were available. This problem could be solved by using directly labelled (with a fluorophore or biotin) PKC antibodies for staining or the Zenon method (Invitrogen) which utilises preformed primary-secondary antibody complexes. Initial trials have been started for both methods but optimisation would be needed for clear results.

I also employed subcellular fractionation as an alternative method which would work with any antibody, even those that are not mono-specific as long as the isoform in question can be clearly identified. To prove that PKC translocation was detectable in response to ICAM-1 stimulation fractionated cell extracts were immunoblotted using antibodies against PKCα and PKCβ_I. In both cases a clear shift of PKC from one subcellular fraction to another was observed, suggesting that ICAM-1 stimulation led to the activation of both PKC isoforms. In contrast, and in comparison to analysis by immunohistochemistry, fractionation protocols were drawn-out and required much more starting material. Furthermore, the information on the intracellular relocalisation was less specific. For instance, biochemically the majority of PKCβ_I was found in the nuclear fraction (pellet 1) following ICAM-1 ligation. Immunocytochemical analysis suggested that translocation occurred to a vesicular compartment in the cytoplasm or the perinuclear region. It is possible that fractionated nuclei were contaminated with other cellular components due to continued association with the cytoskeleton (in particular actin and intermediate filaments).

Taken together, a combination of both immunohistochemistry and fractionation may be required to analyse PKC isoform activation following ICAM-1 stimulation. In our pilot studies, I found clear evidence for the activation of PKCα, PKCβ_I, PKCε and PKCθ in response to ICAM-1

ligation, suggesting that many endothelial PKC isoforms are involved during ICAM-1-mediated TEM.

Chapter 5: ICAM-1-mediated MAP kinase activation in BMVECs

5.1 Introduction

ICAM-1 has been shown not only to have a role in firm adhesion capturing the lymphocyte to the endothelium from the blood flow to recruit it to tissue underneath but also in rendering the endothelium compliant to transmigration. ICAM-1-mediated outside-in signalling is important for this to occur. A number of groups have investigated ICAM-1-mediated signalling in a number of model systems derived from different vascular beds. Within these studies three important MAP kinases, namely ERK, JNK and p38, have been shown to be activated in response to ICAM-1 stimulation. MAP kinases respond to numerous extra- and intracellular stimuli that specifically direct their activity to regulating functions including growth control, cytoprotection and the cellular response to inflammation and stress (Hoefen and Berk, 2002). Generally, growth factors and phorbol esters lead to the activation of ERK1/2 whilst JNK and p38 respond to stress stimuli including cytokine stimulation and osmotic shock (Roux and Blenis, 2004). The response of each of the MAP kinases can lead to the phosphorylation of a number of downstream effector substrate including other kinases, cytoskeletal proteins and transcription factors.

In HUVEC, sustained ERK activation occurs within 30 min of ICAM-1 cross-linking (Lawson et al., 1999). In pulmonary MVEC stimulated with TNF-α, p38 is activated within a few minutes following ICAM-1 cross-linking (Wang and Doerschuk, 2001). In immortalised rat BMVEC JNK activation occurs within 15 min of ICAM-1 cross-linking (Etienne et al., 1998). Thus, the activation of all three major MAP kinases is clearly part of ICAM-1 signalling in ECs. However, major questions remain: firstly, each of these studies has used fundamentally different EC (at different activation states) and therefore it is unclear if all three MAP kinases are activated within the same cell type in response to ICAM-1 activation or if individual MAP kinase activation is cell-type specific. Secondly, it is unclear whether comparable methods of ICAM-1 activation have been used in the aforementioned studies. ICAM-1 can be activated by simple antibody (or ligand) binding (Martinelli et al., 2009), by antibody-mediated cross-linking (Etienne et al., 1998; Lawson et al., 1999; Wang and Doerschuk, 2001), by antibody-coated beads (van Buul et al., 2007b) or by direct T-lymphocyte adhesion (Greenwood et al., 2003a). Each of these activation methods can result in

different intracellular signalling and activation time courses. Taken together, a more detailed analysis in a single EC type should clarify how ERK, JNK and p38 signalling relates to ICAM-1 activation.

5.2 Aim

The aim of this part of the study was to determine if ERK, JNK and p38 were activated in non-cytokine stimulated BMVEC in response to ICAM-1 stimulation. Different ICAM-1 activation methods were to be used to ascertain that MAP kinase activation was relevant. Lastly, if activation occurred, I am interested in the timeframe of activation so that this could be correlated to other previously identified pathways.

5.3 Results

5.3.1 ICAM-1 stimulation mediates the phosphorylation of the endothelial MAP kinases ERK, p38 and JNK

Activation of the three MAP kinases in response to ICAM-1 stimulation was studied in confluent, contact-inhibited GPNT BMVECs which were made quiescent by serum starvation. In a first experimental setup I chose to stimulate ICAM-1 by antibody-mediated cross-linking. This is the most commonly used method of adhesion receptor activation and consists of a primary incubation with ICAM-1 specific antibodies followed by surface clustering of the antibody-ICAM-1 complexes by the addition of secondary antibodies. As also discussed below, the primary incubation has erroneously been considered a neutral period when no signalling is triggered. Therefore investigators have never paid much attention to incubation times, which varied between a few minutes and 1 h. Instead, in such studies activation times relate to incubation with secondary antibody. I performed ICAM-1 cross-linking by incubation with anti-rat ICAM-1 antibody 1A29 for 30 min (by which time primary signalling has usually subsided), followed by washes and

the addition of secondary antibody for different times (Figure 5.1). Lysates were analysed for MAP kinase activation by immunoblotting using specific anti-phospho-antibodies for ERK, JNK and p38 (Figure 5.1A). MAP kinases are activated in response to dual phosphorylation of threonine (Thr) and tyrosine (Tyr) residues in conserved motifs (Thr-X-Tyr) located in the activation loop (Davis, 2000; Clark et al., 2003; Roux and Blenis, 2004). Therefore, phosphorylation is commonly assumed to determine activation of MAP kinases. Antibodies for the specific dual phosphorylation sites for each MAP kinase were used to determine activation of each of the specific MAP kinases of interest: phospho-ERK (Thr 202/Tyr 204), phospho-JNK (Thr 183/Tyr 185) and phospho-p38 (Thr 180/Tyr 182). Within 5 min, significant increases were detected in the cellular content of all three phospho-MAP kinases. ERK phosphorylation increased for 15 min and decreased after that. JNK phosphorylation followed a similar pattern to that of ERK whilst p38 phosphorylation was maintained for at least 45 min. Maximal phosphorylation was 3.5-, 2- and 3-fold for ERK, JNK and p38 respectively (Figure 5.1B). Phosphorylation was specific to ICAM-1 cross-linking since in control experiments using neural iso-type specific control IgG during the primary incubation neither JNK nor p38 displayed significant increases in phosphorylation (Figure 5.2). ERK appeared to display an increase in phosphorylation albeit less than that observed with ICAM-1 cross-linking.

Previous work in the laboratory has shown that incubation of GPNT with primary antibody alone (termed 'ICAM-1 ligation') is sufficient to trigger microaggregation and also ICAM-1 signalling (Martinelli et al., 2009). I therefore wanted to determine if the anti-rat ICAM-1 antibody 1A29 was sufficient to induce phosphorylation of the three MAP kinases. As with the cross-linking experiment GPNT EC were grown to confluency, serum-starved and then stimulated with 1A29 antibody for varying lengths of time before cell extracts were prepared. Immunoblot analysis showed that ERK, JNK and p38 were all strongly phosphorylated in response to ICAM-1 ligation. In fact, phosphorylation occurred more rapidly as when compared to the ICAM-1 cross-linking (Figure 5.3A). ERK and p38 showed significant increase in phosphorylation within 1 min of ICAM-1 ligation whilst for JNK this was seen within 2 min. Maximal phosphorylation was greater than 4-fold for p38 and greater than 3-fold for ERK and JNK (Figure 5.3B). Activatory phosphorylation of all three MAP kinases was all transient and had reverted to control levels within 20 min.

To confirm that the phosphorylation of endothelial ERK, JNK and p38 in response to ICAM-1 stimulation was not species or cell line specific, the immortalised human BMVEC line, hCMEC/D3, and primary rat BMVEC were used to verify the results. MAP kinases of the human D3 cell line

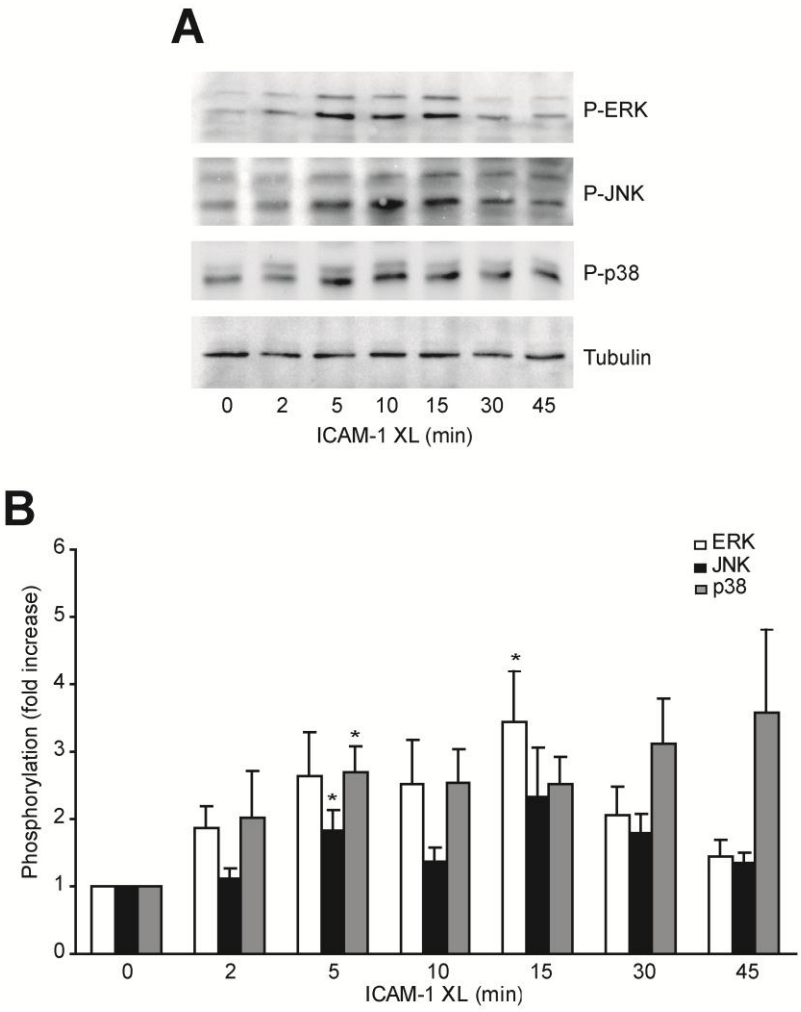

Figure 5.1 Endothelial ERK, JNK and p38 are phosphorylated in response to ICAM-1 cross-linking

(A) GPNT cells were grown to confluency and then stimulated with anti-ICAM-1 antibody (5µg/ml) for 30 min, washed once with HBSS and then stimulated with secondary antibody (10µg/ml) for time indicated before being lysed. Proteins of lysates were then subjected to SDS-PAGE, transferred to nitrocellulose membranes which were then probed with antibodies directed against phospho-ERK, -JNK, -p38 and tubulin as a loading control.

(B) Densitometry quantification of 3 experiments including (A) represented as a fold increase of phosphorylation for the three MAP kinases compared to control. Results are expressed as average means +/- SEM. Student's t test was used to analyse the variances of mean values. *, $P < 0.05$; **, $0.001<P< 0.01$; ***, $P \leq 0.001$

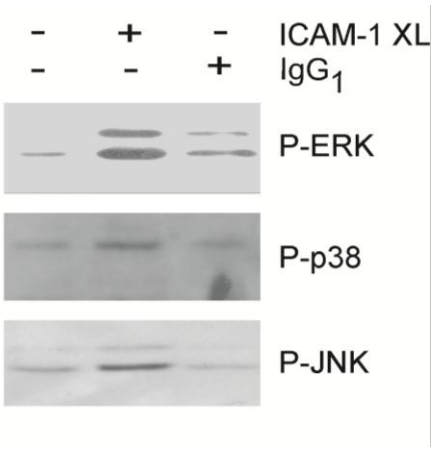

Figure 5.2 Phosphorylation of endothelial ERK, JNK and p38 is a specific response to ICAM-1 cross-linking

GPNTs were grown to confluency, serum-starved and incubated with either anti-ICAM-1 antibody 1A29 or control isotype-matched IgG (5μg/ml) for 30 min followed by a 5 min cross-linking with secondary antibodies. Cells were the lysed and subjected to immunoblotting as described for Figure 5.1.

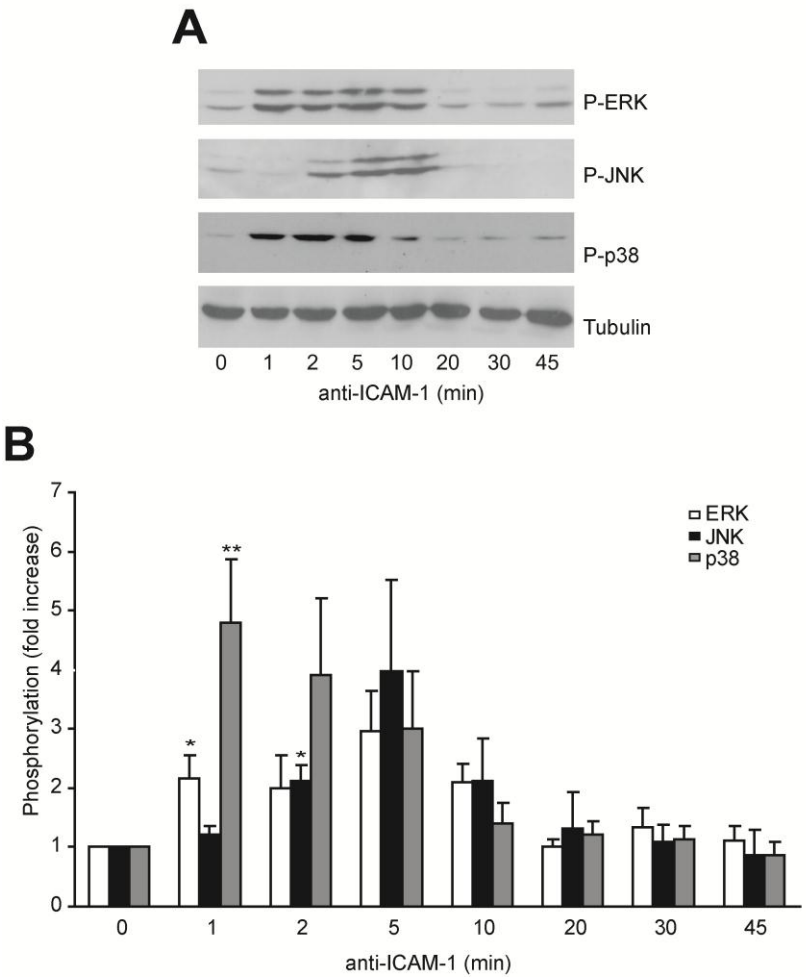

Figure 5.3 ICAM-1 ligation leads to transient phosphorylation of endothelial ERK, JNK and p38.

(A) GPNT cells were grown to confluency and then stimulated with anti-ICAM-1 antibody 1A29 (5µg/ml) for the times indicated and then analysed by western blotting as described in Figure 5.1.

(B) Densitometry quantification of the data from (A) and 2 other independent experiments represented as an average fold increase of phosphorylation for the three MAP kinases compared to control +/- SEM. Variances of mean values were statistically analysed by the Student's t test. *, $P < 0.05$; **, $0.001<P< 0.01$; ***, $P \leq 0.001$

responded in a similar manner to that of GPNT following both ICAM-1 ligation and cross-linking (Figure 5.4). Phosphorylation of MAP kinases appears to be similar to that observed in GPNT EC for both ICAM-1 ligation and cross-linking. Each MAP kinase was phosphorylated within 5 min of stimulation by either ICAM-1 ligation or cross-linking. An apparent difference seems to suggest that ICAM-1 cross-linking in hCMEC/D3s is transient when compared to the sustained response seen in GPNT BMVEC. Overall, this suggested that MAP kinase activation is not cell or species specific.

In primary rat BMVECs, I investigated time points that had previously shown significant phosphorylation of all three kinases following either ICAM-1 ligation or cross-linking in GPNT and hCMEC/D3. Specifically, I studied ICAM-1 ligation at 2 and 5 min and cross-linking at 10 and 20 min. ICAM-1 mediated phosphorylation was observed for all three MAP kinases (Figure 5.5A). Within the time points chosen ERK phosphorylation was strongest following ICAM-1 ligation for 5 min and cross-linking of ICAM-1 for 10 min (Figure 5.5B). Strong JNK activation was observed within 2 min of ICAM-1 ligation and at both times of cross-linking. p38 phosphorylation was equally rapidly induced following ligation and sustained at 10 and 20 min cross-linking. Thus for all three kinases activatory phosphorylation occurred in a similar way in primary and immortalised cells, suggesting that GPNTs were suitable for further studies of ICAM-1-mediated MAP kinase signalling networks.

5.3.2 Lymphocyte adhesion results in the phosphorylation of endothelial ERK, p38 and JNK

Physiologically, the activation and aggregation of endothelial ICAM-1 is triggered by interaction with leukocyte integrin LFA-1 ($\alpha_L\beta_2$ integrin) or MAC-1 ($\alpha_M\beta_2$ integrin) (Hubbard and Rothlein, 2000; Ley et al., 2007; Vestweber, 2007). Thus, I wanted to determine whether adhesion of lymphocytes to GPNTs induced MAP kinase activation and whether such activation was dependent on LFA-1 which is the dominant counter-receptor of ICAM-1 in lymphocytes (Greenwood et al., 1995; Pryce et al., 1997; Lyck et al., 2003). GPNT BMVEC were co-cultured with concanavalin A-activated PLN lymphocytes which adhere efficiently but do not transmigrate (since in contrast to circulating lymphocytes they are not antigen-activated). At various times thereafter adherent lymphocytes were washed off with ice-cold PBS, lysates were prepared and analysed by

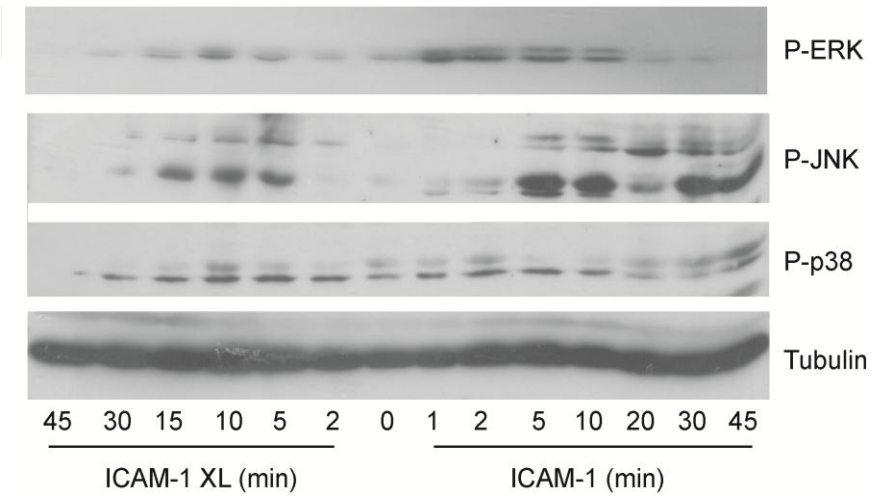

Figure 5.4 ERK, JNK and p38 are phosphorylated in response to ICAM-1 ligation and ICAM-1 cross-linking in human BMVEC (hCMEC/D3)

Western blot analysis of ICAM-1 induced phosphorylation of MAP kinases performed as described in Figures 5.1 and 5.3 with the exception that the human BMVEC cell line hCMEC/D3 was used and mouse anti-human ICAM-1 (CD54) antibody.

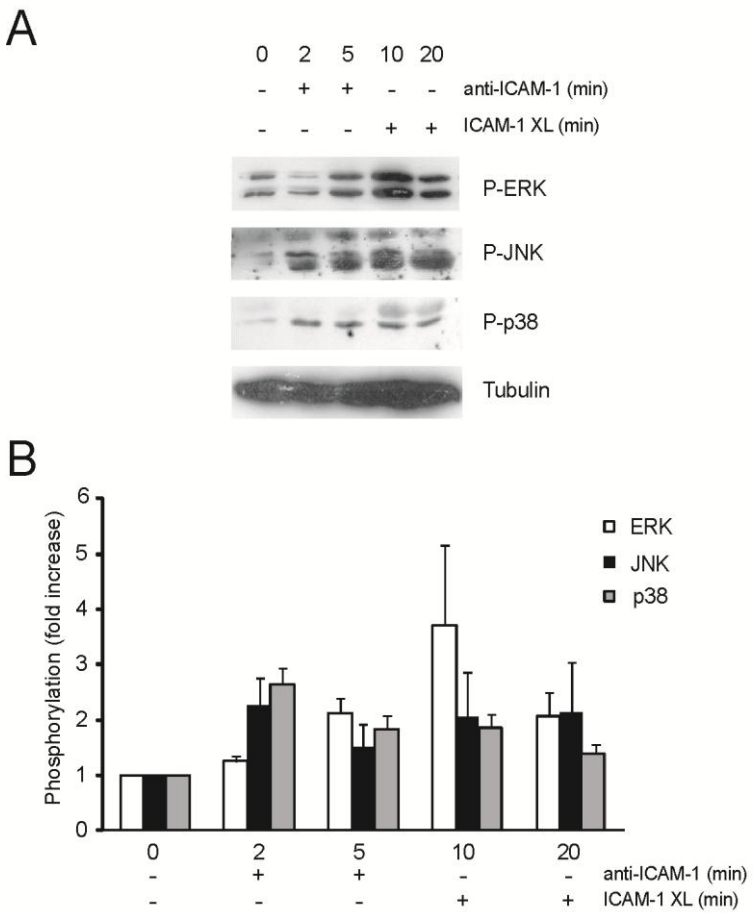

Figure 5.5 ERK, JNK and p38 are phosphorylated in response to ICAM-1 ligation and cross-linking in primary rat BMVEC

(A) Primary rat BMVEC were grown to confluency and stimulated by ICAM-1 ligation or cross-linking as described in Figures 5.1 and 5.3. They were subsequently analysed by immunoblotting.

(B) Densitometry quantification of data from (A) and two other independent experiments. Results are expressed as mean average of fold increase of phosphorylation of the three MAP kinases compared to control +/- SEM. Variances of mean values were statistically analysed by the Student's t test. *, $P < 0.05$; **, $0.001<P< 0.01$; ***, $P \leq 0.001$

immunoblotting with phospho-specific antibodies. Figure 5.6A shows that phosphorylation of ERK, JNK and p38 occurred within 5 min of co-culture and was sustained for at least an hour. Within 15 min of lymphocyte exposure endothelial ERK, JNK and p38 phosphorylation increased significantly by 4-, 2.5- and 2-fold, respectively (Figure 5.6B).

To assess the contribution of the LFA-1-ICAM-1 interaction to MAP kinase activation GPNTs were co-cultured with PLN lymphocytes that had been pre-incubated with function-blocking antibodies to the ICAM-1-ligand LFA-1 (CD18 and CD11α). After 30 min of co-culture endothelial lysates were prepared and analysed. Figure 5.7A shows that incubation with PLN lymphocytes increases MAP kinase phosphorylation and is decreased when PLNs are incubated with function-blocking antibodies. Phosphorylation for all three endothelial MAP kinases was reduced by around 40% when LFA-1 was functionally blocked (Figure 5.7B), suggesting that the interaction with lymphocyte LFA-1 can play an important role in ICAM-1-mediated endothelial MAP kinase activation.

In contrast, when pre-incubated with function-blocking antibodies to the VCAM-1 ligand VLA-4 (CD49) PLN lymphocyte adhesion produced uninhibited MAP kinase phosphorylation (Figure 5.8A and B). In fact, there was some increase in p38 phosphorylation (Figure 5.8B).

5.3.2 Anti-ICAM-1-coated beads mimic receptor ligation and cross-linking

I also used 1A29 antibody bound to fluorescent GFP beads to activate GPNT (as described in Section 2.2.14). Added to quiescent, confluent GPNT they induced rapid and sustained phosphorylation of ERK, JNK and p38 (Figure 5.9A). MAP kinase phosphorylation occurred (and for ERK and JNK peaked) within 5 min of bead addition and was sustained for at least 1 h. Similar results were obtained using 1A29 bound to protein G-Dynabeads (Figure 5.9B). Phosphorylation of p38 detected two distinct bands of different molecular weights. It is likely that these bands correspond to the isoforms p38α and p38β which have not been routinely separated on previous blots. In both sets of experiments MAP kinase phosphorylation seemed to be biphasic over time, with highest levels reached after a few minutes, decreasing thereafter and increasing again towards the latter part of the incubation period. This data suggested that biphasic activation may not be an artefact of the cross-linking strategy.

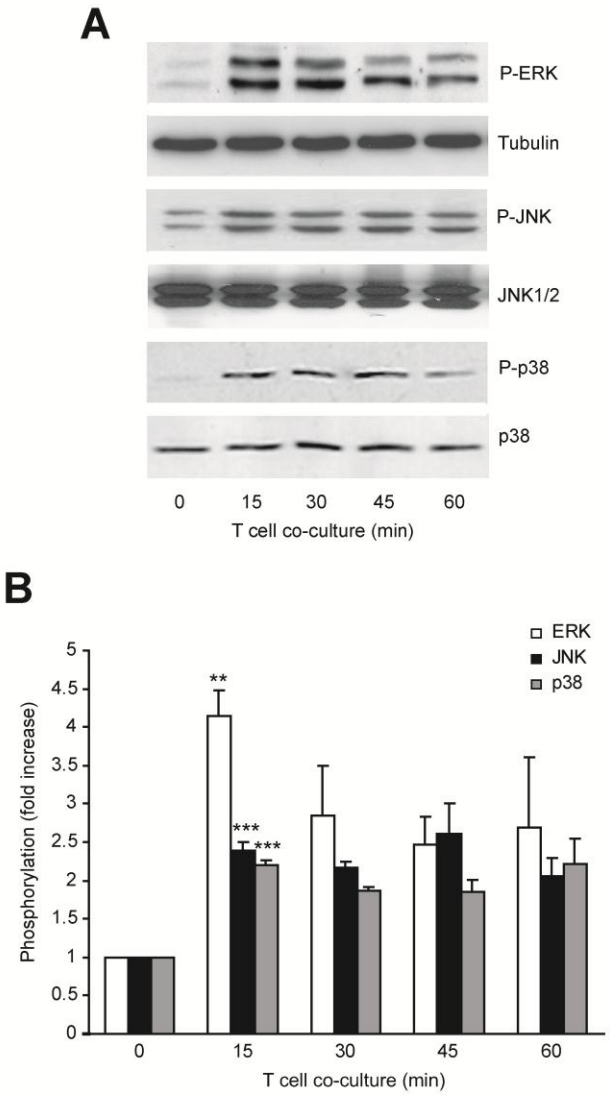

Figure 5.6 Lymphocyte adhesion results in endothelial ERK, JNK and p38 phosphorylation

(A) GPNT BMVEC were grown to confluency, serum-starved and co-cultured with 2 X 10^6/ml concanavalin A-activated rat PLN lymphocytes for the times indicated. Lymphocytes were thoroughly washed off and lysates prepared from the remaining EC monolayers. Lysates were analysed by immunoblotting as described for Figure 5.1 using antibodies against phospho-ERK, -JNK and -p38 and tubulin, JNK1/2 and p38 as loading controls.

(B) Densitometry quantification of 3 experiments including (A) represented as a fold increase changes in the three MAP kinases in relation to control +/- SEM. Variances of mean values were statistically analysed by the Student's t test. *, $P < 0.05$; **, $0.001<P< 0.01$; ***, $P \leq 0.001$

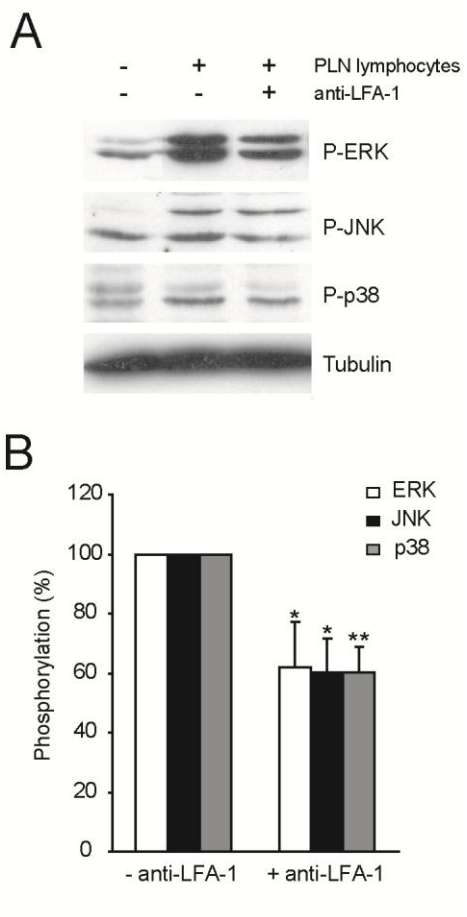

Figure 5.7 Interaction of endothelial ICAM-1 with its counter-receptor LFA-1 on lymphocyte is important for MAP kinase phosphorylation

(A) PLN lymphocytes were pre-incubated with anti-LFA-1 blocking antibodies, CD18 and CD11α, (20μg/ml) for 60 min before addition to GPNTs. Control PLNs were incubated without any antibodies. Following co-culture with GPNT for 30 min PLNs were extensively washed off with ice-cold PBS, lysates prepared and analysed by immunoblotting as described for Figure 5.1. High variability in MAP kinase phosphorylation was observed when compared to GPNT alone and hence the absolute values of inhibition differed greatly. The data shown in Figure 5.7B is expressed as a percent inhibition of maximal activation (PLN lymphocyte alone).

(B) Densitometry quantification of data from (A) and 2 other independent experiments. Mean values are expressed as percent inhibition of maximal activation (-anti-LFA-1) +/- SEM. Student's t test was used for statistical analysis of mean value variance. *, $P < 0.05$; **, $0.001<P< 0.01$; ***, $P \leq 0.001$

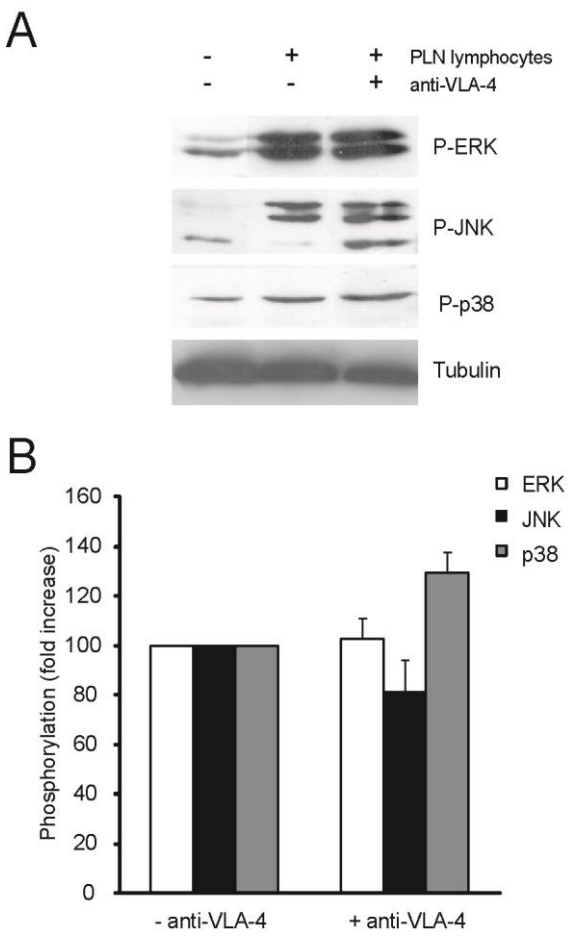

Figure 5.8 Interaction of endothelial VCAM-1 with its counter receptor VLA-4 on lymphocytes is insufficient to induce MAP kinase phosphorylation

(A) As described in Figure 5.7 with the exception that PLN lymphocytes were pre-incubated with the anti-VLA-4 blocking antibody CD49 (20µg/ml). Lysates were prepared and analysed as described in Figure 5.1.

(B) Densitometry quantification of data from (A) and 2 other independent experiments. Mean values are expressed as percent inhibition of maximal activation (-anti-VLA-4) +/- SEM. Variances of mean values were statistically analysed by the Student's t test. *, $P < 0.05$; **, $0.001<P< 0.01$; ***, $P \leq 0.001$

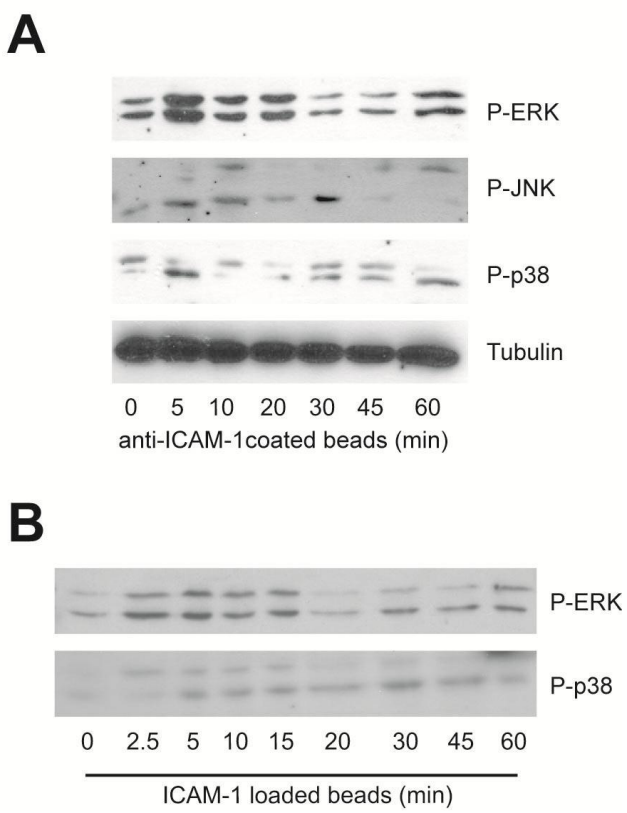

Figure 5.9 Anti-ICAM-1-coated fluorescent beads and protein G-dynabeads as a novel method to induce MAP kinase phosphorylation

(A) Anti-ICAM-1-coated fluorescently labelled beads (0.36 X $10^6/cm^2$) were co-cultured with confluent, serum-starved GPNT EC monolayer for the indicated times. Lysates were prepared and analysed as described for Figure 5.1.

(B) As in (A) with the exception GPNT EC monolayers were co-cultured with anti-ICAM-1-coated protein G-Dynabeads.

5.4 Discussion

When lymphocytes adhere to the vascular endothelium the interaction of LFA-1 and ICAM-1 also induces EC signalling. ICAM-1-mediated signalling causes the activation of the MAP kinases ERK, p38 or JNK; with each case studied in fundamentally different EC model systems (Etienne et al., 1998; Lawson et al., 1999; Wang and Doerschuk, 2001). I show that all three MAP kinases were phosphorylated in the same EC cell line with similar time courses in response to a variety of different ICAM-1 activation modes. Phosphorylation occurred on Thr 202/Tyr 204, Thr 183/Tyr 185 and Thr 180/Tyr 182 for ERK, JNK and p38, respectively, which correlates to kinase activation (Davis, 2000; Roux and Blenis, 2004).

All three MAP kinases in this study were shown to be activated in response to ICAM-1 cross-linking (Figure 5.1) which classically consists of an initial incubation period with primary antibody. Incubation periods with primary antibody have erroneously been considered not to trigger any receptor-dependent signalling. Thus little attention has been paid to primary incubation times which vary from 5 to 60 min dependent on the laboratory. However, work from our laboratory has shown that ligation using anti-ICAM-1 antibodies alone is sufficient to induce ICAM-1 microaggregation and Ca^{2+}, CaMKK, and AMPK signalling (Martinelli et al., 2009). ICAM-1 ligation using primary antibody alone induces ICAM-1 surface clusters which are smaller but more frequent than those seen following cross-linking using a secondary antibody, suggesting that ICAM-1 ligation is an intermediary step in receptor aggregation and cell activation. In support I found that ICAM-1 ligation was also sufficient to activate ERK, JNK and p38 (Figure 5.3). Phosphorylation of all three MAP kinases occurred within 1 to 2 min of ICAM-1 ligation and thus more rapid than compared to ICAM-1 cross-linking. Differences were also notable in the length of activation of the three kinases depending on whether ICAM-1 ligation or cross-linking was carried out. ERK, JNK and p38 showed transient activation which peaked at around 5 min following ICAM-1 ligation, whereas activation was more sustained following cross-linking, with p38 phosphorylation being high for at least 45 min.

It is noteworthy that our experimental conditions of ICAM-1 cross-linking employed the secondary antibody only at a time when MAP kinase phosphorylation in response to activation by primary antibody had completely receded. Overall, our results investigating MAP kinase activation

following ICAM-1 cross-linking corroborate previous data in other model systems. Notable differences were in the timing of MAP kinase phosphorylation and the length of activation. The transient nature of ERK phosphorylation following ICAM-1 cross-linking in GPNT differed to the activation of ERK seen in HUVECs which occurs later at 30 min and is sustained for at least an hour (Lawson et al., 1999). This difference in the activation profile could be due to HUVEC being derived from macrovasculature compared to brain microvasculature giving subtle differences in signalling properties. Alternatively, it may also be due to differences in the cross-linking protocol or the use of a different anti-ICAM-1 antibody. Etienne and colleagues investigated the activation of JNK using the GPNT parent cell line GP8 and the same anti-ICAM-1 antibody 1A29 (Etienne et al., 1998). They observed maximal activation of JNK at 30 min as compared to 5 to 15 min in our study. However, this difference may be explained by differences in the duration with primary antibody. Etienne *et al*. added secondary antibody after 10 min as opposed to the 30 min in our study. Furthermore, these authors also measured c-Jun phosphorylation in JNK immunoprecipitates rather than JNK phosphorylation. As to ICAM-1-induced p38 activation in pulmonary MVEC, the study by Wang and Doerschuk looked at times up to 10 min and transient activation was seen within 2 to 6 min (Wang and Doerschuk, 2001). This is very similar to our observations although I observed much more sustained phosphorylation of p38.

Primary rat BMVECs were also used to ensure that the activation profile seen using GPNTs was not due to their immortalisation. ERK, JNK and p38 phosphorylation in response to ICAM-1 ligation or cross-linking of primary BMVECs matched that of GPNT (Figure 5.5). Whether or not activation profiles were identical cannot be concluded from this data since I did not analyse full time courses. I also analysed MAP kinase activation in a human equivalent to GPNT, the BMVEC line, hCMEC/D3. MAP kinase phosphorylation appeared to occur at a similar rate following ICAM-1 ligation and cross-linking although responses to cross-linking appeared to be more short-lived (Figure 5.4). Taken together and in combination with previous reports, this work suggests that similar MAP kinase signalling cascades act downstream of ICAM-1 in MVEC, irrespective of their origin and species. Thus GPNT cells appear appropriate to study the intricacies and role of endothelial ICAM-1-mediated MAP kinase signalling.

These results give rise to the idea that microaggregation is followed by macroaggregation in the physiological activation of ICAM-1 and that crucially our experimental conditions allow separation of the two activation states.

None of the aforementioned reports on ICAM-1-mediated MAP kinase activation in EC addresses the questions whether such activation can also be induced by the physiological stimulus, which is leukocyte adhesion. Here, I show that lymphocyte adhesion to GPNT induced ERK, JNK and p38 phosphorylation in an LFA-1- (but not VLA-4) dependent manner (Figure 5.7 and 5.8). Phosphorylation of all three MAP kinases occurred within 15 min of lymphocyte adhesion and was sustained for at least 1 h (Figure 5.6). This sustained response was different to that when ICAM-1 antibodies were used. This may have been due to a number of factors. Firstly, lymphocytes do not only adhere to EC via ICAM-1 and adhesion via selectins and other CAMs may also induce MAP kinases (van Buul et al., 2007b; van Buul and Hordijk, 2009). Indeed, I only found a ca. 40% reduction in MAP kinase phosphorylation when LFA-1 was neutralised on lymphocytes. Although, such neutralisation can never be complete, the same treatment of lymphocytes leads to an 80-90% inhibition of migration (Greenwood et al., 1995), suggesting that receptors other than ICAM-1 contributed to MAP kinase activation in response to lymphocyte adhesion. Secondly, ICAM-1 clustering on the EC surface was undoubtedly different in response to lymphocyte adhesion and antibody cross-linking. For instance, LFA-1-ICAM-1 interactions and clustering are restricted to specific areas of the advancing leukocyte (Smith et al., 2005). Similarly, it has also been observed that lymphocytes have preferentially sites of adherence on the EC. In clear contrast antibody-mediated ligation does not occur at preferred areas of the EC cell surface (Turowski et al., 2008). Thus leukocyte adhesion may give rise to a more focused and consequently different MAP kinase response.

Antibody-mediated ICAM-1 ligation or cross-linking are ways to mimic and study part of the lymphocyte adhesion process and ensuing EC signalling. However, they are clearly not reproducing EC signalling in its entirety. Another way to model leukocyte interactions with EC ICAM-1 is by using antibody-coated beads (van Buul et al., 2007b). As shown in Chapter 3, such beads appeared to trigger EC activation only after being lateralised and preferentially immobilised in tri-cellular junctions, areas reported to serve as preferential site of transmigration. Here, I show that the addition of anti-ICAM-1-coated beads to GPNT activated all three MAP kinases in a similar manner to that seen by ICAM-1 ligation and cross-linking. In fact, biphasic MAP kinase phosphorylation appeared to be observed, suggesting that antibody-coated beads mimic ligation (microaggregation) and cross-linking (clustering) of ICAM-1. To eliminate the possibility that this apparent biphasic activation is due to noise background further experiments would need to be carried out. Taken together these results indicate that whilst antibody-coated beads will be useful

to delineate spatio-temporal events of EC ICAM-1 by microscopy, the straightforward use of soluble antibody in ligation or cross-linking experiments is sufficient to study biochemical aspects of ICAM-1-mediated MAP kinase signalling networks.

Overall the results presented in this chapter show that the interaction between LFA-1 and ICAM-1 is not only important for cell adhesion but also leads to significant EC MAP kinase activation. I observed clear differences in the time frame and duration of their phosphorylation, implying that ICAM-1-mediated activation of ERK, JNK and p38 uses distinct pathways and that MAP kinase have distinct roles in leukocyte-EC interaction.

Chapter 6: Upstream mediators of MAP kinase activation

6.1 Introduction

As shown in Chapter 5 MAP kinase activation occurred in response to both ICAM-1 ligation, cross-linking and lymphocyte adhesion. Since the timing and magnitude of ICAM-1-induced activation of the three MAP kinases differed, ERK, JNK and p38 may be operating in different signalling axes fulfilling distinct roles.

Many studies have shown that ICAM-1-mediated signalling leads to activation and phosphorylation of numerous signalling proteins (Durieu-Trautmann et al., 1994; Etienne et al., 1998; Adamson et al., 1999; Etienne-Manneville et al., 2000; Tilghman and Hoover, 2002; Yang et al., 2006a; Yang et al., 2006b). Important examples of components of the EC shown to respond to ICAM-1 stimulation and being involved in TEM include the small GTPase Rho, actin dynamics, Src and PKC. Src activation occurs in response to ICAM-1 engagement in HUVECs and rat BMVEC systems as well as in pulmonary EC suggesting that it is a key mediator of ICAM-1 signalling (Durieu-Trautmann et al., 1994; Etienne-Manneville et al., 2000; Tilghman and Hoover, 2002). Src inhibition using the specific inhibitor PP2 (Hanke et al., 1996) has been shown to abolish ICAM-1-mediated phosphorylation of p38 in TNF-α stimulated pulmonary EC, suggesting Src operates upstream of p38 (Wang et al., 2003).

Activation of endothelial Rho in response to ICAM-1 cross-linking mediates many functions including rearrangements of the actin cytoskeleton (Etienne-Manneville et al., 2000). The exoenzyme C3 transferase selectively inactivates the small GTPases RhoA, RhoB, and RhoC, by inducing ADP-ribosylation both *in vivo* and *in vitro* (Aktories and Hall, 1989). The use of C3 transferase in GPNT cells showed that Rho also operates upstream of ICAM-1-induced JNK activation (Etienne et al., 1998).

Other work by Etienne-Manneville and colleagues has shown that ICAM-1-dependent Src activation in GPNT is downstream of a pathway involving PLCγ, PKC and Ca^{2+} (Etienne-Manneville et al., 2000). Specifically, Src activity was inhibited by overnight incubation with the phorbol ester PMA. PMA stimulates PKC activity but long-term exposure of cells leads to downregulation of PKC

activity. GF109203X, a more specific, direct PKC inhibitor, also prevented the activation of Src in the study.

6.2 Aim

ERK, JNK and p38 are activated in response to ICAM-1 ligation and ICAM-1 cross-linking. Previous work suggests that Src and Rho are important for p38 and JNK activation, respectively, but this has not been fully studied within the same model system. The nature of ERK activation has not been investigated either. The aim of this part of the study is to identify whether Src, Rho, PKC or actin dynamics play a role in the activation of ERK, JNK and p38 during ICAM-1 stimulation of GPNT.

6.3 Results

6.3.1 Rho and Src are upstream of ICAM-1-mediated ERK, JNK and p38 activation

GPNT BMVECs were grown to confluency, serum-starved and then pre-treated with 10µg/ml C3 transferase for 12 h. ICAM-1 was subsequently cross-linked for 10 min as described in Chapter 5. Cells were lysed and phosphorylation of MAP kinases analysed by immunoblotting (Figure 6.1). ICAM-1 cross-linking induced ERK, JNK and p38 phosphorylation as previously described. ERK and p38 phosphorylation was not inhibited following pre-treatment with C3 transferase. In contrast, JNK phosphorylation was completely abolished in response to pre-treatment with C3 transferase. These results therefore implied that JNK, but not ERK or p38, was downstream of ICAM-1-induced Rho activation.

I next tested the involvement of Src family kinases. For this, GPNT EC were grown to confluency, serum-starved and pre-treated with 10µM PP2, a small molecule inhibitor specific for Src family kinases (Hanke et al., 1996), for 30 min. Subsequently, ICAM-1 was cross-linked and EC

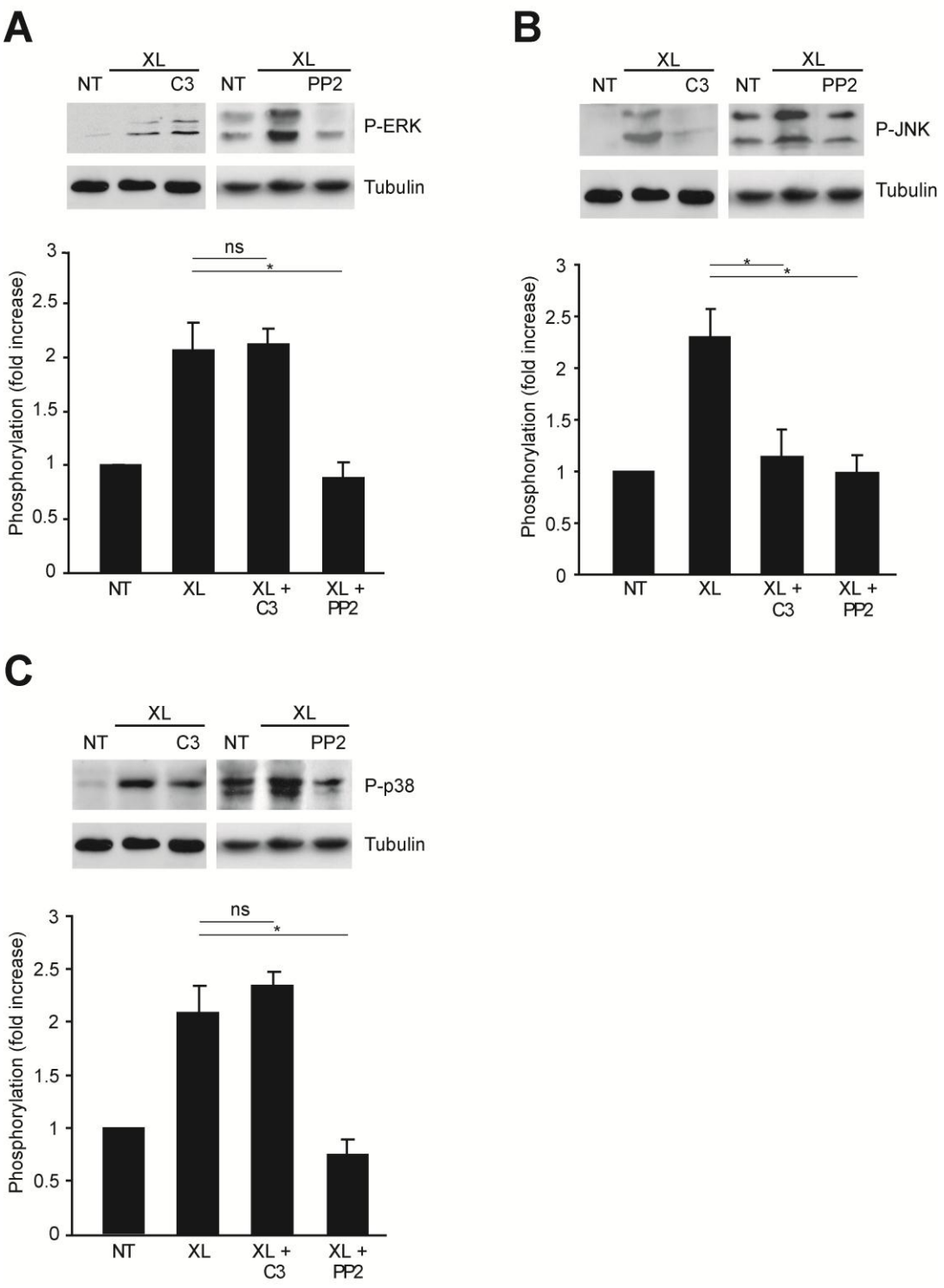

Figure 6.1 Rho and Src family kinase mediate ICAM-1-induced MAP kinase activation

Figure 6.1 figure legends

GPNT were grown to confluency, serum-starved and pre-treated with 10µg/ml C3-transferase for 12 h or 10µM PP2 for 30 min. EC monolayers were washed twice with HBSS and then subjected to ICAM-1 cross-linking for 10 min. Lysates were prepared and phosphorylation of ERK (A), JNK (B) and p38 (C) analysed by immunoblots (as described in Material and Methods and Chapter 5). Densitometric quantifications were derived from at least 3 independent immunoblot analyses, where the phospho-MAP kinase signal was normalised to cell mass (i.e. tubulin signal). Shown are means -/+ SEM. Variances of mean values were statistically analysed by the Student's *t* test. *, $P < 0.05$; **, $0.001<P< 0.01$; ***, $P \leq 0.001$

MAP kinases analysed as described before (Figure 6.1 A-C). Pre-treatment with PP2 abolished ICAM-1-induced phosphorylation of ERK, JNK and p38, suggesting that Src or a related protein kinase acts upstream of ICAM-1-mediated MAP kinase activation.

6.3.2 A PKC is upstream of ICAM-1-mediated ERK and JNK, but not p38 activation

It has been suggested that PKC is involved in ICAM-1-induced Src activation in BMVEC (Etienne-Manneville et al., 2000). I tested the involvement of PKC in ICAM-1-induced MAP kinase activation using PKC isoform selective inhibitors. Table 6.1 shows the three different PKC inhibitors, Gö6976 (Martiny-Baron et al., 1993), GF109203X (Toullec et al., 1991)and Gö6983 (Gschwendt et al., 1996) that were used in this study. Importantly, Gö6976 inhibits the classical isoforms, whilst GF109203X and Gö6983 additionally inhibit the novel and atypical isoforms, respectively.

Table 6.1: Inhibition profile of PKC inhibitors used in study

Compound	PKC isoform inhibited
Gö6976	α, β_I, β_{II}, γ
GF109203X	α, β_I, β_{II}, γ, δ, ε, η, θ
Gö6983	α, β_I, β_{II}, γ, δ, ε, η, θ, ι, ζ

Confluent GPNT ECs were pre-treated for 30 min with 20µM Gö6976, GF109203X or Gö6983 before the effect of ICAM-1 ligation was assessed on MAP kinase phosphorylation (Figure 6.2). ICAM-1-induced ERK and JNK activation was inhibited when EC were pre-treated with Gö6983 (Figure 6.2G and 6.2H) whilst the activation of p38 was not affected (Figure 6.2I). In contrast pre-treatment with Gö6976 and GF109203X did not influence the phosphorylation of ERK, JNK or p38 at all. From this, it can be concluded that an aPKC (PKCι or PKCζ) mediated the activation of ERK and JNK in response to ICAM-1 ligation.

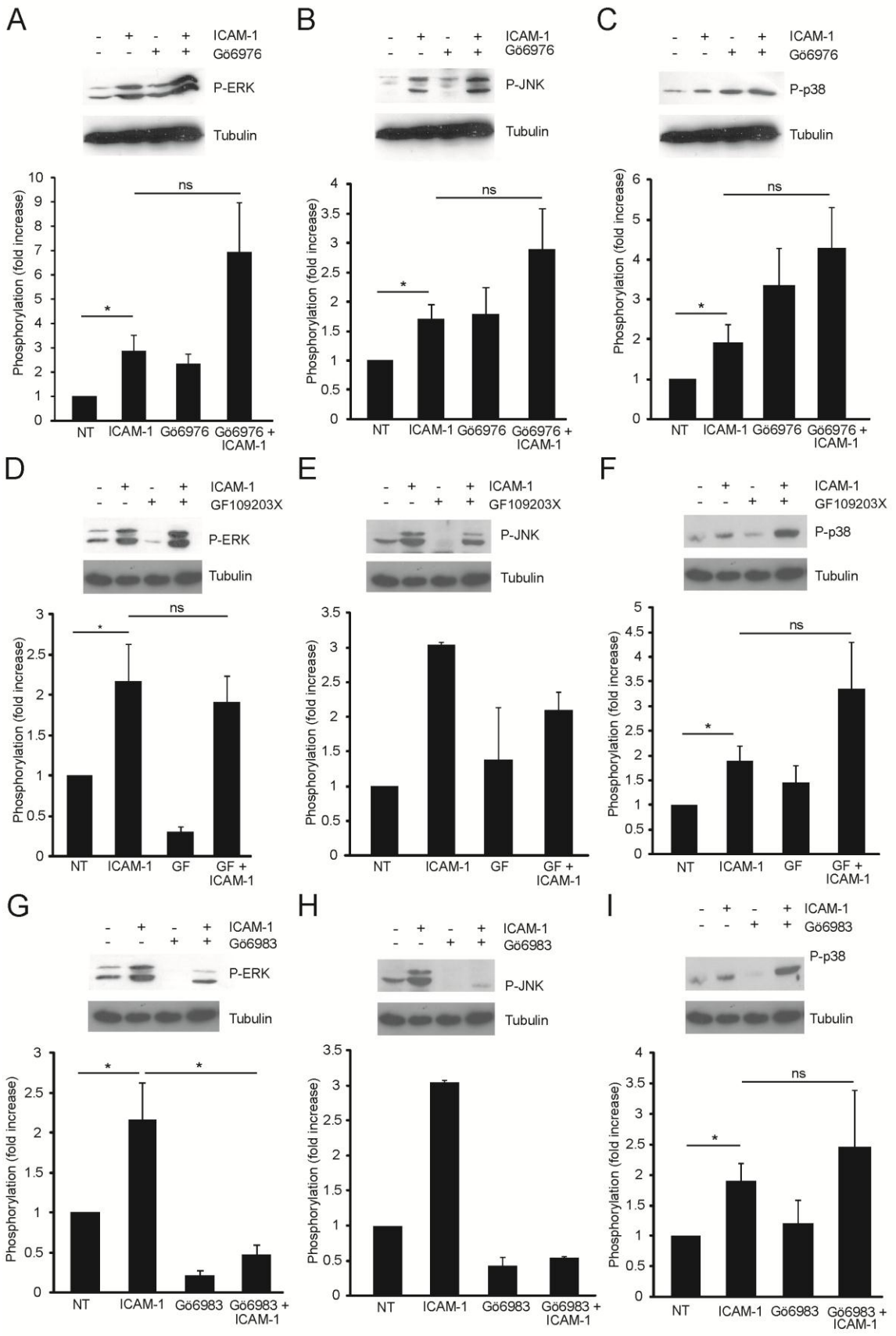
A
ICAM-1
Gö6976
P-ERK
Tubulin
Phosphorylation (fold increase)
ns
*
NT
ICAM-1
Gö6976
Gö6976 + ICAM-1
B
ICAM-1
Gö6976
P-JNK
Tubulin
Phosphorylation (fold increase)
ns
*
NT
ICAM-1
Gö6976
Gö6976 + ICAM-1
C
ICAM-1
Gö6976
P-p38
Tubulin
Phosphorylation (fold increase)
ns
*
NT
ICAM-1
Gö6976
Gö6976 + ICAM-1
D
ICAM-1
GF109203X
P-ERK
Tubulin
Phosphorylation (fold increase)
ns
*
NT
ICAM-1
GF
GF + ICAM-1
E
ICAM-1
GF109203X
P-JNK
Tubulin
Phosphorylation (fold increase)
NT
ICAM-1
GF
GF + ICAM-1
F
ICAM-1
GF109203X
P-p38
Tubulin
Phosphorylation (fold increase)
ns
*
NT
ICAM-1
GF
GF + ICAM-1
G
ICAM-1
Gö6983
P-ERK
Tubulin
Phosphorylation (fold increase)
*
*
NT
ICAM-1
Gö6983
Gö6983 + ICAM-1
H
ICAM-1
Gö6983
P-JNK
Tubulin
Phosphorylation (fold increase)
NT
ICAM-1
Gö6983
Gö6983 + ICAM-1
I
ICAM-1
Gö6983
P-p38
Tubulin
Phosphorylation (fold increase)
ns
*
NT
ICAM-1
Gö6983
Gö6983 + ICAM-1

Figure 6.2 The role of PKC in ICAM-1-induced MAP kinase activation

GPNT were grown to confluency, serum-starved and pre-treated with either 20µM Gö6976, GF109203X or Gö6983 for 60 min. EC monolayers were washed twice with HBSS and then subjected to ICAM-1 ligation for 5 min. Lysates were prepared and phosphorylation of ERK, JNK and p38 analysed by immunoblots as described in Material and Methods and Chapter 5. Densitometric quantifications were derived from at least 3 independent immunoblot analyses, where the phospho-MAP kinase signal was normalised to cell mass (i.e. tubulin signal). Statistical analysis was unable to be carried out for effect of GF109203X and Gö6983 pre-treatment on JNK as data represents 2 independent experiments. Shown are means -/+ SEM. Student's t test was used for statistical analysis of mean value variances. *, $P < 0.05$; **, $0.001<P< 0.01$; ***, $P \leq 0.001$

6.3.3 Actin dynamics control ICAM-1-induced ERK and p38 activation

A number of studies have shown that actin re-arrangements are a primary EC response to leukocyte adhesion or ICAM-1 engagement (Etienne et al., 1998; Adamson et al., 1999; Wojciak-Stothard et al., 1999; Etienne-Manneville et al., 2000; Wang and Doerschuk, 2001; Millan et al., 2006) and EC actin is undoubtedly an important regulator of TEM (Carman et al., 2003; Carman and Springer, 2004). I used cytochalasin D (Cyto D), an inhibitor of actin polymerisation (Brenner and Korn, 1979), to assess the importance of actin dynamics on MAP kinase activation. Serum-starved GPNT EC monolayers were pre-treated using Cyto D for 30 min. ICAM-1 ligation was performed, lysates were prepared and MAP kinase phosphorylation analysed by immunoblots as described before. ERK and p38 phosphorylation was strongly inhibited following pre-treatment with Cyto D (Figure 6.3A). In contrast, ICAM-1-induced JNK activation was not affected (Figure 6.3B). It can be concluded that actin dynamics played an important role in ICAM-1-induced ERK and p38 but not JNK activation.

6.4 Discussion

To understand the interconnection and divergence of ICAM-1-mediated networks I studied MAP kinase activation in relation to previously described mediators of ICAM-1 signalling, namely Src, actin dynamics, Rho and PKC (Etienne et al., 1998; Adamson et al., 1999; Etienne-Manneville et al., 2000; Carman et al., 2003; Carman and Springer, 2004; Millan et al., 2006; Yang et al., 2006b). Actin dynamics were inhibited using Cyto D, which specifically prevents actin polymerisation. To expand these studies, other actin targeting drugs could be used such as jasplakinolide, which has been shown to disrupt filaments (Bubb et al., 1994), or blebbistatin, which inhibits actin myosin II-dependent contractility (Straight et al., 2003). To inhibit the function of Src and PKC, I used small molecule inhibitors, which have been shown to display high selectivity for their target molecules. However, specificity for a single protein kinase is rare (Bain et al., 2007), and accordingly PP2 has been shown to inhibit Src and Src family kinases Lck, Fyn and Hck, (Hanke et al., 1996) whilst the PKC inhibitors used show specificity for range of family members (see Table 6.1). Inhibition of Rho GTPases was achieved using C3 transferase. Again related family members,

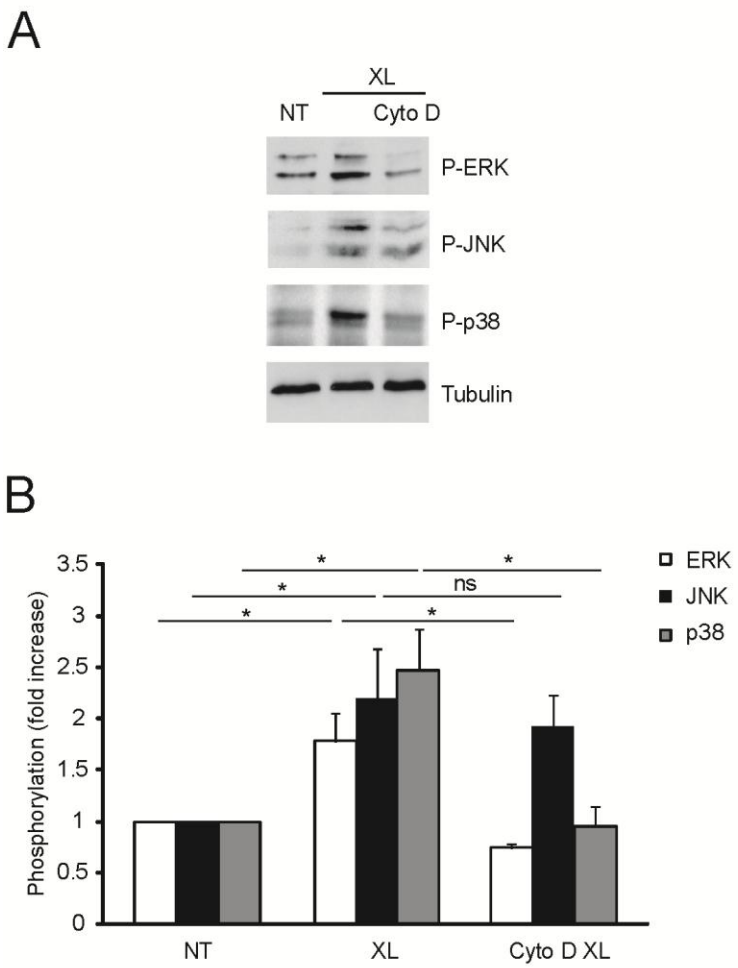

Figure 6.3 Actin dynamics are important for ICAM-1-induced ERK and p38 but not JNK activation

(A) GPNT were grown to confluency, serum-starved and pre-treated with 2µM Cyto D for 30 min. EC monolayers were washed twice with HBSS and then subjected to ICAM-1 cross-linking for 10 min. Lysates were prepared and phosphorylation of ERK, JNK and p38 analysed by immunoblots as described in Material and Methods and Chapter 5.

(B) Densitometric quantification immunoblot analysis was derived from 3 independent experiments including (A). The phospho-MAP kinase signal was normalised to cell mass (i.e. tubulin signal). Shown are means -/+ SEM. Statistical analysis carried out using the Student's t test for variance of mean values. *, $P < 0.05$; **, $0.001<P< 0.01$; ***, $P \leq 0.001$

namely Rho A, B, and C, are sensitive to C3 transferase treatment (Aktories and Hall, 1989). If more specific, and most importantly isoform-specific, inhibition was to be studied small interference RNA would need to be used.

Activation of all three MAP kinases was sensitive to PP2 (or SU6656, data not shown), indicating that Src tyrosine kinase family members are central to ICAM-1 signalling (Figure 6.1). Our data also corroborated previous data showing that Src family kinase was required for p38 activation following ICAM-1 cross-linking of pulmonary MVEC (Wang et al., 2003). Indeed, the involvement of Src family kinase has been demonstrated in many studies of ICAM-1 related signalling and TEM (Tilghman and Hoover, 2002; Yang et al., 2006b; Allingham et al., 2007; Liu et al., 2011). Src family kinases operate very early following ICAM-1 stimulation (Durieu-Trautmann et al., 1994) and could even operate on the level of ICAM-1 phosphorylation itself (Pluskota et al., 2000). Taken together, Src appears to operate early during ICAM-1-induced signalling, regulating many divergent pathways, in particular ERK, JNK and p38.

Beyond Src, as a common signalling denominator, divergence arose (see Figure 6.4). In particular, JNK activation was clearly different from that of ERK and p38. JNK was unique amongst the three MAP kinase as it was shown to be inhibited by C3 transferase, a finding which agrees with a previous study in BMVEC (Etienne et al., 1998). To find Rho as an upstream activator of JNK activity is unusual since in most cases Cdc42 or Rac have been implicated (Marinissen and Gutkind, 2005). Under certain conditions, Rho-dependent activation of the JNK MAP kinase cascade can occur and appears to be primarily mediated by the guanine nucleotide exchange factors Net1 and p115RhoGEF, and the scaffolding protein CNK1 (Alberts and Treisman, 1998; Jaffe et al., 2005) (see also Chapter 9). Future studies will establish whether this ‘non-canonical’ pathway is also involved in mediating ICAM-1 signalling in BMVECs.

The activation of p38 and ERK, but not JNK, was sensitive to actin polymerisation. It is noteworthy that Rho (i.e. C3 transferase sensitive) activity was not required. This suggests that the EC stress fibres frequently reported to be induced following ICAM-1 stimulation (Adamson et al., 1999; Wojciak-Stothard et al., 1999; Millan et al., 2006) are not involved in the activation of p38 or ERK. Instead, the actin-dependent activation of p38 and ERK could be related to our observation that anti-ICAM-1 beads induce luminal surface ruffles (see Chapter 3), which normally are Rac-dependent. Conversely, Rho-dependent activation of JNK did not require actin polymerisation,

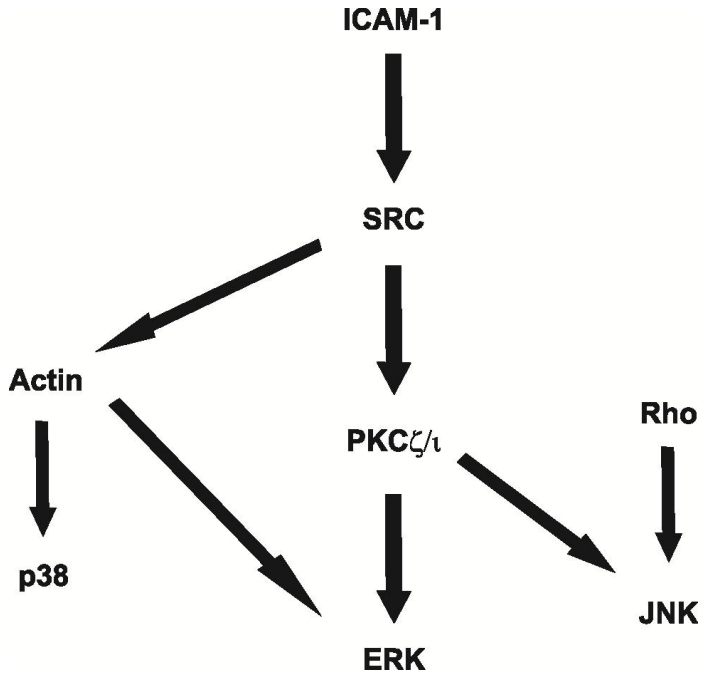

Figure 6.4 Hypothetical signal divergence at the level of Src for MAP kinase activation in response to ICAM-1 stimulation in BMVEC

suggesting that here the GTPase acted directly on the organisation or activation of a MAP kinase.

Results using three different PKC inhibitors also agree with the idea that there is divergence in MAP kinase activation (Figure 6.3). The universal PKC inhibitor, Gö6983 which inhibits all PKC isoforms apart from PKCμ, impacted on the ICAM-1-induced activation of ERK and JNK but not p38. Gö6976 or GF109203X, inhibitors of cPKC or nPKC, respectively, did not affect the activation of any of the three MAP kinases, implying that an aPKC, either PKCι and/or PKCζ was involved in ERK and JNK activation. In contrast lymphocyte migration is sensitive to inhibition with GF109203X (Etienne-Manneville et al., 2000). This strongly suggests an additional GF109203X-sensitive PKC operates either downstream of MAP kinases or entirely independently of MAP kinase during TEM (see also Chapters 7 and 9).

The divergence in signalling from ICAM-1 to MAP kinases strongly suggests that each MAP kinase is involved in a different function within the EC. Given the individual requirements for actin polymerisation differential intracellular localisation of MAP kinase activation is very likely as well. Future studies should focus on determining the intracellular localisation of activated MAP kinase cascades. This could be achieved using bead-coupled rather than soluble antibodies. Furthermore, studies interrogating the functional role of ICAM-1-induced MAP kinase, such as the regulation of gene expression or of lymphocyte migration (see Chapter 7) should be conducted.

Chapter 7: Involvement of ICAM-1-mediated signalling in TEM

7.1 Introduction

The results from Chapters 5 and 6 showed that ICAM-1 stimulation triggered MAP kinase activation with Src, Rho, the actin cytoskeleton and PKC involved upstream of the MAP kinase. As discussed in Chapter 1, endothelial ICAM-1 and downstream signalling makes an essential contribution to leukocyte TEM (reviewed in: Turowski et al., 2005). However, endothelial ICAM-1 signalling also regulates functions which are not directly involved in TEM.

ICAM-1-mediated signalling is important for gene expression. For instance, ICAM-1 engagement can activate the transcription factor AP-1 leading to transcription of IL-1β (Koyama et al., 1996) and ERK-dependent VCAM-1 expression (Lawson et al., 1999). ICAM-1-induced activation of ERK also leads to the induction of IL-8 and RANTES production (Sano et al., 1998).

Another role contributed to ICAM-1 engagement is the regulation of endothelial permeability (Williams and Luscinskas, 2011). ICAM-1-induced permeability arises in response to the interaction formed with its counter β_2 integrin receptor on leukocytes (Sumagin et al., 2008; DiStasi and Ley, 2009) or ICAM-1 antibody ligation (Sumagin et al., 2011). Rolling and adherent leukocytes (Sumagin et al., 2008) which often secrete factors such as neutrophil elastase, ROS and cytokines (DiStasi and Ley, 2009) that lead to localised permeability increases. ICAM-1 cross-linking is sufficient to induce increases in permeability in the absence of leukocyte adhesion and the subsequent activation of EC signalling, even in arterioles which normally are unable to support EC-leukocyte interactions (Sumagin et al., 2011). Increased permeability does not occur following cross-linking of VCAM-1. Different signalling pathways regulate permeability depending on the inflammatory status and degree of ICAM-1 engagement on the endothelium (Williams and Luscinskas, 2011). Dermal MVEC TEER can be altered by expression levels of ICAM-1 which can alter the actin cytoskeleton, TJ and AJ proteins (Clark et al., 2007).

A number of protein kinase signalling pathways have been shown to be involved in endothelial permeability modulation including PKC, Src and the MAP kinases ERK and p38 (Yuan, 2002) which have all been shown to be activated downstream of ICAM-1 engagement (Chapter 6).

Many of the effects are mediated either directly by phosphorylation of other proteins such as FAK, myosin light chain kinase (MLCK) or ERM proteins or indirectly acting on other protein kinases (Yuan, 2002; Koss et al., 2006).

Some of the signal transducers identified in Chapter 5 and 6 have previously been shown to be important in ICAM-1-mediated leukocyte TEM. Neutrophil transmigration across a HUVEC monolayer is significantly inhibited when pre-treated with the Src inhibitors PP2 or SU6656 (Yang et al., 2006b; Allingham et al., 2007). Src plays a role in the adhesion of THP-1 cells to HUVECs and ICAM-1 mediates Src -dependent phosphorylation of cortactin (Tilghman and Hoover, 2002). ICAM-1-mediated cortactin phosphorylation induces actin cytoskeletal changes and facilitates neutrophil TEM across cytokine-stimulated HUVEC monolayers (Yang et al., 2006a; Yang et al., 2006b).

Inhibition of Rho GTPase following pre-treatment of BMVEC with C3 transferase inhibits lymphocyte transmigration (Adamson et al., 1999). Both clustering of cell surface adhesion molecule and monocyte adhesion and spreading is dependent on Rho activity (Wojciak-Stothard et al., 1999). Surprisingly, the endothelial projections that form in response to leukocyte adhesion to the endothelial surface do not require Rho (Carman et al., 2003) although Rac or Cdc42 are important for the transcellular pore formation and subsequent TEM (Carman and Springer, 2004). Another Rho GTPase, RhoG, has also been shown to be important for both the formation of the docking structure and leukocyte TEM acting downstream of RhoA (van Buul et al., 2007a).

The regulation of leukocyte TEM by endothelial actin and actin-based contractility have been extensively studied (reviewed by: Millan and Ridley, 2005). Actin has also been shown to the main cytoskeletal regulator of the transmigration cup and is found enriched in the ICAM-1 projections that form upon leukocyte adhesion, the structural equivalent to committed TEM (Carman et al., 2003; Carman and Springer, 2004; Millan et al., 2006). Inhibition of TEM (Adamson et al., 1999) and adhesion of leukocytes (Wojciak-Stothard et al., 1999) occurs in response to pre-treatment of the endothelium with Cyto D.

PKCs have also been implied to be important in lymphocyte transmigration across BMVEC (Etienne-Manneville et al., 2000). Lymphocyte adhesion to endothelial VCAM-1 generates ROS that activates PKCα involving PTP-1B which is important for TEM (Deem et al., 2007). PKC, acting via a pathway involving RhoA and Src, can also induce actin reorganisation (Brandt et al., 2002).

Of the three MAP kinases, only p38 has been shown to have a role in ICAM-1-mediated TEM. Wang *et al*. show p38 plays a role in the migration of neutrophils to junctions of pulmonary MVEC (Wang and Doerschuk, 2001). Whether p38 inhibition results in inhibition of actual TEM rates has not been addressed in this study. ERK has been proposed to play a role in neutrophil TEM (Stein et al., 2003) although this has not been shown to be dependent upon ICAM-1 engagement.

7.2 Aim

The main aim of this part of the study is to determine whether ICAM-1-mediated activation of the three MAP kinases, ERK, JNK and p38, is involved in TEM. This analysis will be extended to their upstream mediators of MAP kinases, as defined in Chapter 6.

7.3 Results

7.3.1 Endothelial JNK and its upstream kinase, MKK7, regulate lymphocyte transendothelial migration

To analyse whether MAP kinase activation in EC was required for successful lymphocyte migration, GPNT EC were grown to confluency and co-cultured with migratory myelin basic protein-specific IL-2 activated T lymphocytes (PAS) (Beraud et al., 1993). Diapedesis was assessed by time-lapse video microscopy as described in Chapter 2 (Section 2.2.3). Prior to adding T-lymphocytes, GPNT EC were pre-treated with three different kinase inhibitors: UO126 (which inhibits the ERK activating kinase MEK) (Favata et al., 1998), SP600125 (which shows some specificity for JNK) (Bennett et al., 2001) and SB202190 (which is highly specific inhibitor for p38α and β) (Lee et al., 1994). Concentration of treatment was set to 50μM for 1 h, conditions which have been shown to strongly inhibit the respective kinase in GPNT during the treatment and for at least 30 min after withdrawal (including washing of the cells) (R. Blaber and P. Turowski, unpublished results). After 1 h of pre-treatment, inhibitors were washed off to avoid the possibility

of affecting T-lymphocyte function. Then PAS were added and allowed to migrate for 1 h prior to assessing migration rates. Inhibition of ERK and p38 using UO126 and SB202190 did not affect transmigration of lymphocytes (Figure 7.1, black bars). In contrast, pre-treatment of GPNT with SP600125 reduced transmigration of lymphocytes to approximately 40% of control levels, suggesting that JNK, but not ERK or p38, was involved in regulating TEM. SP600125 only inhibited diapedesis not adhesion of lymphocytes to EC (Figure 7.1, grey bars).

SP600125 strongly inhibits JNK *in vitro* and in living cells but has been shown recently to inhibit a variety of other protein kinases, suggesting that SP600125 may not be as specific for JNK as previously thought (Bain et al., 2007). To corroborate a role of JNK in lymphocyte transmigration dominant-negative MAP kinase components were expressed in GPNT. GPNT were transfected using wild-type and dominant-negative versions of MAP kinase kinase 7 (MKK7), one of the specific JNK activating kinases (Yao et al., 1997), and of JNK1/2 plasmids (as described in Section 2.2.2). Two days post-transfection migration was assessed by the standard method described above and in Chapter 2 (Section 2.2.3). Expression of dominant-negative but not wild-type MKK7 and JNK1 significantly reduced migration by around 60% of control levels, similar to what was observed with SP600125 (Figure 7.2, black bars). JNK2 expression did not significantly alter lymphocyte diapedesis, suggesting that JNK1 and one of its activating kinases MKK7 were an important part of ICAM-1-mediated TEM. Again adhesion was not significantly affected by expressing any of the kinases (Figure 7.2, grey bars).

7.3.2 Endothelial Src and Rho are involved in ICAM-1-mediated lymphocyte transmigration

Src and Rho were identified as upstream regulators of JNK (Chapter 6). Both have previously been shown to regulate TEM (Adamson et al., 1999; Greenwood et al., 2003b; Yang et al., 2006b; Allingham et al., 2007). Next, I wanted to confirm that Src and Rho played a role in lymphocyte migration in our model system. GPNT EC monolayers were pre-treated with either 10µg/ml C3 transferase for 16 h or 10µM PP2 for 1 h (Figure 7.3, black bars). Inhibition of Rho using C3 transferase resulted in an 80% inhibition of PAS transmigration, whilst pharmacological inhibition of Src reduced transmigration by 40%, corroborating that both Rho and Src are involved in regulation of ICAM-1-mediated lymphocyte transmigration. Adhesion was not significantly

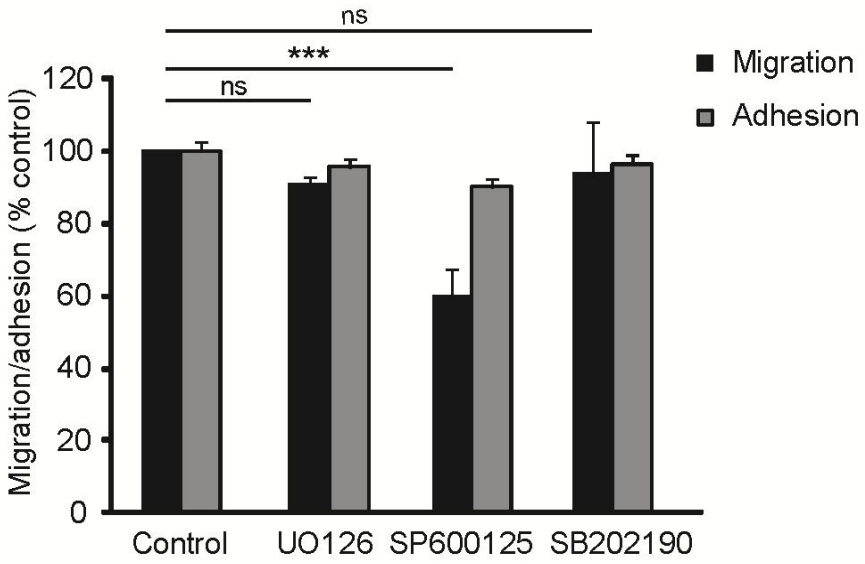

Figure 7.1 Effect of endothelial MAP kinase inhibition on leukocyte transmigration

GPNT cells were grown to confluency in wells of a 96 well plate and then treated with either 50μM UO126 (ERK), SP600125 (JNK), and SB202190 (p38), for 1 h. The cells were washed twice with HBSS before PAS lymphocyte were added. These were left to migrate for 1 h before one field per well was analysed by time-lapsed microscopy. Video recordings were analysed and quantified comparing the number of cells that had migrated under the endothelium to the number that were found above (black bars). Adhesion (grey bars) was analysed by measuring the adhesion of concanavalin-A stimulated PLNs to GPNT pre-treated or not as specified for the migration assay. Values for migration and adhesion are expressed as mean percentages of control from at least 4 independent experiments +/- SEM. Variances of mean values were statistically analysed by the Student's t test. *, $P < 0.05$; **, $0.001<P< 0.01$; ***, $P \leq 0.001$

Adhesion data was kindly provided by Patric Turowski.

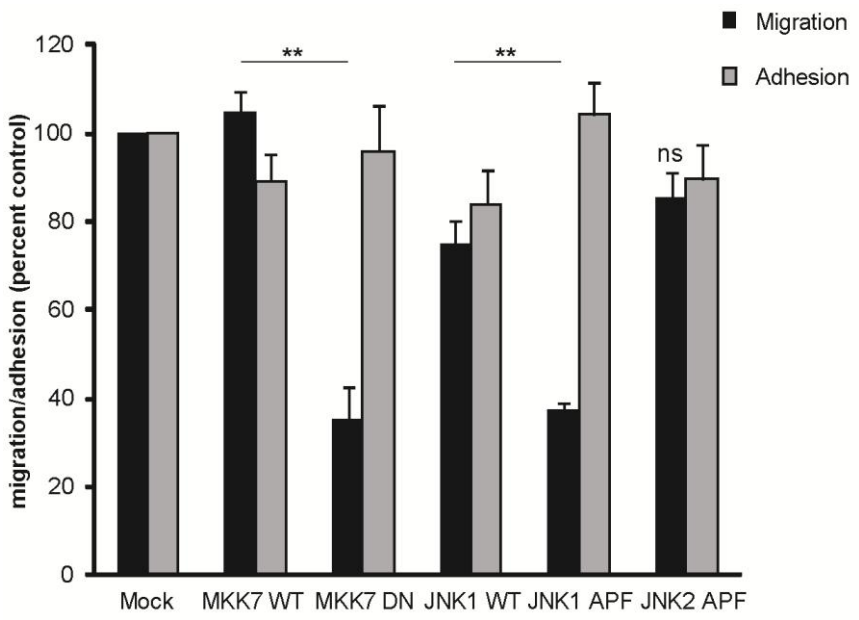

Figure 7.2 Endothelial MKK7 and JNK1 are involved in lymphocyte transmigration

GPNT were nucleofected with 10µg of either wild-type or dominant-negative MKK7, JNK1 or JNK2 and plated into a 96 well plate. Migration (black bars) was assessed as described in Figure 7.1. Adhesion (grey bars), following nucleofection, was determined by comparing the average total number of PAS in the field of view for each transfection. Average values for both migration and adhesion are expressed as a percentage of mock control from 3 independent experiments +/- SEM. Variances of mean values were statistically analysed by the Student's t test. *, $P < 0.05$; **, $0.001<P< 0.01$; ***, $P \leq 0.001$

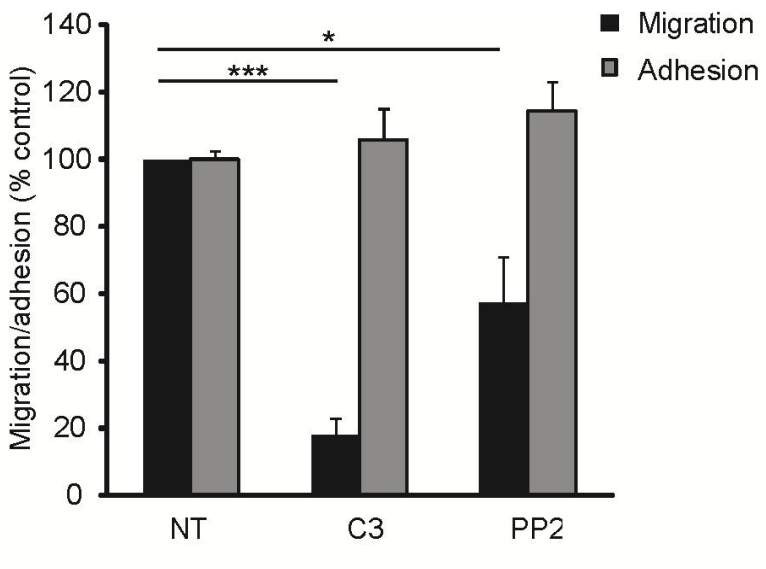

Figure 7.3 Endothelial Src and Rho are important for leukocyte transmigration

GPNT cells were grown to confluency in wells of a 96 well plate and then pre-treated or not with 10µg/ml C3 transferase (Rho) for 16 h or 10µM PP2 (Src) for 1 h. Lymphocyte migration (black bars) and concanavalin-A stimulated PLN adhesion (grey bars) was analysed as described in Figure 7.1. Values are expressed as percentage of control from 3 independent experiments +/- SEM. Variances of mean values were statistically analysed by the Student's t test. *, $P < 0.05$; **, $0.001<P< 0.01$; ***, $P \leq 0.001$

Migration and adhesion data for C3 transferase was kindly provided by Patric Turowksi.

affected by inhibition of Rho or Src (Figure 7.3, grey bars).

7.3.3 PKC isoforms involved in transmigration

PKC family members are involved in lymphocyte transmigration across rat BMVEC. This has been conclusively shown using GF109203X (Etienne-Manneville et al., 2000). I found that Gö6983 but not Gö6976 or GF109203X inhibited ICAM-1-induced MAP kinase activation (Chapter 6) and wanted to determine if they had a similar effect on lymphocyte transmigration. GPNT monolayer was pre-treated with 20μM Gö6976, GF109203X or Gö6983 for 1 h before the PAS migration was assessed (Figure 7.4A). Migration was inhibited following pre-treatment with any of the three compounds to at least 54% of control levels, indicating that at least one PKC isoform was involved in TEM (see discussion). The universal PKC inhibitor Gö6983 did not have an effect on adhesion (Figure 7.4B); demonstrating TEM was inhibited on the level of diapedesis.

7.3.4 JNK and PKC are important for lymphocyte transmigration across primary rat BMVEC

Next I wanted to corroborate the role of endothelial PKC and JNK during TEM across primary rat BMVECs. Cells were isolated from rat brains and grown to confluency (as described in Section 2.2.1.3). Primary rat BMVECs were then pre-treated using Gö6983 and SP600125 as described before and PAS migration rates were assessed. Similarly to our results using GPNT, migration was inhibited by 63% and 60% following pre-treatment using SP600125 and Gö6983, respectively (Figure 7.5).

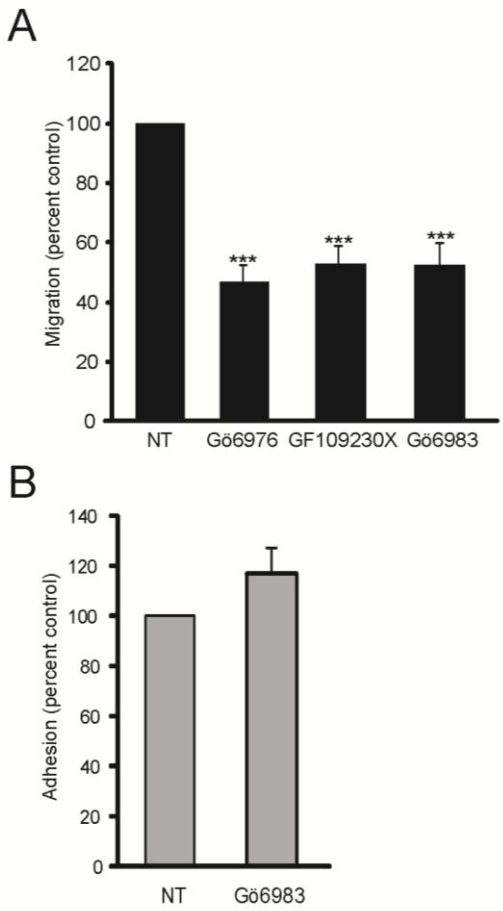

Figure 7.4 PKC is involved in lymphocyte migration

(A) GPNT cells were grown to confluency in wells of a 96 well plate and then treated in presence or absence of 20μM Gö6976, GF109203X or Gö6983 for 1 h. Migration was analysed as previously described in Figure 7.1 and data from 4 independent experiments was expressed as means -/+ SEM.

(B) Confluent GPNT were either left untreated (NT) or pre-treated using 20μM Gö6983 for 1 h. Subsequently PLN adhesion was assessed as described in Figure 7.1. Shown are means -/+ SEM from 3 independent experiments.

Variances of mean values were statistically analysed by the Student's t test. *, $P < 0.05$; **, $0.001<P< 0.01$; ***, $P \leq 0.001$

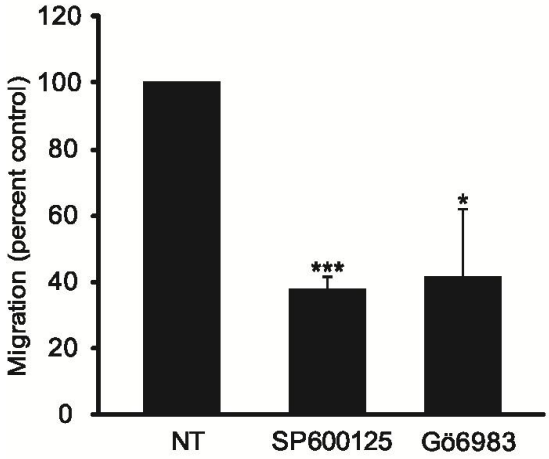

Figure 7.5 Endothelial JNK and PKC are involved in TEM across primary rat BMVEC

Primary rat BMVEC were grown to confluency and PAS transmigration assessed as described for GPNT (Figure 7.1). Prior to addition of T-lymphocytes, the EC were pre-treated with 50μM SP600125 or 20μM Gö6983 for 1 h. Shown are mean migration rates +/- SEM from 3 independent experiments. Student's t test was used for statistical analysis of mean value variance, * $P < 0.05$; ** $0.001<P< 0.01$; ***, $P \leq 0.001$

7.4 Discussion

Here, I showed that ICAM-1-induced JNK, but not ERK or p38, played a key role in lymphocyte transmigration across established or primary BMVECs. This was surprising as it has been reported previously that ERK (Stein et al., 2003) and p38 (Wang and Doerschuk, 2001) are important for neutrophil transmigration. To our knowledge, this is the first report, which implicates endothelial JNK in leukocyte TEM. Involvement of JNK was confirmed by the use of SP600125 and the expression of dominant-negatives of JNK1 and MKK7. In fact the latter experiment did not only provide additional specificity but also indicated that the pathway regulating TEM consists of MKK7 and JNK1 rather than JNK2. The expression of JNK1 and MKK7 dominant-negative inhibited migration to similar levels as seen following EC pre-treatment with SP600125 and hence it is unlikely another SP600125-sensitive kinase, other than JNK, is involved in lymphocyte TEM. Therefore, this experiment justifies the simple use of SP600125 for all future investigations into the involvement of JNK since if another kinase was involved SP600125 would result in greater inhibition than that seen with the dominant-negative expression of JNK1 and MKK7. Furthermore, mediators of ICAM-1-induced activation of JNK as defined in Chapter 6 were also found to be essential for TEM, namely Src family kinases, Rho GTPase and Gö6983-sensitive PKC. In light of publications by Wang *et al.* (Wang and Doerschuk, 2001; Wang et al., 2003) I was surprised not to find an involvement of p38. This discrepancy may reflect a difference of signalling in pulmonary MVEC and BMVEC. Alternatively, Wang *et al*. conducted their study in cytokine- stimulated ECs whilst our analysis focused on TEM across resting, unstimulated EC monolayers. Thus, endothelial p38 may play a differential role during TEM depending on the vascular or inflammatory environment. Unpublished work from our laboratory suggests that ERK and p38 activation is important for inflammatory gene expression and message stabilisation (R. Blaber, Y. Gill and P. Turowski, unpublished).

In line with previous reports, inhibition of Rho using C3 transferase resulted in the greatest inhibition of lymphocyte transmigration (Adamson et al., 1999; Greenwood et al., 2003b). Inhibition of endothelial Src, PKC or JNK reduced TEM to similar levels (by ca. 40 to 50 %). Our data for Src inhibition is in agreement with a recent report showing a similar effect of endothelial Src inhibition on migration of neutrophils across HUVECs (Yang et al., 2006b; Allingham et al., 2007). The only previous study using PKC inhibitors on EC during TEM does not report as strong an

inhibition by GF109203X as I observed (Etienne-Manneville et al., 2000). Our experimental protocol may explain this notable difference: the effect of protein kinase inhibitors targeting the ATP-binding sites is rapidly lost from GPNT as soon as drugs are withdrawn from the culture medium (P. Turowski, unpublished data), presumably due to the presence of highly active drug efflux pumps (Demeuse et al., 2004). Therefore I used higher, but tolerable, drug concentrations and performed the TEM assay within 1 h of withdrawal of the drug, a time when kinase inhibition was still at least 30-50% compared to when the drug was left in the culture medium. Etienne-Manneville *et al.* performed the TEM assay 4 h after withdrawal of PKC inhibitors and may therefore have observed a less potent inhibition of TEM (Etienne-Manneville et al., 2000).

Overall the question remained, why Src, PKC or JNK inhibition led to less potent reduction of TEM as when e.g. Rho GTPase was inhibited using C3 transferase or when ICAM-1 is neutralised using antibodies (Greenwood et al., 1995). For the reason detailed above protein kinase inhibition using ATP-binding site inhibitors was never complete. Even when dominant-negative plasmids were transfected targeting was well below 100% due to limited transfectability of GPNT (on average 60%). Inhibition using C3 transferase or ICAM-1 antibodies presumably induces more complete inhibition since they induce covalent modification or tight binding neutralization, respectively. Alternatively, signalling from other adhesion molecules on the EC have been shown to contribute to TEM (Matheny et al., 2000; Adamson et al., 2002; Mamdouh et al., 2003; van Wetering et al., 2003; Deem and Cook-Mills, 2004; Mamdouh et al., 2008; Mamdouh et al., 2009; Woodfin et al., 2009; Steiner et al., 2010) and may even compensate for the loss of ICAM-1-mediated signalling. Importantly, the use of primary rat BMVEC corroborated the inhibitory effect of SP600125 and Gö6983 on TEM (Figure 7.5), demonstrating that it was not an artefact linked to the immortalised GPNT cell line.

Unexpectedly, all three PKC inhibitors inhibited lymphocyte transmigration to similar levels even Gö6976 and GF109203X which did not have an effect on ICAM-1-JNK signalling (Chapter 6). ICAM-1-JNK signalling was exclusively sensitive to Gö6983, which inhibits also aPKCs in addition to cPKCs and nPKCs, suggesting that either PKCι or PKCζ are involved in the activation of JNK. This suggests that other endothelial PKCs either classical and/or novel are involved in TEM. They could operate in parallel to the ICAM-1-JNK pathway or act downstream of it. Recently, Martinelli *et al*. identified a pathway ICAM-1-induced eNOS activation to VEC phosphorylation (Martinelli et al., 2009). Since this pathway is Ca^{2+}-dependent it is possible that cPKC family members could be

involved. To further investigate which particular PKC isoform(s) are involved more specific tools would need to be utilised. This might be achieved using PKC inhibitors that inhibit only one isoform rather than a whole family, for example the PKCβ specific inhibitor ruboxistaurin (also known as LY333531), or RNAi.

In conclusion, I have shown that endothelial JNK and important upstream regulators are essential for ICAM-1-mediated lymphocyte transmigration. Our results point to an involvement of PKCs at several distinct points of ICAM-1-mediated endothelial compliance to TEM. In fact, our data clearly demonstrates the existence of ICAM-1-induced signalling pathway which has yet to be characterised: in addition to another PKC, Rho-independent actin dynamics have been shown to be important for TEM (Adamson et al., 1999; Carman et al., 2003) but not JNK activation. At this point, it was still unclear what the potential downstream targets of ICAM-1-JNK were and how activation of JNK leads to endothelial compliance to lymphocyte transmigration.

Chapter 8: Paxillin as downstream effector of the ICAM-1-induced JNK pathway

8.1 Introduction

As shown in Chapters 5-7, JNK is an important mediator of endothelial ICAM-1 signalling and of lymphocyte TEM. The downstream target of JNK in this process is unknown. Previously it has been shown that cross-linking of ICAM-1 in BMVEC leads to Rho-dependent tyrosine phosphorylation of the focal adhesion proteins paxillin, FAK and p130Cas (Etienne et al., 1998). Since actin cytoskeletal rearrangements are also important for ICAM-1-mediated TEM (Adamson et al., 1999) and paxillin is a prominent target of JNK (Bogoyevitch and Kobe, 2006), paxillin could be a downstream effector of the ICAM-1-JNK pathway.

Paxillin is a cytoplasmic protein that localises to focal adhesions, primarily to sites of cell adhesion, providing a structural link between the actin cytoskeleton and the ECM (Turner, 1998; Turner, 2000b; Deakin and Turner, 2008). In higher eukaryotes paxillin is found in 3 alternate spliced isoforms, with the principal alpha isoform having a more ubiquitous expression profile than beta or gamma (Schaller, 2001; Brown and Turner, 2004). Paxillin is highly conserved between species, with 90 percent identity found between human and chicken (Turner, 2000a).

Paxillin function is clearly important since mice lacking paxillin are embryonically lethal (Deakin and Turner, 2008). Cells deficient in paxillin have an altered actin cytoskeleton and are unable to spread and migrate normally (Webb et al., 2004). In fact, paxillin has many functions within different cell types which are mediated by multiple protein-protein interaction sites. Paxillin acts as a multi-domain scaffold protein which can interact with numerous structural and signalling proteins including FAK, Src and α_4 integrins (Liu et al., 1999; Turner, 2000b; Deakin and Turner, 2008). The C-terminus of paxillin contains LIM domains that mediate protein-protein interactions and localisation to both the actin cytoskeleton and focal adhesion (Turner, 1998; Brown and Turner, 2004; Deakin and Turner, 2008). Within the N-terminus of paxillin 5 leucine- and aspartate-rich (LD) motifs are present which control most of the signalling activity of paxillin (Brown and Turner, 2004). The LD motifs are specific interaction sites for particular proteins, for

example the LD2 domain provides an interaction site for vinculin, FAK and Pyk2. Paxillin can bind to α_4 integrin and this interaction is important for establishing cell adhesion under conditions of shear stress (Rose, 2006; Manevich et al., 2007) as well as enhancing rates of cell migration (Liu et al., 1999). It has been proposed that paxillin promotes the disassembly of focal adhesion at the leading edge (Deakin and Turner, 2008) or invadopodia (Badowski et al., 2008) thus promoting cell migration.

Phosphorylation of paxillin plays a major role in recruiting signalling components in mediating interactions with focal adhesions and the cytoskeleton (Turner, 1998; Brown and Turner, 2004; Deakin and Turner, 2008). For instance, focal adhesions actively mediate integrin signalling following paxillin phosphorylation in response to cell adhesion (Burridge et al., 1992a; Burridge et al., 1992b; Schaller, 2001; Deakin and Turner, 2008). Consequently, multiple tyrosine, serine and threonine residues of paxillin can be phosphorylated by a plethora of protein kinases, including Src, FAK and members of the MAP kinase family (Deakin and Turner, 2008). Key sites on paxillin involved in its functional activation are Y31 and Y118 which are phosphorylated by FAK and Src (Turner, 1998). In addition, JNK has been shown to phosphorylate S178 (Bogoyevitch and Kobe, 2006).

Paxillin has a central role in co-ordinating and regulating Rho GTPase signalling by indirectly recruiting GEFs, GAPs, small GTPases and other effector proteins (reviewed by: Deakin and Turner, 2008). This is in part mediated by phosphorylation of paxillin. For instance, the adaptor protein CrkII can bind to phosphorylated Y31 and Y118 in response to integrin binding to fibronectin or collagen. This then promotes Rac1-dependent relocalisation of paxillin to focal contacts (Lamorte et al., 2003). Modulation of Rac and Rho signalling can also facilitate the role of paxillin in EC barrier regulation in response to protective or disruptive growth factors (Birukova et al., 2007). Paxillin may also be recruited to sites where FAK and Src are found to interact with ERK which in turns regulates contractility mediated by MLCK (Webb et al., 2004; Deakin and Turner, 2008; Huveneers and Danen, 2009).

Paxillin phosphorylation at residues S178, Y31 or Y118 is important for cell migration in a number of model systems, including normal rat kidney (NRK) cells and human corneal epithelial (HCE) cells (Huang et al., 2003; Kimura et al., 2008; Huang et al., 2008; Rosse et al., 2009). Enhanced migration following phosphorylation has been observed in a number of cell types (Zaidel-Bar et al., 2007) including HCE cells after induction with EGF (Huang et al., 2008). Activated

JNK co-localises with paxillin at focal adhesions in wound margins (Kimura et al., 2008) and pre-treatment of keratocytes and NBT-II cells with SP600125 inhibits migration (Huang et al., 2003). Expression of a non-phosphorylatable mutant of paxillin, S178A, markedly reduces paxillin phosphorylation by MKK7-activated JNK (Huang et al., 2003) and inhibits migration (Huang et al., 2004). PKC is important for JNK-mediated phosphorylation of paxillin in NRK cells and migration as large static focal adhesions form when aPKC is inhibited or siRNA used (Rosse et al., 2009). Neurite extension is mediated by a JNK pathway as inhibition is observed in response to expression of S178A paxillin or pre-treatment with SP600125 (Yamauchi et al., 2006). JNK-mediated phosphorylation of paxillin also reduces its ability to promote microtubule assembly (Bogoyevitch and Kobe, 2006).

It has been hypothesised that S178 paxillin phosphorylation by JNK is a pre-requisite to render paxillin receptive to phosphorylation on residues Y31 and Y118 (Huang et al., 2008). Suppression of JNK activity or expression of S178A paxillin prevents FAK association with paxillin and results in reduced level of tyrosine phosphorylation and inhibition of migration. However, this contradicts work by Ken Jacobson's group as they see no effect on paxillin tyrosine phosphorylation in the presence of S178A paxillin expression (Huang et al., 2003).

8.2 Aim

I hypothesise that paxillin is a downstream effector of ICAM-1-JNK signalling. The aims of this part of the study are to investigate if paxillin is phosphorylated in a JNK-dependent manner during ICAM-1 activation and if paxillin phosphorylation is important for lymphocyte TEM. Lastly, if paxillin is found to be involved in ICAM-1-dependent TEM I would be interested to understand how this relates to the ICAM-1-VEC pathway previously identified in the laboratory.

8.3 Results

8.3.1 ICAM-1-mediated tyrosine phosphorylation of paxillin is dependent on JNK

ICAM-1 cross-linking leads to tyrosine phosphorylation of paxillin in BMVEC (Etienne et al., 1998). I determined the time course of phosphorylation of Y118 in response to ICAM-1 ligation. Confluent GPNT EC were subjected to ICAM-1 ligation for varying lengths of time and then to western blotting using a phospho-specific Y118 paxillin antibody (Figure 8.1A). A 2-fold increase in paxillin phosphorylation occurred within 2 min of primary antibody ligation increasing to a 10-fold increase after 30 min ligation (Figure 8.1B). Cross-linking of ICAM-1 induces a significant 7-fold increase in paxillin phosphorylation. These results show that ICAM-1 engagement, either by ligation or cross-linking, leads to a time-dependent increase of paxillin phosphorylation on Y118.

Since phosphorylation of paxillin on the JNK site S178 has been proposed to be a pre-requisite for phosphorylation on Y31 and 118 by FAK (Huang et al., 2008) I re-examined the GPNT extracts shown in Figure 8.1 using anti-phospho-S178 antibodies. Phosphorylation on S178 was not consistently observed, either following ICAM-1 ligation or cross linking (data not shown). Antibodies from two different suppliers were used without any further success. The inclusion of PP1 and PP2A inhibitor calyculin A during cell lysis did not make any difference to our attempts to detect phosphorylation on S178. A signal was detected in a single experiment using ICAM-1 antibody-coated beads (Figure 8.2). Phosphorylation on S178 was strong at 5 and 60 min of ICAM-1 engagement and appeared to precede Y118 phosphorylation which was strong in the same cell samples at 10-30 min and 60 min. However, this result could never be repeated.

Despite the inability to deliver clear evidence of phosphorylation of paxillin on S178 in response to ICAM-1 activation, tyrosine phosphorylation of paxillin on Y118 could still be dependent on JNK activity. Indeed, pre-treatment of confluent GPNT EC with SP600125 prior to ICAM-1 ligation or cross-linking inhibited Y118 paxillin phosphorylation (Figure 8.3A). SP600125 pre-treatment did affect basal Y118 phosphorylation. Nevertheless, it also prevented anti-ICAM-1 from inducing a quantitative increase of Y118 phosphorylation (Figure 8.3B), suggesting that ICAM-1-mediated paxillin phosphorylation on Y118 is dependent on JNK and that transient S178 phosphorylation could be a pre-requisite.

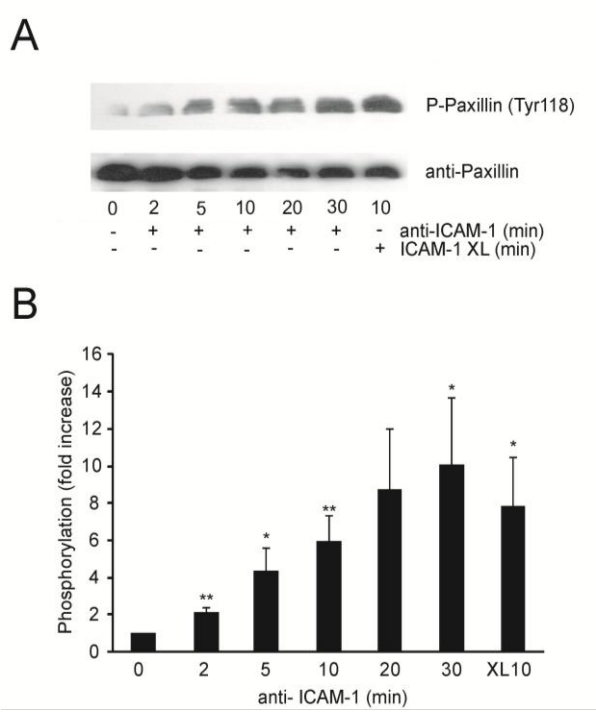

Figure 8.1 ICAM-1 mediates phosphorylation of paxillin Y118

(A) GPNT ECs were grown to confluency, serum-starved and stimulated with anti-ICAM-1 antibody 1A29 to induce ICAM-1 ligation for the indicated times or ICAM-1 cross-linking for 10 min (XL10) as described for Figure 5.1. Cells were lysed and subjected to western blot analysis using phospho-Y118 paxillin antibodies and, as a loading control, anti-paxillin antibodies.

(B) Densitometry quantification of 4 independent experiments as shown in (A). Shown is normalised mean Y118 phosphorylation +/- SEM. Statistical analysis of the variance of mean values was carried out by the Student's t test. *, $P < 0.05$; **, $0.001<P< 0.01$; ***, $P \leq 0.001$

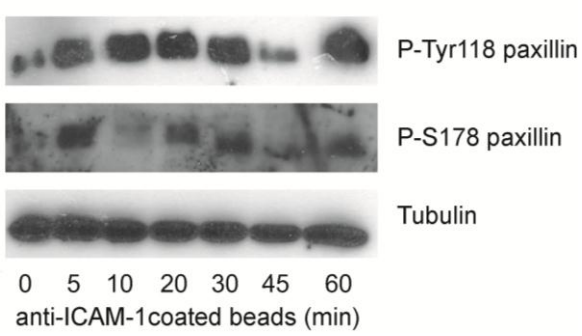

Figure 8.2 Anti-ICAM-1-coated beads can induce phosphorylation of paxillin on Y118 and S178

Confluent, serum-starved GPNT ECs were incubated with 3 anti-ICAM-1-coated beads/EC for the indicated times. Lysates were prepared and analysed as described in Figure 8.1 with the exception that tubulin was used as loading control.

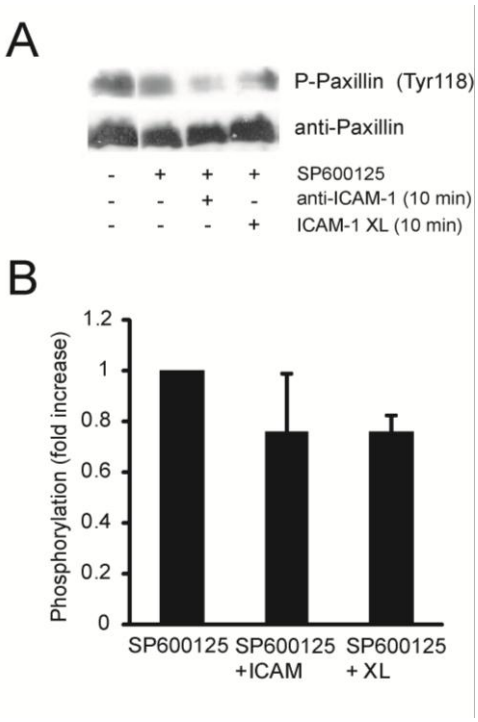

Figure 8.3 ICAM-1-mediated Y118 phosphorylation of paxillin is dependent on JNK

(A) Confluent GPNT EC were serum-starved and pre-treated in the presence or absence of 50µM SP600125 for 1 h before ICAM-1 was ligated or cross-linked (XL) for 10 min. Protein lysates were analysed by western blotting as described in Figure 8.1.

(B) Densitometry quantification of the immunoblots shown in (A) and two other independent experiments. Basal levels of Y118 phosphorylation varied following pre-treatment with SP600125. Therefore, to determine how strongly ICAM-1-induced paxillin phosphorylation was inhibited, densitometric values were normalised and mean -/+ SEM expressed in relation to values obtained from SP600125 treated BMVEC.

8.3.2 Phosphorylation of paxillin is important for lymphocyte TEM

Paxillin was phosphorylated on Y118 in response to ICAM-1 stimulation and in a JNK-dependent manner, suggesting it could mediate endothelial ICAM-1 signalling during TEM. Next, I examined whether paxillin phosphorylation was important for successful lymphocyte TEM. GPNT BMVEC were transfected with plasmids encoding either 10µg of wild-type or phosphorylation-deficient mutants of paxillin, namely the double mutant Y31F/Y118F or S178A. Expression of Y31F/Y118F or S178A paxillin significantly inhibited lymphocyte transmigration (Figure 8.4A, black bars). Inhibition of migration was slightly greater following expression of Y31F/Y118F (58%) than of S178A (68%). Importantly, expression of Y31F/Y118F or S178A paxillin did not inhibit adhesion (Figure 8.4A, grey bars) suggesting that paxillin plays an important role in lymphocyte transmigration, potentially as downstream effector of the JNK pathway. Y118 is efficiently phosphorylated by FAK (Turner, 1998). Inhibition of FAK, using two different pharmacological inhibitors, significantly reduced lymphocyte TEM by at least 50% (Figure 8.4B) further underlining the importance of paxillin phosphorylation on Y118 during TEM.

8.3.3 The JNK-paxillin and eNOS-VEC pathways converge to mediate lymphocyte transmigration

Our laboratory has previously identified a pathway linking AJ modulation to ICAM-1 stimulation during TEM. This pathway involves Ca^{2+}, CaMKK, AMPK and eNOS leading to tyrosine phosphorylation of VEC which in turn regulates TEM (Turowski et al., 2008; Martinelli et al., 2009). Expression of VEC mutated at Y731 is sufficient to inhibit TEM by ca. 40% (Allingham et al., 2007; Turowski et al., 2008). Here, I was interested in the relationship between the phosphorylation of VEC and paxillin during regulation of lymphocyte TEM across GPNT.

I co-transfected plasmids encoding wild-type or phosphorylation-deficient paxillin (Y31F/Y118F or S178A) in combination with wild-type or phosphorylation-deficient (Y731F) VEC (Turowski et al., 2008) into sub-confluent GPNTs. Two days post-transfection lymphocyte transmigration was assessed. As shown before, expression of phosphorylation-deficient VEC or paxillin resulted in significant inhibition of migration. Significantly, the co-expression of VEC and

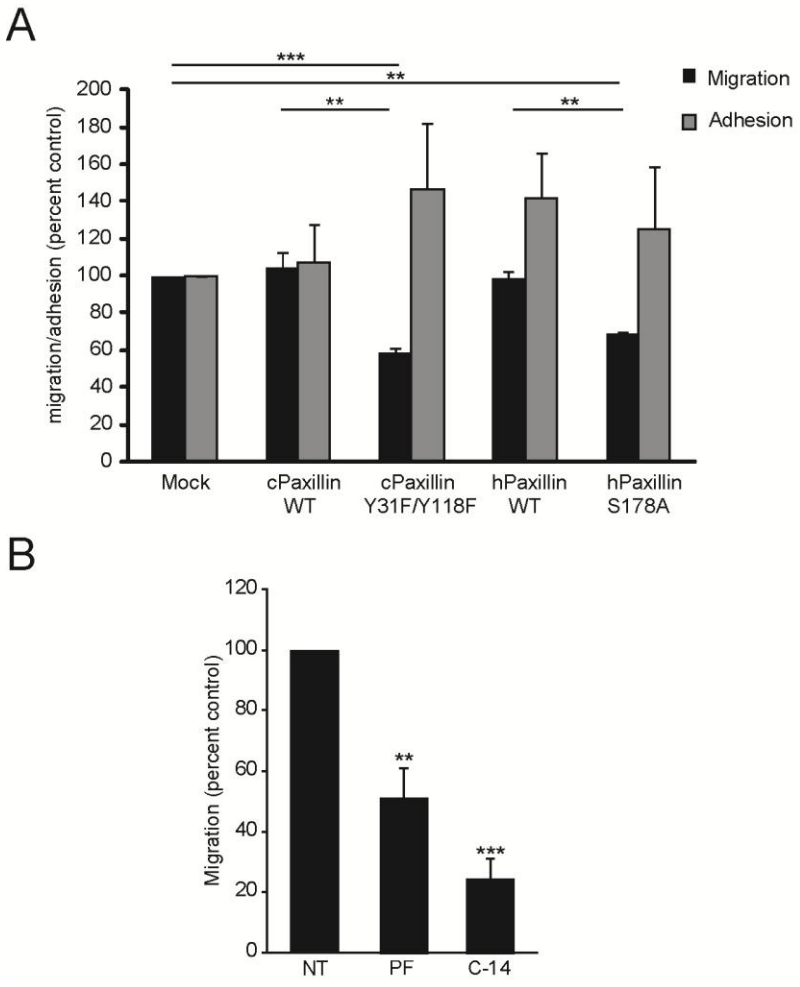

Figure 8.4 Paxillin phosphorylation is important for lymphocyte transmigration

Figure 8.4 figure legends

(A) GPNT EC were transfected with 10μg of each CMV expression plasmid encoding chicken paxillin, either wild-type or with the double phosphorylation site mutations Y31F and Y118F, or human paxillin, either wild-type or phosphorylation-deficient in S178 (S178A). After two days lymphocyte transmigration (black bars) and adhesion (grey bars) were analysed as described in Figure 7.2. Results are shown as mean percentage of control from 3 independent experiments +/- SEM. Statistical analysis of mean value variances was undertaken using the Student's t test. *, $P < 0.05$; **, $0.001<P< 0.01$; ***, $P \leq 0.001$

(B) GPNT were grown to confluency in wells of a 96 well plate and pre-treated with either 10μM PF573228 (PF) or 50μM FAK inhibitor 14 (C-14) for 1 h. Migration was assessed as described in Figure 7.1 with values expressed as percentage of control from 3 independent experiments +/- SEM. Variances of mean values were statistically analysed by the Student's t test. *, $P < 0.05$; **, $0.001<P< 0.01$; ***, $P \leq 0.001$

paxillin phosphorylation-deficient mutants did not result in further inhibition (Figure 8.5). Inhibition of TEM was greater following co-expression of Y31F/Y118F paxillin and Y731F VEC than with any other combination. However, this difference was not significant and appeared to be due to adhesion of lymphocytes also being reduced by ca. 20 % (Figure 8.5A). These results showed that the two pathways, namely JNK-paxillin and eNOS-VEC, were not additive suggesting that they converged to regulate a common effector mechanism.

I also tested whether the JNK pathway regulated VEC phosphorylation. For this GPNT EC monolayers were stimulated using anti-ICAM-1 antibodies following pre-treatment with the MAP kinase inhibitors UO126, SP600125 and SB202190 (see Chapter 6). VEC was then immunoprecipitated from lysates and its tyrosine phosphorylation analysed by immunoblotting (Figure 8.6A). ICAM-1 mediated around a 2.5-fold increase in tyrosine phosphorylation of VEC (Figure 8.6B) in agreement with previous reports (Allingham et al., 2007; Turowski et al., 2008). However, this was not affected by any of the three MAP kinase inhibitor treatments (Figure 8.6B). This data suggests that VEC phosphorylation is not modulated by the JNK-paxillin pathway.

8.3.4 ICAM-1 stimulation mediates association of paxillin and VEC

VEC has been shown to associate with paxillin and FAK in human pulmonary artery EC treated with sphingosine-1-phosphate (Sun et al., 2009). Similarly, oxidized-1-palmitoyl-2-arachidonyl-*sn*-glycero-3-phosphorylcholine induced junctional recruitment of paxillin and association with VEC (Birukova et al., 2007).

I therefore investigated whether paxillin and VEC physically interacted during ICAM-1 stimulation. For this, GPNTs were grown to confluency, serum-starved and subjected to antibody-mediated ICAM-1 ligation. Lysates were prepared at various times and VEC immunoprecipitated using an affinity purified VEC antibody. Subsequently, the association of VEC with paxillin was analysed by immunoblotting immunoprecipitates for the presence of paxillin. As shown in Figure 8.7A, ICAM-1 stimulation induced VEC association with paxillin in a time-dependent manner. Maximal association occurred at 10 min. Furthermore, I found that the association of VEC and paxillin was dependent on JNK activity since it was sensitive to pre-treatment of GPNTs with SP600125 (Figure 8.7B).

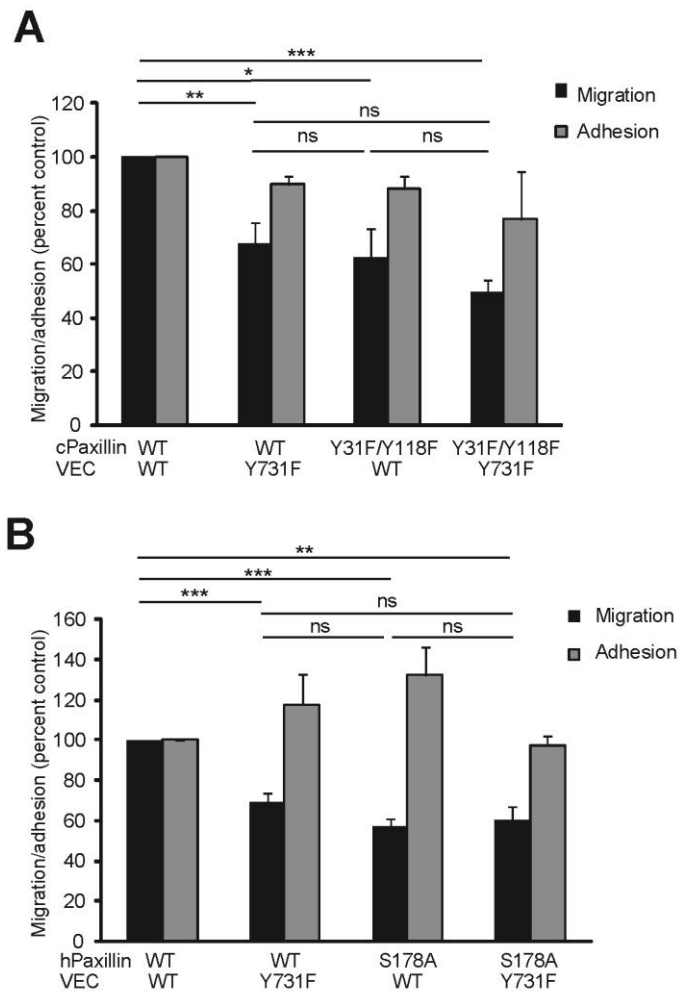

Figure 8.5 Paxillin and VEC converge to mediate lymphocyte transmigration

(A) 10µg of plasmid encoding wild-type or phosphorylation-deficient (Y31F/Y118F) chicken paxillin was co-transfected with 10µg of plasmid encoding wild-type or dominant-negative (Y731F) mouse VEC plasmids into GPNT BMVEC. (B) 10µg of plasmid encoding wild-type or phosphorylation-deficient (S178A) human paxillin was co-transfected with 10µg of plasmid encoding wild-type or dominant-negative (Y731F) mouse VEC plasmids into GPNT BMVEC. (A and B) Two days post-transfection lymphocyte TEM across the transfected EC monolayer was assessed. Migration (black bars) and adhesion (grey bars) were analysed as described in Chapter 7. Results are shown as mean percentage of control from 3 independent experiments +/- SEM. Students t test was used for statistically analysis of the mean value variance. *, $P < 0.05$; **, $0.001<P< 0.01$; ***, $P \leq 0.001$

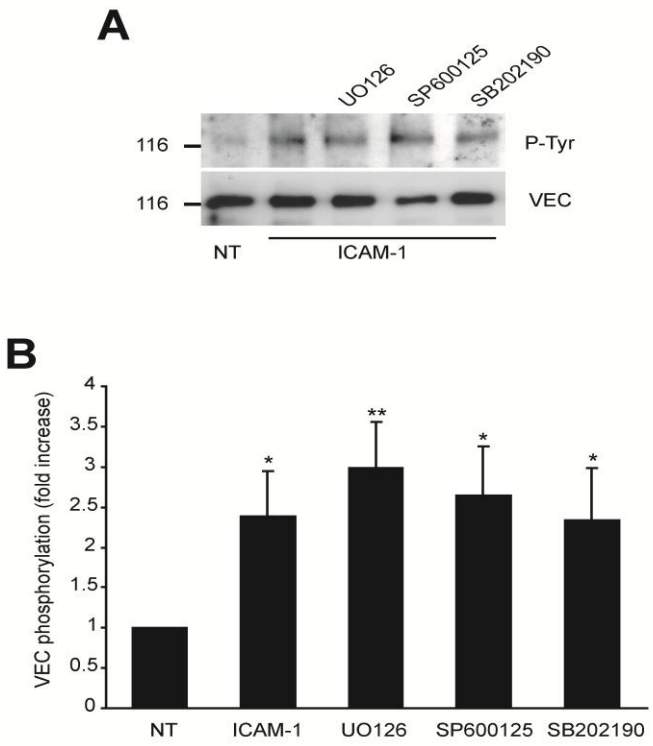

Figure 8.6 VEC phosphorylation is not mediated by endothelial MAP kinases

(A) GPNT cells were grown to confluency, serum-starved and treated with 50μM UO126, SP600125 and SB202190 for 1 h. Cells were subsequently subjected to ICAM-1 ligation for 15 min before they were lysed and VEC immunoprecipitates analysed by western blotting using antibody against phospho-tyrosine (4G10) and VEC.

(B) Densitometry quantification of (A) and three other independent experiments. Results are shown as mean (-/+ SEM) fold increase in VEC phosphorylation compared to control. Variance of mean values was statistically analysed by Students t test. *, $P < 0.05$; **, $0.001<P< 0.01$; ***, $P \leq 0.001$

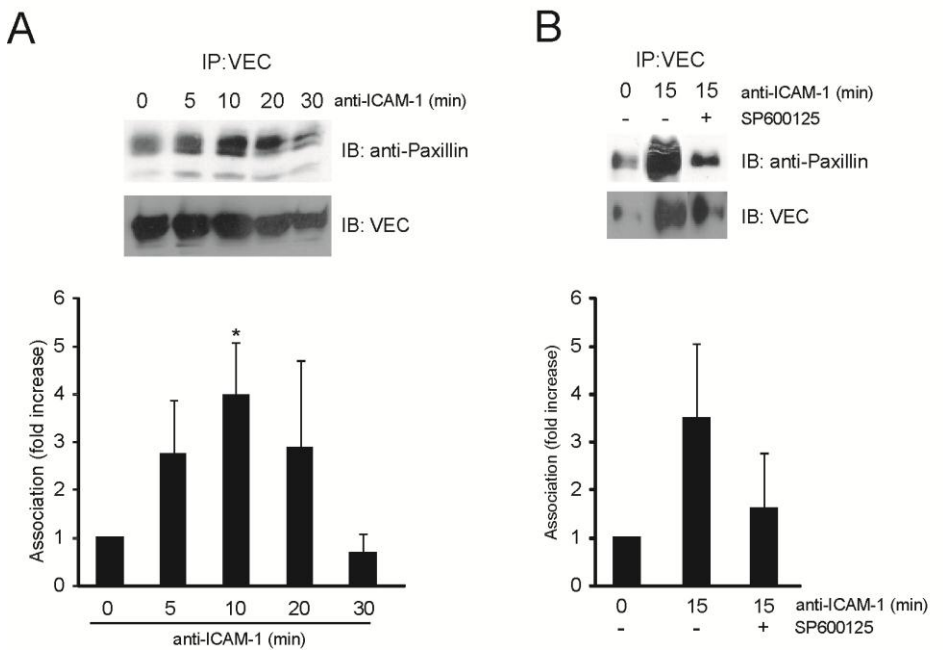

Figure 8.7 ICAM-1 mediates the association of VEC and paxillin in a time- dependent and JNK-dependent manner

(A) Confluent GPNT were serum-starved and subjected to ICAM-1 ligation for the indicated lengths of time before the cells were lysed and VEC immunoprecipitates analysed by western blotting using antibody against anti-paxillin and VEC. Densitometry quantification of five independent experiments expressed as average mean +/- SEM fold increase in paxillin association compared to control. Variance of mean values was statistically analysed by Students t test. *, $P < 0.05$; **, $0.001<P< 0.01$; ***, $P \leq 0.001$

(B) As in (A) with the exception that confluent GPNT were pre-treated with 50μM SP600125 for 1 h and subjected to ICAM-1 ligation for 15 min before analysis. Densitometry quantification of three independent experiments is expressed as an average mean +/- SEM. Mean value variance was statistically analysed by Students t test. *, $P < 0.05$; **, $0.001<P< 0.01$; ***, $P \leq 0.001$

Immunocytochemical analysis of the localisation of paxillin in response to ICAM-1 stimulation also suggested its association with AJ (Figure 8.8). In unstimulated GPNT, diffuse staining of paxillin was found concentrated around the nuclei. Little staining was found resembling classical focal adhesions. Instead some staining appeared to be concentrated at lateral membranes (Figure 8.8 A). Co-staining for phospho-Y118 paxillin revealed that the majority of this form of paxillin was found at lateral membranes. In fact its staining was reminiscent of AJ staining in GPNT (see Figure 3.1, Chapter 3). In response to ICAM-1 engagement for 20 min, the phospho-paxillin staining associated with AJs was strongly induced (Figure 8.8B), corroborating our biochemical association data.

8.3.5 ICAM-1 induces VEC internalisation

At this point, I wanted to elucidate the functional consequence of the VEC-paxillin interaction. In HUVECs, VEGF induces removal of VEC from the cell surface and its accumulation in intracellular vesicles (Gavard and Gutkind, 2006). Here, I tested whether VEC was internalised in GPNT following ICAM-1 stimulation.

Using a protocol adapted from (Gavard and Gutkind, 2006) I studied VEC internalisation biochemically. This protocol assesses the amount of internalised VEC following exposure of live cells to surface proteolysis using trypsin. Surface VEC is completely degraded whilst internalised VEC is protected from proteolysis. Confluent GPNT were serum-starved and subjected to ICAM-1 ligation or cross-linking. Subsequently, cells were placed on ice and treated with trypsin for 30 min. As shown in Figure 8.9 trypsin treatment nearly completely abolished the detection of full-length VEC (instead smaller polypeptides were detected). ICAM-1 ligation rapidly induced the amount of trypsin-protected VEC, suggesting that the full-length protein had been internalised. The amount of trypsin-protected VEC increased 2.5 fold after 5 min. Importantly, the ICAM-1-induced increase in trypsin-protected VEC was sensitive to pre-treatment of GPNT with SP600125, suggesting that JNK induced VEC internalisation.

To further corroborate this, I studied the surface and vesicular immunolocalisation of VEC during ICAM-1 ligation using a protocol adapted from Xiao *et al*. (Xiao et al., 2003). Confluent and serum- starved GPNT were incubated in the presence or absence of VEC at 4°C for 1 h. GPNTs

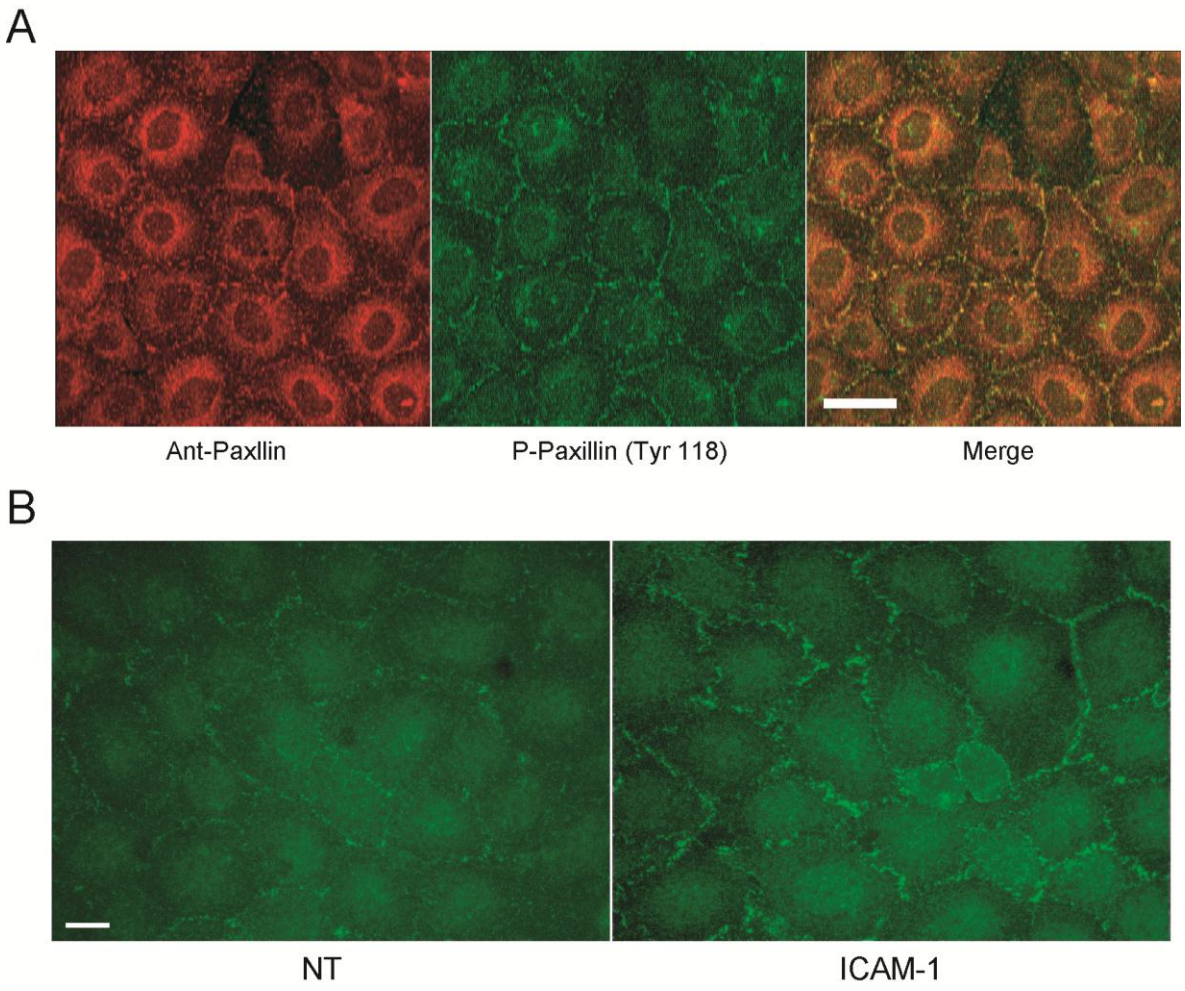

Figure 8.8 Phosphorylated paxillin association with AJs is enhanced following ICAM-1 stimulation

(A) GPNT ECs were grown to confluency, fixed for 15 min in 3.7% formaldehyde followed by ice-cold acetone extraction. ECs were stained for either total paxillin (red) or phospho-paxillin Y118 (green) as described in Section 2.2.14. Staining was analysed by confocal microscopy using the Zeiss LSM 700. (Scale bar: 20µm)

(B) As in (A) except GPNT were stimulated with 5µg/ml ICAM-1 antibody for 20 min before fixation and stained for phospho-paxillin Y118. Immunofluorescence was analysed by epi-fluorescent microscopy using the Zeiss Axiophot (Scale bar: 10µm)

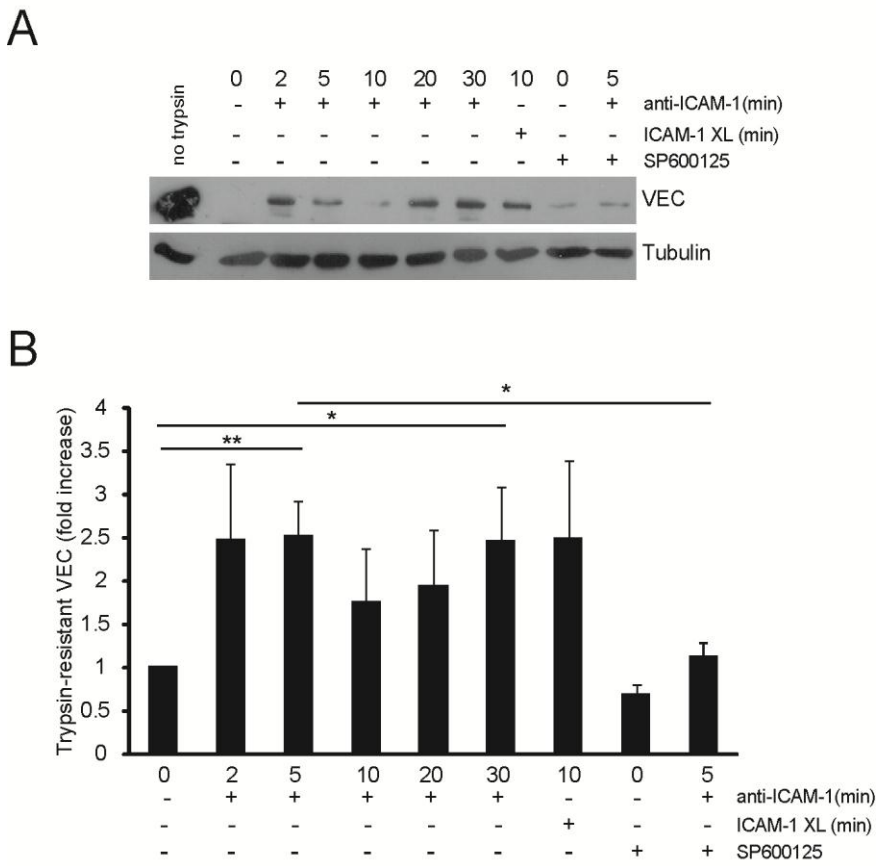

Figure 8.9 VEC is internalised following ICAM-1 stimulation

(A) Confluent, serum-starved GPNT were pre-treated in the presence or absence of 50µM SP600125. Cells were then stimulated with primary anti-ICAM-1 antibody, or subjected to ICAM-1 cross-linking (XL) for the length of times indicated. Trypsinisation was carried out as described in Section 2.2.8. As a control one cell sample was treated with ice-cold PBS for the 30 min incubation rather than trypsin. Lysates were analysed by western blotting for internalised VEC with tubulin as loading control.

(B) Densitometry quantification of (A) and two other independent experiments expressed as a mean average +/- SEM. Variance of the mean values was statistically analysed using the Student's t test. *, $P < 0.05$; **, $0.001<P< 0.01$; ***, $P \leq 0.001$

were then placed at 37°C to allow the antibody bound to VEC to internalise. Cells were fixed and stained for the presence of primary VEC antibody. To distinguish between surface and internalised VEC antibody, cells were also subjected to acid washes before fixation to release surface bound antibody. As shown in Figure 8.10, VEC antibody distribution was primarily junctional when cells were fixed immediately and no acid wash performed (Figure 8.10A), indicating that the antibody bound to VEC in live GPNT cells. In cells that had been returned to 37°C (and VEC allowed to internalise), ICAM-1 ligation led to strong accumulation of the antibody within cells (Figure 8.10C). Indeed, after acid wash VEC antibody was mainly found in cytoplasmic vesicular structures, suggesting that ICAM-1 indeed induced internalisation of VEC.

8.4 Discussion

Within this study I have observed a time-dependent increase in Y118 paxillin phosphorylation in response to ICAM-1 stimulation (Figure 8.1) corroborating the work by Etienne and colleagues who observed significant tyrosine phosphorylation following ICAM-1 cross-linking (Etienne et al., 1998). Maximal phosphorylation of Y118 paxillin occurs at 30 min, a later time point to that observed for JNK phosphorylation in response to ICAM-1 (as shown in Chapter 5). Unfortunately attempts to investigate ICAM-1-mediated S178 paxillin phosphorylation, a designated JNK target (Bogoyevitch and Kobe, 2006) were problematic and were only able to detect it in a one off experiment using anti-ICAM-1-coated beads (Figure 8.2). Phosphorylation of S178 may be too transient and a rapid response to ICAM-1 stimulation which we are unable to detect, although in our lysis buffer calyculin A was included to inhibit phosphatase activities. Nevertheless, S178 phosphorylation appeared to be important for TEM since both phosphorylation-deficient paxillin mutants, namely S178A and Y31F/Y118F, significantly inhibited lymphocyte transmigration but not adhesion (Figure 8.4A). Surprisingly, the paxillin mutants acted as dominant-negatives in the presence of endogenous paxillin. A similar effect of dominant effect of phosphorylation site mutation has also been shown for VEC (Turowski et al., 2008). Migration using both paxillin mutants inhibited migration to similar levels as seen with JNK1 and MKK7 dominant-negative expression and pharmacological inhibitors, such as SP600125. This suggests that paxillin is the only downstream effector of JNK in ICAM-1-mediated TEM.

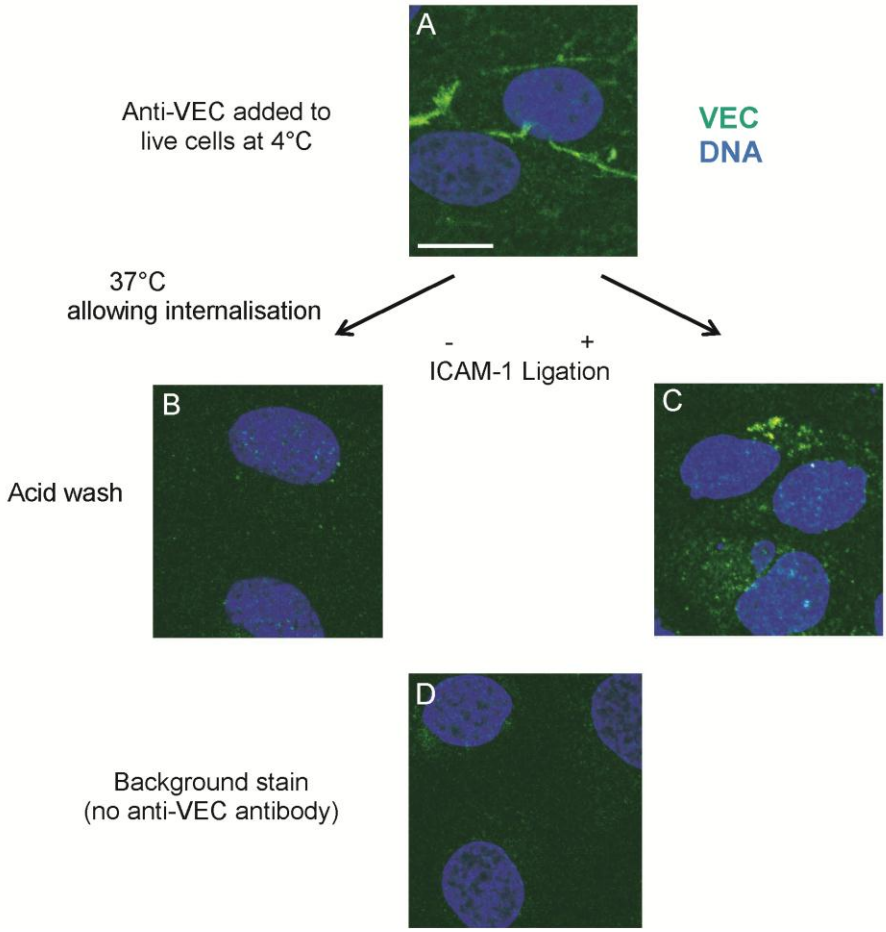

Figure 8.10 VEC becomes internalised in response to ICAM-1 ligation

Confluent and serum-starved GPNT were incubated in the presence (A-C) or absence (D) of 5µg/ml anti-VEC antibody at 4°C for 1 h as described in section 2.2.15. Cells were either (A) fixed immediately or returned to 37°C in absence (B) or presence of (C) anti-ICAM-1 antibody (1A29) for 20 min. Cells were subjected to acid wash (B-D) to release surface bound VEC before cells were fixed and (A-D) processed for IF of primary VEC antibody (as detailed in Section 2.2.14). (Scale bar: 10µm)

ICAM-1-mediated phosphorylation of Y118 paxillin has not been previously studied in conjunction with the potential involvement of JNK. Etienne and colleagues suggested that the focal adhesion proteins, paxillin, FAK and p130cas acted in a Rho-dependent manner to activate JNK (Etienne et al., 1998). From this study I conclude that Y118 phosphorylation is downstream of JNK (Figure 8.3) because it was sensitive to SP600125 treatment (with the assumption that mainly JNK was inhibited as suggested by our transmigration experiments). Our data is in agreement with results from Ken Jacobson's group who show paxillin to be phosphorylated in an MKK7-activated JNK-dependent manner (Huang et al., 2003). This implies that Rho signals via JNK (as shown in Chapter 6 and Etienne et al., 1998) to phosphorylate paxillin on S178 which could either be direct or indirect by phosphorylation of p130cas and FAK which mediate Y118 phosphorylation. Further work is required to analyse whether S178 phosphorylation is a pre-requisite for Y118 paxillin phosphorylation, a hypothesis that has been put forward by Huang and colleagues (Huang et al., 2008).

One caveat of this work is that the involvement of FAK in this pathway has only been studied in TEM assays. FAK has multiple substrates (Guan, 1997; Schlaepfer et al., 1999) which it could be acting on to exert its effects on TEM. Paxillin phosphorylation would need to be studied following EC pre-treatment with the two different FAK inhibitors to corroborate the involvement of FAK.

Some phosphorylated paxillin was already found at the cell junctions (Figure 8.8A) and this increased upon ICAM-1 stimulation (Figure 8.8B). The location of paxillin to the cell junctions put forth the idea that paxillin may play a role in modulating AJs, for example normal turnover of VEC at the AJs. Indeed, VEC and paxillin were found to associate in an ICAM-1-mediated JNK-dependent manner. The two pathways, namely JNK-paxillin and eNOS-VEC, acted independently of one another since VEC phosphorylation was independent of MAP kinase activation (Figure 8.6) and the two pathways were not additive in inhibiting transmigration (Figure 8.5). Therefore, paxillin and VEC cooperated and converged to regulate a common mechanism that leads to internalisation of VEC (Figure 8.9 and 8.10), and thus aiding lymphocyte TEM.

Although I have observed internalisation of VEC it is still not clear where in the EC and within what structures VEC is found. Future work should determine if VEC is recruited to a particular vesicle or cellular compartment and what happens to the VEC when it is there. It is possibly that VEC gets recycled to the AJs following lymphocyte transmigration in a similar manner to the recycling of PECAM-1 via the LBRC (Mamdouh et al., 2003; Muller, 2009; Muller, 2010) or found in

the LBRC itself. Internalised VEC may get degraded via the endosome-lysosomal pathway as dissociation from p120-catenin can lead to clathrin-dependent endocytosis (Xiao et al., 2005).

From these studies I have also not yet determined whether phosphorylation of Y118 occurs before or after association with VEC. It is possible that the phosphorylation of paxillin at this residue could provide a docking structure/interaction site that supports the association of the two proteins. Furthermore, I have not analysed the phosphorylation status of paxillin when associated with VEC, although the immunofluorescence data appeared to suggest that only Y118 phosphorylated paxillin associates with the AJs. To characterise the phosphorylation of paxillin in more detail analysis using S178 detection would be required since I believe that phosphorylation of this residue precedes that of Y118. Using anti-ICAM-1-coated beads may be a more relevant experimental system to use rather than soluble anti-ICAM-1 antibody as it may induce greater phosphorylation via clustering. If S178 phosphorylation is transient I may have to alter the lysis buffer and protocol used as well as looking at earlier time points.

The signalling pathway I have described appears to regulate internalisation of VEC from the AJs. It is still unknown whether the interaction that occurs between paxillin and VEC regulates the internalisation process or whether this interaction occurs in response to the internalisation.

VEC internalisation has been shown previously before in response to leukocyte transmigration (Alcaide et al., 2008), however I show for the first time that this mechanism occurs in an ICAM-1-dependent manner. I have yet to show that internalisation of VEC, via its association with paxillin, is important for lymphocyte TEM. To verify this I would need to test a internalisation resistant VEC mutant where the important EMD motif at residues 562-564 is substituted by a triple alanine substitution (EMD-AAA) (Xiao et al., 2003; Xiao et al., 2005).

Future work would also include studying the effect of transfecting all possible combinations of paxillin phosphorylation-deficient and constitutively-active (Y to E) mutant with phosphorylation-deficient (Y731F) and constitutively-active (Y731E) VEC. This would allow us to determine whether VEC Y731E is capable of driving internalisation on its own or whether paxillin is definitely required for this mechanism.

9. Discussion and Outlook

9.1. Expansion and annotation of the ICAM-1 signalling network regulating TEM

In this thesis the role of endothelial MAP kinases in ICAM-1-mediated lymphocyte TEM has been investigated. A co-culture system of BMVEC and antigen-specific lymphocytes, which is entirely dependent on ICAM-1 but not VCAM-1 activation for TEM (Greenwood et al., 1995), has been used in combination with biochemical and cytological methods interrogating ICAM-1 signalling following antibody ligation.

Through this work I have been able to establish a signalling network which interlinks and assigns roles to many proteins previously recognised to act downstream of endothelial ICAM-1 including Rho, actin, Src, JNK, PKC, paxillin, FAK and VEC (Turowski et al., 2005; Wittchen, 2009). Although many of these proteins have already been shown to be important for TEM, I show mechanistic interaction and expand on their role during TEM (see Figure 9.1 for a schematic summary). JNK was found to be central to this network. In fact, endothelial JNK is the MAP kinase that had previously not been implicated in TEM. In terms of mediating dynamic movement JNK has so far been shown to mediate cell migration, i.e. locomotion of cells during dorsal closure in *drosophila* (Xia and Karin, 2004; Bogoyevitch and Kobe, 2006) and wound closure in NRK cell cultures (Rosse et al., 2009). Although our findings assign an apparently different and new role to JNK it was striking to find essentially the same regulation of paxillin phosphorylation during TEM. JNK and aPKC also control paxillin phosphorylation in NRK cell wound closure (Rosse et al., 2009). However, whilst in this pathway MKK4 mediates JNK activation I found evidence that MKK7 was the kinase responsible for JNK1 activation during TEM. Nevertheless, MKK4 may still be important in signalling since for maximal activation phosphorylation of both threonine and tyrosine is required with each site being preferentially phosphorylated by MKK4 or MKK7 (Cuenda, 2000).

Upstream of JNK I found Src, Rho and aPKC. Whilst Src and Rho have frequently been implicated in TEM and endothelial ICAM-1 signalling, the involvement of aPKC was a novel finding. Previous studies by Etienne *et al*. identified a GF109203X sensitive PKC, i.e. not the PKCι or PKCζ

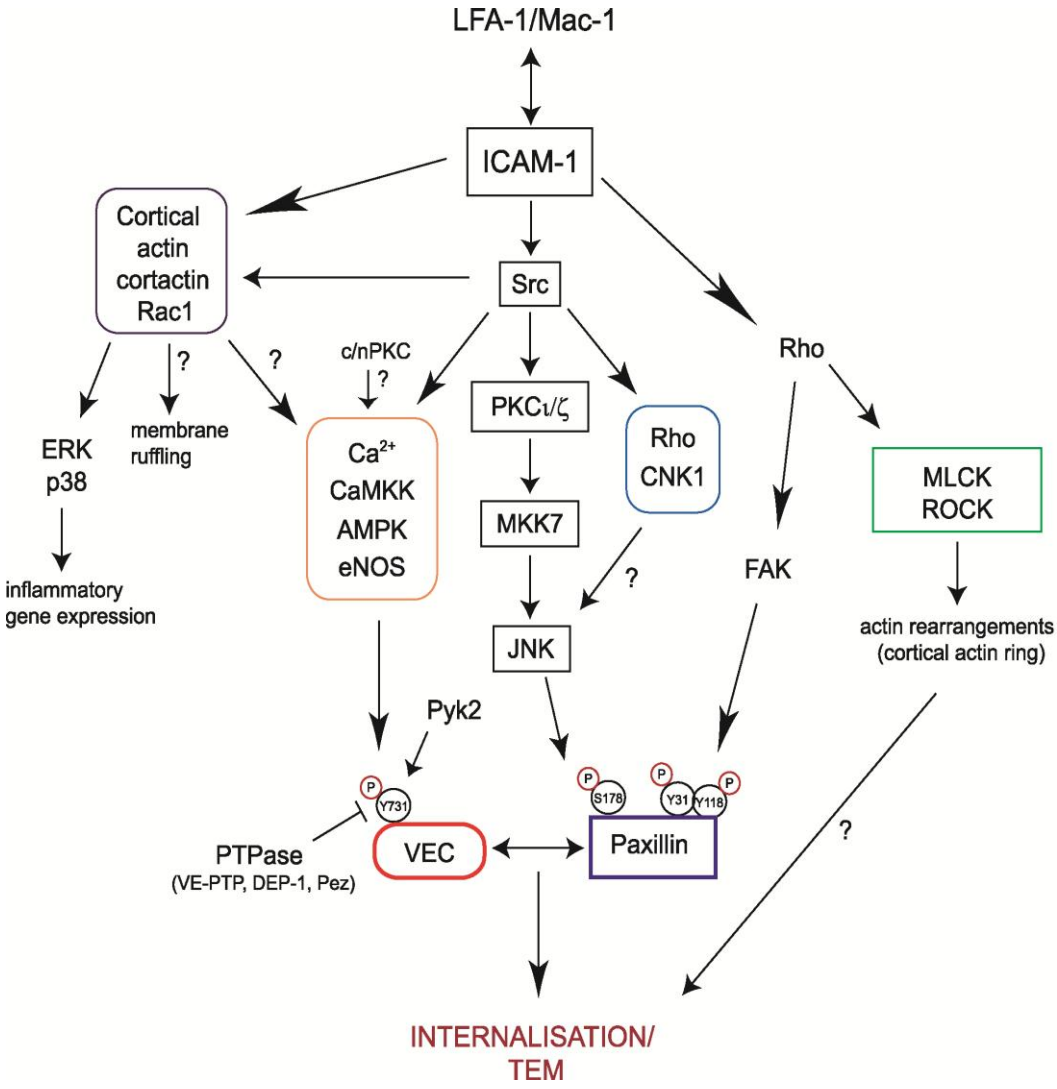

Figure 9.1 Schematic summary of endothelial signalling initiated following ICAM-1 engagement

isoform. In many systems aPKC has been shown to act upstream of JNK activation (Rosse et al., 2009). It has also been found to cooperate with Rho in the activation of many signalling pathways. Obviously our studies do not identify the precise linkage of Src, Rho, aPKC and JNK. Additional studies using RNAi and interaction analysis would be required for that.

Etienne *et al*. proposed an activation mechanism by which Rho-regulated paxillin, FAK and p130cas acted upstream of JNK (Etienne et al., 1998). Indeed, it has been shown that the adaptor protein CrkII can mediate JNK activation in a p130cas-dependent manner (Girardin and Yaniv, 2001). Here I show that Rho was instrumental in the activation of JNK. This was somewhat surprising since JNK signalling is normally found downstream of activated Rac or Cdc42 (Marinissen and Gutkind, 2005). This suggested that other scaffolds and adaptors may be involved during ICAM-1-induced JNK phosphorylation. The non-canonical scaffold CNK1 interacts with the Rho-specific GEFs as well as MLK3 or MKK7, in the regulation of JNK (Jaffe et al., 2005). Thus CNK1 could be the link between Rho and JNK in ICAM-1-mediated TEM. I performed experiments which suggest that this could indeed be the case: preliminary assays showed that the expression of dominant-negative (W493A) CNK1 in GPNT inhibited lymphocyte TEM to similar levels than seen following neutralisation of JNK1 (Figure 9.2A). Moreover, expression of dominant-negative (W493A) CNK1 appeared to inhibit ICAM-1-induced JNK phosphorylation (Figure 9.2B). Further work should consolidate this data and interrogate the biochemical interaction of CNK1 and JNK and the potential role of GEFs such as Net1 or p115RhoGEF, both of which have been shown to regulate the JNK cascade under certain circumstances (Alberts and Treisman, 1998; Marinissen and Gutkind, 2005). Scaffolds, such as CNK1 are important in compartmentalising signalling modules so that they act only in areas of the cell where required.

FAK has been shown to be phosphorylated in response to ICAM-1 cross-linking in a Rho-dependent manner (Etienne-Manneville et al., 2000). Although I have not formally shown that FAK phosphorylated paxillin in response to ICAM-1 activation, I have detected phosphorylation at Y118 which has been identified as a bona fide site for FAK (Turner, 1998; Deakin and Turner, 2008). In support of a role for FAK in ICAM-1-mediated paxillin phosphorylation I found that pharmacological FAK inhibition suppressed lymphocyte TEM (Figure 8.4B). Taken together the data from this study and that by Etienne-Manneville and colleagues (Etienne-Manneville et al., 2000) indicates that Rho regulates paxillin tyrosine phosphorylation through JNK (via S178) and FAK. Further work into the role of FAK in lymphocyte TEM is required to verify its role and its

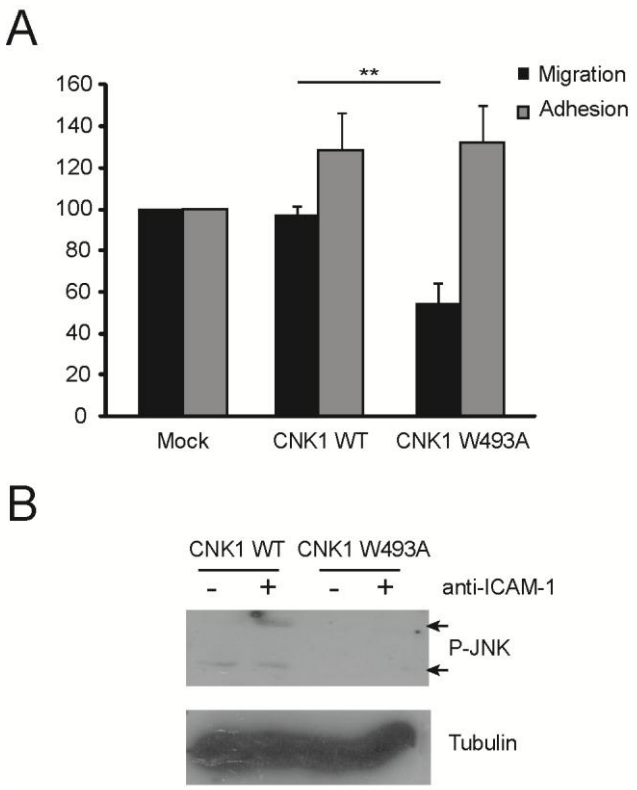

Figure 9.2 The non-canonical scaffold protein CNK1 appears to be important for lymphocyte TEM and ICAM-1-mediated JNK phosphorylation

(A) As described in Figure 7.2 GPNT were nucleofected with 10µg of either wild-type or dominant-negative (W493A) hCNK1. Migration (black bars) was assessed as described in Figure 7.1. Adhesion (grey bars) was determined as described in Figure 7.2. Average values for both migration and adhesion are expressed as a percentage of mock control from 3 independent experiments +/- SEM. Variances of mean values were statistically analysed by the Student's t test. *, $P < 0.05$; **, $0.001<P< 0.01$; ***, $P \leq 0.001$

(B) GPNT were transfected with 10µg of either wild-type or dominant-negative (W493A) CNK1, serum-starved overnight and subjected to ICAM-1 ligation for 5 min. Cells were lysed and subjected to immunoblotting as described for Figure 5.1.

position downstream of Rho in the regulation of paxillin. Phosphorylated FAK has been shown to interact with Src (Guan, 1997; Schlaepfer et al., 1999) and could therefore be part of the immediate early activation similar to cortactin (see below).

Ultimately our data demonstrated that the JNK-paxillin pathway regulated VEC internalisation. Therefore this signalling axis converges with that regulating VEC phosphorylation (Turowski et al., 2008; Martinelli et al., 2009) which is also required for its internalisation (Alcaide et al., 2008). Since JNK did not modulate VEC phosphorylation but enhanced association with paxillin, I postulate that paxillin and the actin cytoskeleton play an important part in AJ internalisation during TEM. Taken together, our findings of converging pathways also suggest that AJ modulation is highly important in facilitation of leukocyte migration across EC barriers.

VEC phosphorylation in response to ICAM-1 appears to be mediated by Pyk2 (Allingham et al., 2007) but a direct role for Src cannot be excluded (Adam et al., 2010). Our laboratory has shown that VEC phosphorylation is downstream of localised NO production by eNOS (Martinelli et al., 2009). NO has been shown to regulate PTPases directly by reversible oxidation of the active site cysteine (i.e. by S-nitrosylation) (Barrett et al., 2005). Thus a number of AJ-associated PTPases could be locally and transiently inactivated, triggering VEC hyperphosphorylation and internalisation. Prominent AJ-associated PTPases are VE-PTP (Nottebaum et al., 2008), DEP-1 (Density enhanced PTP-1) (Grazia et al., 2003) and Pez (Wadham et al., 2003), which have been shown to regulate proteins in VEC complexes including β-catenin, plakoglobin and p120-catenin and potentially AJ protein kinases (Takahashi et al., 1999b; Holsinger et al., 2002; Grazia et al., 2003; Wadham et al., 2003; Jandt et al., 2003; Nottebaum et al., 2008). It will be important to determine whether VEC hyperphosphorylation is predominantly regulated through the activation of protein kinases or the inactivation of protein phosphatases. The low cellular content in phospho-tyrosine (0.1 % or less) suggest that in most cases dephosphorylation is heavily regulated (Sun and Tonks, 1994).

9.2. Unassigned Signalling

9.2.1. ICAM-1-induced membrane ruffling

I provide the first report of visual ICAM-1-stimulated EC activation following bead engagement on the EC surface. The induction of membrane ruffles are linked to Rac activation (Ridley, 1994), suggesting that Rac also operates downstream of ICAM-1. Preliminary biochemical analysis by pull-down assays showed the rapid activation of Rac1 following ICAM-1 ligation (R. Martinelli and P. Turowski, unpublished). Rac has not yet been found downstream of ICAM-1-mediated TEM and future studies could focus on the role of this GTPases.

Recently, Rac has been shown to form a complex with RhoGDI and aPKC which induces membrane ruffling in response to Src activation and plasma membrane recruitment of DAG kinase (DGKα) (Chianale et al., 2010). Rac is also required for cortactin translocation to the cell membrane where it can interact with the actin cytoskeleton (Weed and Parsons, 2001). Cortactin can bind to actin related protein (Arp) 2/3 complex which has been shown to be activated by Wiskott - Aldrich syndrome proteins (WASp) that are effector proteins of Rac-mediated actin polymerisation. Thus cortactin may be involved in the response typified by the induction of membrane ruffles. Src-mediated cortactin phosphorylation is important for TEM and thought to be an immediate early event in ICAM-1 signalling, occurring in seconds rather than minutes (Durieu-Trautmann et al., 1994; Tilghman and Hoover, 2002; Yang et al., 2006a; Yang et al., 2006b). In contrast I have observed membrane ruffles after ca. 15 min suggesting they may not be part of the immediate-early ICAM-1 signalling. Paxillin has also been shown to regulate Rac1 signalling via CrkII (Petit et al., 2000; Deakin and Turner, 2008). Thus Rac1 activation and the induction of membrane ruffles could be a slightly later response downstream of JNK activation. Only careful time course analysis and specific neutralisation experiment will distinguish between these different possibilities.

9.2.2 Rho-independent actin rearrangements

Another open question is how the membrane ruffling may be related to other Rho-independent actin re-arrangements. These include the formation and the dynamics of the transmigration cup (Barreiro et al., 2002; Carman et al., 2003; Carman and Springer, 2004) and the regulation of VEC (Turowski et al., 2008; Martinelli et al., 2009) and ERK and p38 phosphorylation (Chapter 5).

Based on the identification of a number of actin-associated proteins in physical contact with the cytoplasmic tail of ICAM-1, it has been suggested that a primary signal of ICAM-1 activation could be generated by the actin cytoskeleton (Etienne et al., 1998; Adamson et al., 1999; Carman et al., 2003; Carman and Springer, 2004; Millan et al., 2006; Kanters et al., 2008). For instance, filamin B is important for both TEM and the lateral motility of ICAM-1 to the site of adhesion and docking structure that forms (Kanters et al., 2008). Filamin B influences the localisation and activity of Rac1 altering the EC signalling involved in cell adhesion and migration (Valle-Perez et al., 2010). Thus it appears filamin B could potentially act at several different levels in migration and may influence Rho-independent signalling downstream of ICAM-1.

Other filamins may be involved. Another family member, filamin A, can simultaneously bind MKK4, MKK7γ and MKK7β bringing them into close proximity enhancing stress-induced JNK activation *in vivo*, without directly binding JNK (Nakagawa et al., 2010). Rho GTPases, including Rac, Rho, Cdc42 and Ral1, can bind to filamin A (Ohta et al., 1999) and therefore it seems that filamins can integrate cell adhesion and signalling molecules acting as a scaffold (Kim and McCulloch, 2011).

The possible involvement of filamin A and/or filamin B in the different pathways detailed above and shown in Figure 9.1 could be studied using siRNA for particular isoforms as described (Kanters et al., 2008). Other ICAM-1-associating proteins could obviously also be involved such as α-actinin (Carpen et al., 1992), ERM proteins (Heiska et al., 1998) or indeed cortactin. The use of other actin drugs such as jasplakinolide, latrunculin (Spector et al., 1983) or blebbistatin during TEM and cytological analysis of ICAM-1 signalling could also shed further light on the role of actin dynamics.

9.2.3 Classical and novel PKC isoforms

From transmigration assays I observed that all PKC inhibitors led to a significant inhibition in TEM although not all inhibitors influenced inhibition of MAP kinases ERK and JNK. The universal inhibitor Gö6983 influenced ERK and JNK phosphorylation suggesting multiple PKCs may regulate TEM due to differences in the upstream signalling between these two MAP kinases. A cPKC and/or nPKC could well be involved in the regulation of VEC phosphorylation since that also requires Ca^{2+} (Martinelli et al., 2009). Indeed, preliminary data also showed that inhibition of cPKC prevented ICAM-1-mediated eNOS activation (unpublished data).

Cell-cell interactions have been shown to be regulated by cPKC and nPKCs. This is mediated by a regulated spatio-temporal cascade of PKC activation and translocation to cell contact sites (Quittau-Prevostel et al., 2004; Collazos et al., 2006; Diouf et al., 2009). In the pituitary gland $PKC\beta_I$ is generally translocated and activated to the plasma membrane followed by specific recruitment of PKCα and then PKCε to the cell-cell contacts. Cell-cell contact sites forming between different cell types also have similar spatio-temporal co-ordinated PKC activation cascades. For example a PKC cascade occurs during the loose interaction of human fibroblast and cancer epithelial cells, (Louis et al., 2005) and recruitment of PKCθ to the cSMAC when APCs and T-lymphocytes interact (Altman and Villalba, 2003; Yokosuka et al., 2008; Praveen et al., 2009). Recently, a PKC cascade involving PKCε, PKCη and PKCθ has been described during MTOC reorganisation towards the APC at the IS in response to DAG (Quann et al., 2011). Involvement of PKCα, PKCε and PKCδ has been shown during respiratory burst and phagocytosis in RAW264.7 cells (macrophage-like) and hence found to accumulate at these sites after rapid translocation to the membrane (Larsen et al., 2000). Indeed, I have started to explore the possibility of such a PKC signalling cascade operating during leukocyte-EC interactions by using plasmids encoding GFP tagged versions of PKC isoforms.

9.2.4 The role of ERK and p38 during ICAM-1-mediated TEM

ERK and p38 were found not to play a role in lymphocyte TEM or actin rearrangements even though they were found to be phosphorylated downstream of ICAM-1 stimulation. This was in contrast to other work showing the involvement of ERK (Stein et al., 2003) and p38 (Wang and

Doerschuk, 2001) in neutrophil TEM. The discrepancy of these observations may lie in the different EC systems used. Our data was generated using ECs which were not subjected to inflammatory cytokine prior to TEM assays or signalling studies whilst neutrophil TEM is dependent on exposing the endothelium to strong cytokine stimulation. Thus, our co-culture systems models basic TEM, also utilised during immune-surveillance, when JNK but not ERK or p38 appeared to be involved.

Since MAP kinases have been implicated in inflammatory gene expression (Roux and Blenis, 2004; Gaestel, 2006), work in the laboratory has focused on such a potential role of ICAM-1-induced ERK and p38 signalling. The result of this work has shown that ERK and p38 regulate ICAM-1-induced gene expression of inflammatory genes such as VCAM-1, Cox-2 or ICAM-1 itself. Regulation was found to occur on both the transcriptional (involving ERK and p38 driven transcription) and post-transcriptional level (via p38-mediated mRNA stabilisation) (R. Blaber, J. McKenzie and P. Turowski, unpublished observation). Thus, it appears possible that lymphocyte adhesion through engagement of ICAM-1 mediates further expression of endothelial inflammatory (and adhesion) proteins resulting to recruitment of further immune cells to an inflamed region. Indeed, multiple leukocytes can cross the same region of the endothelium (Shaw et al., 2001). However, if this is true a number of observations could be predicted for TEM *in vitro*. 1. Early but not late TEM is independent of EC gene expression. 2. Late TEM rates are higher than early rates. 3. ERK and p38 inhibition (or the general inhibition of gene expression) inhibits the late increase in TEM rates. 4. Prior TEM renders the EC area where TEM occurred more 'permissive' to subsequent TEM. Preliminary results from our laboratory demonstrated that hypothesis 1, 2 and 3 were correct for TEM across GPNT, (Y. Gill, J. Greenwood and P.Turowski, unpublished), suggesting that ERK and p38 could play an instrumental role in orchestrating differential leukocyte egress at the BBB (and possibly other vascular beds).

9.3. VEC internalisation

The activity of the eNOS-VEC and JNK-paxillin pathways lead to the internalisation of VEC. This could facilitate the transmigration of leukocytes via a paracellular route or even transcellular route (Mamdouh et al., 2003; Mamdouh et al., 2008; Mamdouh et al., 2009). VEC has been shown to be internalised in response to VEGF stimulation (Gavard and Gutkind, 2006), dissociation from p120-

catenin (Xiao et al., 2003) and in response to EC infected with viruses (Gorbunova et al., 2010). Dissociation of VEC homophilic interactions is important for VEC displacement and the subsequent gap formation during TEM (Shaw et al., 2001; Carman and Springer, 2004; Woodfin et al., 2011). Therefore internalisation of VEC appears to be the driving force in pore formation and could involve other AJ complex proteins such as β-catenin and p120-catenin, which have already been shown to be important in VEC displacement (Xiao et al., 2003; Alcaide et al., 2008). JNK can bind and phosphorylate β-catenin controlling cell adhesion and AJ formation (Lee et al., 2009).

To our knowledge this is the first experimental demonstration of the involvement of paxillin in VEC internalisation and turnover. However this novel role of paxillin is consistent with other observations. A similar JNK-paxillin pathway has been described in the regulation of the exocyst complex during NRK cell migration (Rosse et al., 2009). The exocyst is an octameric protein complex involved in vesicle trafficking and has also been implicated in establishing and maintaining epithelial polarity by regulating the delivery of membrane to the basolateral plasma membrane (Nejsum and Nelson, 2009). Moreover, exocyst-mediated vesicular trafficking also regulates E-cadherin delivery to the plasma membrane (Langevin et al., 2005). It is conceivable that JNK-paxillin plays a prominent role in all of these processes. I have observed the induction of distinctive filamentous actin in cortical areas of ICAM-1 stimulated GPNT (Figure 9.3). Induction was sensitive to SP600125, but not UO126 or SB202190, suggesting that it was also regulated by JNK. This cortical actin was also sensitive to blebbistatin (but not other actin drugs; P.Turowski, unpublished data) and thus reminiscent of the cortical actin seen during the maturation of epithelial cell-cell contacts (Zhang et al., 2005). Since this coincides with exocyst activity and vesicular trafficking being initiated (Nejsum and Nelson, 2009) it is likely that this fine contractile cortical actin network plays a dynamic role during this process. Our current working model going forward is the hypothesis that vesicular transport which is regulated by the exocyst or an exocyst-like complex works in cooperation with paxillin and cortical actin regulates AJ internalization during TEM (and other processes affecting EC barrier function).

It is still not clear how JNK could influence the cortical actin ring induction. A structural link between JNK and actin could be provided by p150-Spir, a member of the WASp family protein (Otto et al., 2000a). JNK may simply regulate the spatial organisation of cortical actin by paxillin phosphorylation (Xia and Karin, 2004) whilst Rho via Rho kinase (ROCK) or MLCK induces contractile fibres (see also Figure 9.3) (Pellegrin and Mellor, 2007). Thus paxillin would act as an

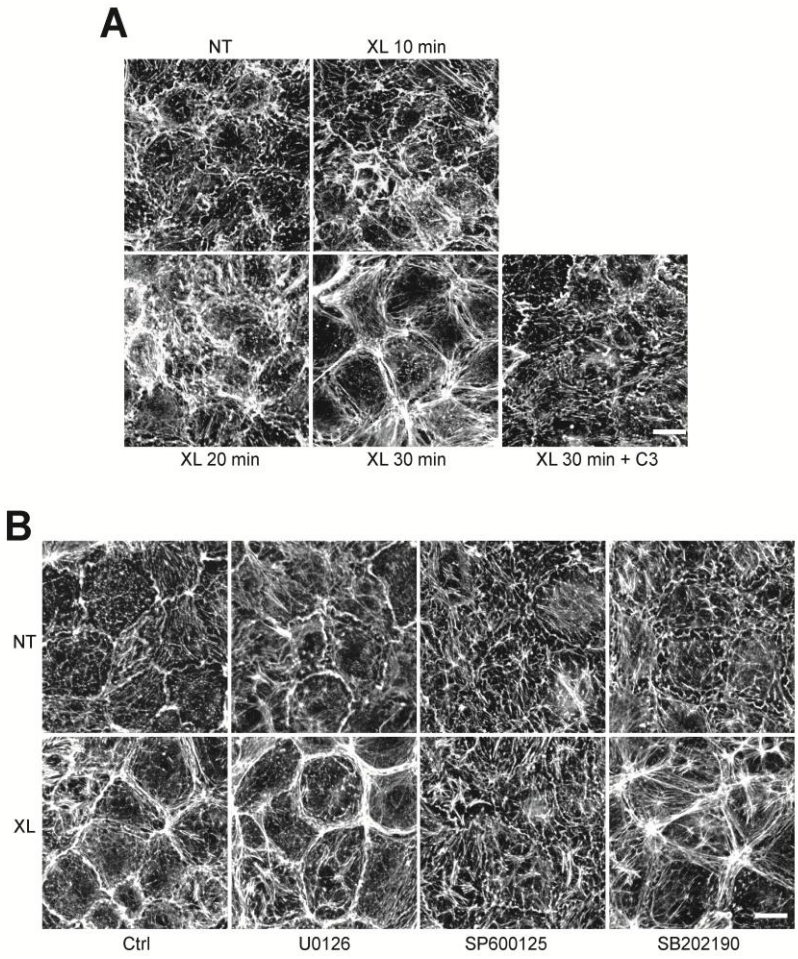

Figure 9.3 Cortical actin rearrangements occur in a Rho- and JNK-dependent manner

(A) Confluent GPNT cells were serum-starved and either left untreated (NT) or ICAM-1 cross-linked (XL) for the indicated lengths of time. Alternatively, GPNT were pre-treated with 10µg/ml C3 transferase for 12 h prior to ICAM-1 XL. At the indicated times cells were fixed and stained for F-actin (as described in Section 2.2.14).

(B) As described in (A) except confluent GPNT EC monolayers were left untreated or pre-treated with 50µM UO126, SP600125 or SB202190 for 1 h before ICAM-1 cross-linking for 20 min.

Figure kindly provided by Patric Turowski

anchor for the actin cytoskeleton during VEC internalisation (see also Figure 9.1).

Internalised VEC could be part of the same recycling compartment described for PECAM-1 and named the LBRC (Mamdouh et al., 2003; Mamdouh et al., 2008; Mamdouh et al., 2009; Muller, 2009; Muller, 2010). A similar compartment, the vesiculo-vacuolar organelles (VVO) may also be related to the mechanism observed for VEC internalisation (Dvorak et al., 1996; Dvorak and Feng, 2001). These membrane compartments are found concentrated near lateral EC borders and are intimately involved in the passage of macromolecules and leukocytes across the vasculature. The presence of VVO is often associated with increased vascular permeability.

The use of anti-ICAM-1-coated beads should allow investigation into the spatial details of VEC internalisation. Soluble anti-ICAM-1 antibodies are likely to induce universal changes such as an actin ring forming along the entire cortical area of the cell. It is highly likely that ICAM-1 clustering with beads would induce a localised actin and endocytic response and their interaction with any of the players of the pathway discussed in this thesis will be highly informative. Further mechanistic information could also be obtained by assessing VEC-paxillin complex formation and VEC internalisation after the transfection of dominant-negative, non-phosphorylatable versions of VEC and/or paxillin. This would show whether internalisation is dependent on phosphorylation on both proteins and whether the requirement for phosphorylation is gradual or simultaneous.

9.4. Location, location, location

This thesis did not address where proteins phosphorylated in response to ICAM-1 are localised and whether translocation from one cellular compartment to another is required. Due to the observed differences in activation kinetics in response to ICAM-1 ligation and ICAM-1 cross-linking, it is likely that endothelial ERK, JNK and p38 are activated and operate within different areas of the EC. Given their role in inflammatory gene expression ERK and p38 are likely to be translocated to the nucleus in response to ICAM-1 activation. JNK would be expected to translocate to (or be activated near) AJs. Localisation studies could be performed following ICAM-1 activation by soluble antibodies. However, this is likely to lead to uniform and ubiquitous EC activation and occlude the spatio-temporal restrictions that may operate during TEM. Ideally

leukocyte should be used to undertake such studies but this approach is complicated by the majority of proteins to be studied being present in both the leukocyte and the EC. Therefore it is believed that addition of anti-ICAM-1-coated beads constitute the best available experimental model to study the spatial arrangement of the MAP kinase in relation to VEC internalisation and the actin cytoskeleton.

Other important technologies to be used for future EC spatio-temporal analysis during TEM are undoubtedly fluorescent energy transfer methods which allow us to interrogate the interaction of our main players in living cells. For instance it is unclear whether paxillin and VEC interact directly or via a third protein.

9.5 Final Summary

In conclusion I have determined a functional link between many components previously found to be phosphorylated, and subsequently activated, downstream of ICAM-1 engagement. I have demonstrated that divergence arises at the level of Src leading to an aPKC-JNK pathway that is important in mediating lymphocyte TEM whilst ERK and p38 have been shown by others in the laboratory to be important in ICAM-1-mediated gene expression. JNK activation, which normally is found downstream of Rac or Cdc42, is found to be dependent on Rho. Due to this I hypothesise that the non-canonical scaffold CNK1 may be the functional linker between Rho and JNK with preliminary work showing CNK1 to be important in TEM. JNK can phosphorylate the focal adhesion protein paxillin which converges with the eNOS-VEC pathway to aid transmigration by a novel mechanism in which VEC becomes internalised. This occurs in response to ICAM-1 inducing the association of paxillin and VEC, which I have shown both biochemically and by immunohistochemistry. Internalisation of VEC may involve the exocyst, or an exocyst-like complex, which is important for vesicular transport and may be important in aiding the delivery of extra membrane to the site of TEM, in a similar way to the LBRC which recycles PECAM-1 to the junctions.

I further demonstrated the first visual evidence of EC activation in response to ICAM-1 engagement on the endothelial surface that induces membrane ruffling, a response often

associated to Rac activation. This suggests that Rac is activated in response to ICAM-1 and may be mediated via a novel pathway or converges with the pathway I have described.

This study has contributed to a better understanding of lymphocyte TEM across the specialised BBB or BRB which is a more tightly regulated process due to the presence of TJs. Excessive infiltration of lymphocytes into the brain can have detrimental, rather than beneficial, effects leading to development of autoimmune diseases such as MS. The pathway I have established is likely to be important in other vascular beds as well as being utilised by other leukocyte sub-sets, such as neutrophils and monocytes. The involvement of CNK1, due to it appearing to have restricted non-ubiquitous functions, and the potential involvement of an exocyst-like structure could constitute novel therapeutic targets which could be exploited for treatment of inflammatory disorders. However, the main contribution of this study has been to structure the role of known downstream targets of ICAM-1 during lymphocyte TEM.

10. Appendices

10.1 *Rattus norvegius* PKC isoform alignment

```
alpha           ------------------------------------------------------------
beta            ----------------------AGGCTCTCTCAAACTTCTGCCGCAGCTCTTCATTGCC 37
gamma           ------------------------------------------------------------
zeta            ------------------------------------------------------------
iota            ATGTTTCTACTCCGTCTTTTTACACGGTGTGCATTTATCATTGTAACATCCCAGAAAAGT 60
delta           ------------------------------------------------------------
theta           ------------------------------------------------------------
epsilon         ------------------------------------------------------------
mu              ----------------------------------CCGGGCCGCGCGCCCTGTCCCCGCG 25

alpha           ------------------------------------------------------------
beta            CTCGCTTCCTTCCGGCGGCACCGGCACATTAAAGTACTCGCCTTCTTCCTGGCTTAGTAA 97
gamma           ------------------------------------------------------------
zeta            ------------------------------------------------------------
iota            TTTGAGCAGCGTGGCTTTAGAATGAAGCCAATTTCGGTTCTCATTCTGTCGTACCGTCAC 120
delta           ------------------------------------------------------------
theta           ------------------------------------------------------------
epsilon         ------------------------------------------------------------
mu              CGCGGACTTTCCCGGAAAGTTTGGTGGTTGTTTTCGGCCGCCGCAGGCAGCGGCGCCGCG 85

alpha           ------------------------------------------------------------
beta            CTTGAACCTCATCTCCTTGAACCTTCGGGTACTTAGGCGTTCAATCCTTTCTTGGGCAC 157
gamma           ------------------------------------------------------------
zeta            ------------------------------------------------------------
iota            CTGCGAACCCCTGAAATCCATTCCGCTCCACCTTCAACTACTACCATCACCTCTGGCTCC 180
delta           ------------------------------------------------------------
theta           ------------------------------------------------------------
epsilon         ------------------------------------------------------------
mu              CCCCACCTCCGCCAAACTTTGGGGCTCACTCGCGCCATGAGCGCCCCTCCGCTACTACGG 145

alpha           ------------------------------------------------------------
beta            CCGAGGTGCTCATCTTAACGCACCCCAGGGCCTAGGACAGGGTGCCAGGGGCGCGGCTCA 217
gamma           ------------------------------------------------------------
zeta            ------------------------------------------------------------
iota            GCCACCAAGGGCACAATGGATTTGCCAAAATGCAAAGGAAAACCCAAGAAAGGACGGTCG 240
delta           ------------------------------------------------------------
theta           ------------------------------------------------------------
epsilon         ------------------------------------------------------------
mu              CCGCCTAGCCCGCTGCTGCCCGCCGCGGCCGCTGTGGCCGC-CGCCGCTGCTGCGCTGGT 204

alpha           ------------------------------------------------------------
beta            GATCTGTCCAGCGCAGTCTGCGGTCCTCGCGCCGCAGCGTGCGGCTAAGAACACTTGGCT 277
gamma           ------------------------------------------------------------
zeta            ------------------------------------------------------------
iota            GAAGAAATTCGAAAGGACCGCTGCGCAGTTAAATTCCAGCGAGATGTCACTGGTGCATCT 300
delta           ---GAATTCCGGGGGCGGCGGCCGCGGGGATCCCGCGAGCGGCCCCTGAACATCTACCCTT 57
theta           ------------------------------------------------------------
```

```
epsilon         ------------------------------------------------------------
mu              CCCGGGCTCCGGGCCCGCGCCCTTCCCAGCGCCTGGGGCCGCCCCGGCGGGGGGCATCTC 264

alpha           ------------------------------------------------------------
beta            GGGGGGCCTGCGGGTTGCGGTGTGTGTGTATATGTGTGTGTGTCTGAGTCTGTGTGTGCG 337
gamma           ------------------------------------------------------------
zeta            ------------------------------------------------------------
iota            CTTGCTAATATAATCGCCGAGAGGAATCAGAAACTAGAGGTTCCCAGTGTGGGAGGAGGG 360
delta           CTTGCCGGGACCCGGGAGGTCCCCACTGGCCTCCGGGCCCGTCCTGATCAGACTCGTGTC 117
theta           ------------------------------------------------------------
epsilon         ------------------------------------------------------------
mu              GTTCCATCTGCAGATCGGCCTGAGCCGCGAGCCGGTGCTGCTCCTTCAGGACTCCTCTGG 324

alpha           ------------------------------------------------------------
beta            TTTGCTGGTGGTGCCGATATGTAAAGCAGCTGGCGGCTCTGGGCGGGGCCTGGGTTCCAT 397
gamma           ------------------------------------------------------------
zeta            ------------------------------------------------------------
iota            GCACAGAATCCTATAATTCTAAACTGCTGTGGGTCCTGGAGATCATCAATCCTGCCTTCT 420
delta           GACCTCCCCGTCCACGCGCATCCGGGAGAGCCGCGCCACGAGACGGACCCGGGCCCGCCG 177
theta           ------------------------------------------------------------
epsilon         -----GAATTCCGGAATCCGGCGAGGAAATACATGCACTCGCTGAGAATCGCCGGCGCCA 55
mu              CGACTACAGCCTGGCGCATGTCCGGGAGATGGCTTGCTCCATCGTGGACCAGAAGTTCCC 384

alpha           ---------------GCCGCGAGTAGGAAGCGCGAGCGCCAGGCGCCG-GGCTG---TCA 41
beta            GCAAATGAAGGAGGAGGGGCTACCCTGGGGCTCCGCCTCCCTCCCCCGCAGCTGGGGCCA 457
gamma           ------------------------------------CCTAGATGCCCCAGTCT---TCT 20
zeta            ------------------------------------------------------------
iota            GCTGAGGAAAAGCGAAGTGGAAAAGCCAGTAACAGCCCTTACCCTATCACGTGTGAAATG 480
delta           GGACCCCTGGTGTCTGGCCCTGCGTCGAGAGGCTGGTGACTGCCACCCATAAGCTCCAGC 237
theta           -------AGGCGCGCGTCCCTGAGCCGGC------GTGGCGAGCGCCCTCTGGCCGGTGT 47
epsilon         GGACGC--AGCGCCACAAGGTGTAGCGAGTGAGTGGGGTGGGGCAAGAGGGGACCCAGGA 113
mu              TGAATGTGGCTTCTATGGACTCTATGACAAGATCCTGCTTTTCCGTCACGATCCTGCCTC 444

alpha           GTGAGCGTGGGGCCAGCCAGAG--AGCGAGAGAGCCGGAGAGAGCCAGAGAGAGC--CAG 97
beta            GCGGTGCCAAGCACAGCTGGACC-AGCGGCAGCAGCTGGGCGAGTGACAGCCCAG--CAA 514
gamma           ACTGCTCTGACCCCACCCGCTT----TCTCCCGGCTCGGTACAGCTGGTGCC-------- 68
zeta            ------------------------------------------------------------
iota            AGGGTCCTGGCGGTCTTTGAAC-----TTAGATACTCAAGCTGTTCTCAGGACTT--CTA 533
delta           TTCAGCCTCGGCTTACTCCCCT-----CAGGGGCTTGCAGGCTGAGGCCTGCCCT--CGG 290
theta           CGCCGCC-CGGAGTACCCTC----------GGGTCGCCAGGCCCGCGCCAGTCCC--CGC 94
epsilon         GTCCCCC-CAGGCTCCCAGCGC-----GCCTGCTCCTGCTCTTCAATCCTGCCCT--CGG 165
mu              TGAAAACATCCTTCAGCTGGTAAAAATCGCAAGTGACATTCAGGAGGGCGATCTTATTGA 504

alpha           AGAGAGCGGCTCAGCTCCCAGCTCCAAGCAGCGCAGCGCCC-GCCCGGCTCTCCCCGGCC 156
beta            CGCGCGCGCGGCCGCCGCCAGAGCCGGC--GCGAAGGGGCA-GCGCGGCCCTGCGGTCCC 571
gamma           ---GGGGGGTGCTGCTTTCTGCCCTGCGCTGCGCACCGTTA-GTGC--CCTGCCCCTGTC 122
zeta            ------------------------------------------------------------
iota            TGCCTACAAGTCCCGGGAAGCGC----AAGACAGAAAAC-G-CGGCACCCTGTACCTAAG 587
delta           ACGCGGCTGACCAGCCTCTCCCTCTCTTCCACACTTTGG-A-CTTCTCTTTGGACCTCCT 348
theta           CATCGGAGCAGCAGCGGC---------ACTGCGCTG-GG-A-CTGCGGCCACGACACC-- 140
epsilon         GGCGGACGGAGTGACCCCCGC------CCCGACCATGGT-A-GTGTTCAATGGCCTTCTT 217
mu              AGTGGTCCTGTCAGCTTCAGCCACCTTCGAAGACTTCCAGATCCGGCCTCACGCTCTCTT 564

alpha           ACCGCCGCCACCACCGCACCTCA-GCACCGC-CACCTCGGCCGCCGCCCCCGCCCACCCC 214
beta            CGGGCGGCAGCAGCGGCCGCCTA-GTCCCGCGCCTCTCCGGGCTTACAGCCCCCGGTCCC 630
gamma           CTTCCGATCTCAGAGTCTGCGGA-GTGCCCC-------------TATCGCCGTCCA-CCT 167
zeta            ------------------------------------------------------------
```

```
iota            GAACAAATCCCAGAATCCCACCG-GGACTCCAAATCCCAGAATCCCGCGCAGCAAATACA 646
delta           AAAAAGGCTCCATCATGGCACCG-TTCCTGCGCATCTCCTTCAATTCCTATGAGCTGGGC 407
theta           ---AGGGAACAACCATGTCACCG-TTTCTTCGAATTGGTTTATCCAACTTTGACTGTGGG 196
epsilon         ----AAGATCAA---AATCTGCG-AGGCCGTGAGCTTGAAGCCCACAGCCTGGTCGCTGC 269
mu              CGTTCATTCATACAGAGCCCCTGCTTTCTGTGATCACTGTGGAGAAATGCTGTGGGGACT 624
alpha           GGCCCTCCCCGGC---TGCTGCTCCCCGGCGGAGGCAAGAGGTGGTTGGGGGGGACCATG 271
beta            GCCGCCCCGGGGC---CGCCACCTCTCGGGGCTCCCCCCAGTCCCCGCGCGCGCAAGATG 687
gamma           GTTTCCTCAGAAA---AAAGGCCAGCTCGTGATCCCT---GCTGCGTTCCTGGGGCCATG 221
zeta            ------------------------------------------------------------
iota            TCCCGGAAGCGTGGCGGGAGCGAACGTGGTGGGAGGGGCCGTGGCGGGAGGCGTGTTGTG 706
delta           TCCCTGCAGGCGG---AGGACGACGCAAGCCAGCCTTTCTGTGCCGTGA--AGATGAAGG 462
theta           ACCTGTCAAGCTTGTCAGGGAGAGGCGGTGAACCCCTACTGTGCCGTGC--TTGTCAAAG 254
epsilon         GCCATGCGGTGGG---ACCCCGGCCCCAGACGTTCCTTCTGGACCCCTACATTGCCCTTA 326
mu              GGTGCGCCAAGGC----CTTAAATGTGAAGGATGTGGCCTGAATTACCATAAGAGATGTG 680

alpha           GCTGAC--GTTTACCCGGCCAACGACTCCACGGCGTCTCAGGACGTGGCCAACCGCTTCG 329
beta            GCTGACCCGGCTGCGGGGCCGCCG--CCGAGCGAGGGCGAGGAGAGCACGGTGCGCTTCG 745
gamma           GCGGGTCTGGGT-CCTGGCGGGGG---CGACTCAGAAGGGGGACCCCGACCCCTGTTTTG 277
zeta            ------------------------------------------------------------
iota            CAGAGCGGAGGGAGGAGCGCCGGGGCTCGGGCTGTGGCGGCGAAGCGACCCTTCGCTCGC 766
delta           AGGCACTCACCACAGACCGAGGGAAGACTCTGGTACAGAAGAAGCCCACCATGTACCCTG 522
theta           AGTATGTGGAATCAGAAAACGGGCAGATGTACATCCAGAAAAAGCCGACCATGTACCCGC 314
epsilon         ACGTGGACGACTCGCGCATCGGCCAAACAGCCACCAAGCAGAAGACCAACA---GTCCGG 383
mu              CATTTAAAATCCCCAACAATTGCA-GTGGAGTGAGAAGGAGAAGGCTCTCAAATGTTTCC 739

alpha           CCCGCAAAGGGGCGCTGAGGCAGAAGAACGTGCATGAGGTGAAAGACCACAAATTCATCG 389
beta            CCCGCAAAGGCGCCCTCCGGCAGAAGAACGTGCACGAGGTGAAGAACCACAAATTCACCG 805
gamma           CA-GAAAGGGGGCGCTGAGGCAGAAGGTGGTCCACGAGGTGAAGAGCCACAAGTTCACCG 336
zeta            -----CGAGGCGGGTGCCGTCGGTCC------CGCGCTGCGC--GCTCCCTTCCGCGTTC 47
iota            TCTGGCGGGTTAGGCGT-GTTGGTCCGGGAGGCGGGCGGCCACGGCTTCCCGACAGGCTC 825
delta           AGTGGAAGTCAACATTC-GACGCCCACATCTATGAAGGCCGTGTCATCCAGATCGTGCTG 581
theta           CTTGGGACAGCACCTTT-GATGCCCACATTAACAAGGGAAGGGTGATGCAGATCATCGTG 373
epsilon         CCTGGCACGATGAGTTC-GTCACTGATGTGTGCAATGGGCGCAAGATCGAGCTGGCTGTC 442
mu              CTCACTGGACTGGGTACTGTCCGCACAGCGTCTGCGGAGTTCTCCACC-AGTGCCCCCGA 798
                                  *

alpha           CCCGCTTCTTCAAGCAACCCACCTTCTGCAGCCACTGCACCGACTTCATCTGGGGGTTTG 449
beta            CCCGCTTCTTCAAGCAGCCCACCTTCTGCAGCCACTGCACCGACTTCATTTGGGGCTTCG 865
gamma           CTCGTTTCTTCAAGCAGCCAACCTTCTGCAGTCACTGTACCGACTTCATCTGGGGCATTG 396
zeta            CGCCGTCTGC--CCCGCCTGGCAACCCGGCCCTGCTCGGGGGCCGCTAGCCATGGCCGGA 105
iota            GGGAGGCCGAGACCCTCGCGGCG-CCCGGCGCTGCCCGGATCCCCTCAGCCTCCAGCGGA 884
delta           ATGCGGGCAGCTGAAGACCCCATGTCGGAGGTGACCGTGGGCGTGTCAGTGCTGGCTGAG 641
theta           AAAGGCAAAAATGTAGACCTCATATCAGAAACCACCGTGGAGCTCTACTCCCTGGCAGAG 433
epsilon         TTTCACGATGCTCCTATCGGCTACGACGACTTCGTGGCCAACTGCACCATCCAGTTCGAG 502
mu              TGAGCCTCTACTGTCTCCTGTGAGCCCTGGCTTTGAGCAAAAGTCTCCATCTGAGTCATT 858

alpha           GAAAACAAGGCTTCCAGTGCCAAGTTTGCTGTTTTGTGGTTCACAAGAGGTGCCATGAGT 509
beta            GGAAACAGGGATTCCAGTGTCAAGTCTGCTGCTTTGTTGTACACAAGCGCTGCCATGAAT 925
gamma           GAAAGCAGGGCCTGCAATGTCAAGTCTGCAGCTTTGTGGTTCACCGCCGATGCCACGAAT 456
zeta            GTGCCCTGGACACA--GCGCTGACGGC--GGCTGGCGGAGT-GCGCCATGCCCAGCAGGA 160
iota            GAGGCGGGGGAGTGAGGAGATGCCGACCCAGAGGGACAGCA-GCACCATGTCTCACACGG 943
delta           -CGCTGCAAGAAGA--ACAACGGCAAGGCTGAGTTCTGGCT-GGACCTGCAGCCTCAGGC 697
theta           -AGATGCCGCAAGA--ACAATGGGCGGACAGAAATATGGTT-AGAGCTGAAACCTCAAGG 489
epsilon         GAGCTGCTGCAGAATGGGAGCCGTCACTTCGAGGACTGGAT-TGATCTGGAGCCAGAAGG 561
mu              TATCGGTCGTGAGAAGAGGTCAAATTCTCAGTCATATGTTGGACGGCCGATTCAGCTCGA 918
                                          *

alpha           TTGTTACTTTCTCT---TGTCCGGGTGCGGATAAGGGACCTGACACTGATGACCCCAGAA 566
beta            TCGTCACGTTCTCC---TGCCCTGGTGCAGACAAGGGCCCGGCCTCTGATGACCCACGGA 982
gamma           TTGTGACCTTCGAG---TGTCCAGGAGCTGGAAAGGGCCCCCAGACGGACGACCCTCGCA 513
```

```
zeta            CCGACCCCAAGATG---GACCGGAGCGGCGGCCGC---GTCCGTCTGAAGGCGCACTACG 214
iota            TCGCGTGCGGCGGC---GGCGGGGACCATTCCCACCAGGTCCGGGTGAAAGCCTACTACC 1000
delta           CAAGGTGCTGATGT---GTGTGCAGTATTTCCTGGAGGATGGGG----ATTGCAAACAGT 750
theta           CCGAATGCTAATGA---ATGCAAGATACTTTCTGGAA-ATGAGT----GACACAAAGGAC 541
epsilon         --AAAAGTCTACGT---GATCATCGATCTCTCGGGATCATCGGGCGAAGCCCCTAAAGAC 616
mu              CAAGCTCCTGATGTCTAAGGTGAAGGTGCCACACACCTTTGTCATCCACTCCTACACACG 978

alpha           GCAAGCACAAGTTCAAAATCCACACCTATGGAAGCCCTACCTTCTGTGA--------TCA 618
beta            GCAAACACAAGTTTAAGATCCACACCTACTCCAGCCCTACCTTCTGTGA--------CCA 1034
gamma           ACAAGCACAAGTTCCGTCTGCACAGCTACAGCAGTCCCACCTTCTGCGA--------CCA 565
zeta            GCGGGGACATCCTGATTACCAGCGTGGACCCCACGACAACTTTCCAGGA--------CCT 266
iota            GCGGGGATATTATGATAACACACTTCGAGCCTTCCATCTCCTTTGAAGG--------ACT 1052
delta           CCATGCGTAGTGAGGAGGAGGCCATGTTCCCAACTATGA-ACCGCCGTG--------GAG 801
theta           ATGAGTGAATTTGAGAACGAAGGATTCTTTGCACTGCATCACCGCCGAG--------GCG 593
epsilon         AATGAAGAACGAGTGTTTAGGGAGCGGATGCGGCCAAGGAAGCGCCAAG--------GGG 668
mu              GCCCACGGTCTGCCAGTTCTGTAAGAAGCTCCTCAAGGGCCTCTTCCGGCAGGGTTTGCA 1038

alpha           CTGTGGGTCCCTGCTCTAC--GGACTTATCCACCAAGGGATGAAATGCGACACCTGCGAC 676
beta            CTGTGGATCACTGCTGTAT--GGGCTCATCCACCAGGGGATGAAATGCGACACCTGTATG 1092
gamma           CTGTGGTTCCCTCCTCTAC--GGGCTGGTGCACCAGGGCATGAAATGTTCCTGTTGCGAA 623
zeta            CTGTGAGGAAGTGCGAGACATGTGTGGCCTGCACCAGCAGCACCCACTCACCCTCAAGTG 326
iota            TTGCAGTGAGGTTCGAGATATGTGTTCTTTTGACAATGAGCAGCCATTCACCATGAAATG 1112
delta           CCATTAAACAGGCCAAGAT-----TCACTACATCAAGAACCACGAGTTCATCGCCACCTT 856
theta           CCATCAAACAAGCCAAAGT-----CCACCACGTCAAGTGTCACGAGTTCACAGCCACCTT 648
epsilon         CTGTCAGGCG---CAGGGT-----CCACCAGGTCAATGGCCACAAGTTCATGGCCACCTA 720
mu              GTGCAAAGATTGCCGATTCAACTGTCACAAACGCTGTGCACCAAAAGTACCAAACAACTG 1098
                             *                   *

alpha           ATG--AATGTTCACAAGCAGTGCG-----TGATCAATGTCCCCAGCCTCTGCGGAATGGA 729
beta            ATG--AATGTCCACAAGCGCTGCG-----TGATGAACGTCCCCAGCCTCTGTGGCACCGA 1145
gamma           ATG--AATGTGCACCGACGCTGTG-----TGCGCAGCGTGCCCTCCCTTTGCGGCGTGGA 676
zeta            GGTGGACAGTGAAGGTGACCCTTG-----TACTGTGTCCTCACAGATGGAGCTGGAGGAG 381
iota            GATAGATGAGGAAGGAGACCCGTG-----CACAGTGTCTTCTCAGTTGGAGTTGGAAGAG 1167
delta           CTT---TGGGCAGCCCACCTTCTG-----TTCTGTGTGCAAAGAGTTTGTCTGGGCCTC 908
theta           TTT---CCCTCAACCCACGTTCTG-----CTCTGTCTGCCATGAATTTGTCTGGGGGCTG 700
epsilon         CTT---GCGGCAGCCCACCTACTG-----CTCCCACTGTAGGGATTTCATCTGGGGTGTC 772
mu              CTTGGGCGAAGTGACCATCAATGGAGAATTGCTTAGCCCTGGGGCAGAGTCTGATGTTGT 1158
                                      *

alpha           TCACACAGAGAAGAGGGGGCGGATTTACCTGAAGGCAGAGGT---CACAGATGAAAAGCT 786
beta            CCACACAGAACGCCGTGGCCGCATCTACATCCAGGCCCACAT---CGACAGGGAGGTCCT 1202
gamma           CCATACAGAGCGCCGTGGACGTCTGCAACTGGAAATCCGGGCTCCCACATCAGATGAGAT 736
zeta            GCCTTCCGCCTGGCCTGTCAGGGCAGGGACGAAGTGCTCATCATCCACGTTTTCCCAAGC 441
iota            GCTTTCAGGCTGTATGAGTTGAACAAGGATTCTGAACTCCTGATCCACGTGTTCCCGTGT 1227
delta           A---ACAAGCAAGGCTACAAATGCAGGCAATGCAACGCTGCCATCCATAAGAAATGCATC 965
theta           A---ACAAGCAGGGCTACCAGTGCCGACAATGTAATGCAGCGATTCACAAGAAGTGCATC 757
epsilon         ATAGGAAAACAGGGATATCAATGTCAAGTTTGTACCTGCGTCGTCCACAAACGATGCCAT 832
mu              CATGGAAGAAGGGAGCGATGACAATGACAGCGAACGGAACAGTGGACTCATGGATGACAT 1218

alpha           GCACGTCACCGTACGAGATGCAAAAAATCTAATC---CCTATGGATCCAAATGGG----- 838
beta            CATCGTTGTTGTAAGAGATGCTAAAAATCTGGTA---CCTATGGACCCCAACGGC----- 1254
gamma           CCATATTACTGTGGGTGAGGCCCGGAACCTCATT---CCTATGGACCCCAATGGC----- 788
zeta            ATCCCAGAACAACCGGGCATGCCTTGTCCTGGAG---AAGACAAGTCCATCTACC----- 493
iota            GTACCAGAGCGTCCTGGAATGCCTTGCCCAGGGG---AAGACAAGTCCATTTACC----- 1279
delta           G-ACAAGATTATCGGCCGCTGCACTGGCACTGCT---ACCAATAGCCGGGACACC----- 1016
theta           G-ATAAAGTGATAGCCAAGTGCACAGGATCGGCG---ATCAATAGTCGAGAGACC----- 808
epsilon         G-AGCTCATTATTACGAAGTGCGCTGG----GCT---A--AAGAAACAGGAAACC----- 877
mu              GGACGAGGCCATGGTCCAGGACACTGAGATGGCTTTGGCGGAGGGTCAGAGTGACGGTGC 1278
                                                                  *
```

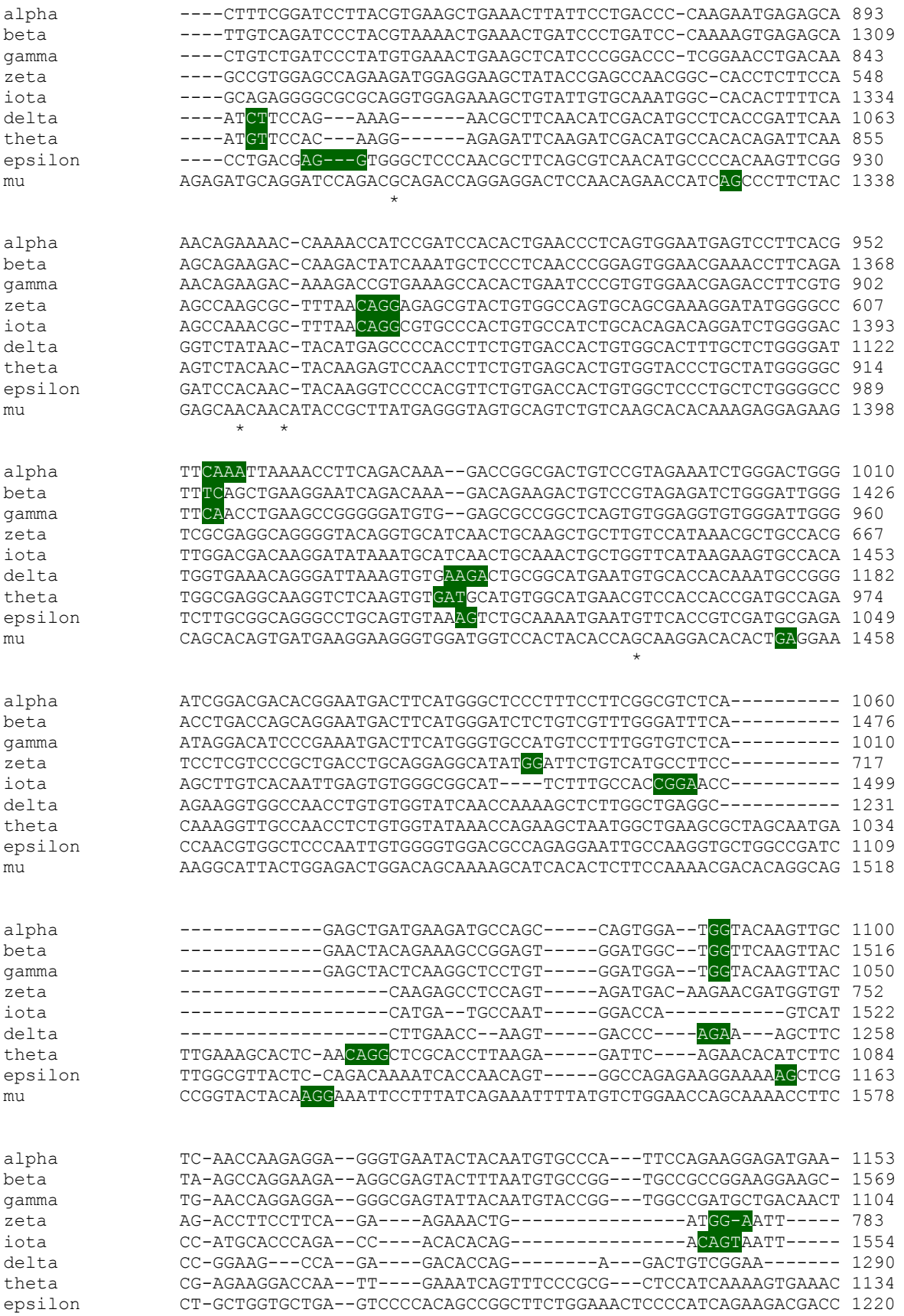
alpha ----CTTTCGGATCCTTACGTGAAGCTGAAACTTATTCCTGACCC-CAAGAATGAGAGCA 893
beta ----TTGTCAGATCCCTACGTAAAACTGAAACTGATCCCTGATCC-CAAAAGTGAGAGCA 1309
gamma ----CTGTCTGATCCCTATGTGAAACTGAAGCTCATCCCGGACCC-TCGGAACCTGACAA 843
zeta ----GCCGTGGAGCCAGAAGATGGAGGAAGCTATACCGAGCCAACGGC-CACCTCTTCCA 548
iota ----GCAGAGGGGCGCGCAGGTGGAGAAAGCTGTATTGTGCAAATGGC-CACACTTTTCA 1334
delta ----ATCTTCCAG---AAAG------AACGCTTCAACATCGACATGCCTCACCGATTCAA 1063
theta ----ATGTTCCAC---AAGG------AGAGATTCAAGATCGACATGCCACACAGATTCAA 855
epsilon ----CCTGACGAG---GTGGGCTCCCAACGCTTCAGCGTCAACATGCCCCACAAGTTCGG 930
mu AGAGATGCAGGATCCAGACGCAGACCAGGAGGACTCCAACAGAACCATCAGCCCTTCTAC 1338
alpha AACAGAAAAC-CAAAACCATCCGATCCACACTGAACCCTCAGTGGAATGAGTCCTTCACG 952
beta AGCAGAAGAC-CAAGACTATCAAATGCTCCCTCAACCCGGAGTGGAACGAAACCTTCAGA 1368
gamma AACAGAAGAC-AAAGACCGTGAAAGCCACACTGAATCCCGTGTGGAACGAGACCTTCGTG 902
zeta AGCCAAGCGC-TTTAACAGGAGAGCGTACTGTGGCCAGTGCAGCGAAAGGATATGGGGCC 607
iota AGCCAAACGC-TTTAACAGGCGTGCCCACTGTGCCATCTGCACAGACAGGATCTGGGGAC 1393
delta GGTCTATAAC-TACATGAGCCCCACCTTCTGTGACCACTGTGGCACTTTGCTCTGGGGAT 1122
theta AGTCTACAAC-TACAAGAGTCCAACCTTCTGTGAGCACTGTGGTACCCTGCTATGGGGGC 914
epsilon GATCCACAAC-TACAAGGTCCCCACGTTCTGTGACCACTGTGGCTCCCTGCTCTGGGGCC 989
mu GAGCAACAACATACCGCTTATGAGGGTAGTGCAGTCTGTCAAGCACACAAAGAGGAGAAG 1398
alpha TTCAAATTAAAACCTTCAGACAAA--GACCGGCGACTGTCCGTAGAAATCTGGGACTGGG 1010
beta TTTCAGCTGAAGGAATCAGACAAA--GACAGAAGACTGTCCGTAGAGATCTGGGATTGGG 1426
gamma TTCAACCTGAAGCCGGGGGATGTG--GAGCGCCGGCTCAGTGTGGAGGTGTGGGATTGGG 960
zeta TCGCGAGGCAGGGGTACAGGTGCATCAACTGCAAGCTGCTTGTCCATAAACGCTGCCACG 667
iota TTGGACGACAAGGATATAAATGCATCAACTGCAAACTGCTGGTTCATAAGAAGTGCCACA 1453
delta TGGTGAAACAGGGATTAAAGTGTGAAGACTGCGGCATGAATGTGCACCACAAATGCCGGG 1182
theta TGGCGAGGCAAGGTCTCAAGTGTGATGCATGTGGCATGAACGTCCACCACCGATGCCAGA 974
epsilon TCTTGCGGCAGGGCCTGCAGTGTAAAGTCTGCAAAATGAATGTTCACCGTCGATGCGAGA 1049
mu CAGCACAGTGATGAAGGAAGGGTGGATGGTCCACTACACCAGCAAGGACACACTGAGGAA 1458
alpha ATCGGACGACACGGAATGACTTCATGGGCTCCCTTTCCTTCGGCGTCTCA---------- 1060
beta ACCTGACCAGCAGGAATGACTTCATGGGATCTCTGTCGTTTGGGATTTCA---------- 1476
gamma ATAGGACATCCCGAAATGACTTCATGGGTGCCATGTCCTTTGGTGTCTCA---------- 1010
zeta TCCTCGTCCCGCTGACCTGCAGGAGGCATATGGATTCTGTCATGCCTTCC---------- 717
iota AGCTTGTCACAATTGAGTGTGGGCGGCAT----TCTTTGCCACCGGAACC---------- 1499
delta AGAAGGTGGCCAACCTGTGTGGTATCAACCAAAAGCTCTTGGCTGAGGC---------- 1231
theta CAAAGGTTGCCAACCTCTGTGGTATAAACCAGAAGCTAATGGCTGAAGCGCTAGCAATGA 1034
epsilon CCAACGTGGCTCCCAATTGTGGGGTGGACGCCAGAGGAATTGCCAAGGTGCTGGCCGATC 1109
mu AAGGCATTACTGGAGACTGGACAGCAAAAGCATCACACTCTTCCAAAACGACACAGGCAG 1518
alpha ----------GAGCTGATGAAGATGCCAGC-----CAGTGGA--TGGTACAAGTTGC 1100
beta ----------GAACTACAGAAAGCCGGAGT-----GGATGGC--TGGTTCAAGTTAC 1516
gamma ----------GAGCTACTCAAGGCTCCTGT-----GGATGGA--TGGTACAAGTTAC 1050
zeta ----------CAAGAGCCTCCAGT-----AGATGAC-AAGAACGATGGTGT 752
iota ----------CATGA--TGCCAAT-----GGACCA----------GTCAT 1522
delta ----------CTTGAACC--AAGT-----GACCC----AGAA---AGCTTC 1258
theta TTGAAAGCACTC-AACAGGCTCGCACCTTAAGA-----GATTC----AGAACACATCTTC 1084
epsilon TTGGCGTTACTC-CAGACAAAATCACCAACAGT-----GGCCAGAGAAGGAAAAAGCTCG 1163
mu CCGGTACTACAAGGAAATTCCTTTATCAGAAATTTTATGTCTGGAACCAGCAAAACCTTC 1578
alpha TC-AACCAAGAGGA--GGGTGAATACTACAATGTGCCCA---TTCCAGAAGGAGATGAA- 1153
beta TA-AGCCAGGAAGA--AGGCGAGTACTTTAATGTGCCGG---TGCCGCCGGAAGGAAGC- 1569
gamma TG-AACCAGGAGGA--GGGCGAGTATTACAATGTACCGG---TGGCCGATGCTGACAACT 1104
zeta AG-ACCTTCCTTCA--GA----AGAAACTG----------ATGG-AATT----- 783
iota CC-ATGCACCCAGA--CC----ACACACAG----------ACAGTAATT----- 1554
delta CC-GGAAG---CCA--GA----GACACCAG--------A---GACTGTCGGAA------- 1290
theta CG-AGAAGGACCAA--TT----GAAATCAGTTTCCCGCG---CTCCATCAAAAGTGAAAC 1134
epsilon CT-GCTGGTGCTGA--GTCCCCACAGCCGGCTTCTGGAAACTCCCCATCAGAAGACGACC 1220

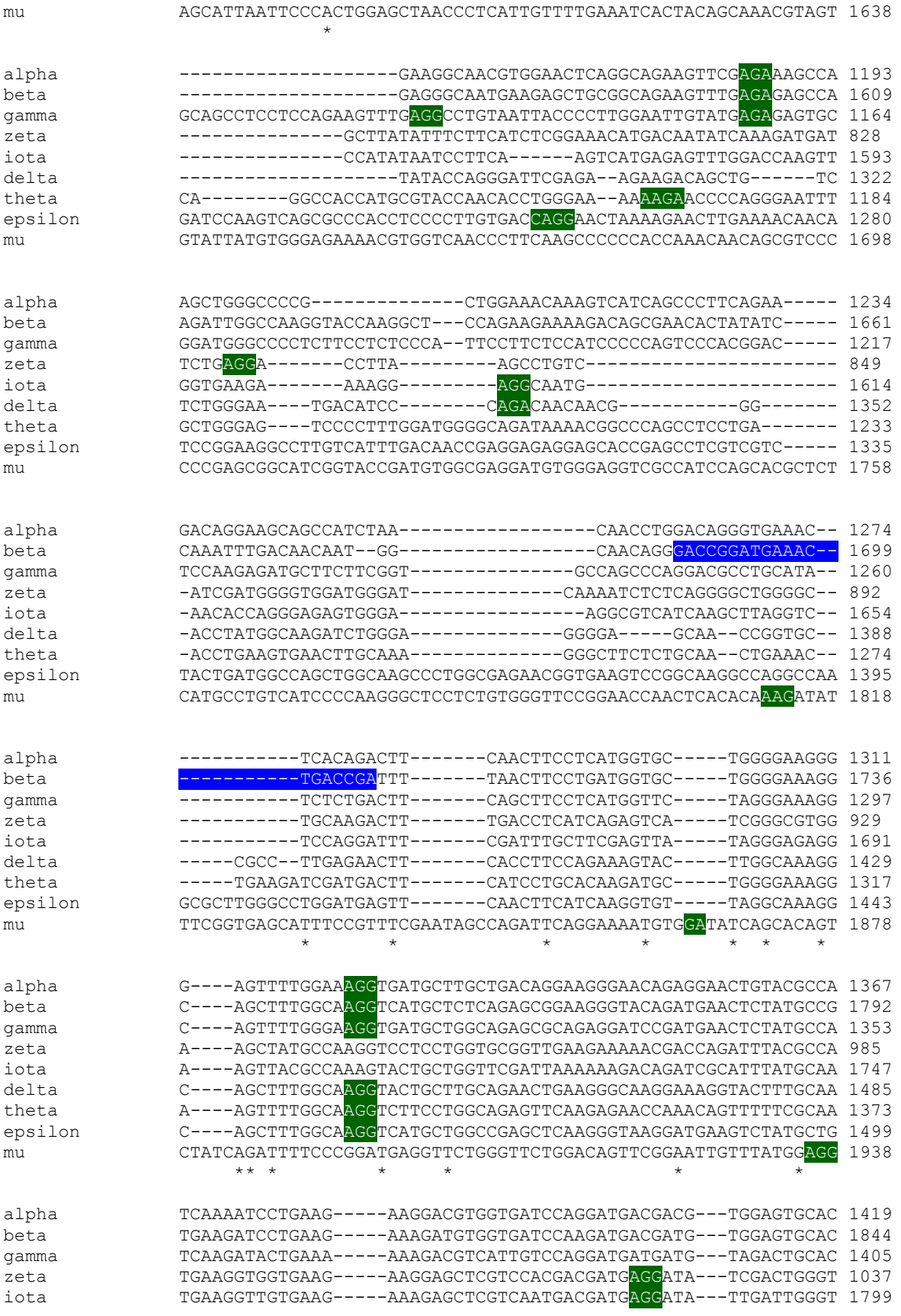
mu AGCATTAATTCCCACTGGAGCTAACCCTCATTGTTTTGAAATCACTACAGCAAACGTAGT 1638
alpha ----------GAAGGCAACGTGGAACTCAGGCAGAAGTTCGAGAAAGCCA 1193
beta ----------GAGGGCAATGAAGAGCTGCGGCAGAAGTTTGAGAGAGCCA 1609
gamma GCAGCCTCCTCCAGAAGTTTGAGGCCTGTAATTACCCCTTGGAATTGTATGAGAGAGTGC 1164
zeta ----------GCTTATATTTCTTCATCTCGGAAACATGACAATATCAAAGATGAT 828
iota ----------CCATATAATCCTTCA------AGTCATGAGAGTTTGGACCAAGTT 1593
delta ----------TATACCAGGGATTCGAGA--AGAAGACAGCTG------TC 1322
theta CA--------GGCCACCATGCGTACCAACACCTGGGAA--AAAAGAACCCCAGGGAATTT 1184
epsilon GATCCAAGTCAGCGCCCACCTCCCCTTGTGACCAGGAACTAAAAGAACTTGAAAACAACA 1280
mu GTATTATGTGGGAGAAAACGTGGTCAACCCTTCAAGCCCCCCACCAAACAACAGCGTCCC 1698
alpha AGCTGGGCCCCG----------CTGGAAACAAAGTCATCAGCCCTTCAGAA----- 1234
beta AGATTGGCCAAGGTACCAAGGCT---CCAGAAGAAAAGACAGCGAACACTATATC----- 1661
gamma GGATGGGCCCCTCTTCCTCTCCCA--TTCCTTCTCCATCCCCCAGTCCCACGGAC----- 1217
zeta TCTGAGGA-------CCTTA---------AGCCTGTC---------- 849
iota GGTGAAGA-------AAAGG---------AGGCAATG---------- 1614
delta TCTGGGAA----TGACATCC--------CAGACAACAACG----------GG------- 1352
theta GCTGGGAG----TCCCCTTTGGATGGGGCAGATAAAACGGCCCAGCCTCCTGA------- 1233
epsilon TCCGGAAGGCCTTGTCATTTGACAACCGAGGAGAGGAGCACCGAGCCTCGTCGTC----- 1335
mu CCCGAGCGGCATCGGTACCGATGTGGCGAGGATGTGGGAGGTCGCCATCCAGCACGCTCT 1758
alpha GACAGGAAGCAGCCATCTAA----------CAACCTGGACAGGGTGAAAC-- 1274
beta CAAATTTGACAACAAT--GG----------CAACAGGGACCGGATGAAAC-- 1699
gamma TCCAAGAGATGCTTCTTCGGT----------GCCAGCCCAGGACGCCTGCATA-- 1260
zeta -ATCGATGGGGTGGATGGGAT----------CAAAATCTCTCAGGGGCTGGGGC-- 892
iota -AACACCAGGGAGAGTGGGA----------AGGCGTCATCAAGCTTAGGTC-- 1654
delta -ACCTATGGCAAGATCTGGGA----------GGGGA-----GCAA--CCGGTGC-- 1388
theta -ACCTGAAGTGAACTTGCAAA----------GGGCTTCTCTGCAA--CTGAAAC-- 1274
epsilon TACTGATGGCCAGCTGGCAAGCCCTGGCGAGAACGGTGAAGTCCGGCAAGGCCAGGCCAA 1395
mu CATGCCTGTCATCCCCAAGGGCTCCTCTGTGGGTTCCGGAACCAACTCACACAAAGATAT 1818
alpha ----------TCACAGACTT-------CAACTTCCTCATGGTGC-----TGGGGAAGGG 1311
beta ----------TGACCGATTT-------TAACTTCCTGATGGTGC-----TGGGGAAAGG 1736
gamma ----------TCTCTGACTT-------CAGCTTCCTCATGGTTC-----TAGGGAAAGG 1297
zeta ----------TGCAAGACTT-------TGACCTCATCAGAGTCA-----TCGGGCGTGG 929
iota ----------TCCAGGATTT-------CGATTTGCTTCGAGTTA-----TAGGGAGAGG 1691
delta -----CGCC--TTGAGAACTT-------CACCTTCCAGAAAGTAC-----TTGGCAAAGG 1429
theta -----TGAAGATCGATGACTT-------CATCCTGCACAAGATGC-----TGGGGAAAGG 1317
epsilon GCGCTTGGGCCTGGATGAGTT-------CAACTTCATCAAGGTGT-----TAGGCAAAGG 1443
mu TTCGGTGAGCATTTCCGTTTCGAATAGCCAGATTCAGGAAAATGTGGATATCAGCACAGT 1878
alpha G----AGTTTTGGAAAGGTGATGCTTGCTGACAGGAAGGGAACAGAGGAACTGTACGCCA 1367
beta C----AGCTTTGGCAAGGTCATGCTCTCAGAGCGGAAGGGTACAGATGAACTCTATGCCG 1792
gamma C----AGTTTTGGGAAGGTGATGCTGGCAGAGCGCAGAGGATCCGATGAACTCTATGCCA 1353
zeta A----AGCTATGCCAAGGTCCTCCTGGTGCGGTTGAAGAAAAACGACCAGATTTACGCCA 985
iota A----AGTTACGCCAAAGTACTGCTGGTTCGATTAAAAAAGACAGATCGCATTTATGCAA 1747
delta C----AGCTTTGGCAAGGTACTGCTTGCAGAACTGAAGGGCAAGGAAAGGTACTTTGCAA 1485
theta A----AGTTTTGGCAAGGTCTTCCTGGCAGAGTTCAAGAGAACCAAACAGTTTTTCGCAA 1373
epsilon C----AGCTTTGGCAAGGTCATGCTGGCCGAGCTCAAGGGTAAGGATGAAGTCTATGCTG 1499
mu CTATCAGATTTTCCCGGATGAGGTTCTGGGTTCTGGACAGTTCGGAATTGTTTATGGAGG 1938
alpha TCAAAATCCTGAAG-----AAGGACGTGGTGATCCAGGATGACGACG---TGGAGTGCAC 1419
beta TGAAGATCCTGAAG-----AAAGATGTGGTGATCCAAGATGACGATG---TGGAGTGCAC 1844
gamma TCAAGATACTGAAA-----AAAGACGTCATTGTCCAGGATGATGATG---TAGACTGCAC 1405
zeta TGAAGGTGGTGAAG-----AAGGAGCTCGTCCACGACGATGAGGATA---TCGACTGGGT 1037
iota TGAAGGTTGTGAAG-----AAAGAGCTCGTCAATGACGATGAGGATA---TTGATTGGGT 1799

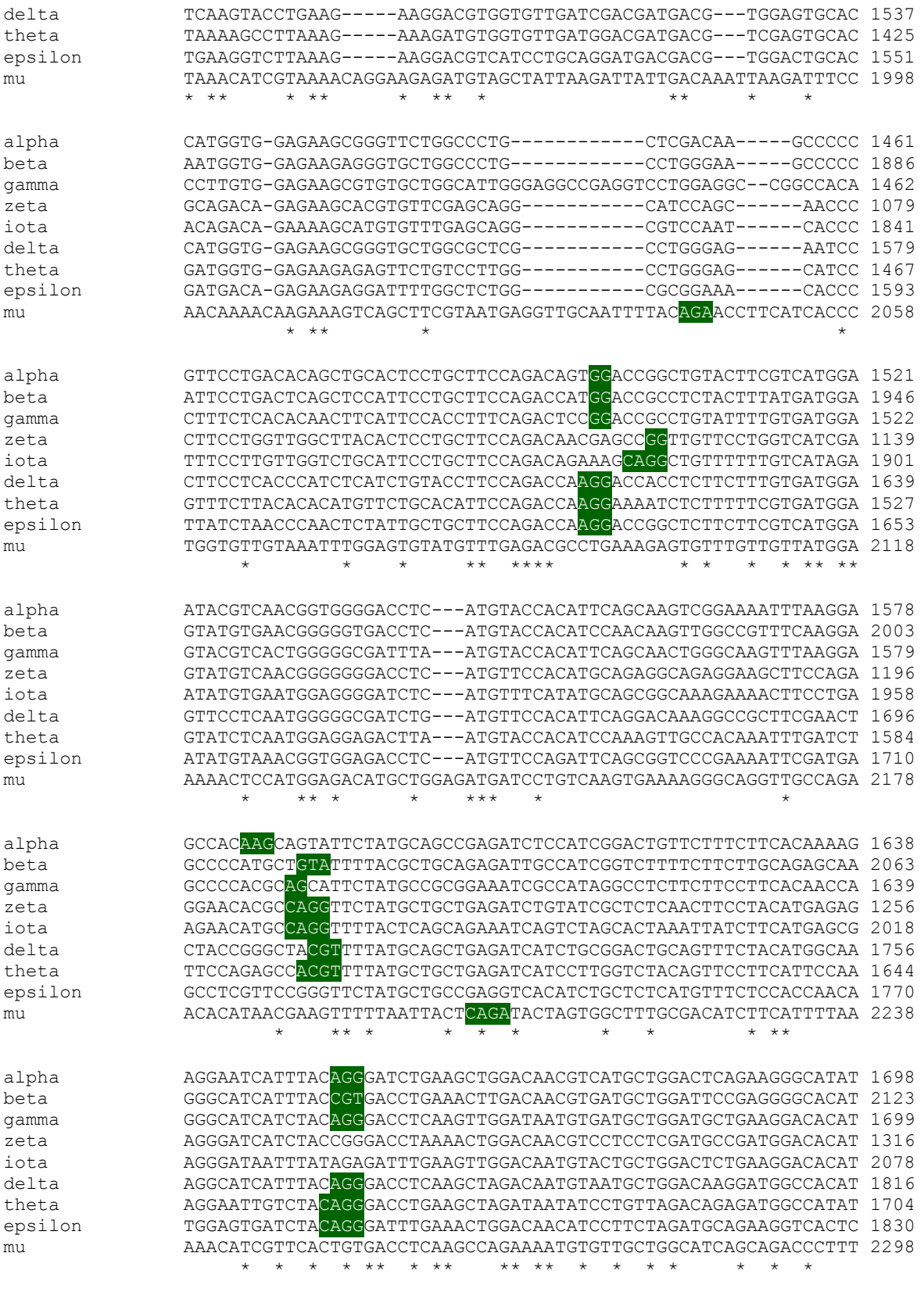
delta TCAAGTACCTGAAG-----AAGGACGTGGTGTTGATCGACGATGACG---TGGAGTGCAC 1537
theta TAAAAGCCTTAAAG-----AAAGATGTGGTGTTGATGGACGATGACG---TCGAGTGCAC 1425
epsilon TGAAGGTCTTAAAG-----AAGGACGTCATCCTGCAGGATGACGACG---TGGACTGCAC 1551
mu TAAACATCGTAAAACAGGAAGAGATGTAGCTATTAAGATTATTGACAAATTAAGATTTCC 1998
alpha CATGGTG-GAGAAGCGGGTTCTGGCCCTG----------CTCGACAA-----GCCCCC 1461
beta AATGGTG-GAGAAGAGGGTGCTGGCCCTG----------CCTGGGAA-----GCCCCC 1886
gamma CCTTGTG-GAGAAGCGTGTGCTGGCATTGGGAGGCCGAGGTCCTGGAGGC--CGGCCACA 1462
zeta GCAGACA-GAGAAGCACGTGTTCGAGCAGG----------CATCCAGC------AACCC 1079
iota ACAGACA-GAAAAGCATGTGTTTGAGCAGG----------CGTCCAAT------CACCC 1841
delta CATGGTG-GAGAAGCGGGTGCTGGCGCTCG----------CCTGGGAG------AATCC 1579
theta GATGGTG-GAGAAGAGAGTTCTGTCCTTGG----------CCTGGGAG------CATCC 1467
epsilon GATGACA-GAGAAGAGGATTTTGGCTCTGG----------CGCGGAAA------CACCC 1593
mu AACAAAACAAGAAAGTCAGCTTCGTAATGAGGTTGCAATTTTACAGAACCTTCATCACCC 2058
alpha GTTCCTGACACAGCTGCACTCCTGCTTCCAGACAGTGGACCGGCTGTACTTCGTCATGGA 1521
beta ATTCCTGACTCAGCTCCATTCCTGCTTCCAGACCATGGACCGCCTCTACTTTATGATGGA 1946
gamma CTTTCTCACACAACTTCATTCCACCTTTCAGACTCCGGACCGCCTGTATTTTGTGATGGA 1522
zeta CTTCCTGGTTGGCTTACACTCCTGCTTCCAGACAACGAGCCGGTTGTTCCTGGTCATCGA 1139
iota TTTCCTTGTTGGTCTGCATTCCTGCTTCCAGACAGAAAGCAGGCTGTTTTTTGTCATAGA 1901
delta CTTCCTCACCCATCTCATCTGTACCTTCCAGACCAAGGACCACCTCTTCTTTGTGATGGA 1639
theta GTTTCTTACACACATGTTCTGCACATTCCAGACCAAGGAAAATCTCTTTTTCGTGATGGA 1527
epsilon TTATCTAACCCAACTCTATTGCTGCTTCCAGACCAAGGACCGGCTCTTCTTCGTCATGGA 1653
mu TGGTGTTGTAAATTTGGAGTGTATGTTTGAGACGCCTGAAAGAGTGTTTGTTGTTATGGA 2118
alpha ATACGTCAACGGTGGGGACCTC---ATGTACCACATTCAGCAAGTCGGAAAATTTAAGGA 1578
beta GTATGTGAACGGGGGTGACCTC---ATGTACCACATCCAACAAGTTGGCCGTTTCAAGGA 2003
gamma GTACGTCACTGGGGGCGATTTA---ATGTACCACATTCAGCAACTGGGCAAGTTTAAGGA 1579
zeta GTATGTCAACGGGGGGGACCTC---ATGTTCCACATGCAGAGGCAGAGGAAGCTTCCAGA 1196
iota ATATGTGAATGGAGGGGATCTC---ATGTTTCATATGCAGCGGCAAAGAAAACTTCCTGA 1958
delta GTTCCTCAATGGGGGCGATCTG---ATGTTCCACATTCAGGACAAAGGCCGCTTCGAACT 1696
theta GTATCTCAATGGAGGAGACTTA---ATGTACCACATCCAAAGTTGCCACAAATTTGATCT 1584
epsilon ATATGTAAACGGTGGAGACCTC---ATGTTCCAGATTCAGCGGTCCCGAAAATTCGATGA 1710
mu AAAACTCCATGGAGACATGCTGGAGATGATCCTGTCAAGTGAAAAGGGCAGGTTGCCAGA 2178
alpha GCCACAAGCAGTATTCTATGCAGCCGAGATCTCCATCGGACTGTTCTTTCTTCACAAAAG 1638
beta GCCCCATGCTGTATTTTACGCTGCAGAGATTGCCATCGGTCTTTTCTTCTTGCAGAGCAA 2063
gamma GCCCCACGCAGCATTCTATGCCGCGGAAATCGCCATAGGCCTCTTCTTCCTTCACAACCA 1639
zeta GGAACACGCCAGGTTCTATGCTGCTGAGATCTGTATCGCTCTCAACTTCCTACATGAGAG 1256
iota AGAACATGCCAGGTTTTACTCAGCAGAAATCAGTCTAGCACTAAATTATCTTCATGAGCG 2018
delta CTACCGGGCTACGTTTTATGCAGCTGAGATCATCTGCGGACTGCAGTTTCTACATGGCAA 1756
theta TTCCAGAGCCACGTTTTATGCTGCTGAGATCATCCTTGGTCTACAGTTCCTTCATTCCAA 1644
epsilon GCCTCGTTCCGGGTTCTATGCTGCCGAGGTCACATCTGCTCTCATGTTTCTCCACCAACA 1770
mu ACACATAACGAAGTTTTTAATTACTCAGATACTAGTGGCTTTGCGACATCTTCATTTTAA 2238
alpha AGGAATCATTTACAGGGATCTGAAGCTGGACAACGTCATGCTGGACTCAGAAGGGCATAT 1698
beta GGGCATCATTTACCGTGACCTGAAACTTGACAACGTGATGCTGGATTCCGAGGGGCACAT 2123
gamma GGGCATCATCTACAGGGACCTCAAGTTGGATAATGTGATGCTGGATGCTGAAGGACACAT 1699
zeta AGGGATCATCTACCGGGACCTAAAACTGGACAACGTCCTCCTCGATGCCGATGGACACAT 1316
iota AGGGATAATTTATAGAGATTTGAAGTTGGACAATGTACTGCTGGACTCTGAAGGACACAT 2078
delta AGGCATCATTTACAGGGACCTCAAGCTAGACAATGTAATGCTGGACAAGGATGGCCACAT 1816
theta AGGAATTGTCTACAGGGACCTGAAGCTAGATAATATCCTGTTAGACAGAGATGGCCATAT 1704
epsilon TGGAGTGATCTACAGGGATTTGAAACTGGACAACATCCTTCTAGATGCAGAAGGTCACTC 1830
mu AAACATCGTTCACTGTGACCTCAAGCCAGAAAATGTGTTGCTGGCATCAGCAGACCCTTT 2298
alpha CAAAATCGC-CGACTTCGGGAT----GTGCAAGGAACACATGATGGACGGGGTCACGACC 1753
beta CAAAATCGC-TGACTTTGGCAT----GTGTAAAGAGAATATCTGGGATGGGGTGACAACC 2178

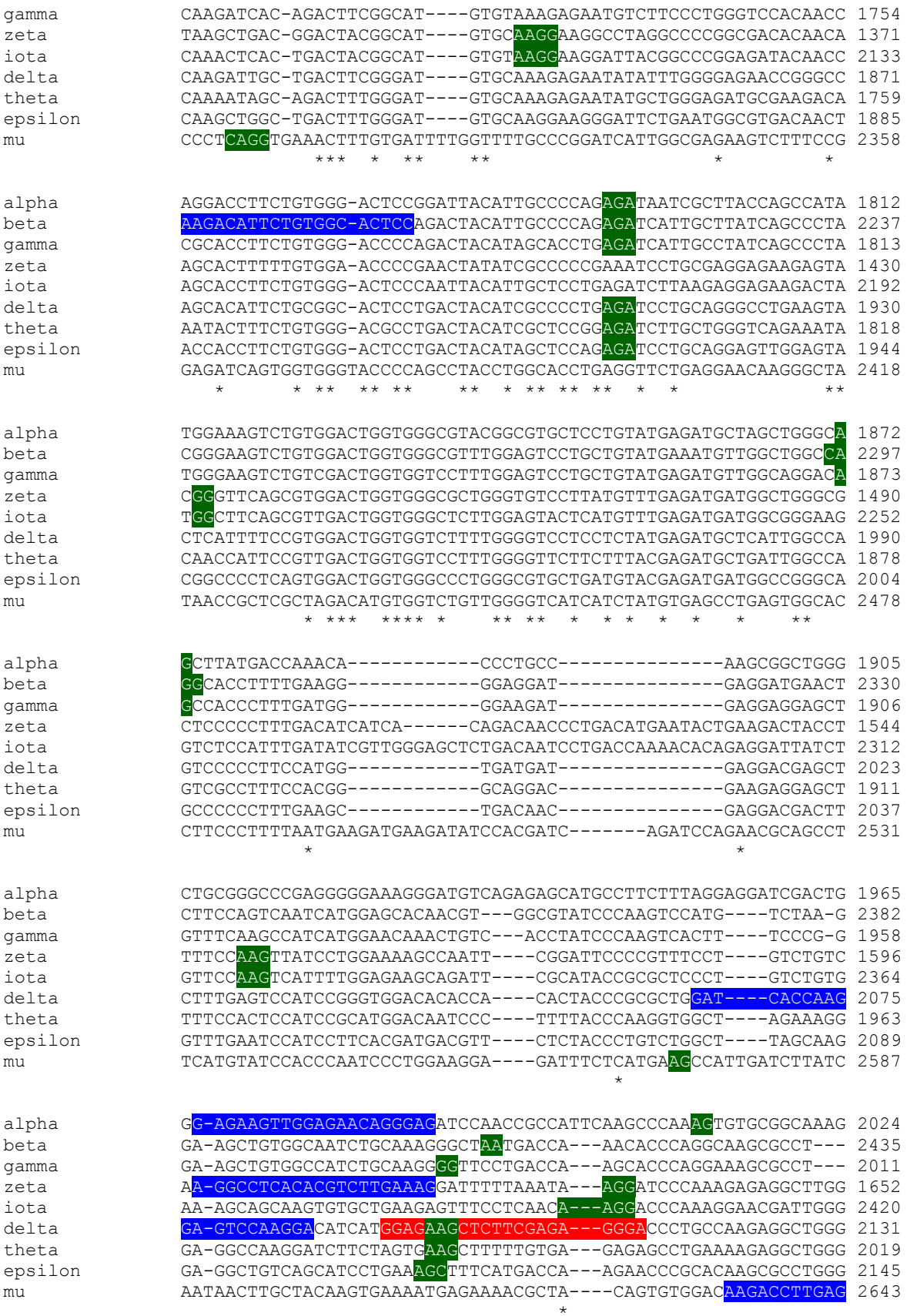
gamma CAAGATCAC-AGACTTCGGCAT----GTGTAAAGAGAATGTCTTCCCTGGGTCCACAACC 1754
zeta TAAGCTGAC-GGACTACGGCAT----GTGCAAGGAAGGCCTAGGCCCCGGCGACACAACA 1371
iota CAAACTCAC-TGACTACGGCAT----GTGTAAGGAAGGATTACGGCCCGGAGATACAACC 2133
delta CAAGATTGC-TGACTTCGGGAT----GTGCAAAGAGAATATATTTGGGGAGAACCGGGCC 1871
theta CAAAATAGC-AGACTTTGGGAT----GTGCAAAGAGAATATGCTGGGAGATGCGAAGACA 1759
epsilon CAAGCTGGC-TGACTTTGGGAT----GTGCAAGGAAGGGATTCTGAATGGCGTGACAACT 1885
mu CCCTCAGGTGAAACTTTGTGATTTTGGTTTTGCCCGGATCATTGGCGAGAAGTCTTTCCG 2358
alpha AGGACCTTCTGTGGG-ACTCCGGATTACATTGCCCCAGAGATAATCGCTTACCAGCCATA 1812
beta AAGACATTCTGTGGC-ACTCCAGACTACATTGCCCCAGAGATCATTGCTTATCAGCCCTA 2237
gamma CGCACCTTCTGTGGG-ACCCCAGACTACATAGCACCTGAGATCATTGCCTATCAGCCCTA 1813
zeta AGCACTTTTTGTGGA-ACCCCGAACTATATCGCCCCCGAAATCCTGCGAGGAGAAGAGTA 1430
iota AGCACCTTCTGTGGG-ACTCCCAATTACATTGCTCCTGAGATCTTAAGAGGAGAAGACTA 2192
delta AGCACATTCTGCGGC-ACTCCTGACTACATCGCCCCTGAGATCCTGCAGGGCCTGAAGTA 1930
theta AATACTTTCTGTGGG-ACGCCTGACTACATCGCTCCGGAGATCTTGCTGGGTCAGAAATA 1818
epsilon ACCACCTTCTGTGGG-ACTCCTGACTACATAGCTCCAGAGATCCTGCAGGAGTTGGAGTA 1944
mu GAGATCAGTGGTGGGTACCCCAGCCTACCTGGCACCTGAGGTTCTGAGGAACAAGGGCTA 2418
alpha TGGAAAGTCTGTGGACTGGTGGGCGTACGGCGTGCTCCTGTATGAGATGCTAGCTGGGCA 1872
beta CGGGAAGTCTGTGGACTGGTGGGCGTTTGGAGTCCTGCTGTATGAAATGTTGGCTGGCCA 2297
gamma TGGGAAGTCTGTCGACTGGTGGTCCTTTGGAGTCCTGCTGTATGAGATGTTGGCAGGACA 1873
zeta CGGGTTCAGCGTGGACTGGTGGGCGCTGGGTGTCCTTATGTTTGAGATGATGGCTGGGCG 1490
iota TGGCTTCAGCGTTGACTGGTGGGCTCTTGGAGTACTCATGTTTGAGATGATGGCGGGAAG 2252
delta CTCATTTTCCGTGGACTGGTGGTCTTTTGGGGTCCTCCTCTATGAGATGCTCATTGGCCA 1990
theta CAACCATTCCGTTGACTGGTGGTCCTTTGGGGTTCTTCTTTACGAGATGCTGATTGGCCA 1878
epsilon CGGCCCCTCAGTGGACTGGTGGGCCCTGGGCGTGCTGATGTACGAGATGATGGCCGGGCA 2004
mu TAACCGCTCGCTAGACATGTGGTCTGTTGGGGTCATCATCTATGTGAGCCTGAGTGGCAC 2478
alpha GCTTATGACCAAACA------------CCCTGCC---------------AAGCGGCTGGG 1905
beta GGCACCTTTTGAAGG------------GGAGGAT---------------GAGGATGAACT 2330
gamma GCCACCCTTTGATGG------------GGAAGAT---------------GAGGAGGAGCT 1906
zeta CTCCCCCTTTGACATCATCA------CAGACAACCCTGACATGAATACTGAAGACTACCT 1544
iota GTCTCCATTTGATATCGTTGGGAGCTCTGACAATCCTGACCAAAACACAGAGGATTATCT 2312
delta GTCCCCCTTCCATGG------------TGATGAT---------------GAGGACGAGCT 2023
theta GTCGCCTTTCCACGG------------GCAGGAC---------------GAAGAGGAGCT 1911
epsilon GCCCCCCTTTGAAGC------------TGACAAC---------------GAGGACGACTT 2037
mu CTTCCCTTTTAATGAAGATGAAGATATCCACGATC-------AGATCCAGAACGCAGCCT 2531
alpha CTGCGGGCCCGAGGGGGAAAGGGATGTCAGAGAGCATGCCTTCTTTAGGAGGATCGACTG 1965
beta CTTCCAGTCAATCATGGAGCACAACGT---GGCGTATCCCAAGTCCATG----TCTAA-G 2382
gamma GTTTCAAGCCATCATGGAACAAACTGTC---ACCTATCCCAAGTCACTT----TCCCG-G 1958
zeta TTTCCAAGTTATCCTGGAAAAGCCAATT----CGGATTCCCCGTTTCCT----GTCTGTC 1596
iota GTTCCAAGTCATTTTGGAGAAGCAGATT----CGCATACCGCGCTCCCT----GTCTGTG 2364
delta CTTTGAGTCCATCCGGGTGGACACACCA----CACTACCCGCGCTGGAT----CACCAAG 2075
theta TTTCCACTCCATCCGCATGGACAATCCC----TTTTACCCAAGGTGGCT----AGAAAGG 1963
epsilon GTTTGAATCCATCCTTCACGATGACGTT----CTCTACCCTGTCTGGCT----TAGCAAG 2089
mu TCATGTATCCACCCAATCCCTGGAAGGA----GATTTCTCATGAAGCCATTGATCTTATC 2587
alpha GG-AGAAGTTGGAGAACAGGGAGATCCAACCGCCATTCAAGCCCAAAGTGTGCGGCAAAG 2024
beta GA-AGCTGTGGCAATCTGCAAAGGGCTAATGACCA---AACACCCAGGCAAGCGCCT--- 2435
gamma GA-AGCTGTGGCCATCTGCAAGGGGTTCCTGACCA---AGCACCCAGGAAAGCGCCT--- 2011
zeta AA-GGCCTCACACGTCTTGAAAGGATTTTTAAATA---AGGATCCCAAAGAGAGGCTTGG 1652
iota AA-AGCAGCAAGTGTGCTGAAGAGTTTCCTCAACA---AGGACCCAAAGGAACGATTGGG 2420
delta GA-GTCCAAGGACATCATGGAGAAGCTCTTCGAGA---GGGACCCTGCCAAGAGGCTGGG 2131
theta GA-GGCCAAGGATCTTCTAGTGAAGCTTTTTGTGA---GAGAGCCTGAAAAGAGGCTGGG 2019
epsilon GA-GGCTGTCAGCATCCTGAAAGCTTTCATGACCA---AGAACCCGCACAAGCGCCTGGG 2145
mu AATAACTTGCTACAAGTGAAAATGAGAAAACGCTA----CAGTGTGGACAAGACCTTGAG 2643

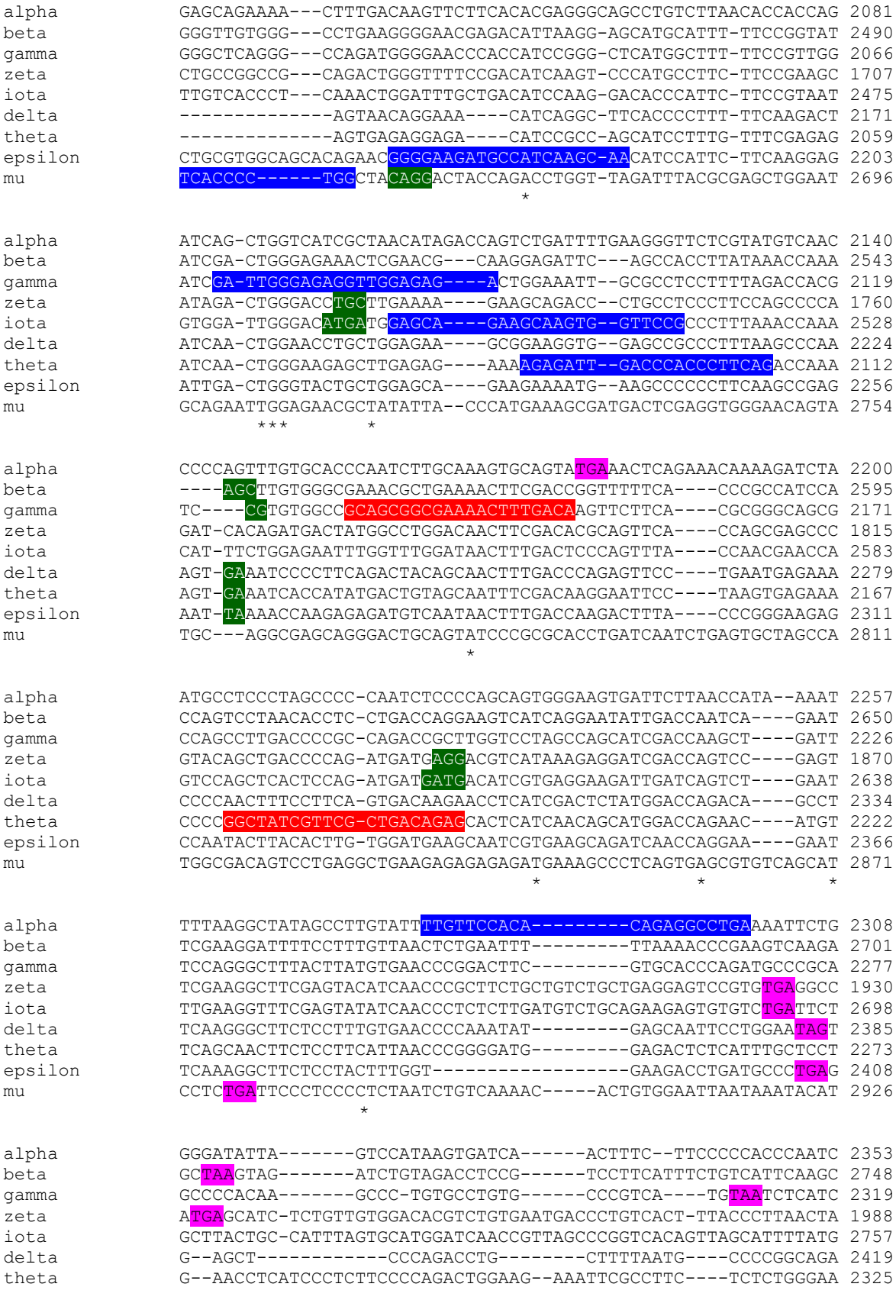
alpha GAGCAGAAAA---CTTTGACAAGTTCTTCACACGAGGGCAGCCTGTCTTAACACCACCAG 2081
beta GGGTTGTGGG---CCTGAAGGGGAACGAGACATTAAGG-AGCATGCATTT-TTCCGGTAT 2490
gamma GGGCTCAGGG---CCAGATGGGGAACCCACCATCCGGG-CTCATGGCTTT-TTCCGTTGG 2066
zeta CTGCCGGCCG---CAGACTGGGTTTTCCGACATCAAGT-CCCATGCCTTC-TTCCGAAGC 1707
iota TTGTCACCCT---CAAACTGGATTTGCTGACATCCAAG-GACACCCATTC-TTCCGTAAT 2475
delta --------------AGTAACAGGAAA----CATCAGGC-TTCACCCCTTT-TTCAAGACT 2171
theta --------------AGTGAGAGGAGA----CATCCGCC-AGCATCCTTTG-TTTCGAGAG 2059
epsilon CTGCGTGGCAGCACAGAACGGGGAAGATGCCATCAAGC-AACATCCATTC-TTCAAGGAG 2203
mu TCACCCC------TGGCTACAGGACTACCAGACCTGGT-TAGATTTACGCGAGCTGGAAT 2696
alpha ATCAG-CTGGTCATCGCTAACATAGACCAGTCTGATTTTGAAGGGTTCTCGTATGTCAAC 2140
beta ATCGA-CTGGGAGAAACTCGAACG---CAAGGAGATTC---AGCCACCTTATAAACCAAA 2543
gamma ATCGA-TTGGGAGAGGTTGGAGAG----ACTGGAAATT--GCGCCTCCTTTTAGACCACG 2119
zeta ATAGA-CTGGGACCTGCTTGAAAA----GAAGCAGACC--CTGCCTCCCTTCCAGCCCCA 1760
iota GTGGA-TTGGGACATGATGGAGCA----GAAGCAAGTG--GTTCCGCCCTTTAAACCAAA 2528
delta ATCAA-CTGGAACCTGCTGGAGAA----GCGGAAGGTG--GAGCCGCCCTTTAAGCCCAA 2224
theta ATCAA-CTGGGAAGAGCTTGAGAG----AAAAGAGATT--GACCCACCCTTCAGACCAAA 2112
epsilon ATTGA-CTGGGTACTGCTGGAGCA----GAAGAAAATG--AAGCCCCCCTTCAAGCCGAG 2256
mu GCAGAATTGGAGAACGCTATATTA--CCCATGAAAGCGATGACTCGAGGTGGGAACAGTA 2754
alpha CCCCAGTTTGTGCACCCAATCTTGCAAAGTGCAGTATGAAACTCAGAAACAAAAGATCTA 2200
beta ----AGCTTGTGGGCGAAACGCTGAAAACTTCGACCGGTTTTTCA----CCCGCCATCCA 2595
gamma TC----CGTGTGGCCGCAGCGGCGAAAACTTTGACAAGTTCTTCA----CGCGGGCAGCG 2171
zeta GAT-CACAGATGACTATGGCCTGGACAACTTCGACACGCAGTTCA----CCAGCGAGCCC 1815
iota CAT-TTCTGGAGAATTTGGTTTGGATAACTTTGACTCCCAGTTTA----CCAACGAACCA 2583
delta AGT-GAAATCCCCTTCAGACTACAGCAACTTTGACCCAGAGTTCC----TGAATGAGAAA 2279
theta AGT-GAAATCACCATATGACTGTAGCAATTTCGACAAGGAATTCC----TAAGTGAGAAA 2167
epsilon AAT-TAAAACCAAGAGAGATGTCAATAACTTTGACCAAGACTTTA----CCCGGGAAGAG 2311
mu TGC---AGGCGAGCAGGGACTGCAGTATCCCGCGCACCTGATCAATCTGAGTGCTAGCCA 2811
alpha ATGCCTCCCTAGCCCC-CAATCTCCCCAGCAGTGGGAAGTGATTCTTAACCATA--AAAT 2257
beta CCAGTCCTAACACCTC-CTGACCAGGAAGTCATCAGGAATATTGACCAATCA----GAAT 2650
gamma CCAGCCTTGACCCCGC-CAGACCGCTTGGTCCTAGCCAGCATCGACCAAGCT----GATT 2226
zeta GTACAGCTGACCCCAG-ATGATGAGGACGTCATAAAGAGGATCGACCAGTCC----GAGT 1870
iota GTCCAGCTCACTCCAG-ATGATGATGACATCGTGAGGAAGATTGATCAGTCT----GAAT 2638
delta CCCCAACTTTCCTTCA-GTGACAAGAACCTCATCGACTCTATGGACCAGACA----GCCT 2334
theta CCCCGGCTATCGTTCG-CTGACAGAGCACTCATCAACAGCATGGACCAGAAC----ATGT 2222
epsilon CCAATACTTACACTTG-TGGATGAAGCAATCGTGAAGCAGATCAACCAGGAA----GAAT 2366
mu TGGCGACAGTCCTGAGGCTGAAGAGAGAGAGATGAAAGCCCTCAGTGAGCGTGTCAGCAT 2871
alpha TTTAAGGCTATAGCCTTGTATTTTGTTCCACA---------CAGAGGCCTGAAAATTCTG 2308
beta TCGAAGGATTTTCCTTTGTTAACTCTGAATTT---------TTAAAACCCGAAGTCAAGA 2701
gamma TCCAGGGCTTTACTTATGTGAACCCGGACTTC---------GTGCACCCAGATGCCCGCA 2277
zeta TCGAAGGCTTCGAGTACATCAACCCGCTTCTGCTGTCTGCTGAGGAGTCCGTGTGAGGCC 1930
iota TTGAAGGTTTCGAGTATATCAACCCTCTCTTGATGTCTGCAGAAGAGTGTGTCTGATTCT 2698
delta TCAAGGGCTTCTCCTTTGTGAACCCCAAATAT---------GAGCAATTCCTGGAATAGT 2385
theta TCAGCAACTTCTCCTTCATTAACCCGGGGATG---------GAGACTCTCATTTGCTCCT 2273
epsilon TCAAAGGCTTCTCCTACTTTGGT----------------GAAGACCTGATGCCCTGAG 2408
mu CCTCTGATTCCCTCCCCTCTAATCTGTCAAAAC-----ACTGTGGAATTAATAAATACAT 2926
alpha GGGATATTA-------GTCCATAAGTGATCA------ACTTTC--TTCCCCCACCCAATC 2353
beta GCTAAGTAG-------ATCTGTAGACCTCCG------TCCTTCATTTCTGTCATTCAAGC 2748
gamma GCCCCACAA-------GCCC-TGTGCCTGTG------CCCGTCA----TGTAATCTCATC 2319
zeta ATGAGCATC-TCTGTTGTGGACACGTCTGTGAATGACCCTGTCACT-TTACCCTTAACTA 1988
iota GCTTACTGC-CATTTAGTGCATGGATCAACCGTTAGCCCGGTCACAGTTAGCATTTTATG 2757
delta G--AGCT------------CCCAGACCTG--------CTTTTAATG----CCCCGGCAGA 2419
theta G--AACCTCATCCCTCTTCCCCAGACTGGAAG--AAATTCGCCTTC----TCTCTGGGAA 2325

```
epsilon          A--AACTGC----------TTCACATGGA-----------GTTAGC----TCACTGCAAG 2441
mu               ACGGTCAGG----TTTAACATTTGCCTTGCAGAACTGCCATTATTTTCTGTCAGATGAGA 2982

alpha            CCAAACCAAAAAAACATTATCTTAGTGGATGATGACATAATATACAGAGTATAGT--TTAA 2411
beta             TCAA--CAGCTATCATGAGAGACAAGCGAGACACCTCCAACTTCGACAAAGAGT--TCA- 2803
gamma            TGCTGCCGCTAGGTGT--TCCCAGTGC-TCCCTCCGCCAAGTTGGCTGTAACTC--CCAT 2374
zeta             CAG--CATATGCATGCCAGGCCAGACACCGAGGCTCCAAGCAGCCAGAGAGGG---ATGC 2043
iota             TTGTCCCTACAGAAATCTCTCTCAATATC----CTGTTAGCGACTATAGGAATC--ATAT 2811
delta            GTAGGCCCATCTGCCCTGGTTTGCATCCT----CACTGCCCAT-GAAGAAGAGT--GGGT 2472
theta            CTGGTTCAAGTAACACTTCTGGGGGTCTC----TTTTTCACGTTGGAGAAGAG---AAGA 2378
epsilon          GAGGGT------------GTTGAGA---C----AATCCCGTGTTGCAGAGG--------- 2473
mu               ACAAAGCTGTTAAACTGTTAGCACTGTTGATGTATCTGAGTTGCCAAGACAAATCAACAG 3042

alpha            TTATGTA-GAAGTCACATCTGGCTTCAAGTTAATTCTTTCTAGGAAACAAAGAGACTTGG 2470
beta             CCAGGCA-GCCTGTGGAACTGACTCCCA-CTGACAAACTCTTCATCATGA----ACTTGG 2857
gamma            CCACCCCCATCCCCGCCTCTAGTCCGAATTTTAGGTCTCTTAAACCACCCAA--CCTTCT 2432
zeta             TGGCCACCAAGACCGCAGAGGGGGCACCCAACAGGCACTTCTAGACAGAGCA-ATCTC-- 2100
iota             AGCTAAGCAGAGCTAAAAAAACAGAAACTAGTT--TCCTGACAGTCATGTCA-AACTCCA 2868
delta            GACTGGTGATTCCTGCTGCTG-------CCCCCTCTTCCTCGGAG--------AGTCTGG 2517
theta            AACACTCAACCTCGAAAGCAGGGAGGACCGCTGAGCTCCTCGAGGGACACGC-AGCACAA 2437
epsilon          --CTCAGAATGTCTCGAACTA--------TTCGTCCTCCCCAGAGC---CCC-AGTCCCA 2519
mu               AAGCATTTGTATTTTGTGTGACCAACTGTGTTGTATTAACAAAAGTTCCCGGAAACACTA 3102

alpha            ACCCTATTT--TTTGGTACGATTTAATATATTCTCCATACCTTTCATATT-TTGGATTTT 2527
beta             ACCAAAATGAATTTGCTGGCTTCTCGTATACTAACCCAGAGTTTGTCATT-AATGTGTAG 2916
gamma            GGCCTCTTTCACGCGCCCCAAGTGGGTTCTAGACGCTGTTCCCCAGCATTGCTGGCATTT 2492
zeta             -TTGTGTCCAGGC-CCCAGAGGCTGGCTTTGTGCTGGAAGGAACCA-CTTCCTGTGCCCA 2157
iota             GTTATGCTTGCTC-TCCAGAGGCT--CCTAATGAGAAAGGACAGTGTCTTTGTGTAAAGG 2925
delta            CTCCTGTTGGCTGGGCTCACAGTACTTCCTCTGTGAACTGTTTGTGAATTTGCCTTCCTT 2577
theta            ACCATGTCTCCTTCACTAATGGCA-TCATCCTGTTATATCTCCTGGAATCTCTCTCACCG 2496
epsilon          CATCTGCTCTCTT-ATTTATTGCA-TCCCCTCATCCCAGGCCCTG-----TCCTTCCCCA 2572
mu               AACTTGTTA---TTGTGAATGATTTATGTTATATTTAATACATTAAACCTGTCTCCACTG 3159

alpha            CACTATCCAAATCAAC-CAGAGATAATAAAGTGAACCCACCTGAA---CTCAAGGGATGG 2583
beta             GTGAATGCAGATT--C-CATCGCTGAGCCTGTGTGTAAGGCTGCAG-GCTGAATGTCTAT 2972
gamma            TAAACTTCAAACAGTCTCTAGGGCCTTTCTGTGTTCTAGGTTCGTT-GTGCTGAGCCCTG 2551
zeta             TGGCGGCCC----TACCAGAGGGTGAGACAGCCACGCCGT----CTTGAAAGGCGCACAT 2209
iota             AAACAGCCTAGCTTGTCAAAGAAAGCCTCTGCTGCGTTGTGACACTCAGTGGGATGACAT 2985
delta            TTGC--CATCG------GAGGGAAACTGTAAATCCTGTGTGTCATT-ACTTGAATG-TAG 2627
theta            CAGC--CCTAG------AAGTTAGACCATTGTTAACTCTAGTCATTTACTTGAAAGATGG 2548
epsilon          CCCT--CCCAG------TGACCAGAAGGCCCTCTTTGGTCCAGACTCACCAAGATCACAG 2624
mu               TGCCTTTGCAA------ATCAGTGTTTTTCCTACCAGAGCCTCATTTTGGTGAGAGCCAG 3213

alpha            AAACATTTCTG----CCCAAGATATCTTTGGAATTAAAGAACAGGAAGCCCAAACAGAAA 2639
beta             TATCAATTCCAGTCTTCCAGGATTCATGGTGCCTCTGTTGGCATCCGTCATGTGGAGAGC 3032
gamma            GTTTTTCCCCA----CCCCCAACATCTGGATGCTGTTCCAACTCTTCCCAGAAACCCCAC 2607
zeta             CTTCCACAGAGACAGAACTCGATGCACTGATCCGCTCCAGGAAAAGTTAGCGTGTAATGC 2269
iota             CATCAGTCT--CCCACAGTTGTCACTTTGGGTTAAGGCATGGAAGGCTTAATTGTAGAGT 3043
delta            TTATTGA---------AATATATATTATATATATGCACATATATATAATAGGCTGTATAT 2678
theta            TTCCCGATC---CTGCGAACGATTCGAAATGTAATTCTGCTCTTGTCGTTGACAAGAGCT 2605
epsilon          ATTTGAACT---G---CGTCTGCTCTGTGTGCAGTGCTAGGTCTGGAGTAGCC---GTCC 2675
mu               CTCCAAT---------CCATGACACCATTGTGTTTGGTGTGCCCCTATTGATAGTGGTGT 3264

alpha            ACAAAGAGAGGCAGAGTCTCATATATTCAAGACCTCGTTGCTTCTATTTTCT------GC 2693
beta             TTGTCTTAGAGGGCTTTTCTTTGTATGTATAGCTTGCTAGTTTGTTTTCTAC------AT 3086
gamma            TCCGTGTGGGGTTCTAGACTCTATCTTGGTAGTTTTATGCCTTCTCTCTCCCTAGACCAC 2667
zeta             CCTGAGGAATA--AAGTGTA-CTGATGATGTCGAAGCTTCCTCTGATGCCTTTTTTCTGT 2326
```

```
iota            GGAGGGCCATGCTAAATATATCTGCTAGTGTTACTGGTTTCTG-AGTTCCCTCAGTTTGA 3102
delta           ATTGCTCAGTATAGAAAGCATGTAGGAGACTGGTGATGTGTTGACCTTTTTTTAAAAAAA 2738
theta           GCTGGTTGGTG-ACGAACCAAGGTGCAAGTGGAACAGATTTCTCAAGACCGGGAGGGCAG 2664
epsilon         ACCCACAACCC--TGAAGCAGCCCGGAATTC---------------------------- 2704
mu              TGTAAGCAAACTCTTGAAGAGTAGATAATCTGCCGGTGTTCTGTGAACAACTCAA---AA 3321

alpha           TTCAATGGAAACAGTCCCTAGAGTCTGAG-AGGGCAGGATGA---ACCTGAT-CACTGTT 2748
beta            TTCAAAATGTTTAGT--TTAGAATAAGTGCATTGCCCACTGA---TAGAGGTACAATTTT 3141
gamma           GTTGGGAGAAATAGTCTCATGAGATTGCCTGCTCCAGACTAAGATTCCAGATCAGCTCTC 2727
zeta            GGCACCCGCCTGATGTCCCCAATGCAGCCCCCCACACGAGGAGGAGCTGCGCTTTCCAAG 2386
iota            ATCCTCCTATAAATCTTCTCATTACTTTGGGTAATTTAAAGAA-----GCAGTTATCAAA 3157
delta           ACCATATGT-ATACGTGTGTATGT-ATACATCTACACACGTATA---CATATATGTATGT 2793
theta           ATTGCCTGTCATGGAAGTCGATTCCACTCAACCACAGAGAAGGA---CCCACTAACCCGC 2721
epsilon         ------------------------------------------------------------
mu              TGCACAGTGGGTGGGGTGGGGGGGGAGAATGAAAGATGAGGAGAAGGCGTATAAGTGCTA 3381

alpha           CCCAATCATCATAG-CACAACCATAGTGC--ATAGTTTGAAAATGAAAGAAAACTTCAGA 2805
beta            CCAGACTTCCAGAAACTCATCCAATGAACCAACAGTGTCAAAACTTAACTGTGTCCGATA 3201
gamma           TGCATCCTTCAAGGCCCCTCCTACCTCCACTTCAGTTGTAGAATTAAGTGGGAGGCTGGG 2787
zeta            CAGGCAGAACGTAGGCAGGGGACGGGCACCCAAGTGCCTGCAGGGATGTTGTGC-TGCAA 2445
iota            TTGATACACAATTGACTTGTTTTATTAA--GAATTGGGTTCTAAGTTATTATCTGTGTTT 3215
delta           ATGTATGTATGTATGTATGTATATATGACCAAAAGAAAAGAGAGCACAAGCTACCTGAAC 2853
theta           ATCGTCCTGCGCATGTCTGTGGAAATGTCGATGGCAGAAGGGAGGGAAAGGGATGTGA-T 2780
epsilon         ------------------------------------------------------------
mu              AGATTGACTTGCATGAAAACAGTTCTACTGTGTGGTGTCAGATCCTCTGCCTGTCTGGTG 3441

alpha           CAGATGTTCGTTGAATCTATCATATGTACTCCCCTGCTCGGTTGATAACTATCTCGATAA 2865
beta            CCAAAATGC-TTCAGTAT-TTGTA---ATTTTTAAAGTCAGATGCTGATGTTCCTGGTCA 3256
gamma           CTC-CGTGT-TCCAGGCCACCTCC----CTTCCATGTTCTGGGGATTCCTGGCATGCACG 2841
zeta            CAAGAATTGTTACAG--ATTCGGAACGTTTTCTAAATCCCGGTAAGTTCTGTTGTTAATA 2503
iota            CAAAAACTAACACAGTGATTTATTTTGTGTTTTTAATTTTTCTTTTTCTTTTTTTTTACA 3275
delta           CACAGGATTGTTTATGTGTGTATAAATAAACACTGAATGGTAAAAAACCGGA-ATTC--- 2909
theta           GGGATGTTCTCCAATAAACTTA-GCGTGAAACTTGAGATTTACAAACCCGTTCGTTCTGG 2839
epsilon         ------------------------------------------------------------
mu              TGCCTCAGTGTATTTAACTCTAGTGAGTGCACCTCATTATGTGGAGCCACTGCACTAAGC 3501

alpha           CTCATTCTTTTTAAGAGGCCAAAATCATCTAAGGACTTTGCTAA-ACAAACATG--TGAA 2922
beta            --AAGTTTTTACAGTTACTCTCGAATATCTCCTTTGAATGCTAC-CTAAGCATGACCGGT 3313
gamma           GAGGATTCTCTC------CCCGACTTTTCTCAGTCAGCTTTTGTTCTAGATTTGTTCCAG 2895
zeta            TTTAACAAGTATTTTCATACCTAGGG----CAGCTAACCGTGGT-AGGCTGAAGCCGAAG 2558
iota            ATAAGGGGTTAGCTTCTGAGCTTGCCTCTTCCGTGAATACTAGC-ATAATGATACCTGAC 3334
delta           ------------------------------------------------------------
theta           CCAGCCCTGAAATTCACAAGGCAGCGG---AAAGTAAGGGGTGA-GGTGCAGAGCCTTTG 2895
epsilon         ------------------------------------------------------------
mu              CTAAATGCCTTAG---ACTGTAAACTGCTTTACATACCAGATGCATTTCCTCCTTTCTTA 3558

alpha           ATCATTTCAGATCAAGGATAAACCATGTG--TA-TGTTCATTTTAATCTCTGGGAGATGA 2979
beta            ATTTTTAAAAGTTGTGAGTAAGCTTTGCAGTTACTGTGAACTCTTGTCTCTTGGAGGAAA 3373
gamma           AACCCTTCACTGCTCACCTGCCCCGTGCA--TGGCTCCAGCCTTGGTCGGAATCACACAC 2953
zeta            G----GACACCCCGGCCAGGTTGGT---GGC-GCTGTTCCCACCAGCCCA-------GCC 2603
iota            GTGCAGAGACCCAGGCTGCATGGGAATAGGCAGCTGCTCAGGTAAAGGAGAAAGGAGGAG 3394
delta           ------------------------------------------------------------
theta           TCACCAACAGGAAGGGTAAGGATGTTTCGGATGTGGTGCATCTCATTCCCACAGAAGTAA 2955
epsilon         ------------------------------------------------------------
mu              CAATAGCAACTGTATCAAGGAAAACCAGCAACCCACCAAATGTTGGCCTTTTGTGTATTT 3618

alpha           CTCTTCAATCCAGGGT-GCCATCAGTAATCATGCCACTG---TTCACGAGTGTTGTTAGC 3035
beta            CTTTTTGTTTAAGAATTGGTATGATTAAATGAATTCATA---TATGC------------- 3417
```

```
gamma           ACACACACACACACACACACACACACACACACACACACACA---CACACACCCCTTGTCCTC 3010
zeta            CGTTCGGACTCTGAAGGGGGGGAAATTGGATCACGGAGA---TTCTAAAACATTGCTCAC 2660
iota            TGTACCGTAGCTGCAGAAAGAACAATGGTAGTATTCTGTCTCTTCTGGAGAATGAGTCCT 3454
delta           ------------------------------------------------------------
theta           AGTCCAACCAACGAAGGCAGGGCAGTTTACTGCTGCCAA----TCAAACCTTCTCTTCCC 3011
epsilon         ------------------------------------------------------------
mu              TTGAATAATAAGAAATAAATACTCTTTTCAAAGTT----------------------- 3653


alpha           CA-ACCCCCCGCCACATAATAATATTTTGCTACCTTTGTGGGTACCCTTCCTAGGAAGCT 3094
beta            ------------------------------------------------------------
gamma           CGCAGTGCCTGCCACTTTCTGGGACTTTCTCATCCCCCACGCCCTTCCTTTATCCTCTCC 3070
zeta            C----------------------------------------------------------- 2661
iota            GTAGCTGGTGGTTAAGATTTGATGTAAATAATGAGGAGGCTCTCGCTTCTTACCCTACTT 3514
delta           ------------------------------------------------------------
theta           TCTTGTTCTGGCTGATTTCTCTGTCAGCGTCGGCATTCGTCATCGTCCTCCCGTTGCACA 3071
epsilon         ------------------------------------------------------------
mu              ------------------------------------------------------------


alpha           AAAATGTATGCCCCATCCCCTTTTGTACTATTTATTTAATAAGCCGCAGTGTCGTTTATG 3154
beta            ------------------------------------------------------------
gamma           CACCCAGACACAGCTGCTGGAGAATAAATTTGGAGCTCTCGAG----------------- 3113
zeta            ------------------------------------------------------------
iota            AGAAAAGCATTCCATGTCTTCAGGGGAGGCGGAGTGAATATATTTTTATTATTTAGTATA 3574
delta           ------------------------------------------------------------
theta           AGAAATGAAGTACATGACTCTTGTGAGAGAAAGAAAACCAATCCCATATCATGTTGCTCC 3131
epsilon         ------------------------------------------------------------
mu              ------------------------------------------------------------


alpha           AAAGTACAATGTATAGTAACTTAATCAAAGTACTGACTAGCATCAGTCCCTATAGGTTGA 3214
beta            ------------------------------------------------------------
gamma           ------------------------------------------------------------
zeta            ------------------------------------------------------------
iota            TGGGAAAATAATTTATCTGCTAAGTAGAATGTCTTAACTACTTGTGATTCCTTCCCCAGA 3634
delta           ------------------------------------------------------------
theta           TGGTGATTCGGTGACAAATAAGTCCCTCTTTAGGCATCCTGCAAGACAAACGACCCACGC 3191
epsilon         ------------------------------------------------------------
mu              ------------------------------------------------------------


alpha           TTTTCCTCCTTTCTCTAGCCCCACATCCACTTAGAGATGAGAAAAAAAAGAGTATATTTT 3274
beta            ------------------------------------------------------------
gamma           ------------------------------------------------------------
zeta            ------------------------------------------------------------
iota            GTACATTATCTGTACTTTGAGAGCTTTTCGTGGAGTCTGCAGTGAAGCTCAAGACCAGTA 3694
delta           ------------------------------------------------------------
theta           ATGCTATTTCCACTAGTCAGCCCTGTTGAGTTGGAGTACTAATTAGACACTTAGAGTCTC 3251
epsilon         ------------------------------------------------------------
mu              ------------------------------------------------------------


alpha           GGGTTCCAATTCCCAGTTCTAATTGAATGGCACACATGGAGCTGTAGGATCAAGACACTT 3334
beta            ------------------------------------------------------------
gamma           ------------------------------------------------------------
zeta            ------------------------------------------------------------
iota            CTGGTGACTTGATAGCTGTGTGACACATCCAGTACAGACCAGTACTGGTGACTTGATAGC 3754
delta           ------------------------------------------------------------
theta           GCGTGCTGTTTGTATATTTTGATGGGATGTTGTGATGATGACGTACGTGGACGTGTAAAA 3311
epsilon         ------------------------------------------------------------
mu              ------------------------------------------------------------
```

```
alpha           TATGCTTATATCAACTCAAAGATGTTTTCTTGCTAGAAGGATTTTAATATGTTTTGCGAG 3394
beta            ------------------------------------------------------------
gamma           ------------------------------------------------------------
zeta            ------------------------------------------------------------
iota            TGTGTAACACATCCCAGTTCGGGCTCTTCCTGAGTTTTTGTGTCTAGGTAACAAGTGTGA 3814
delta           ------------------------------------------------------------
theta           CGGAATAAAAGAAGAAAAGAAAGATG---------------------------------- 3337
epsilon         ------------------------------------------------------------
mu              ------------------------------------------------------------

alpha           TGCATCATGCAATGGATTTTGCATGTTTATAATAAACCTTAATAACAAGTTAATCTATAT 3454
beta            ------------------------------------------------------------
gamma           ------------------------------------------------------------
zeta            ------------------------------------------------------------
iota            TACAGTACAGTCCATTCAGGGCAGAGTCTTCAGTTCTCCACAATATTTTTATTAACAGTA 3874
delta           ------------------------------------------------------------
theta           ------------------------------------------------------------
epsilon         ------------------------------------------------------------
mu              ------------------------------------------------------------

alpha           TATTGATATAATTGTATCAAGTATAAAGAGTATTATGATAATTTTATAAGACACAATTGT 3514
beta            ------------------------------------------------------------
gamma           ------------------------------------------------------------
zeta            ------------------------------------------------------------
iota            GTATTTAGCAATCTTTTATTTAAAGAAGCACCATTTTAAGCACCATTCTGCTGTTTATTT 3934
delta           ------------------------------------------------------------
theta           ------------------------------------------------------------
epsilon         ------------------------------------------------------------
mu              ------------------------------------------------------------

alpha           GCTATATTTGTGATGCTCATGTTTCCAGTCTGCTTTAAGATTAAGTGTTAGCTTTATTCA 3574
beta            ------------------------------------------------------------
gamma           ------------------------------------------------------------
zeta            ------------------------------------------------------------
iota            TAAATATTTTTATATAAAGGACTTTAAAATGGTCACCTAAACAAGCTACCATTGTCAAAT 3994
delta           ------------------------------------------------------------
theta           ------------------------------------------------------------
epsilon         ------------------------------------------------------------
mu              ------------------------------------------------------------

alpha           TTGCTGCTGGGGCCTCTATTACCCGCTACCCCACACACTGGCACTCTATCAGATATATTA 3634
beta            ------------------------------------------------------------
gamma           ------------------------------------------------------------
zeta            ------------------------------------------------------------
iota            CAGTAGACTTAGTTTCATGAATGCTGTACGGTGTTGAGCTTATAAGGCTTCAAACACGTA 4054
delta           ------------------------------------------------------------
theta           ------------------------------------------------------------
epsilon         ------------------------------------------------------------
mu              ------------------------------------------------------------

alpha           ATTTTTTAATGTAGATGTAATTTTAAAATGAATGGCTACTTTACACGTTTAACTAGGCTT 3694
beta            ------------------------------------------------------------
gamma           ------------------------------------------------------------
zeta            ------------------------------------------------------------
iota            GTCATTGAAGACATCTCTGAGGATGCCACATTTCATTACAAGTGTAAGTTGTGTCAAGTT 4114
delta           ------------------------------------------------------------
theta           ------------------------------------------------------------
```

```
epsilon         ------------------------------------------------------------
mu              ------------------------------------------------------------

alpha           TTACTATA-------------------------------------------------------- 3702
beta            ------------------------------------------------------------
gamma           ------------------------------------------------------------
zeta            ------------------------------------------------------------
iota            GGGTCGTGCATTTTCTTAAATAATGAAAGACTGGGAGCCGTGAAAACCTCCACTGAGGAA 4174
delta           ------------------------------------------------------------
theta           ------------------------------------------------------------
epsilon         ------------------------------------------------------------
mu              ------------------------------------------------------------

alpha           ------------------------------------------------------------
beta            ------------------------------------------------------------
gamma           ------------------------------------------------------------
zeta            ------------------------------------------------------------
iota            AGCCAACCAGGGACCATCAGTCGGTCGAGGCAGCTCAGCACCTGATGACCTGATGCCTGG 4234
delta           ------------------------------------------------------------
theta           ------------------------------------------------------------
epsilon         ------------------------------------------------------------
mu              ------------------------------------------------------------

alpha           ------------------------------------------------------------
beta            ------------------------------------------------------------
gamma           ------------------------------------------------------------
zeta            ------------------------------------------------------------
iota            AACCCACAAGCTGAGAGGAAGGACAGACCAGCTCCCACAGGCTGGCACCCGTGGCACGCA 4294
delta           ------------------------------------------------------------
theta           ------------------------------------------------------------
epsilon         ------------------------------------------------------------
mu              ------------------------------------------------------------

alpha           ------------------------------------------------------------
beta            ------------------------------------------------------------
gamma           ------------------------------------------------------------
zeta            ------------------------------------------------------------
iota            CGAGGCCCTCCCTGCAGGACATAACTGTGAGGGAGCAGACAAGGGAGTGCAGTGAATGCA 4354
delta           ------------------------------------------------------------
theta           ------------------------------------------------------------
epsilon         ------------------------------------------------------------
mu              ------------------------------------------------------------

alpha           ------------------------------------------------------------
beta            ------------------------------------------------------------
gamma           ------------------------------------------------------------
zeta            ------------------------------------------------------------
iota            CACCTAGAGGCAGATGTTTGTGCACACTTCATGTTTAAGAAGCGCGGGTTTCCCTGAGAT 4414
delta           ------------------------------------------------------------
theta           ------------------------------------------------------------
epsilon         ------------------------------------------------------------
mu              ------------------------------------------------------------

alpha           ------------------------------------------------------------
beta            ------------------------------------------------------------
gamma           ------------------------------------------------------------
zeta            ------------------------------------------------------------
```

```
iota            CTAGAACATTCTTAAATCAAAAGGCAGTGTTCACGTCCTAAGCTTGTGGGGAGTTCTGAG 4474
delta           ------------------------------------------------------------
theta           ------------------------------------------------------------
epsilon         ------------------------------------------------------------
mu              ------------------------------------------------------------

alpha           ------------------------------------------------------------
beta            ------------------------------------------------------------
gamma           ------------------------------------------------------------
zeta            ------------------------------------------------------------
iota            ATATCTATGACCTAAGTGGGGCTTCTCCCTTGGGGCACTTCAGACTGAGCCTTGTTAAAG 4534
delta           ------------------------------------------------------------
theta           ------------------------------------------------------------
epsilon         ------------------------------------------------------------
mu              ------------------------------------------------------------

alpha           ------------------------------------------------------------
beta            ------------------------------------------------------------
gamma           ------------------------------------------------------------
zeta            ------------------------------------------------------------
iota            TGCAGTGCCGAGCCTGCCTGGGAGTCTTCTGGGACTTGATATTTCATCGTGAGAAGCATT 4594
delta           ------------------------------------------------------------
theta           ------------------------------------------------------------
epsilon         ------------------------------------------------------------
mu              ------------------------------------------------------------

alpha           ------------------------------------------------------------
beta            ------------------------------------------------------------
gamma           ------------------------------------------------------------
zeta            ------------------------------------------------------------
iota            TTCGTCAAGGTATTCTTTATCTTGTGGCCATATTTCTTACTGGAGTGTGAGTCTGTGTTT 4654
delta           ------------------------------------------------------------
theta           ------------------------------------------------------------
epsilon         ------------------------------------------------------------
mu              ------------------------------------------------------------

alpha           ------------------------------------------------------------
beta            ------------------------------------------------------------
gamma           ------------------------------------------------------------
zeta            ------------------------------------------------------------
iota            TTTGTGATAAAACATTTTAAGAAGGGGAAATCAGTAAATTATCATGCATTTATCAACAAA 4714
delta           ------------------------------------------------------------
theta           ------------------------------------------------------------
epsilon         ------------------------------------------------------------
mu              ------------------------------------------------------------

alpha           ------------------------------------------------------------
beta            ------------------------------------------------------------
gamma           ------------------------------------------------------------
zeta            ------------------------------------------------------------
iota            TTTAGATGAATAAATTCAAGTTATATGTCTTCCCTGCCCTCATCCCCAACAAAACTTATC 4774
delta           ------------------------------------------------------------
theta           ------------------------------------------------------------
epsilon         ------------------------------------------------------------
mu              ------------------------------------------------------------

alpha           ------------------------------------------------------------
```

```
beta            ------------------------------------------------------------
gamma           ------------------------------------------------------------
zeta            ------------------------------------------------------------
iota            CGTTTCTGCCAATACCGTACAAATGATGAACATTTTTCTATGATGAGGTTCTCACCATAA 4834
delta           ------------------------------------------------------------
theta           ------------------------------------------------------------
epsilon         ------------------------------------------------------------
mu              ------------------------------------------------------------

alpha           ------------------------------------------------------------
beta            ------------------------------------------------------------
gamma           ------------------------------------------------------------
zeta            ------------------------------------------------------------
iota            TTAAGGTGGTCTTTGTTTTTAAATCTTTCTGTTGTTGTTGATAACTAATAAGACAACGTA 4894
delta           ------------------------------------------------------------
theta           ------------------------------------------------------------
epsilon         ------------------------------------------------------------
mu              ------------------------------------------------------------

alpha           ------------------------------------------------------------
beta            ------------------------------------------------------------
gamma           ------------------------------------------------------------
zeta            ------------------------------------------------------------
iota            CTATGTATGCTTTATACAGAATTATTACAATGATTTTAGTTCCGTTCTTGTTTTCTGTCC 4954
delta           ------------------------------------------------------------
theta           ------------------------------------------------------------
epsilon         ------------------------------------------------------------
mu              ------------------------------------------------------------

alpha           ------------------------------------------------------------
beta            ------------------------------------------------------------
gamma           ------------------------------------------------------------
zeta            ------------------------------------------------------------
iota            TTCCGAGCCATGCCAAATCTGTATGTTATGGAAATGTTCTCAGAATCCTGCCAGGGGAAT 5014
delta           ------------------------------------------------------------
theta           ------------------------------------------------------------
epsilon         ------------------------------------------------------------
mu              ------------------------------------------------------------

alpha           ------------------------------------------------------------
beta            ------------------------------------------------------------
gamma           ------------------------------------------------------------
zeta            ------------------------------------------------------------
iota            GCAGTGTGGACGGGCAGTGATTGGCACTTGGTGTCATAGAAATTACTTACCTTGCATAAG 5074
delta           ------------------------------------------------------------
theta           ------------------------------------------------------------
epsilon         ------------------------------------------------------------
mu              ------------------------------------------------------------

alpha           ------------------------------------------------------------
beta            ------------------------------------------------------------
gamma           ------------------------------------------------------------
zeta            ------------------------------------------------------------
iota            CTCGTGGTTGGATCGGTTATCACGTGTAGCTGGATGGATATCTAGTCCTGTGTTCTTGTT 5134
delta           ------------------------------------------------------------
theta           ------------------------------------------------------------
epsilon         ------------------------------------------------------------
mu              ------------------------------------------------------------
```

```
alpha           ------------------------------------------------------------
beta            ------------------------------------------------------------
gamma           ------------------------------------------------------------
zeta            ------------------------------------------------------------
iota            GTCGGTACTCACCTTAGAAACTTGTTTTGATTTTTGTCATGTAGAACACTGCCTTGTTCA 5194
delta           ------------------------------------------------------------
theta           ------------------------------------------------------------
epsilon         ------------------------------------------------------------
mu              ------------------------------------------------------------


alpha           ------------------------------------------------------------
beta            ------------------------------------------------------------
gamma           ------------------------------------------------------------
zeta            ------------------------------------------------------------
iota            CTATAATGTAACTGTATTTGTATAATTTTTTTACATTAAGATCTTAAAATAAAATGTTTA 5254
delta           ------------------------------------------------------------
theta           ------------------------------------------------------------
epsilon         ------------------------------------------------------------
mu              ------------------------------------------------------------

alpha           ---------
beta            ---------
gamma           ---------
zeta            ---------
iota            ATACCTATG 5263
delta           ---------
theta           ---------
epsilon         ---------
mu              ---------
```

Start/stop codon

Intron/exon boundary

Primer Set 1

Primer Set 2

10.2 *Rattus norvegius* PKC isoform alignment

```
delta           GAATTCCGGGGCGGCGGCCGCGGGGATCCCGCGAGCGGCCCCTGAACATCTACCCTTCTT 60
theta           ------------------------------------------------------------
eta             ------------------------------------------------------------
epsilon         ------------------------------------------------------------

delta           GCCGGGACCCGGGAGGTCCCCACTGGCCTCCGGGCCCGTCCTGATCAGACTCGTGTCGAC 120
theta           ------------------------------------------------------------
eta             ------------------------------------------------------------
epsilon         ----------------------------------------------------------GA 2

delta           CTCCCCGTCCACGCGCATCCGGGAGAGCCGCGCCACGAGACGGACCCGGGCCCGCCGGGA 180
theta           ------------------------------------------------------------
eta             ----GGGAAGGAGGGGAGGGGA-AGGTCCCTCGGAGGAGGCGGAATGGCCGGTCGCAGGG 55
epsilon         ATTCCGGAATCCGGCGAGGAAATACATGCACTCGCTGAG----AATCGCCGGCGCCAGGA 58

delta           CCC----CTGGTGTCTGGCCCTGCGTCGAGAGGCTGGTGACTGCCACCCATAAGCTCCAG 236
theta           --------AGGCGCGCGTCCCTGAGCCGGC------GTGGCGAGCGCCCTCTGGCCGGTG 46
eta             GGCTTGGGTGCTGCTTCTCCCGGGAGCTGCCTCCACGAGCGTGGCTGCGGAGAGGACTGC 115
epsilon         CGC---AGCGCCACAAGGTGTAGCGAGTGAGTG---GGGTGGGGCAAGAGGGGACCCAGG 112
                         *           *           * *     *

delta           CTTCAGCCTCGGCTTACTCCCCTCAGGGGCTTGCAGGCTGAGGCCTGCCCTCGGACGCGG 296
theta           TCGCCGCC-CGGAGTACCCTC-----GGGTCGCCAGGCCCGCGCCAGTCCCCGCCATCGG 100
eta             CTTGAGCCCGGGCTCTCCGTTCCCCGGTGCCAGCCAGCCCG-GCC--CCCTCGGGGCTCC 172
epsilon         AGTCCCCCCAGGCTCCCAGCGCGCCTGCTCCTGCTCTTCAA-TCCTGCCCTCGGGGCGGA 171
                      **  **    *         *      *         **   ** **

delta           CTGACCAGCCTCTCCCTCTCTTCCACACTTTGGACTTCTCTTTGGACCTCCTAAAAAGGC 356
theta           AGCAGCAGCGGCAC-------TGCGC---TGGGACTGCGGCCACGACACC-----AGGGA 145
eta             GGCAGCAGCGCCAGCATGTCGTCCGG-CACGATGAAGTTCAATGGCTATCT----GAGGG 227
epsilon         CGGAGTGACCCCCG-----CCCCGAC-CATGGTAGTGTTCAATGGCCTTCT----TAAGA 221
                   *    *  *                                 *    *       *

delta           TCCATCATGGCACCGTTCCTGCGCATCTCCTTCAATTCCTATGAGCTGGGCTCCCTGCAG 416
theta           ACAACCATGTCACCGTTTCTTCGAATTGGTTTATCCAACTTTGACTGTGGGACCTGTCAA 205
eta             TCCGC---ATCGGAGAGGCAGTGGGGCTGCAGCCCACCCGCTGGTCCCTGCGGCACTCGC 284
epsilon         TCAAA---ATCTGCGAGGCCGTGAGCTTGAAGCCCACAGCCTGGTCGCTGCGCCATGCGG 278
                 *        *   *   *   *                  **      *   *   *

delta           GCG---GAGGACGACGCAAGCCAGCCTTTCTGTGCCGTGAAGATGAAGGAGGCACTCACC 473
theta           GCTTGTCAGGGAGAGGCGGTGAACCCCTACTGTGCCGTGCTTGTCAAAGAGTATGTGGAA 265
eta             T----CTTCAAAAAGGGCCACCAGCTGCTGGACCCCTACCTGACGGTGAGCGTAGACCAG 340
epsilon         TGGGACCCCGGCCCCAGACGTTC-CTTCTGGACCCCTACATTGCCCTTAACGTGGACGAC 337
                               *         **

delta           ACAGACCGAGGGAAGACTCTGGTACAGAAGAAGCCCACCATGTACCCTGAGTGGAAGTCA 533
theta           TCAGAAAACGGGCAGATGTACATCCAGAAAAAGCCGACCATGTACCCGCCTTGGGACAGC 325
eta             GTACGCGTGGGCCAGACCAGCACAAAGCAGAAGACTAACA---AACCCACCTACAACGAG 397
epsilon         TCGCGCATCGGCCAAACAGCCACCAAGCAGAAGACCAACA---GTCCGGCCTGGCACGAT 394
                       **  * *         ** * *** * * **     **    *   *

delta           ACATTCGACGCCCACATCTATGAAGGCCGTGTCATCCAGAT---CGTGCTGATGCGGGCA 590
theta           ACCTTTGATGCCCACATTAACAAGGGAAGGGTGATGCAGAT---CATCGTGAAAGGCAAA 382
```

```
eta             GAGTTCTGCACCAATGTCTCCGACGGCGGCCACCTGGAGCTAGCCGTCTTCCACGAGACG 457
epsilon         GAGTTCGTCACTGATGTGTGCAATGGGCGCAAGATCGAGCTGGCTGTCTTTCACGATGCT 454
                   **     *  *  *     * **  *     *  ** *     *  *

delta           GCTGAAGACC----CCATGTCGGAGGTGACCGTGGGCGTGTCAGTGCTG-GCTGAGCGCT 645
theta           AATGTAGACC----TCATATCAGAAACCACCGTGGAGCTCTACTCCCTG-GCAGAGAGAT 437
eta             CCCCTGGGCTATGACCACTTTGTGGCCAACTGCACGCTGCAGTTCCAGGAGCTGTTGCGC 517
epsilon         CCTATCGGCTACGACGACTTCGTGGCCAACTGCACCATCCAGTTCGAGGAGCTGCTGCAG 514
                      * *       *  *       ** *                * ** *

delta           GCAAGAAGAACAACGGCAA-GGCTGAGTTCTGGCTGGACCTGCAGCCTCAGGCCAAGGTG 704
theta           GCCGCAAGAACAATGGGCG-GACAGAAATATGGTTAGAGCTGAAACCTCAAGGCCGAATG 496
eta             ACGGCCGGCACATCGGACACCTTCGAGGGCTGGGTGGATCTGGAGCCTGAGGGGAAAGTG 577
epsilon         AATGGGAGC-CGTCA-----CTTCGAGGACTGGATTGATCTGGAGCCAGAAGGAAAAGTC 568
                       *  *            **    *** * ** *** * **  * *     *

delta           CTGATGTGTGTGCAGTATTTCCTGGAGGATGGGGATTGCAAACAGT--CCATGCGTAGT- 761
theta           CTAATGAATGCAAGATACTTTCTGGAA-ATGAGTGACACAAAGGAC--ATGAGTGAATTT 553
eta             TTCGTG-GTAATAACCCTAACAGGGAGCTTCACTGAAGCCACTCT---CCAGAGAGACCG 633
epsilon         TACGTG-ATCATCGATCTCTCGGGATCATCGGGCGAAGCCCCTAAAGACAATGAAGAACG 627
                    **  *            *             *             *

delta           GAGGAGGAGGCCATGTTCCCA-ACTATGAACCGCCGTGGAGCCATTAAACAGGCCAAGAT 820
theta           GAGAACGAAGGATTCTTTGCA-CTGCATCACCGCCGAGGCGCCATCAAACAAGCCAAAGT 612
eta             CATCTTCAAGCATTTTA------CCAGGAAGCGCCAACGGGCTATGCGAAG---GAGAGT 684
epsilon         AGTGTTTAGGGAGCGGATGCGGCCAAGGAAGCGCCAAGGGGCTGTCAGGCG---CAGGGT 684
                       * *                  * ****   * **  *          *   *

delta           TCACTACATCAAGAACCACGAGTTCATCGCCACCTTCTTTGGGCAGCCCACCTTCTGTTC 880
theta           CCACCACGTCAAGTGTCACGAGTTCACAGCCACCTTTTTCCCTCAACCCACGTTCTGCTC 672
eta             CCATCAAGTCAACGGACACAAGTTCATGGCCACATACCTGAGGCAGCCCACCTACTGCTC 744
epsilon         CCACCAGGTCAATGGCCACAAGTTCATGGCCACCTACTTGCGGCAGCCCACCTACTGCTC 744
                 **  *  ****    *** ******  ***** *   *    ** ***** * *** **

delta           TGTGTGCAAAGAGTTTGTCTGGGG---CCTCAACAAGCAAGGCTACAAATGCAGGCAATG 937
theta           TGTCTGCCATGAATTTGTCTGGGG---GCTGAACAAGCAGGGCTACCAGTGCCGACAATG 729
eta             TCACTGCCGGGAGTTCATCTGGGAGTATTTGGGAAACAGGGTTATCAATGCCAAGTGTG 804
epsilon         CCACTGTAGGGATTTCATCTGGGGTGTCATAGGAAAACAGGGATATCAATGTCAAGTTTG 804
                    **    ** **  *******     *    ** ** ** **  * **       **

delta           CAACGCTGCCATCCATAAGAAATGCATCGACAAGATTATCGGCCGCTGCACTGGCACTGC 997
theta           TAATGCAGCGATTCACAAGAAGTGCATCGATAAAGTGATAGCCAAGTGCACAGGATCGGC 789
eta             CACCTGCGTCGTCCATAAACGCTGCCATCACCTAATTGTTACAGCCTGCACTTGCCAAAA 864
epsilon         TACCTGCGTCGTCCACAAACGATGCCATGAGCTCATTATTACGAAGTGCGCTGGGCTAAA 864
                 *     *   * ** **    ***    *     *  *       *** *  *

delta           TACC---AATAGCCGGGACACCATCTTCCAGAAAGAACGCTTCAACATCGACATGCCTCA 1054
theta           GATC---AATAGTCGAGAGACCATGTTCCACAAGGAGAGATTCAAGATCGACATGCCACA 846
eta             CAATATTAACAAAGTGGATGCCAAGATCGCAGAGCAACGGTTTGGCATCAACATCCCACA 924
epsilon         GAAA---CAGGAAACCCCTGACGAGGTGGGCTCCCAACGCTTCAGCGTCAACATGCCCCA 921
                 *     *           *    *        *  * **     ** **** ** **

delta           CCGATTCAAGGTCTATAACTACATGAGCCCCACCTTCTGTGACCACTGTGGCACTTTGCT 1114
theta           CAGATTCAAAGTCTACAACTACAAGAGTCCAACCTTCTGTGAGCACTGTGGTACCCTGCT 906
eta             CAAGTTCAACGTTCACAACTACAAGGTGCCCACGTTCTGCGACCACTGTGGCTCCCTGCT 984
epsilon         CAAGTTCGGGATCCACAACTACAAGGTCCCCACGTTCTGTGACCACTGTGGCTCCCTGCT 981
                *   ***    *  * ******* *   ** ** ***** ** ********  *  ****

delta           CTGGGGATTGGTGAAACAGGGATTAAAGTGTGAAGACTGCGGCATGAATGTGCACCACAA 1174
theta           ATGGGGGCTGGCGAGGCAAGGTCTCAAGTGTGATGCATGTGGCATGAACGTCCACCACCG 966
eta             CTGGGGGATAATGCGACAAGGACTTCAGTGTAAAATATGTAAGATGAACGTACATATTCG 1044
epsilon         CTGGGGCCTCTTGCGGCAGGGCCTGCAGTGTAAAGTCTGCAAAATGAATGTTCACCGTCG 1041
                 *****  *   *   ** **  *  ***** *    **    ***** ** **
```

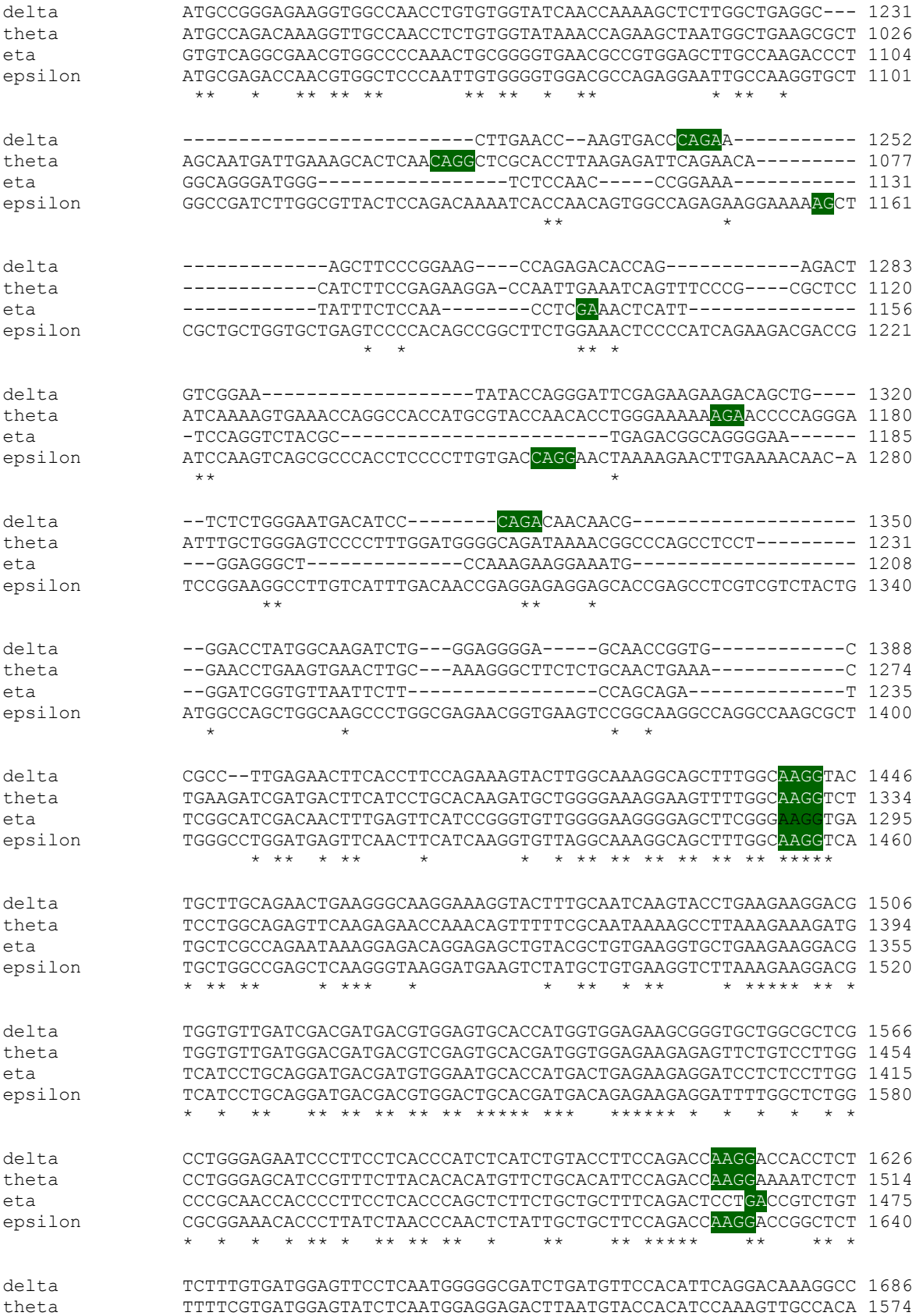
delta ATGCCGGGAGAAGGTGGCCAACCTGTGTGGTATCAACCAAAAGCTCTTGGCTGAGGC--- 1231
theta ATGCCAGACAAAGGTTGCCAACCTCTGTGGTATAAACCAGAAGCTAATGGCTGAAGCGCT 1026
eta GTGTCAGGCGAACGTGGCCCCAAACTGCGGGGTGAACGCCGTGGAGCTTGCCAAGACCCT 1104
epsilon ATGCGAGACCAACGTGGCTCCCAATTGTGGGGTGGACGCCAGAGGAATTGCCAAGGTGCT 1101
delta ----------CTTGAACC--AAGTGACCCAGAA---------- 1252
theta AGCAATGATTGAAAGCACTCAACAGGCTCGCACCTTAAGAGATTCAGAACA--------- 1077
eta GGCAGGGATGGG----------TCTCCAAC-----CCGGAAA---------- 1131
epsilon GGCCGATCTTGGCGTTACTCCAGACAAAATCACCAACAGTGGCCAGAGAAGGAAAAAGCT 1161
delta ----------AGCTTCCCGGAAG----CCAGAGACACCAG----------AGACT 1283
theta ----------CATCTTCCGAGAAGGA-CCAATTGAAATCAGTTTCCCG----CGCTCC 1120
eta ----------TATTTCTCCAA--------CCTCGAAACTCATT---------- 1156
epsilon CGCTGCTGGTGCTGAGTCCCCACAGCCGGCTTCTGGAAACTCCCCATCAGAAGACGACCG 1221
delta GTCGGAA----------TATACCAGGGATTCGAGAAGAAGACAGCTG---- 1320
theta ATCAAAAGTGAAACCAGGCCACCATGCGTACCAACACCTGGGAAAAAAGAGACCCCAGGGA 1180
eta -TCCAGGTCTACGC----------TGAGACGGCAGGGGAA------ 1185
epsilon ATCCAAGTCAGCGCCCACCTCCCCTTGTGACCAGGAACTAAAAGAACTTGAAAACAAC-A 1280
delta --TCTCTGGGAATGACATCC--------CAGACAACAACG---------- 1350
theta ATTTGCTGGGAGTCCCCTTTGGATGGGGCAGATAAAACGGCCCAGCCTCCT--------- 1231
eta ---GGAGGGCT----------CCAAAGAAGGAAATG---------- 1208
epsilon TCCGGAAGGCCTTGTCATTTGACAACCGAGGAGAGGAGCACCGAGCCTCGTCGTCTACTG 1340
delta --GGACCTATGGCAAGATCTG---GGAGGGGA-----GCAACCGGTG----------C 1388
theta --GAACCTGAAGTGAACTTGC---AAAGGGCTTCTCTGCAACTGAAA----------C 1274
eta --GGATCGGTGTTAATTCTT----------CCAGCAGA----------T 1235
epsilon ATGGCCAGCTGGCAAGCCCTGGCGAGAACGGTGAAGTCCGGCAAGGCCAGGCCAAGCGCT 1400
delta CGCC--TTGAGAACTTCACCTTCCAGAAAGTACTTGGCAAAGGCAGCTTTGGCAAGGTAC 1446
theta TGAAGATCGATGACTTCATCCTGCACAAGATGCTGGGGAAAGGAAGTTTTGGCAAGGTCT 1334
eta TCGGCATCGACAACTTTGAGTTCATCCGGGTGTTGGGGAAGGGGAGCTTCGGGAAGGTGA 1295
epsilon TGGGCCTGGATGAGTTCAACTTCATCAAGGTGTTAGGCAAAGGCAGCTTTGGCAAGGTCA 1460
delta TGCTTGCAGAACTGAAGGGCAAGGAAAGGTACTTTGCAATCAAGTACCTGAAGAAGGACG 1506
theta TCCTGGCAGAGTTCAAGAGAACCAAACAGTTTTTCGCAATAAAAGCCTTAAAGAAAGATG 1394
eta TGCTCGCCAGAATAAAGGAGACAGGAGAGCTGTACGCTGTGAAGGTGCTGAAGAAGGACG 1355
epsilon TGCTGGCCGAGCTCAAGGGTAAGGATGAAGTCTATGCTGTGAAGGTCTTAAAGAAGGACG 1520
delta TGGTGTTGATCGACGATGACGTGGAGTGCACCATGGTGGAGAAGCGGGTGCTGGCGCTCG 1566
theta TGGTGTTGATGGACGATGACGTCGAGTGCACGATGGTGGAGAAGAGAGTTCTGTCCTTGG 1454
eta TCATCCTGCAGGATGACGATGTGGAATGCACCATGACTGAGAAGAGGATCCTCTCCTTGG 1415
epsilon TCATCCTGCAGGATGACGACGTGGACTGCACGATGACAGAGAAGAGGATTTTGGCTCTGG 1580
delta CCTGGGAGAATCCCTTCCTCACCCATCTCATCTGTACCTTCCAGACCAAGGACCACCTCT 1626
theta CCTGGGAGCATCCGTTTCTTACACACATGTTCTGCACATTCCAGACCAAGGAAAATCTCT 1514
eta CCCGCAACCACCCCTTCCTCACCCAGCTCTTCTGCTGCTTTCAGACTCCTGACCGTCTGT 1475
epsilon CGCGGAAACACCCTTATCTAACCCAACTCTATTGCTGCTTCCAGACCAAGGACCGGCTCT 1640
delta TCTTTGTGATGGAGTTCCTCAATGGGGGCGATCTGATGTTCCACATTCAGGACAAAGGCC 1686
theta TTTTCGTGATGGAGTATCTCAATGGAGGAGACTTAATGTACCACATCCAAAGTTGCCACA 1574

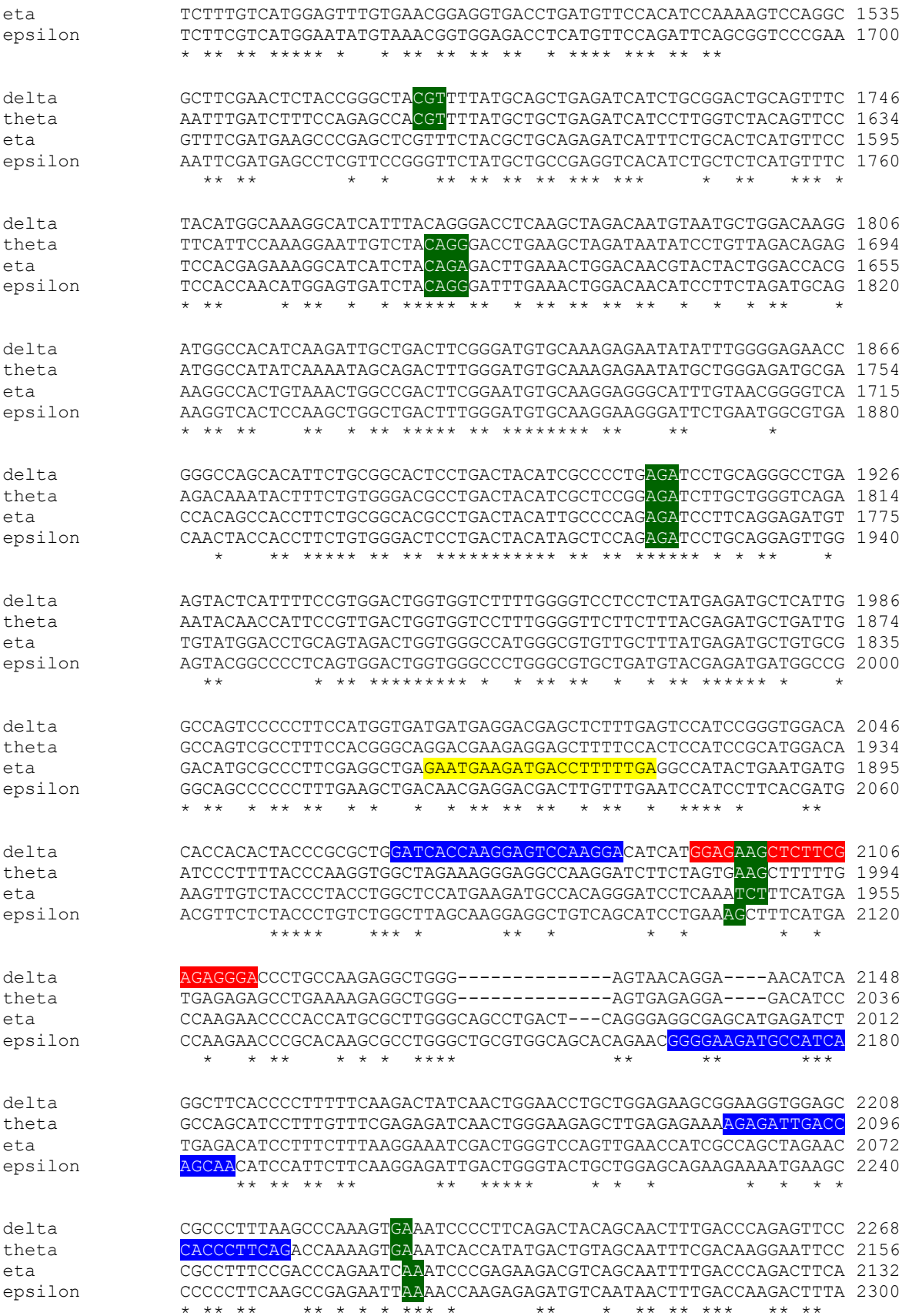
eta TCTTTGTCATGGAGTTTGTGAACGGAGGTGACCTGATGTTCCACATCCAAAAGTCCAGGC 1535
epsilon TCTTCGTCATGGAATATGTAAACGGTGGAGACCTCATGTTCCAGATTCAGCGGTCCCGAA 1700
delta GCTTCGAACTCTACCGGGCTACGTTTTATGCAGCTGAGATCATCTGCGGACTGCAGTTTC 1746
theta AATTTGATCTTTCCAGAGCCACGTTTTATGCTGCTGAGATCATCCTTGGTCTACAGTTCC 1634
eta GTTTCGATGAAGCCCGAGCTCGTTTCTACGCTGCAGAGATCATTTCTGCACTCATGTTCC 1595
epsilon AATTCGATGAGCCTCGTTCCGGGTTCTATGCTGCCGAGGTCACATCTGCTCTCATGTTTC 1760
delta TACATGGCAAAGGCATCATTTACAGGGACCTCAAGCTAGACAATGTAATGCTGGACAAGG 1806
theta TTCATTCCAAAGGAATTGTCTACAGGGACCTGAAGCTAGATAATATCCTGTTAGACAGAG 1694
eta TCCACGAGAAAGGCATCATCTACAGAGACTTGAAACTGGACAACGTACTACTGGACCACG 1655
epsilon TCCACCAACATGGAGTGATCTACAGGGATTTGAAACTGGACAACATCCTTCTAGATGCAG 1820
delta ATGGCCACATCAAGATTGCTGACTTCGGGATGTGCAAAGAGAATATATTTGGGGAGAACC 1866
theta ATGGCCATATCAAAATAGCAGACTTTGGGATGTGCAAAGAGAATATGCTGGGAGATGCGA 1754
eta AAGGCCACTGTAAACTGGCCGACTTCGGAATGTGCAAGGAGGGCATTTGTAACGGGGTCA 1715
epsilon AAGGTCACTCCAAGCTGGCTGACTTTGGGATGTGCAAGGAAGGGATTCTGAATGGCGTGA 1880
delta GGGCCAGCACATTCTGCGGCACTCCTGACTACATCGCCCCTGAGATCCTGCAGGGCCTGA 1926
theta AGACAAATACTTTCTGTGGGACGCCTGACTACATCGCTCCGGAGATCTTGCTGGGTCAGA 1814
eta CCACAGCCACCTTCTGCGGCACGCCTGACTACATTGCCCCAGAGATCCTTCAGGAGATGT 1775
epsilon CAACTACCACCTTCTGTGGGACTCCTGACTACATAGCTCCAGAGATCCTGCAGGAGTTGG 1940
delta AGTACTCATTTTCCGTGGACTGGTGGTCTTTTGGGGTCCTCCTCTATGAGATGCTCATTG 1986
theta AATACAACCATTCCGTTGACTGGTGGTCCTTTGGGGTTCTTCTTTACGAGATGCTGATTG 1874
eta TGTATGGACCTGCAGTAGACTGGTGGGCCATGGGCGTGTTGCTTTATGAGATGCTGTGCG 1835
epsilon AGTACGGCCCCTCAGTGGACTGGTGGGCCCTGGGCGTGCTGATGTACGAGATGATGGCCG 2000
delta GCCAGTCCCCCTTCCATGGTGATGATGAGGACGAGCTCTTTGAGTCCATCCGGGTGGACA 2046
theta GCCAGTCGCCTTTCCACGGGCAGGACGAAGAGGAGCTTTTCCACTCCATCCGCATGGACA 1934
eta GACATGCGCCCTTCGAGGCTGAGAATGAAGATGACCTTTTTGAGGCCATACTGAATGATG 1895
epsilon GGCAGCCCCCCTTTGAAGCTGACAACGAGGACGACTTGTTTGAATCCATCCTTCACGATG 2060
delta CACCACACTACCCGCGCTGGATCACCAAGGAGTCCAAGGACATCATGGAGAAGCTCTTCG 2106
theta ATCCCTTTTACCCAAGGTGGCTAGAAAGGGAGGCCAAGGATCTTCTAGTGAAGCTTTTTG 1994
eta AAGTTGTCTACCCTACCTGGCTCCATGAAGATGCCACAGGGATCCTCAAATCTTTCATGA 1955
epsilon ACGTTCTCTACCCTGTCTGGCTTAGCAAGGAGGCTGTCAGCATCCTGAAAGCTTTCATGA 2120
delta AGAGGGACCCTGCCAAGAGGCTGGG--------------AGTAACAGGA----AACATCA 2148
theta TGAGAGAGCCTGAAAAGAGGCTGGG--------------AGTGAGAGGA----GACATCC 2036
eta CCAAGAACCCCACCATGCGCTTGGGCAGCCTGACT---CAGGGAGGCGAGCATGAGATCT 2012
epsilon CCAAGAACCCGCACAAGCGCCTGGGCTGCGTGGCAGCACAGAACGGGGAAGATGCCATCA 2180
delta GGCTTCACCCCTTTTTCAAGACTATCAACTGGAACCTGCTGGAGAAGCGGAAGGTGGAGC 2208
theta GCCAGCATCCTTTGTTTCGAGAGATCAACTGGGAAGAGCTTGAGAGAAAAGAGATTGACC 2096
eta TGAGACATCCTTTCTTTAAGGAAATCGACTGGGTCCAGTTGAACCATCGCCAGCTAGAAC 2072
epsilon AGCAACATCCATTCTTCAAGGAGATTGACTGGGTACTGCTGGAGCAGAAGAAAATGAAGC 2240
delta CGCCCTTTAAGCCCAAAGTGAAATCCCCTTCAGACTACAGCAACTTTGACCCAGAGTTCC 2268
theta CACCCTTCAGACCAAAAGTGAAATCACCATATGACTGTAGCAATTTCGACAAGGAATTCC 2156
eta CGCCTTTCCGACCCAGAATCAAATCCCGAGAAGACGTCAGCAATTTTGACCCAGACTTCA 2132
epsilon CCCCCTTCAAGCCGAGAATTAAAACCAAGAGAGATGTCAATAACTTTGACCAAGACTTTA 2300

```
delta           TGAATGAGAAACCCCAACTTTCCTTCAGTGACAAGAACCTCATCGACTCTATGGACCAGA 2328
theta           TAAGTGAGAAACCCCGGCTATCGTTCGCTGACAGAGCACTCATCAACAGCATGGACCAGA 2216
eta             TAAAAGAAGAGCCTGTTTTAACTCCGATCGATGAGGGACATCTTCCTATGATTAACCAGG 2192
epsilon         CCCGGGAAGAGCCAATACTTACACTTGTGGATGAAGCAATCGTGAAGCAGATCAACCAGG 2360
                     **  * **     *  *       **           *       **  *****

delta           CAGCCTTCAAGGGCTTCTCCTTTGTGAACCCCAAATATGAGCAATT------CCTGGAAT 2382
theta           ACATGTTCAGCAACTTCTCCTTCATTAACCCGGGGATGGAGACTCT------CATTTGCT 2270
eta             ATGAGTTTAGAAACTTTTCCTATGTGTCACCAGAATTGCAACCGTA-------GCCTTAT 2245
epsilon         AAGAATTCAAAGGCTTCTCCTACTTTGGTGAAGACCTGATGCCCTGAGAAACTGCTTCAC 2420
                     ** *    *** ****   *

delta           AGTGAGCT------------CCCAGACCTG------CTTTTAATGCCCCGGCAGAGTAGG 2424
theta           CCTGAACCTCATCCCTCTTCCCCAGACTGGAAGAAATTCGCCTTCTCTCTGGGAACTGGT 2330
eta             GGGAAGC-AACAAAGAGAAAGGGGGATCTTTCCAGAGATTTCTTGTGTGGGAAGTCCCCA 2304
epsilon         ATGGAGTTAGCTCACTGCAAGGAGGGTGTTGAGACA-ATCCCGTGTTGCAGAGGCTCAGA 2479
                    *                   *                   *     *

delta           CCCATCTGCCCTGGTTTGCATCCTCACTGCCCAT-GAAGAAGAGTGGGTGACTGGTGATT 2483
theta           TCAAGTAACACTTCTGGGGGTCTCTTTTTCACGTTGGAGAAGAGAAGA-AACACTCAACC 2389
eta             GCTCCT---GCCTTTTAACACCACCTTCACCTTC-ACGGAGCAAATGTTCACAACTCTGC 2360
epsilon         ATGTCTCGAACTATTCGTCCTCCCCAGAGCCCCA-GTCCCACATCTGCTCTCTTATTTAT 2538
                          *   *      *       *           *   *    *

delta           CCTGCTGCTG-------CCCCCTCTTCCTCGGAG-------AGTCTGGCTCCTGTTGGCT 2529
theta           TCGAAAGCAGGGAGGACCGCTGAGCTCCTCGAGGGACACGCAGCACAAACCATGTCTCCT 2449
eta             -GAAGGGCGGAGCCTCAAGAGAGCCACTCTGTCAA-----GTCCCGGGGAGCCATGGTAC 2414
epsilon         TGCATCCCCTCATCCCAGGCCCTGTCCTTCCCCAC-----CCTCCCAGTGACCAGAAGGC 2593
                       *                *

delta           GGGCTCACAGTACTTCCTCTGTGAACTGTTTGTGAATTTGCCTTCCTTTTGCCATCGGAG 2589
theta           TCACTAATGGCATCATC-CTGTTATATCTCCTGGAATCTCTCTCACCGCAGCCCTAGAAG 2508
eta             ACTTCGGTAGTTGATACTGAGGTAAGATGTTACAGAGACGTGCACCGCCCACCCCGGAGT 2474
epsilon         -CCTCTTTGGTCCAGACTCAC-CAAGAT--CACAGATTTGAACTGCGTCTGCTCTG---T 2646
                         *      *      *           *         *     *

delta           GGAAACTGTAAATCCTGTGTGTCATT-ACTTGAATG-TAGTTATTGA------AATATAT 2641
theta           TTAGACCATTGTTAACTCTAGTCATTTACTTGAAAGATGGTTCCCGATCCTGCGAACGAT 2568
eta             CTCCATGGCTTTCAGGCTTGGAGTAAAGGACAGAAGCCAAAAGAAGAG-----ATGCTGG 2529
epsilon         GTGCAGTGCT---AGGTCTGGAGTAGCCGTCCACCCACAACCCTGAAG-----CAGCCCG 2698
                    *               *                          *

delta           ATTATATATATGCACATATATATAATAGGCTGTATATATTGCTCAGTATAGAAAGCATGT 2701
theta           TCGAAATGTAATTCTGCTCTTGTCGTTGACAAGAGCTGCTGGTTGGTG-ACGAACCAAGG 2627
eta             GTAACACAGGAGGTCCTAGGGATCCTCAGCCAAACAGGCTTCTTGTTTTTAACTTCAAGA 2589
epsilon         G-AATTC------------------------------------------------------ 2704
                   *

delta           AGGAGACTGGTGATGTGTTGACCTTTTTTTAAAAAAAACCATATGT-ATACGTGT-GTAT 2759
theta           TGCAAGTGGAACAGATTTCTCAAGACCGGGAGGGCAGATTGCCTGTCATGGAAGTCGATT 2687
eta             GACAAATCTAGACTTTCCGTGGAGCACCCCACACTGTTCTTCACGCCAATAGTGCAGTCT 2649
epsilon         ------------------------------------------------------------

delta           GTATACATCTACACACGTATACATATATGTATGTATGTATGTATGTATGTATGTATATAT 2819
theta           CCACTCAACCACAGAGAAGGACCCACTAACCCGCATCGTCCTGCGCATGTCTGTGGAAAT 2747
eta             GCGAAAGATCAAATGCTGATGAAGAAGTTAAAAGTCTCTCTAGGGAAACGGACGGCATTC 2709
epsilon         ------------------------------------------------------------

delta           GACCAAAAGAAAAGAGAGCACAAGCTACCTGAACCACAGGATTGTTTATGTGTGTATAAA 2879
theta           GTCGATGGCAGAAGGGAGGGAAAGGGATGTGA-TGGGATGTTCTCCAATAAACTTAGCGT 2806
```

```
eta             TAAGCAGACTGATTCGCTTCGAAGAAACCGCAGTTGGGCGTCCTTCAAGCTCCCAACCTA 2769
epsilon         ------------------------------------------------------------

delta           TAAACACTGAATGGTAAAAAA-CCGGA-ATTC---------------------------- 2909
theta           GAAAC-TTGAGATTTACAAAC-CCGTTCGTTCTGGCCAGCCCTGAAATTCACAAGGCAGC 2864
eta             AACCCAGTGTTGAGAACAGAGGTTGGACACCACGACGACCTCTGTTGTCTTGACAACAGC 2829
epsilon         ------------------------------------------------------------

delta           ------------------------------------------------------------
theta           GGAAAGTAAGGGGTGAGGTGCAGAGCCTTTGTCACCAACAGGAAGGGTAAGGATGTTTCG 2924
eta             TCAAGTGTCTTGAGTCTCTTCCTTCCAGTAACTAGATATTTATTGAGTGTCAAATAAAAA 2889
epsilon         ------------------------------------------------------------

delta           ------------------------------------------------------------
theta           GATGTGGTGCATCTCATTCCCACAGAAGTAAAGTCCAACCAACGAAGGCAGGGCAGTTTA 2984
eta             GGTGCCATACTCTTCAGTAGTGTACACGGTAGAGTCACCTTCATGATGCCTTTACTCGTT 2949
epsilon         ------------------------------------------------------------

delta           ------------------------------------------------------------
theta           CTGCTGCCAATCAAACCTTCTCTTCCCTCTTGTTCTGGCTGATTTCTCTGTCAGCGTCGG 3044
eta             CTGGGGTCCACCTAATGGTGTTCGCACTCTGCGAAAGGCCTCTCCACATTGCATATAGGT 3009
epsilon         ------------------------------------------------------------

delta           ------------------------------------------------------------
theta           CATTCGTCATCGTCCTCCCGTTGCACAAGAAATGA-AGTACATGACTCTTGTGAGAGAAA 3103
eta             CTGTCTTCTTTGTCTCCTGTTCATAGAAGGGCCACCACCACAGTAGTGCGGTCAGCAGGC 3069
epsilon         ------------------------------------------------------------

delta           ------------------------------------------------------------
theta           GAAAACCAATCCCATATCATGTTGCTCCTGGTGATTCGGTGACAAATAAGTCCCTCTTTA 3163
eta             GGGCTTCCGCTGCATGCCACCTGCTGACTGGCCGGTGGAATCTAATCTCCACATCCTTCA 3129
epsilon         ------------------------------------------------------------

delta           ------------------------------------------------------------
theta           GGCATCCT--GCAAGACAAACGACCCACGCATGCTATTTCCACTAGTCAGCCCTGTTGAG 3221
eta             TCCCACGTCGACTCATTGGCGAAGAAGTCCGTGCCACTCCCATCCTCGAACACGTGTGTG 3189
epsilon         ------------------------------------------------------------

delta           ------------------------------------------------------------
theta           TTGGAGTACTAATTAGACACTTAGAGTCTCGCGTGCTGTTTGTATATTTTGATGGGATGT 3281
eta             GCAGGTCCATCGGCCGCCTACTTGAGTTATGTTTCAGAGACAAAGAAGGTTGTTTGATAC 3249
epsilon         ------------------------------------------------------------

delta           ------------------------------------------------------------
theta           TGTGATGATGACGTACGTGGACGTGTAAAACGGAATAAAAGAAGAAAAGAAAGATG---- 3337
eta             TCACATTAATAAGAAGCTCTGGGTCTTGTAAACAAGGCCGACGACAGAGGTGTACCTTTT 3309
epsilon         ------------------------------------------------------------

delta           ------------------------------------------------------------
theta           ------------------------------------------------------------
eta             CATGTGTAACCATATATACAGTTGAAAAAATTTTATCTGGCTGGAAATAAAGGCATTTTT 3369
epsilon         ------------------------------------------------------------
```

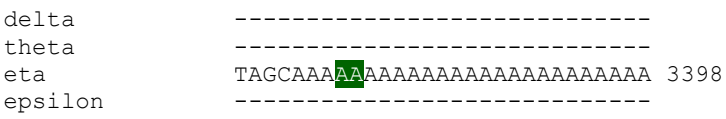

Start/stop codon

Intron/exon boundary

Primer Set 1 from original alignment

Primer Set 2 from original alignment

PKC Eta primers

11. References

Abbott,N.J., Hughes,C.C., Revest,P.A., and Greenwood,J. (1992). Development and characterisation of a rat brain capillary endothelial culture: towards an in vitro blood-brain barrier. *J. Cell Sci.* **103 (Pt 1),** 23-37.

Abbott,N.J., Ronnback,L., and Hansson,E. (2006). Astrocyte-endothelial interactions at the blood-brain barrier. *Nat. Rev. Neurosci.* **7,** 41-53.

Adam,A.P., Sharenko,A.L., Pumiglia,K., and Vincent,P.A. (2010). Src-induced tyrosine phosphorylation of VE-cadherin is not sufficient to decrease barrier function of endothelial monolayers. *J. Biol. Chem.* **285,** 7045-7055.

Adamson,P., Etienne,S., Couraud,P.O., Calder,V., and Greenwood,J. (1999). Lymphocyte migration through brain endothelial cell monolayers involves signaling through endothelial ICAM-1 via a rho-dependent pathway. *J. Immunol.* **162,** 2964-2973.

Adamson,P., Wilbourn,B., Etienne-Manneville,S., Calder,V., Beraud,E., Milligan,G., Couraud,P.O., and Greenwood,J. (2002). Lymphocyte trafficking through the blood-brain barrier is dependent on endothelial cell heterotrimeric G-protein signaling. *FASEB J.* **16,** 1185-1194.

Ager,A. (2003). Inflammation: Border crossings. *Nature* **421,** 703-705.

Aird,W.C. (2003). Endothelial cell heterogeneity. *Crit Care Med.* **31,** S221-S230.

Aird,W.C. (2004). Endothelium as an organ system. *Crit Care Med.* **32,** S271-S279.

Aird,W.C. (2007a). Phenotypic heterogeneity of the endothelium: I. Structure, function, and mechanisms. *Circ. Res.* **100,** 158-173.

Aird,W.C. (2007b). Phenotypic heterogeneity of the endothelium: II. Representative vascular beds. *Circ. Res.* **100,** 174-190.

Aird,W.C. (2008). Endothelium in health and disease. *Pharmacol. Rep.* **60,** 139-143.

Aktories,K. and Hall,A. (1989). Botulinum ADP-ribosyltransferase C3: a new tool to study low molecular weight GTP-binding proteins. *Trends Pharmacol. Sci.* **10,** 415-418.

Alberts,A.S. and Treisman,R. (1998). Activation of RhoA and SAPK/JNK signalling pathways by the RhoA-specific exchange factor mNET1. *EMBO J.* **17,** 4075-4085.

Alcaide,P., Newton,G., Auerbach,S., Sehrawat,S., Mayadas,T.N., Golan,D.E., Yacono,P., Vincent,P., Kowalczyk,A., and Luscinskas,F.W. (2008). p120-Catenin regulates leukocyte transmigration through an effect on VE-cadherin phosphorylation. *Blood* **112,** 2770-2779.

Allingham,M.J., van Buul,J.D., and Burridge,K. (2007). ICAM-1-mediated, Src- and Pyk2-dependent vascular endothelial cadherin tyrosine phosphorylation is required for leukocyte transendothelial migration. *J. Immunol.* **179,** 4053-4064.

Allt,G. and Lawrenson,J.G. (2001). Pericytes: cell biology and pathology. *Cells Tissues. Organs* **169,** 1-11.

Altman,A. and Villalba,M. (2003). Protein kinase C-theta (PKCtheta): it's all about location, location, location. *Immunol. Rev.* **192,** 53-63.

Antonetti,D.A., Barber,A.J., Hollinger,L.A., Wolpert,E.B., and Gardner,T.W. (1999). Vascular endothelial growth factor induces rapid phosphorylation of tight junction proteins occludin and zonula occluden 1. A potential mechanism for vascular permeability in diabetic retinopathy and tumors. *J. Biol. Chem.* **274,** 23463-23467.

Antonetti,D.A., Barber,A.J., Khin,S., Lieth,E., Tarbell,J.M., and Gardner,T.W. (1998). Vascular permeability in experimental diabetes is associated with reduced endothelial occludin content: vascular endothelial growth factor decreases occludin in retinal endothelial cells. Penn State Retina Research Group. *Diabetes* **47,** 1953-1959.

Asada,M., Irie,K., Morimoto,K., Yamada,A., Ikeda,W., Takeuchi,M., and Takai,Y. (2003). ADIP, a novel Afadin- and alpha-actinin-binding protein localized at cell-cell adherens junctions. *J. Biol. Chem.* **278,** 4103-4111.

Aurrand-Lions,M., Duncan,L., Ballestrem,C., and Imhof,B.A. (2001). JAM-2, a novel immunoglobulin superfamily molecule, expressed by endothelial and lymphatic cells. *J. Biol. Chem.* **276,** 2733-2741.

Badowski,C., Pawlak,G., Grichine,A., Chabadel,A., Oddou,C., Jurdic,P., Pfaff,M., Albiges-Rizo,C., and Block,M.R. (2008). Paxillin phosphorylation controls invadopodia/podosomes spatiotemporal organization. *Mol. Biol. Cell* **19,** 633-645.

Bain,J., Plater,L., Elliott,M., Shpiro,N., Hastie,C.J., McLauchlan,H., Klevernic,I., Arthur,J.S., Alessi,D.R., and Cohen,P. (2007). The selectivity of protein kinase inhibitors: a further update. *Biochem. J.* **408,** 297-315.

Balda,M.S. and Anderson,J.M. (1993). Two classes of tight junctions are revealed by ZO-1 isoforms. *Am. J. Physiol* **264,** C918-C924.

Balda,M.S., Garrett,M.D., and Matter,K. (2003). The ZO-1-associated Y-box factor ZONAB regulates epithelial cell proliferation and cell density. *J. Cell Biol.* **160,** 423-432.

Balda,M.S. and Matter,K. (2000a). The tight junction protein ZO-1 and an interacting transcription factor regulate ErbB-2 expression. *EMBO J.* **19,** 2024-2033.

Balda,M.S. and Matter,K. (2000b). Transmembrane proteins of tight junctions. *Semin. Cell Dev. Biol.* **11,** 281-289.

Balda,M.S. and Matter,K. (2003). Epithelial cell adhesion and the regulation of gene expression. *Trends Cell Biol.* **13,** 310-318.

Balda,M.S. and Matter,K. (2008). Tight junctions at a glance. *J. Cell Sci.* **121,** 3677-3682.

Balda,M.S. and Matter,K. (2009). Tight junctions and the regulation of gene expression. *Biochim. Biophys. Acta* **1788,** 761-767.

Balda,M.S., Whitney,J.A., Flores,C., Gonzalez,S., Cereijido,M., and Matter,K. (1996). Functional dissociation of paracellular permeability and transepithelial electrical resistance and disruption of the apical-basolateral intramembrane diffusion barrier by expression of a mutant tight junction membrane protein. *J. Cell Biol.* **134,** 1031-1049.

Baluk,P., Fuxe,J., Hashizume,H., Romano,T., Lashnits,E., Butz,S., Vestweber,D., Corada,M., Molendini,C., Dejana,E. et al. (2007). Functionally specialized junctions between endothelial cells of lymphatic vessels. *J. Exp. Med.* **204,** 2349-2362.

Bardin,N., Blot-Chabaud,M., Despoix,N., Kebir,A., Harhouri,K., Arsanto,J.P., Espinosa,L., Perrin,P., Robert,S., Vely,F. et al. (2009). CD146 and its soluble form regulate monocyte transendothelial migration. *Arterioscler. Thromb. Vasc. Biol.* **29,** 746-753.

Barreiro,O., Yanez-Mo,M., Serrador,J.M., Montoya,M.C., Vicente-Manzanares,M., Tejedor,R., Furthmayr,H., and Sanchez-Madrid,F. (2002). Dynamic interaction of VCAM-1 and ICAM-1 with moesin and ezrin in a novel endothelial docking structure for adherent leukocytes. *J. Cell Biol.* **157,** 1233-1245.

Barrett,D.M., Black,S.M., Todor,H., Schmidt-Ullrich,R.K., Dawson,K.S., and Mikkelsen,R.B. (2005). Inhibition of protein-tyrosine phosphatases by mild oxidative stresses is dependent on S-nitrosylation. *J. Biol. Chem.* **280,** 14453-14461.

Bazzoni,G. and Dejana,E. (2004). Endothelial cell-to-cell junctions: molecular organization and role in vascular homeostasis. *Physiol Rev.* **84,** 869-901.

Bennett,B.L., Sasaki,D.T., Murray,B.W., O'Leary,E.C., Sakata,S.T., Xu,W., Leisten,J.C., Motiwala,A., Pierce,S., Satoh,Y. et al. (2001). SP600125, an anthrapyrazolone inhibitor of Jun N-terminal kinase. *Proc. Natl. Acad. Sci. U. S. A* **98,** 13681-13686.

Beraud,E., Balzano,C., Zamora,A.J., Varriale,S., Bernard,D., and Ben Nun,A. (1993). Pathogenic and non-pathogenic T lymphocytes specific for the encephalitogenic epitope of myelin basic protein: functional characteristics and vaccination properties. *J. Neuroimmunol.* **47,** 41-53.

Birukova,A.A., Malyukova,I., Poroyko,V., and Birukov,K.G. (2007). Paxillin-beta-catenin interactions are involved in Rac/Cdc42-mediated endothelial barrier-protective response to oxidized phospholipids. *Am. J. Physiol Lung Cell Mol. Physiol* **293,** L199-L211.

Bixel,G., Kloep,S., Butz,S., Petri,B., Engelhardt,B., and Vestweber,D. (2004). Mouse CD99 participates in T-cell recruitment into inflamed skin. *Blood* **104,** 3205-3213.

Bixel,M.G., Petri,B., Khandoga,A.G., Khandoga,A., Wolburg-Buchholz,K., Wolburg,H., Marz,S., Krombach,F., and Vestweber,D. (2007). A CD99-related antigen on endothelial cells mediates neutrophil but not lymphocyte extravasation in vivo. *Blood* **109,** 5327-5336.

Bogoyevitch,M.A. and Kobe,B. (2006). Uses for JNK: the many and varied substrates of the c-Jun N-terminal kinases. *Microbiol. Mol. Biol. Rev.* **70,** 1061-1095.

Bradfield,P.F., Scheiermann,C., Nourshargh,S., Ody,C., Luscinskas,F.W., Rainger,G.E., Nash,G.B., Miljkovic-Licina,M., Aurrand-Lions,M., and Imhof,B.A. (2007). JAM-C regulates unidirectional monocyte transendothelial migration in inflammation. *Blood* **110,** 2545-2555.

Brandt,D., Gimona,M., Hillmann,M., Haller,H., and Mischak,H. (2002). Protein kinase C induces actin reorganization via a Src- and Rho-dependent pathway. *J. Biol. Chem.* **277,** 20903-20910.

Brenner,S.L. and Korn,E.D. (1979). Substoichiometric concentrations of cytochalasin D inhibit actin polymerization. Additional evidence for an F-actin treadmill. *J. Biol. Chem.* **254,** 9982-9985.

Bretscher,A., Edwards,K., and Fehon,R.G. (2002). ERM proteins and merlin: integrators at the cell cortex. *Nat. Rev. Mol. Cell Biol.* **3,** 586-599.

Brown,M.C. and Turner,C.E. (2004). Paxillin: adapting to change. *Physiol Rev.* **84,** 1315-1339.

Bubb,M.R., Senderowicz,A.M., Sausville,E.A., Duncan,K.L., and Korn,E.D. (1994). Jasplakinolide, a cytotoxic natural product, induces actin polymerization and competitively inhibits the binding of phalloidin to F-actin. *J. Biol. Chem.* **269,** 14869-14871.

Burns,A.R., Walker,D.C., Brown,E.S., Thurmon,L.T., Bowden,R.A., Keese,C.R., Simon,S.I., Entman,M.L., and Smith,C.W. (1997). Neutrophil transendothelial migration is independent of tight junctions and occurs preferentially at tricellular corners. *J. Immunol.* **159,** 2893-2903.

Burridge,K., Petch,L.A., and Romer,L.H. (1992a). Signals from focal adhesions. *Curr. Biol.* **2,** 537-539.

Burridge,K., Turner,C.E., and Romer,L.H. (1992b). Tyrosine phosphorylation of paxillin and pp125FAK accompanies cell adhesion to extracellular matrix: a role in cytoskeletal assembly. *J. Cell Biol.* **119,** 893-903.

Butcher,E.C. (1991). Leukocyte-endothelial cell recognition: three (or more) steps to specificity and diversity. *Cell* **67,** 1033-1036.

Carman,C.V. (2009). Mechanisms for transcellular diapedesis: probing and pathfinding by 'invadosome-like protrusions'. *J. Cell Sci.* **122,** 3025-3035.

Carman,C.V., Jun,C.D., Salas,A., and Springer,T.A. (2003). Endothelial cells proactively form microvilli-like membrane projections upon intercellular adhesion molecule 1 engagement of leukocyte LFA-1. *J. Immunol.* **171,** 6135-6144.

Carman,C.V., Sage,P.T., Sciuto,T.E., de la Fuente,M.A., Geha,R.S., Ochs,H.D., Dvorak,H.F., Dvorak,A.M., and Springer,T.A. (2007). Transcellular diapedesis is initiated by invasive podosomes. *Immunity.* **26,** 784-797.

Carman,C.V. and Springer,T.A. (2004). A transmigratory cup in leukocyte diapedesis both through individual vascular endothelial cells and between them. *J. Cell Biol.* **167,** 377-388.

Carman,C.V. and Springer,T.A. (2008). Trans-cellular migration: cell-cell contacts get intimate. *Curr. Opin. Cell Biol.* **20,** 533-540.

Carmena,D. and Sardini,A. (2007). Lifespan regulation of conventional protein kinase C isotypes. *Biochem. Soc. Trans.* **35,** 1043-1045.

Carpen,O., Pallai,P., Staunton,D.E., and Springer,T.A. (1992). Association of intercellular adhesion molecule-1 (ICAM-1) with actin-containing cytoskeleton and alpha-actinin. *J. Cell Biol.* **118,** 1223-1234.

Carpenter,A.C. and Alexander,J.S. (2008). Endothelial PKC delta activation attenuates neutrophil transendothelial migration. *Inflamm. Res.* **57,** 216-229.

Cayrol,R., Wosik,K., Berard,J.L., Dodelet-Devillers,A., Ifergan,I., Kebir,H., Haqqani,A.S., Kreymborg,K., Krug,S., Moumdjian,R. et al. (2008). Activated leukocyte cell adhesion molecule promotes leukocyte trafficking into the central nervous system. *Nat. Immunol.* **9,** 137-145.

Cernuda-Morollon,E. and Ridley,A.J. (2006). Rho GTPases and leukocyte adhesion receptor expression and function in endothelial cells. *Circ. Res.* **98,** 757-767.

Chan,P.Y. and Aruffo,A. (1993). VLA-4 integrin mediates lymphocyte migration on the inducible endothelial cell ligand VCAM-1 and the extracellular matrix ligand fibronectin. *J. Biol. Chem.* **268,** 24655-24664.

Chang,L. and Karin,M. (2001). Mammalian MAP kinase signalling cascades. *Nature* **410,** 37-40.

Chianale,F., Rainero,E., Cianflone,C., Bettio,V., Pighini,A., Porporato,P.E., Filigheddu,N., Serini,G., Sinigaglia,F., Baldanzi,G. et al. (2010). Diacylglycerol kinase alpha mediates HGF-induced Rac activation and membrane ruffling by regulating atypical PKC and RhoGDI. *Proc. Natl. Acad. Sci. U. S. A* **107,** 4182-4187.

Clark,A.R., Dean,J.L., and Saklatvala,J. (2003). Post-transcriptional regulation of gene expression by mitogen-activated protein kinase p38. *FEBS Lett.* **546,** 37-44.

Clark,P.R., Manes,T.D., Pober,J.S., and Kluger,M.S. (2007). Increased ICAM-1 expression causes endothelial cell leakiness, cytoskeletal reorganization and junctional alterations. *J. Invest Dermatol.* **127,** 762-774.

Collazos,A., Diouf,B., Guerineau,N.C., Quittau-Prevostel,C., Peter,M., Coudane,F., Hollande,F., and Joubert,D. (2006). A spatiotemporally coordinated cascade of protein kinase C activation controls isoform-selective translocation. *Mol. Cell Biol.* **26,** 2247-2261.

Constantin,G., Laudanna,C., Brocke,S., and Butcher,E.C. (1999). Inhibition of experimental autoimmune encephalomyelitis by a tyrosine kinase inhibitor. *J. Immunol.* **162,** 1144-1149.

Cook-Mills,J.M. and Deem,T.L. (2005). Active participation of endothelial cells in inflammation. *J. Leukoc. Biol.* **77,** 487-495.

Corbalan-Garcia,S. and Gomez-Fernandez,J.C. (2006). Protein kinase C regulatory domains: the art of decoding many different signals in membranes. *Biochim. Biophys. Acta* **1761,** 633-654.

Couty,J.P., Rampon,C., Leveque,M., Laran-Chich,M.P., Bourdoulous,S., Greenwood,J., and Couraud,P.O. (2007). PECAM-1 engagement counteracts ICAM-1-induced signaling in brain vascular endothelial cells. *J. Neurochem.* **103,** 793-801.

Crane,I.J. and Liversidge,J. (2008). Mechanisms of leukocyte migration across the blood-retina barrier. *Semin. Immunopathol.* **30,** 165-177.

Cuenda,A. (2000). Mitogen-activated protein kinase kinase 4 (MKK4). *Int. J. Biochem. Cell Biol.* **32,** 581-587.

Daneman,R. and Rescigno,M. (2009). The gut immune barrier and the blood-brain barrier: are they so different? *Immunity.* **31,** 722-735.

Dasgupta,B. and Muller,W.A. (2008). Endothelial Src kinase regulates membrane recycling from the lateral border recycling compartment during leukocyte transendothelial migration. *Eur. J. Immunol.* **38,** 3499-3507.

Davis,R.J. (2000). Signal transduction by the JNK group of MAP kinases. *Cell* **103,** 239-252.

Deakin,N.O. and Turner,C.E. (2008). Paxillin comes of age. *J. Cell Sci.* **121,** 2435-2444.

Deem,T.L., Abdala-Valencia,H., and Cook-Mills,J.M. (2007). VCAM-1 activation of endothelial cell protein tyrosine phosphatase 1B. *J. Immunol.* **178,** 3865-3873.

Deem,T.L. and Cook-Mills,J.M. (2004). Vascular cell adhesion molecule 1 (VCAM-1) activation of endothelial cell matrix metalloproteinases: role of reactive oxygen species. *Blood* **104,** 2385-2393.

Dejana,E. (2004). Endothelial cell-cell junctions: happy together. *Nat. Rev. Mol. Cell Biol.* **5,** 261-270.

Dejana,E., Orsenigo,F., and Lampugnani,M.G. (2008). The role of adherens junctions and VE-cadherin in the control of vascular permeability. *J. Cell Sci.* **121,** 2115-2122.

Dejana,E., Orsenigo,F., Molendini,C., Baluk,P., and McDonald,D.M. (2009). Organization and signaling of endothelial cell-to-cell junctions in various regions of the blood and lymphatic vascular trees. *Cell Tissue Res.* **335,** 17-25.

Demeuse,P., Fragner,P., Leroy-Noury,C., Mercier,C., Payen,L., Fardel,O., Couraud,P.O., and Roux,F. (2004). Puromycin selectively increases mdr1a expression in immortalized rat brain endothelial cell lines. *J. Neurochem.* **88,** 23-31.

Dietrich,J.B. (2002). The adhesion molecule ICAM-1 and its regulation in relation with the blood-brain barrier. *J. Neuroimmunol.* **128,** 58-68.

Dimmeler,S., Fleming,I., Fisslthaler,B., Hermann,C., Busse,R., and Zeiher,A.M. (1999). Activation of nitric oxide synthase in endothelial cells by Akt-dependent phosphorylation. *Nature* **399,** 601-605.

Diouf,B., Collazos,A., Labesse,G., Macari,F., Choquet,A., Clair,P., Gauthier-Rouviere,C., Guerineau,N.C., Jay,P., Hollande,F. et al. (2009). A 20-amino acid module of protein kinase C{epsilon} involved in translocation and selective targeting at cell-cell contacts. *J. Biol. Chem.* **284,** 18808-18815.

DiStasi,M.R. and Ley,K. (2009). Opening the flood-gates: how neutrophil-endothelial interactions regulate permeability. *Trends Immunol.* **30,** 547-556.

Dodelet-Devillers,A., Cayrol,R., van Horssen,J., Haqqani,A.S., de Vries,H.E., Engelhardt,B., Greenwood,J., and Prat,A. (2009). Functions of lipid raft membrane microdomains at the blood-brain barrier. *J. Mol. Med. (Berl)* **87,** 765-774.

Durieu-Trautmann,O., Chaverot,N., Cazaubon,S., Strosberg,A.D., and Couraud,P.O. (1994). Intercellular adhesion molecule 1 activation induces tyrosine phosphorylation of the cytoskeleton-associated protein cortactin in brain microvessel endothelial cells. *J. Biol. Chem.* **269,** 12536-12540.

Dvorak,A.M. and Feng,D. (2001). The vesiculo-vacuolar organelle (VVO). A new endothelial cell permeability organelle. *J. Histochem. Cytochem.* **49,** 419-432.

Dvorak,A.M., Kohn,S., Morgan,E.S., Fox,P., Nagy,J.A., and Dvorak,H.F. (1996). The vesiculo-vacuolar organelle (VVO): a distinct endothelial cell structure that provides a transcellular pathway for macromolecular extravasation. *J. Leukoc. Biol.* **59,** 100-115.

Dyer,L.A. and Patterson,C. (2010). Development of the endothelium: an emphasis on heterogeneity. *Semin. Thromb. Hemost.* **36,** 227-235.

Eberle,F., Dubreuil,P., Mattei,M.G., Devilard,E., and Lopez,M. (1995). The human PRR2 gene, related to the human poliovirus receptor gene (PVR), is the true homolog of the murine MPH gene. *Gene* **159,** 267-272.

Ebnet,K., Suzuki,A., Ohno,S., and Vestweber,D. (2004). Junctional adhesion molecules (JAMs): more molecules with dual functions? *J. Cell Sci.* **117,** 19-29.

Engelhardt,B. (2003). Development of the blood-brain barrier. *Cell Tissue Res.* **314,** 119-129.

Engelhardt,B. (2008). Immune cell entry into the central nervous system: involvement of adhesion molecules and chemokines. *J. Neurol. Sci.* **274,** 23-26.

Engelhardt,B. and Ransohoff,R.M. (2005). The ins and outs of T-lymphocyte trafficking to the CNS: anatomical sites and molecular mechanisms. *Trends Immunol.* **26,** 485-495.

Engelhardt,B. and Sorokin,L. (2009). The blood-brain and the blood-cerebrospinal fluid barriers: function and dysfunction. *Semin. Immunopathol.* **31,** 497-511.

Etienne,S., Adamson,P., Greenwood,J., Strosberg,A.D., Cazaubon,S., and Couraud,P.O. (1998). ICAM-1 signaling pathways associated with Rho activation in microvascular brain endothelial cells. *J. Immunol.* **161,** 5755-5761.

Etienne-Manneville,S., Manneville,J.B., Adamson,P., Wilbourn,B., Greenwood,J., and Couraud,P.O. (2000). ICAM-1-coupled cytoskeletal rearrangements and transendothelial lymphocyte migration involve intracellular calcium signaling in brain endothelial cell lines. *J. Immunol.* **165,** 3375-3383.

Favata,M.F., Horiuchi,K.Y., Manos,E.J., Daulerio,A.J., Stradley,D.A., Feeser,W.S., Van Dyk,D.E., Pitts,W.J., Earl,R.A., Hobbs,F. et al. (1998). Identification of a novel inhibitor of mitogen-activated protein kinase kinase. *J. Biol. Chem.* **273,** 18623-18632.

Fehon,R.G., McClatchey,A.I., and Bretscher,A. (2010). Organizing the cell cortex: the role of ERM proteins. *Nat. Rev. Mol. Cell Biol.* **11,** 276-287.

Fields,A.P. and Regala,R.P. (2007). Protein kinase C iota: human oncogene, prognostic marker and therapeutic target. *Pharmacol. Res.* **55,** 487-497.

Frank,R.N., Turczyn,T.J., and Das,A. (1990). Pericyte coverage of retinal and cerebral capillaries. *Invest Ophthalmol. Vis. Sci.* **31,** 999-1007.

Friedl,P. and Weigelin,B. (2008). Interstitial leukocyte migration and immune function. *Nat. Immunol.* **9,** 960-969.

Frohman,E.M., Racke,M.K., and Raine,C.S. (2006). Multiple sclerosis--the plaque and its pathogenesis. *N. Engl. J. Med.* **354,** 942-955.

Fukuhara,A., Irie,K., Nakanishi,H., Takekuni,K., Kawakatsu,T., Ikeda,W., Yamada,A., Katata,T., Honda,T., Sato,T. et al. (2002a). Involvement of nectin in the localization of junctional adhesion molecule at tight junctions. *Oncogene* **21,** 7642-7655.

Fukuhara,A., Irie,K., Yamada,A., Katata,T., Honda,T., Shimizu,K., Nakanishi,H., and Takai,Y. (2002b). Role of nectin in organization of tight junctions in epithelial cells. *Genes Cells* **7,** 1059-1072.

Fukuhara,T., Shimizu,K., Kawakatsu,T., Fukuyama,T., Minami,Y., Honda,T., Hoshino,T., Yamada,T., Ogita,H., Okada,M. et al. (2004). Activation of Cdc42 by trans interactions of the cell adhesion molecules nectins through c-Src and Cdc42-GEF FRG. *J. Cell Biol.* **166,** 393-405.

Fulton,D., Gratton,J.P., McCabe,T.J., Fontana,J., Fujio,Y., Walsh,K., Franke,T.F., Papapetropoulos,A., and Sessa,W.C. (1999). Regulation of endothelium-derived nitric oxide production by the protein kinase Akt. *Nature* **399,** 597-601.

Furuse,M., Fujita,K., Hiiragi,T., Fujimoto,K., and Tsukita,S. (1998). Claudin-1 and -2: novel integral membrane proteins localizing at tight junctions with no sequence similarity to occludin. *J. Cell Biol.* **141,** 1539-1550.

Furuse,M., Hirase,T., Itoh,M., Nagafuchi,A., Yonemura,S., Tsukita,S., and Tsukita,S. (1993). Occludin: a novel integral membrane protein localizing at tight junctions. *J. Cell Biol.* **123,** 1777-1788.

Furuse,M., Itoh,M., Hirase,T., Nagafuchi,A., Yonemura,S., Tsukita,S., and Tsukita,S. (1994). Direct association of occludin with ZO-1 and its possible involvement in the localization of occludin at tight junctions. *J. Cell Biol.* **127,** 1617-1626.

Furuse,M. and Tsukita,S. (2006). Claudins in occluding junctions of humans and flies. *Trends Cell Biol.* **16,** 181-188.

Gaestel,M. (2006). MAPKAP kinases - MKs - two's company, three's a crowd. *Nat. Rev. Mol. Cell Biol.* **7,** 120-130.

Garrido-Urbani,S., Bradfield,P.F., Lee,B.P., and Imhof,B.A. (2008). Vascular and epithelial junctions: a barrier for leucocyte migration. *Biochem. Soc. Trans.* **36,** 203-211.

Gavard,J. and Gutkind,J.S. (2006). VEGF controls endothelial-cell permeability by promoting the beta-arrestin-dependent endocytosis of VE-cadherin. *Nat. Cell Biol.* **8,** 1223-1234.

Geraldes,P. and King,G.L. (2010). Activation of protein kinase C isoforms and its impact on diabetic complications. *Circ. Res.* **106,** 1319-1331.

Girardin,S.E. and Yaniv,M. (2001). A direct interaction between JNK1 and CrkII is critical for Rac1-induced JNK activation. *EMBO J.* **20,** 3437-3446.

Gismondi,A., Jacobelli,J., Strippoli,R., Mainiero,F., Soriani,A., Cifaldi,L., Piccoli,M., Frati,L., and Santoni,A. (2003). Proline-rich tyrosine kinase 2 and Rac activation by chemokine and integrin receptors controls NK cell transendothelial migration. *J. Immunol.* **170,** 3065-3073.

Gorbunova,E., Gavrilovskaya,I.N., and Mackow,E.R. (2010). Pathogenic hantaviruses Andes virus and Hantaan virus induce adherens junction disassembly by directing vascular endothelial cadherin internalization in human endothelial cells. *J. Virol.* **84,** 7405-7411.

Gratton,J.P., Bernatchez,P., and Sessa,W.C. (2004). Caveolae and caveolins in the cardiovascular system. *Circ. Res.* **94,** 1408-1417.

Grazia,L.M., Zanetti,A., Corada,M., Takahashi,T., Balconi,G., Breviario,F., Orsenigo,F., Cattelino,A., Kemler,R., Daniel,T.O. et al. (2003). Contact inhibition of VEGF-induced proliferation requires vascular endothelial cadherin, beta-catenin, and the phosphatase DEP-1/CD148. *J. Cell Biol.* **161,** 793-804.

Greenwood,J., Amos,C.L., Walters,C.E., Couraud,P.O., Lyck,R., Engelhardt,B., and Adamson,P. (2003a). Intracellular domain of brain endothelial intercellular adhesion molecule-1 is essential for T lymphocyte-mediated signaling and migration. *J. Immunol.* **171,** 2099-2108.

Greenwood,J., Walters,C.E., Pryce,G., Kanuga,N., Beraud,E., Baker,D., and Adamson,P. (2003b). Lovastatin inhibits brain endothelial cell Rho-mediated lymphocyte migration and attenuates experimental autoimmune encephalomyelitis. *FASEB J.* **17,** 905-907.

Greenwood,J., Wang,Y., and Calder,V.L. (1995). Lymphocyte adhesion and transendothelial migration in the central nervous system: the role of LFA-1, ICAM-1, VLA-4 and VCAM-1. off. *Immunology* **86,** 408-415.

Griner,E.M. and Kazanietz,M.G. (2007). Protein kinase C and other diacylglycerol effectors in cancer. *Nat. Rev. Cancer* **7,** 281-294.

Gschwendt,M., Dieterich,S., Rennecke,J., Kittstein,W., Mueller,H.J., and Johannes,F.J. (1996). Inhibition of protein kinase C mu by various inhibitors. Differentiation from protein kinase c isoenzymes. *FEBS Lett.* **392,** 77-80.

Guan,J.L. (1997). Role of focal adhesion kinase in integrin signaling. *Int. J. Biochem. Cell Biol.* **29,** 1085-1096.

Guezguez,B., Vigneron,P., Lamerant,N., Kieda,C., Jaffredo,T., and Dunon,D. (2007). Dual role of melanoma cell adhesion molecule (MCAM)/CD146 in lymphocyte endothelium interaction: MCAM/CD146 promotes rolling via microvilli induction in lymphocyte and is an endothelial adhesion receptor. *J. Immunol.* **179,** 6673-6685.

Guillemin,G.J. and Brew,B.J. (2004). Microglia, macrophages, perivascular macrophages, and pericytes: a review of function and identification. *J. Leukoc. Biol.* **75,** 388-397.

Hamilton,N.B., Attwell,D., and Hall,C.N. (2010). Pericyte-mediated regulation of capillary diameter: a component of neurovascular coupling in health and disease. *Front Neuroenergetics.* **2**.

Hanke,J.H., Gardner,J.P., Dow,R.L., Changelian,P.S., Brissette,W.H., Weringer,E.J., Pollok,B.A., and Connelly,P.A. (1996). Discovery of a novel, potent, and Src family-selective tyrosine kinase inhibitor. Study of Lck- and FynT-dependent T cell activation. *J. Biol. Chem.* **271,** 695-701.

Harhaj,N.S., Felinski,E.A., Wolpert,E.B., Sundstrom,J.M., Gardner,T.W., and Antonetti,D.A. (2006). VEGF activation of protein kinase C stimulates occludin phosphorylation and contributes to endothelial permeability. *Invest Ophthalmol. Vis. Sci.* **47,** 5106-5115.

Hawkins,B.T. and Davis,T.P. (2005). The blood-brain barrier/neurovascular unit in health and disease. *Pharmacol. Rev.* **57,** 173-185.

Heiska,L., Alfthan,K., Gronholm,M., Vilja,P., Vaheri,A., and Carpen,O. (1998). Association of ezrin with intercellular adhesion molecule-1 and -2 (ICAM-1 and ICAM-2). Regulation by phosphatidylinositol 4, 5-bisphosphate. *J. Biol. Chem.* **273,** 21893-21900.

Hickey,W.F. (1999). Leukocyte traffic in the central nervous system: the participants and their roles. *Semin. Immunol.* **11,** 125-137.

Hickey,W.F. (2001). Basic principles of immunological surveillance of the normal central nervous system. *Glia* **36,** 118-124.

Hoefen,R.J. and Berk,B.C. (2002). The role of MAP kinases in endothelial activation. *Vascul. Pharmacol.* **38,** 271-273.

Holsinger,L.J., Ward,K., Duffield,B., Zachwieja,J., and Jallal,B. (2002). The transmembrane receptor protein tyrosine phosphatase DEP1 interacts with p120(ctn). *Oncogene* **21,** 7067-7076.

Honda,T., Shimizu,K., Fukuhara,A., Irie,K., and Takai,Y. (2003a). Regulation by nectin of the velocity of the formation of adherens junctions and tight junctions. *Biochem. Biophys. Res. Commun.* **306,** 104-109.

Honda,T., Shimizu,K., Kawakatsu,T., Fukuhara,A., Irie,K., Nakamura,T., Matsuda,M., and Takai,Y. (2003b). Cdc42 and Rac small G proteins activated by trans-interactions of nectins are involved in activation of c-Jun N-terminal kinase, but not in association of nectins and cadherin to form adherens junctions, in fibroblasts. *Genes Cells* **8,** 481-491.

Huang,C., Jacobson,K., and Schaller,M.D. (2004). A role for JNK-paxillin signaling in cell migration. *Cell Cycle* **3,** 4-6.

Huang,C., Rajfur,Z., Borchers,C., Schaller,M.D., and Jacobson,K. (2003). JNK phosphorylates paxillin and regulates cell migration. *Nature* **424,** 219-223.

Huang,M.T., Larbi,K.Y., Scheiermann,C., Woodfin,A., Gerwin,N., Haskard,D.O., and Nourshargh,S. (2006). ICAM-2 mediates neutrophil transmigration in vivo: evidence for stimulus specificity and a role in PECAM-1-independent transmigration. *Blood* **107,** 4721-4727.

Huang,Z., Yan,D.P., and Ge,B.X. (2008). JNK regulates cell migration through promotion of tyrosine phosphorylation of paxillin. *Cell Signal.* **20,** 2002-2012.

Hubbard,A.K. and Rothlein,R. (2000). Intercellular adhesion molecule-1 (ICAM-1) expression and cell signaling cascades. *Free Radic. Biol. Med.* **28,** 1379-1386.

Huber,D., Balda,M.S., and Matter,K. (2000). Occludin modulates transepithelial migration of neutrophils. *J. Biol. Chem.* **275,** 5773-5778.

Huveneers,S. and Danen,E.H. (2009). Adhesion signaling - crosstalk between integrins, Src and Rho. *J. Cell Sci.* **122,** 1059-1069.

Ilan,N. and Madri,J.A. (2003). PECAM-1: old friend, new partners. *Curr. Opin. Cell Biol.* **15,** 515-524.

Imhof,B.A. and Aurrand-Lions,M. (2004). Adhesion mechanisms regulating the migration of monocytes. *Nat. Rev. Immunol.* **4,** 432-444.

Ionescu,C.V., Cepinskas,G., Savickiene,J., Sandig,M., and Kvietys,P.R. (2003). Neutrophils induce sequential focal changes in endothelial adherens junction components: role of elastase. *Microcirculation.* **10,** 205-220.

Issekutz,A.C., Rowter,D., and Springer,T.A. (1999). Role of ICAM-1 and ICAM-2 and alternate CD11/CD18 ligands in neutrophil transendothelial migration. *J. Leukoc. Biol.* **65,** 117-126.

Jaffe,A.B., Hall,A., and Schmidt,A. (2005). Association of CNK1 with Rho guanine nucleotide exchange factors controls signaling specificity downstream of Rho. *Curr. Biol.* **15,** 405-412.

Jandt,E., Denner,K., Kovalenko,M., Ostman,A., and Bohmer,F.D. (2003). The protein-tyrosine phosphatase DEP-1 modulates growth factor-stimulated cell migration and cell-matrix adhesion. *Oncogene* **22,** 4175-4185.

Johannes,F.J., Prestle,J., Eis,S., Oberhagemann,P., and Pfizenmaier,K. (1994). PKCu is a novel, atypical member of the protein kinase C family. *J. Biol. Chem.* **269,** 6140-6148.

Kanters,E., van Rijssel,J., Hensbergen,P.J., Hondius,D., Mul,F.P., Deelder,A.M., Sonnenberg,A., van Buul,J.D., and Hordijk,P.L. (2008). Filamin B mediates ICAM-1-driven leukocyte transendothelial migration. *J. Biol. Chem.* **283,** 31830-31839.

Kawakami,T., Kawakami,Y., and Kitaura,J. (2002). Protein kinase C beta (PKC beta): normal functions and diseases. *J. Biochem.* **132,** 677-682.

Kawakatsu,T., Ogita,H., Fukuhara,T., Fukuyama,T., Minami,Y., Shimizu,K., and Takai,Y. (2005). Vav2 as a Rac-GDP/GTP exchange factor responsible for the nectin-induced, c-Src- and Cdc42-mediated activation of Rac. *J. Biol. Chem.* **280,** 4940-4947.

Kawakatsu,T., Shimizu,K., Honda,T., Fukuhara,T., Hoshino,T., and Takai,Y. (2002). Trans-interactions of nectins induce formation of filopodia and Lamellipodia through the respective activation of Cdc42 and Rac small G proteins. *J. Biol. Chem.* **277,** 50749-50755.

Kikkawa,U., Matsuzaki,H., and Yamamoto,T. (2002). Protein kinase C delta (PKC delta): activation mechanisms and functions. *J. Biochem.* **132,** 831-839.

Kim,H. and McCulloch,C.A. (2011). Filamin A mediates interactions between cytoskeletal proteins that control cell adhesion. *FEBS Lett.* **585,** 18-22.

Kimura,K., Teranishi,S., Yamauchi,J., and Nishida,T. (2008). Role of JNK-dependent serine phosphorylation of paxillin in migration of corneal epithelial cells during wound closure. *Invest Ophthalmol. Vis. Sci.* **49,** 125-132.

Kobayashi,H., Boelte,K.C., and Lin,P.C. (2007). Endothelial cell adhesion molecules and cancer progression. *Curr. Med. Chem.* **14,** 377-386.

Konopatskaya,O. and Poole,A.W. (2010). Protein kinase Calpha: disease regulator and therapeutic target. *Trends Pharmacol. Sci.* **31,** 8-14.

Koss,M., Pfeiffer,G.R., Wang,Y., Thomas,S.T., Yerukhimovich,M., Gaarde,W.A., Doerschuk,C.M., and Wang,Q. (2006). Ezrin/radixin/moesin proteins are phosphorylated by TNF-alpha and modulate permeability increases in human pulmonary microvascular endothelial cells. *J. Immunol.* **176,** 1218-1227.

Koyama,Y., Tanaka,Y., Saito,K., Abe,M., Nakatsuka,K., Morimoto,I., Auron,P.E., and Eto,S. (1996). Cross-linking of intercellular adhesion molecule 1 (CD54) induces AP-1 activation and IL-1beta transcription. *J. Immunol.* **157,** 5097-5103.

Krause,G., Winkler,L., Mueller,S.L., Haseloff,R.F., Piontek,J., and Blasig,I.E. (2008). Structure and function of claudins. *Biochim. Biophys. Acta* **1778,** 631-645.

Krizbai,I., Szabo,G., Deli,M., Maderspach,K., Lehel,C., Olah,Z., Wolff,J.R., and Joo,F. (1995). Expression of protein kinase C family members in the cerebral endothelial cells. *J. Neurochem.* **65,** 459-462.

Kumar,P., Shen,Q., Pivetti,C.D., Lee,E.S., Wu,M.H., and Yuan,S.Y. (2009). Molecular mechanisms of endothelial hyperpermeability: implications in inflammation. *Expert. Rev. Mol. Med.* **11,** e19.

Kunt,T., Forst,T., Kazda,C., Harzer,O., Engelbach,M., Lobig,M., Beyer,J., and Pfutzner,A. (2007). The beta-specific protein kinase C inhibitor ruboxistaurin (LY333531) suppresses glucose-induced adhesion of human monocytes to endothelial cells in vitro. *J. Diabetes Sci. Technol.* **1,** 929-935.

Kuramitsu,K., Ikeda,W., Inoue,N., Tamaru,Y., and Takai,Y. (2008). Novel role of nectin: implication in the co-localization of JAM-A and claudin-1 at the same cell-cell adhesion membrane domain. *Genes Cells* **13,** 797-805.

Lamorte,L., Rodrigues,S., Sangwan,V., Turner,C.E., and Park,M. (2003). Crk associates with a multimolecular Paxillin/GIT2/beta-PIX complex and promotes Rac-dependent relocalization of Paxillin to focal contacts. *Mol. Biol. Cell* **14,** 2818-2831.

Lang,G.E. (2007). Pharmacological treatment of diabetic retinopathy. *Ophthalmologica* **221,** 112-117.

Langevin,J., Morgan,M.J., Sibarita,J.B., Aresta,S., Murthy,M., Schwarz,T., Camonis,J., and Bellaiche,Y. (2005). Drosophila exocyst components Sec5, Sec6, and Sec15 regulate DE-Cadherin trafficking from recycling endosomes to the plasma membrane. *Dev. Cell* **9,** 365-376.

Larsen,E.C., DiGennaro,J.A., Saito,N., Mehta,S., Loegering,D.J., Mazurkiewicz,J.E., and Lennartz,M.R. (2000). Differential requirement for classic and novel PKC isoforms in respiratory burst and phagocytosis in RAW 264.7 cells. *J. Immunol.* **165,** 2809-2817.

Lawson,C., Ainsworth,M., Yacoub,M., and Rose,M. (1999). Ligation of ICAM-1 on endothelial cells leads to expression of VCAM-1 via a nuclear factor-kappaB-independent mechanism. *J. Immunol.* **162,** 2990-2996.

Lawson,C. and Wolf,S. (2009). ICAM-1 signaling in endothelial cells. *Pharmacol. Rep.* **61,** 22-32.

Lee,J.C., Laydon,J.T., McDonnell,P.C., Gallagher,T.F., Kumar,S., Green,D., McNulty,D., Blumenthal,M.J., Heys,J.R., Landvatter,S.W. et al. (1994). A protein kinase involved in the regulation of inflammatory cytokine biosynthesis. *Nature* **372,** 739-746.

Lee,M.H., Koria,P., Qu,J., and Andreadis,S.T. (2009). JNK phosphorylates beta-catenin and regulates adherens junctions. *FASEB J.* **23,** 3874-3883.

Lee,S., Choi,I., and Hong,Y.K. (2010). Heterogeneity and plasticity of lymphatic endothelial cells. *Semin. Thromb. Hemost.* **36,** 352-361.

Lehmann,J.C., Jablonski-Westrich,D., Haubold,U., Gutierrez-Ramos,J.C., Springer,T., and Hamann,A. (2003). Overlapping and selective roles of endothelial intercellular adhesion molecule-1 (ICAM-1) and ICAM-2 in lymphocyte trafficking. *J. Immunol.* **171,** 2588-2593.

Ley,K., Laudanna,C., Cybulsky,M.I., and Nourshargh,S. (2007). Getting to the site of inflammation: the leukocyte adhesion cascade updated. *Nat. Rev. Immunol.* **7,** 678-689.

Liebner,S., Corada,M., Bangsow,T., Babbage,J., Taddei,A., Czupalla,C.J., Reis,M., Felici,A., Wolburg,H., Fruttiger,M. et al. (2008). Wnt/beta-catenin signaling controls development of the blood-brain barrier. *J. Cell Biol.* **183,** 409-417.

Liebner,S., Fischmann,A., Rascher,G., Duffner,F., Grote,E.H., Kalbacher,H., and Wolburg,H. (2000). Claudin-1 and claudin-5 expression and tight junction morphology are altered in blood vessels of human glioblastoma multiforme. *Acta Neuropathol.* **100,** 323-331.

Liu,G., Vogel,S.M., Gao,X., Javaid,K., Hu,G., Danilov,S.M., Malik,A.B., and Minshall,R.D. (2011). Src phosphorylation of endothelial cell surface intercellular adhesion molecule-1 mediates neutrophil adhesion and contributes to the mechanism of lung inflammation. *Arterioscler. Thromb. Vasc. Biol.* **31,** 1342-1350.

Liu,S., Thomas,S.M., Woodside,D.G., Rose,D.M., Kiosses,W.B., Pfaff,M., and Ginsberg,M.H. (1999). Binding of paxillin to alpha4 integrins modifies integrin-dependent biological responses. *Nature* **402,** 676-681.

Lopez,M., Aoubala,M., Jordier,F., Isnardon,D., Gomez,S., and Dubreuil,P. (1998). The human poliovirus receptor related 2 protein is a new hematopoietic/endothelial homophilic adhesion molecule. *Blood* **92,** 4602-4611.

Lopez,M., Eberle,F., Mattei,M.G., Gabert,J., Birg,F., Bardin,F., Maroc,C., and Dubreuil,P. (1995). Complementary DNA characterization and chromosomal localization of a human gene related to the poliovirus receptor-encoding gene. *Gene* **155,** 261-265.

Lou,O., Alcaide,P., Luscinskas,F.W., and Muller,W.A. (2007). CD99 is a key mediator of the transendothelial migration of neutrophils. *J. Immunol.* **178,** 1136-1143.

Louis,K., Guerineau,N., Fromigue,O., Defamie,V., Collazos,A., Anglard,P., Shipp,M.A., Auberger,P., Joubert,D., and Mari,B. (2005). Tumor cell-mediated induction of the stromal factor stromelysin-3 requires heterotypic cell contact-dependent activation of specific protein kinase C isoforms. *J. Biol. Chem.* **280,** 1272-1283.

Ludwig,R.J., Hardt,K., Hatting,M., Bistrian,R., Diehl,S., Radeke,H.H., Podda,M., Schon,M.P., Kaufmann,R., Henschler,R. et al. (2009). Junctional adhesion molecule (JAM)-B supports lymphocyte rolling and adhesion through interaction with alpha4beta1 integrin. *Immunology* **128,** 196-205.

Luster,A.D., Alon,R., and von Andrian,U.H. (2005). Immune cell migration in inflammation: present and future therapeutic targets. *Nat. Immunol.* **6,** 1182-1190.

Lyck,R., Reiss,Y., Gerwin,N., Greenwood,J., Adamson,P., and Engelhardt,B. (2003). T-cell interaction with ICAM-1/ICAM-2 double-deficient brain endothelium in vitro: the cytoplasmic tail of endothelial ICAM-1 is necessary for transendothelial migration of T cells. *Blood* **102,** 3675-3683.

Mackay,C.R. (2008). Moving targets: cell migration inhibitors as new anti-inflammatory therapies. *Nat. Immunol.* **9,** 988-998.

Male,D., Rahman,J., Pryce,G., Tamatani,T., and Miyasaka,M. (1994). Lymphocyte migration into the CNS modelled in vitro: roles of LFA-1, ICAM-1 and VLA-4. *Immunology* **81,** 366-372.

Mamdouh,Z., Chen,X., Pierini,L.M., Maxfield,F.R., and Muller,W.A. (2003). Targeted recycling of PECAM from endothelial surface-connected compartments during diapedesis. *Nature* **421,** 748-753.

Mamdouh,Z., Kreitzer,G.E., and Muller,W.A. (2008). Leukocyte transmigration requires kinesin-mediated microtubule-dependent membrane trafficking from the lateral border recycling compartment. *J. Exp. Med.* **205,** 951-966.

Mamdouh,Z., Mikhailov,A., and Muller,W.A. (2009). Transcellular migration of leukocytes is mediated by the endothelial lateral border recycling compartment. *J. Exp. Med.* **206,** 2795-2808.

Mandai,K., Nakanishi,H., Satoh,A., Obaishi,H., Wada,M., Nishioka,H., Itoh,M., Mizoguchi,A., Aoki,T., Fujimoto,T. et al. (1997). Afadin: A novel actin filament-binding protein with one PDZ domain localized at cadherin-based cell-to-cell adherens junction. *J. Cell Biol.* **139,** 517-528.

Mandai,K., Nakanishi,H., Satoh,A., Takahashi,K., Satoh,K., Nishioka,H., Mizoguchi,A., and Takai,Y. (1999). Ponsin/SH3P12: an l-afadin- and vinculin-binding protein localized at cell-cell and cell-matrix adherens junctions. *J. Cell Biol.* **144,** 1001-1017.

Manevich,E., Grabovsky,V., Feigelson,S.W., and Alon,R. (2007). Talin 1 and paxillin facilitate distinct steps in rapid VLA-4-mediated adhesion strengthening to vascular cell adhesion molecule 1. *J. Biol. Chem.* **282,** 25338-25348.

Manning,A.M. and Davis,R.J. (2003). Targeting JNK for therapeutic benefit: from junk to gold? *Nat. Rev. Drug Discov.* **2,** 554-565.

Marinissen,M.J. and Gutkind,J.S. (2005). Scaffold proteins dictate Rho GTPase-signaling specificity. *Trends Biochem. Sci.* **30,** 423-426.

Martelli,A.M., Evangelisti,C., Nyakern,M., and Manzoli,F.A. (2006). Nuclear protein kinase C. *Biochim. Biophys. Acta* **1761,** 542-551.

Martinelli,R., Gegg,M., Longbottom,R., Adamson,P., Turowski,P., and Greenwood,J. (2009). ICAM-1-mediated endothelial nitric oxide synthase activation via calcium and AMP-activated protein kinase is required for transendothelial lymphocyte migration. *Mol. Biol. Cell* **20,** 995-1005.

Martiny-Baron,G. and Fabbro,D. (2007). Classical PKC isoforms in cancer. *Pharmacol. Res.* **55,** 477-486.

Martiny-Baron,G., Kazanietz,M.G., Mischak,H., Blumberg,P.M., Kochs,G., Hug,H., Marme,D., and Schachtele,C. (1993). Selective inhibition of protein kinase C isozymes by the indolocarbazole Go 6976. *J. Biol. Chem.* **268,** 9194-9197.

Matharu,N.M., McGettrick,H.M., Salmon,M., Kissane,S., Vohra,R.K., Rainger,G.E., and Nash,G.B. (2008). Inflammatory responses of endothelial cells experiencing reduction in flow after conditioning by shear stress. *J. Cell Physiol* **216,** 732-741.

Matheny,H.E., Deem,T.L., and Cook-Mills,J.M. (2000). Lymphocyte migration through monolayers of endothelial cell lines involves VCAM-1 signaling via endothelial cell NADPH oxidase. *J. Immunol.* **164,** 6550-6559.

Matter,K. and Balda,M.S. (2003). Signalling to and from tight junctions. *Nat. Rev. Mol. Cell Biol.* **4,** 225-236.

McCarthy,K.M., Francis,S.A., McCormack,J.M., Lai,J., Rogers,R.A., Skare,I.B., Lynch,R.D., and Schneeberger,E.E. (2000). Inducible expression of claudin-1-myc but not occludin-VSV-G results in aberrant tight junction strand formation in MDCK cells. *J. Cell Sci.* **113 Pt 19,** 3387-3398.

McGettrick,H.M., Hunter,K., Moss,P.A., Buckley,C.D., Rainger,G.E., and Nash,G.B. (2009). Direct observations of the kinetics of migrating T cells suggest active retention by endothelial cells with continual bidirectional migration. *J. Leukoc. Biol.* **85,** 98-107.

Meier,M. and King,G.L. (2000). Protein kinase C activation and its pharmacological inhibition in vascular disease. *Vasc. Med.* **5,** 173-185.

Millan,J., Hewlett,L., Glyn,M., Toomre,D., Clark,P., and Ridley,A.J. (2006). Lymphocyte transcellular migration occurs through recruitment of endothelial ICAM-1 to caveola- and F-actin-rich domains. *Nat. Cell Biol.* **8,** 113-123.

Millan,J. and Ridley,A.J. (2005). Rho GTPases and leucocyte-induced endothelial remodelling. *Biochem. J.* **385,** 329-337.

Miller,D.H., Khan,O.A., Sheremata,W.A., Blumhardt,L.D., Rice,G.P., Libonati,M.A., Willmer-Hulme,A.J., Dalton,C.M., Miszkiel,K.A., and O'Connor,P.W. (2003). A controlled trial of natalizumab for relapsing multiple sclerosis. *N. Engl. J. Med.* **348,** 15-23.

Minshall,R.D., Vandenbroucke,E.E., Holinstat,M., Place,A.T., Tiruppathi,C., Vogel,S.M., Nieuw Amerongen,G.P., Mehta,D., and Malik,A.B. (2010). Role of protein kinase Czeta in thrombin-induced RhoA activation and inter-endothelial gap formation of human dermal microvessel endothelial cell monolayers. *Microvasc. Res.*

Miyahara,M., Nakanishi,H., Takahashi,K., Satoh-Horikawa,K., Tachibana,K., and Takai,Y. (2000). Interaction of nectin with afadin is necessary for its clustering at cell-cell contact sites but not for its cis dimerization or trans interaction. *J. Biol. Chem.* **275,** 613-618.

Miyasaka,M. and Tanaka,T. (2004). Lymphocyte trafficking across high endothelial venules: dogmas and enigmas. *Nat. Rev. Immunol.* **4,** 360-370.

Mochly-Rosen,D., Khaner,H., and Lopez,J. (1991). Identification of intracellular receptor proteins for activated protein kinase C. *Proc. Natl. Acad. Sci. U. S. A* **88,** 3997-4000.

Moll,T., Dejana,E., and Vestweber,D. (1998). In vitro degradation of endothelial catenins by a neutrophil protease. *J. Cell Biol.* **140,** 403-407.

Montagnani,M., Chen,H., Barr,V.A., and Quon,M.J. (2001). Insulin-stimulated activation of eNOS is independent of Ca2+ but requires phosphorylation by Akt at Ser(1179). *J. Biol. Chem.* **276,** 30392-30398.

Morita,K., Sasaki,H., Furuse,M., and Tsukita,S. (1999). Endothelial claudin: claudin-5/TMVCF constitutes tight junction strands in endothelial cells. *J. Cell Biol.* **147,** 185-194.

Morrison,M.E. and Racaniello,V.R. (1992). Molecular cloning and expression of a murine homolog of the human poliovirus receptor gene. *J. Virol.* **66,** 2807-2813.

Muller,W.A. (2009). Mechanisms of transendothelial migration of leukocytes. *Circ. Res.* **105,** 223-230.

Muller,W.A. (2010). Mechanisms of Leukocyte Transendothelial Migration. *Annu. Rev. Pathol.*

Murakami,T., Felinski,E.A., and Antonetti,D.A. (2009). Occludin phosphorylation and ubiquitination regulate tight junction trafficking and vascular endothelial growth factor-induced permeability. *J. Biol. Chem.* **284,** 21036-21046.

Nakagawa,K., Sugahara,M., Yamasaki,T., Kajiho,H., Takahashi,S., Hirayama,J., Minami,Y., Ohta,Y., Watanabe,T., Hata,Y. et al. (2010). Filamin associates with stress signalling kinases MKK7 and MKK4 and regulates JNK activation. *Biochem. J.* **427,** 237-245.

Nakashima,S. (2002). Protein kinase C alpha (PKC alpha): regulation and biological function. *J. Biochem.* **132,** 669-675.

Nasdala,I., Wolburg-Buchholz,K., Wolburg,H., Kuhn,A., Ebnet,K., Brachtendorf,G., Samulowitz,U., Kuster,B., Engelhardt,B., Vestweber,D. et al. (2002). A transmembrane tight junction protein selectively expressed on endothelial cells and platelets. *J. Biol. Chem.* **277,** 16294-16303.

Nejsum,L.N. and Nelson,W.J. (2009). Epithelial cell surface polarity: the early steps. *Front Biosci.* **14,** 1088-1098.

Nitta,T., Hata,M., Gotoh,S., Seo,Y., Sasaki,H., Hashimoto,N., Furuse,M., and Tsukita,S. (2003). Size-selective loosening of the blood-brain barrier in claudin-5-deficient mice. *J. Cell Biol.* **161,** 653-660.

Nottebaum,A.F., Cagna,G., Winderlich,M., Gamp,A.C., Linnepe,R., Polaschegg,C., Filippova,K., Lyck,R., Engelhardt,B., Kamenyeva,O. et al. (2008). VE-PTP maintains the endothelial barrier via plakoglobin and becomes dissociated from VE-cadherin by leukocytes and by VEGF. *J. Exp. Med.* **205,** 2929-2945.

Nourshargh,S., Hordijk,P.L., and Sixt,M. (2010). Breaching multiple barriers: leukocyte motility through venular walls and the interstitium. *Nat. Rev. Mol. Cell Biol.* **11,** 366-378.

Oh,H.M., Lee,S., Na,B.R., Wee,H., Kim,S.H., Choi,S.C., Lee,K.M., and Jun,C.D. (2007). RKIKK motif in the intracellular domain is critical for spatial and dynamic organization of ICAM-1: functional implication for the leukocyte adhesion and transmigration. *Mol. Biol. Cell* **18,** 2322-2335.

Ohta,Y., Suzuki,N., Nakamura,S., Hartwig,J.H., and Stossel,T.P. (1999). The small GTPase RalA targets filamin to induce filopodia. *Proc. Natl. Acad. Sci. U. S. A* **96,** 2122-2128.

Oliver,G. and Alitalo,K. (2005). The lymphatic vasculature: recent progress and paradigms. *Annu. Rev. Cell Dev. Biol.* **21,** 457-483.

Oppenheimer-Marks,N., Davis,L.S., Bogue,D.T., Ramberg,J., and Lipsky,P.E. (1991). Differential utilization of ICAM-1 and VCAM-1 during the adhesion and transendothelial migration of human T lymphocytes. *J. Immunol.* **147,** 2913-2921.

Osada,S., Mizuno,K., Saido,T.C., Akita,Y., Suzuki,K., Kuroki,T., and Ohno,S. (1990). A phorbol ester receptor/protein kinase, nPKC eta, a new member of the protein kinase C family predominantly expressed in lung and skin. *J. Biol. Chem.* **265,** 22434-22440.

Otto,I.M., Raabe,T., Rennefahrt,U.E., Bork,P., Rapp,U.R., and Kerkhoff,E. (2000a). The p150-Spir protein provides a link between c-Jun N-terminal kinase function and actin reorganization. *Curr. Biol.* **10,** 345-348.

Otto,V.I., Gloor,S.M., Frentzel,S., Gilli,U., Ammann,E., Hein,A.E., Folkers,G., Trentz,O., Kossmann,T., and Morganti-Kossmann,M.C. (2002). The production of macrophage inflammatory protein-2 induced by soluble intercellular adhesion molecule-1 in mouse astrocytes is mediated by src tyrosine kinases and p42/44 mitogen-activated protein kinase. *J. Neurochem.* **80,** 824-834.

Otto,V.I., Heinzel-Pleines,U.E., Gloor,S.M., Trentz,O., Kossmann,T., and Morganti-Kossmann,M.C. (2000b). sICAM-1 and TNF-alpha induce MIP-2 with distinct kinetics in astrocytes and brain microvascular endothelial cells. *J. Neurosci. Res.* **60,** 733-742.

Pachter,J.S., de Vries,H.E., and Fabry,Z. (2003). The blood-brain barrier and its role in immune privilege in the central nervous system. *J. Neuropathol. Exp. Neurol.* **62,** 593-604.

Parekh,D.B., Ziegler,W., and Parker,P.J. (2000). Multiple pathways control protein kinase C phosphorylation. *EMBO J.* **19,** 496-503.

Parker,P.J. and Murray-Rust,J. (2004). PKC at a glance. *J. Cell Sci.* **117,** 131-132.

Patel,K.D., Cuvelier,S.L., and Wiehler,S. (2002). Selectins: critical mediators of leukocyte recruitment. *Semin. Immunol.* **14,** 73-81.

Pearce,L.R., Komander,D., and Alessi,D.R. (2010). The nuts and bolts of AGC protein kinases. *Nat. Rev. Mol. Cell Biol.* **11,** 9-22.

Pellegrin,S. and Mellor,H. (2007). Actin stress fibres. *J. Cell Sci.* **120,** 3491-3499.

Pepper,M.S. and Skobe,M. (2003). Lymphatic endothelium: morphological, molecular and functional properties. *J. Cell Biol.* **163,** 209-213.

Peppiatt,C.M., Howarth,C., Mobbs,P., and Attwell,D. (2006). Bidirectional control of CNS capillary diameter by pericytes. *Nature* **443,** 700-704.

Perriere,N., Demeuse,P., Garcia,E., Regina,A., Debray,M., Andreux,J.P., Couvreur,P., Scherrmann,J.M., Temsamani,J., Couraud,P.O. et al. (2005). Puromycin-based purification of rat brain capillary endothelial cell cultures. Effect on the expression of blood-brain barrier-specific properties. *J. Neurochem.* **93,** 279-289.

Perry,V.H., Nicoll,J.A., and Holmes,C. (2010). Microglia in neurodegenerative disease. *Nat. Rev. Neurol.* **6,** 193-201.

Petit,V., Boyer,B., Lentz,D., Turner,C.E., Thiery,J.P., and Valles,A.M. (2000). Phosphorylation of tyrosine residues 31 and 118 on paxillin regulates cell migration through an association with CRK in NBT-II cells. *J. Cell Biol.* **148,** 957-970.

Pluskota,E., Chen,Y., and D'Souza,S.E. (2000). Src homology domain 2-containing tyrosine phosphatase 2 associates with intercellular adhesion molecule 1 to regulate cell survival. *J. Biol. Chem.* **275,** 30029-30036.

Potter,M.D., Barbero,S., and Cheresh,D.A. (2005). Tyrosine phosphorylation of VE-cadherin prevents binding of p120- and beta-catenin and maintains the cellular mesenchymal state. *J. Biol. Chem.* **280,** 31906-31912.

Praveen,K., Zheng,Y., Rivas,F., and Gajewski,T.F. (2009). Protein kinase Ctheta focusing at the cSMAC is a consequence rather than cause of TCR signaling and is dependent on the MEK/ERK pathway. *J. Immunol.* **182,** 6022-6030.

Pryce,G., Male,D., Campbell,I., and Greenwood,J. (1997). Factors controlling T-cell migration across rat cerebral endothelium in vitro. *J. Neuroimmunol.* **75,** 84-94.

Quann,E.J., Liu,X., Altan-Bonnet,G., and Huse,M. (2011). A cascade of protein kinase C isozymes promotes cytoskeletal polarization in T cells. *Nat. Immunol.* **12,** 647-654.

Quittau-Prevostel,C., Delaunay,N., Collazos,A., Vallentin,A., and Joubert,D. (2004). Targeting of PKCalpha and epsilon in the pituitary: a highly regulated mechanism involving a GD(E)E motif of the V3 region. *J. Cell Sci.* **117,** 63-72.

Rahman,A. and Fazal,F. (2009). Hug tightly and say goodbye: role of endothelial ICAM-1 in leukocyte transmigration. *Antioxid. Redox. Signal.* **11,** 823-839.

Ransohoff,R.M. and Perry,V.H. (2009). Microglial physiology: unique stimuli, specialized responses. *Annu. Rev. Immunol.* **27,** 119-145.

Regina,A., Romero,I.A., Greenwood,J., Adamson,P., Bourre,J.M., Couraud,P.O., and Roux,F. (1999). Dexamethasone regulation of P-glycoprotein activity in an immortalized rat brain endothelial cell line, GPNT. *J. Neurochem.* **73,** 1954-1963.

Reiss,Y., Hoch,G., Deutsch,U., and Engelhardt,B. (1998). T cell interaction with ICAM-1-deficient endothelium in vitro: essential role for ICAM-1 and ICAM-2 in transendothelial migration of T cells. *Eur. J. Immunol.* **28,** 3086-3099.

Reymond,N., Fabre,S., Lecocq,E., Adelaide,J., Dubreuil,P., and Lopez,M. (2001). Nectin4/PRR4, a new afadin-associated member of the nectin family that trans-interacts with nectin1/PRR1 through V domain interaction. *J. Biol. Chem.* **276,** 43205-43215.

Reymond,N., Garrido-Urbani,S., Borg,J.P., Dubreuil,P., and Lopez,M. (2005). PICK-1: a scaffold protein that interacts with Nectins and JAMs at cell junctions. *FEBS Lett.* **579,** 2243-2249.

Ridley,A.J. (1994). Membrane ruffling and signal transduction. *Bioessays* **16,** 321-327.

Rocha,S.F. and Adams,R.H. (2009). Molecular differentiation and specialization of vascular beds. *Angiogenesis.* **12,** 139-147.

Roffey,J., Rosse,C., Linch,M., Hibbert,A., McDonald,N.Q., and Parker,P.J. (2009). Protein kinase C intervention: the state of play. *Curr. Opin. Cell Biol.* **21,** 268-279.

Romero,I.A., Amos,C.L., Greenwood,J., and Adamson,P. (2002). Ezrin and moesin co-localise with ICAM-1 in brain endothelial cells but are not directly associated. *Brain Res. Mol. Brain Res.* **105,** 47-59.

Rose,D.M. (2006). The role of the alpha4 integrin-paxillin interaction in regulating leukocyte trafficking. *Exp. Mol. Med.* **38,** 191-195.

Rosse,C., Formstecher,E., Boeckeler,K., Zhao,Y., Kremerskothen,J., White,M.D., Camonis,J.H., and Parker,P.J. (2009). An aPKC-exocyst complex controls paxillin phosphorylation and migration through localised JNK1 activation. *PLoS. Biol.* **7,** e1000235.

Rosse,C., Linch,M., Kermorgant,S., Cameron,A.J., Boeckeler,K., and Parker,P.J. (2010). PKC and the control of localized signal dynamics. *Nat. Rev. Mol. Cell Biol.* **11,** 103-112.

Roux,P.P. and Blenis,J. (2004). ERK and p38 MAPK-activated protein kinases: a family of protein kinases with diverse biological functions. *Microbiol. Mol. Biol. Rev.* **68,** 320-344.

Rubin,L.L. and Staddon,J.M. (1999). The cell biology of the blood-brain barrier. *Annu. Rev. Neurosci.* **22,** 11-28.

Rudini,N. and Dejana,E. (2008). Adherens junctions. *Curr. Biol.* **18,** R1080-R1082.

Rykx,A., De Kimpe,L., Mikhalap,S., Vantus,T., Seufferlein,T., Vandenheede,J.R., and Van Lint,J. (2003). Protein kinase D: a family affair. *FEBS Lett.* **546,** 81-86.

Saitou,M., Furuse,M., Sasaki,H., Schulzke,J.D., Fromm,M., Takano,H., Noda,T., and Tsukita,S. (2000). Complex phenotype of mice lacking occludin, a component of tight junction strands. *Mol. Biol. Cell* **11,** 4131-4142.

Sakakibara,A., Furuse,M., Saitou,M., Ando-Akatsuka,Y., and Tsukita,S. (1997). Possible involvement of phosphorylation of occludin in tight junction formation. *J. Cell Biol.* **137,** 1393-1401.

Sano,H., Nakagawa,N., Chiba,R., Kurasawa,K., Saito,Y., and Iwamoto,I. (1998). Cross-linking of intercellular adhesion molecule-1 induces interleukin-8 and RANTES production through the activation of MAP kinases in human vascular endothelial cells. *Biochem. Biophys. Res. Commun.* **250,** 694-698.

Sans,E., Delachanal,E., and Duperray,A. (2001). Analysis of the roles of ICAM-1 in neutrophil transmigration using a reconstituted mammalian cell expression model: implication of ICAM-1 cytoplasmic domain and Rho-dependent signaling pathway. *J. Immunol.* **166,** 544-551.

Satoh-Horikawa,K., Nakanishi,H., Takahashi,K., Miyahara,M., Nishimura,M., Tachibana,K., Mizoguchi,A., and Takai,Y. (2000). Nectin-3, a new member of immunoglobulin-like cell adhesion molecules that shows homophilic and heterophilic cell-cell adhesion activities. *J. Biol. Chem.* **275,** 10291-10299.

Schaller,M.D. (2001). Paxillin: a focal adhesion-associated adaptor protein. *Oncogene* **20,** 6459-6472.

Schenkel,A.R., Mamdouh,Z., Chen,X., Liebman,R.M., and Muller,W.A. (2002). CD99 plays a major role in the migration of monocytes through endothelial junctions. *Nat. Immunol.* **3,** 143-150.

Schlaepfer,D.D., Hauck,C.R., and Sieg,D.J. (1999). Signaling through focal adhesion kinase. *Prog. Biophys. Mol. Biol.* **71,** 435-478.

Schnoor,M., Lai,F.P., Zarbock,A., Klaver,R., Polaschegg,C., Schulte,D., Weich,H.A., Oelkers,J.M., Rottner,K., and Vestweber,D. (2011). Cortactin deficiency is associated with reduced neutrophil recruitment but increased vascular permeability in vivo. *J. Exp. Med.* **208,** 1721-1735.

Shaw,S.K., Bamba,P.S., Perkins,B.N., and Luscinskas,F.W. (2001). Real-time imaging of vascular endothelial-cadherin during leukocyte transmigration across endothelium. *J. Immunol.* **167,** 2323-2330.

Shirai,Y. and Saito,N. (2002). Activation mechanisms of protein kinase C: maturation, catalytic activation, and targeting. *J. Biochem.* **132,** 663-668.

Simmons,D.L. (2005). Anti-adhesion therapies. *Curr. Opin. Pharmacol.* **5,** 398-404.

Smith,A., Bracke,M., Leitinger,B., Porter,J.C., and Hogg,N. (2003). LFA-1-induced T cell migration on ICAM-1 involves regulation of MLCK-mediated attachment and ROCK-dependent detachment. *J. Cell Sci.* **116,** 3123-3133.

Smith,A., Carrasco,Y.R., Stanley,P., Kieffer,N., Batista,F.D., and Hogg,N. (2005). A talin-dependent LFA-1 focal zone is formed by rapidly migrating T lymphocytes. *J. Cell Biol.* **170,** 141-151.

Sobel,R.A., Mitchell,M.E., and Fondren,G. (1990). Intercellular adhesion molecule-1 (ICAM-1) in cellular immune reactions in the human central nervous system. *Am. J. Pathol.* **136,** 1309-1316.

Spector,I., Shochet,N.R., Kashman,Y., and Groweiss,A. (1983). Latrunculins: novel marine toxins that disrupt microfilament organization in cultured cells. *Science* **219,** 493-495.

Springer,T.A. (1994). Traffic signals for lymphocyte recirculation and leukocyte emigration: the multistep paradigm. *Cell* **76,** 301-314.

Stahmann,N., Woods,A., Carling,D., and Heller,R. (2006). Thrombin activates AMP-activated protein kinase in endothelial cells via a pathway involving Ca2+/calmodulin-dependent protein kinase kinase beta. *Mol. Cell Biol.* **26,** 5933-5945.

Stamatovic,S.M., Dimitrijevic,O.B., Keep,R.F., and Andjelkovic,A.V. (2006). Protein kinase Calpha-RhoA cross-talk in CCL2-induced alterations in brain endothelial permeability. *J. Biol. Chem.* **281,** 8379-8388.

Stan,R.V. (2002). Structure and function of endothelial caveolae. *Microsc. Res. Tech.* **57,** 350-364.

Steeber,D.A., Tang,M.L., Green,N.E., Zhang,X.Q., Sloane,J.E., and Tedder,T.F. (1999). Leukocyte entry into sites of inflammation requires overlapping interactions between the L-selectin and ICAM-1 pathways. *J. Immunol.* **163,** 2176-2186.

Stein,B.N., Gamble,J.R., Pitson,S.M., Vadas,M.A., and Khew-Goodall,Y. (2003). Activation of endothelial extracellular signal-regulated kinase is essential for neutrophil transmigration: potential involvement of a soluble neutrophil factor in endothelial activation. *J. Immunol.* **171,** 6097-6104.

Steinberg,S.F. (2008). Structural basis of protein kinase C isoform function. *Physiol Rev.* **88,** 1341-1378.

Steiner,O., Coisne,C., Cecchelli,R., Boscacci,R., Deutsch,U., Engelhardt,B., and Lyck,R. (2010). Differential roles for endothelial ICAM-1, ICAM-2, and VCAM-1 in shear-resistant T cell arrest, polarization, and directed crawling on blood-brain barrier endothelium. *J. Immunol.* **185,** 4846-4855.

Stevenson,B.R., Siliciano,J.D., Mooseker,M.S., and Goodenough,D.A. (1986). Identification of ZO-1: a high molecular weight polypeptide associated with the tight junction (zonula occludens) in a variety of epithelia. *J. Cell Biol.* **103,** 755-766.

Straight,A.F., Cheung,A., Limouze,J., Chen,I., Westwood,N.J., Sellers,J.R., and Mitchison,T.J. (2003). Dissecting temporal and spatial control of cytokinesis with a myosin II Inhibitor. *Science* **299,** 1743-1747.

Sumagin,R., Kuebel,J.M., and Sarelius,I.H. (2011). Leukocyte rolling and adhesion both contribute to regulation of microvascular permeability to albumin via ligation of ICAM-1. *Am. J. Physiol Cell Physiol*.

Sumagin,R., Lomakina,E., and Sarelius,I.H. (2008). Leukocyte-endothelial cell interactions are linked to vascular permeability via ICAM-1-mediated signaling. *Am. J. Physiol Heart Circ. Physiol* **295,** H969-H977.

Sumagin,R. and Sarelius,I.H. (2010). Intercellular Adhesion Molecule-1 Enrichment near Tricellular Endothelial Junctions Is Preferentially Associated with Leukocyte Transmigration and Signals for Reorganization of These Junctions To Accommodate Leukocyte Passage. *J. Immunol.*

Sun,H. and Tonks,N.K. (1994). The coordinated action of protein tyrosine phosphatases and kinases in cell signaling. *Trends Biochem. Sci.* **19,** 480-485.

Sun,M.K. and Alkon,D.L. (2009). Protein kinase C activators as synaptogenic and memory therapeutics. *Arch. Pharm. (Weinheim)* **342,** 689-698.

Sun,X., Shikata,Y., Wang,L., Ohmori,K., Watanabe,N., Wada,J., Shikata,K., Birukov,K.G., Makino,H., Jacobson,J.R. et al. (2009). Enhanced interaction between focal adhesion and adherens junction proteins: involvement in sphingosine 1-phosphate-induced endothelial barrier enhancement. *Microvasc. Res.* **77,** 304-313.

Suzuki,T., Elias,B.C., Seth,A., Shen,L., Turner,J.R., Giorgianni,F., Desiderio,D., Guntaka,R., and Rao,R. (2009). PKC eta regulates occludin phosphorylation and epithelial tight junction integrity. *Proc. Natl. Acad. Sci. U. S. A* **106,** 61-66.

Tachibana,K., Nakanishi,H., Mandai,K., Ozaki,K., Ikeda,W., Yamamoto,Y., Nagafuchi,A., Tsukita,S., and Takai,Y. (2000). Two cell adhesion molecules, nectin and cadherin, interact through their cytoplasmic domain-associated proteins. *J. Cell Biol.* **150,** 1161-1176.

Takahashi,K., Nakanishi,H., Miyahara,M., Mandai,K., Satoh,K., Satoh,A., Nishioka,H., Aoki,J., Nomoto,A., Mizoguchi,A. et al. (1999a). Nectin/PRR: an immunoglobulin-like cell adhesion molecule recruited to cadherin-based adherens junctions through interaction with Afadin, a PDZ domain-containing protein. *J. Cell Biol.* **145,** 539-549.

Takahashi,T., Takahashi,K., Mernaugh,R., Drozdoff,V., Sipe,C., Schoecklmann,H., Robert,B., Abrahamson,D.R., and Daniel,T.O. (1999b). Endothelial localization of receptor tyrosine phosphatase, ECRTP/DEP-1, in developing and mature renal vasculature. *J. Am. Soc. Nephrol.* **10,** 2135-2145.

Takai,Y., Irie,K., Shimizu,K., Sakisaka,T., and Ikeda,W. (2003). Nectins and nectin-like molecules: roles in cell adhesion, migration, and polarization. *Cancer Sci.* **94,** 655-667.

Takai,Y., Miyoshi,J., Ikeda,W., and Ogita,H. (2008). Nectins and nectin-like molecules: roles in contact inhibition of cell movement and proliferation. *Nat. Rev. Mol. Cell Biol.* **9,** 603-615.

Takai,Y. and Nakanishi,H. (2003). Nectin and afadin: novel organizers of intercellular junctions. *J. Cell Sci.* **116,** 17-27.

Tan,S.L. and Parker,P.J. (2003). Emerging and diverse roles of protein kinase C in immune cell signalling. *Biochem. J.* **376,** 545-552.

Thompson,P.W., Randi,A.M., and Ridley,A.J. (2002). Intercellular adhesion molecule (ICAM)-1, but not ICAM-2, activates RhoA and stimulates c-fos and rhoA transcription in endothelial cells. *J. Immunol.* **169,** 1007-1013.

Thompson,R.D., Wakelin,M.W., Larbi,K.Y., Dewar,A., Asimakopoulos,G., Horton,M.A., Nakada,M.T., and Nourshargh,S. (2000). Divergent effects of platelet-endothelial cell adhesion molecule-1 and beta 3 integrin blockade on leukocyte transmigration in vivo. *J. Immunol.* **165,** 426-434.

Tilghman,R.W. and Hoover,R.L. (2002). The Src-cortactin pathway is required for clustering of E-selectin and ICAM-1 in endothelial cells. *FASEB J.* **16,** 1257-1259.

Toullec,D., Pianetti,P., Coste,H., Bellevergue,P., Grand-Perret,T., Ajakane,M., Baudet,V., Boissin,P., Boursier,E., Loriolle,F. et al. (1991). The bisindolylmaleimide GF 109203X is a potent and selective inhibitor of protein kinase C. *J. Biol. Chem.* **266,** 15771-15781.

Treisman,R. (1996). Regulation of transcription by MAP kinase cascades. *Curr. Opin. Cell Biol.* **8,** 205-215.

Tse,D. and Stan,R.V. (2010). Morphological heterogeneity of endothelium. *Semin. Thromb. Hemost.* **36,** 236-245.

Tsukita,S., Furuse,M., and Itoh,M. (2001). Multifunctional strands in tight junctions. *Nat. Rev. Mol. Cell Biol.* **2,** 285-293.

Turner,C.E. (1998). Paxillin. *Int. J. Biochem. Cell Biol.* **30,** 955-959.

Turner,C.E. (2000a). Paxillin and focal adhesion signalling. *Nat. Cell Biol.* **2,** E231-E236.

Turner,C.E. (2000b). Paxillin interactions. *J. Cell Sci.* **113 Pt 23,** 4139-4140.

Turowski,P., Adamson,P., and Greenwood,J. (2005). Pharmacological targeting of ICAM-1 signaling in brain endothelial cells: potential for treating neuroinflammation. *Cell Mol. Neurobiol.* **25,** 153-170.

Turowski,P., Martinelli,R., Crawford,R., Wateridge,D., Papageorgiou,A.P., Lampugnani,M.G., Gamp,A.C., Vestweber,D., Adamson,P., Dejana,E. et al. (2008). Phosphorylation of vascular endothelial cadherin controls lymphocyte emigration. *J. Cell Sci.* **121,** 29-37.

Valle-Perez,B., Martinez,V.G., Lacasa-Salavert,C., Figueras,A., Shapiro,S.S., Takafuta,T., Casanovas,O., Capella,G., Ventura,F., and Vinals,F. (2010). Filamin B plays a key role in vascular endothelial growth factor-induced endothelial cell motility through its interaction with Rac-1 and Vav-2. *J. Biol. Chem.* **285,** 10748-10760.

van Buul,J.D., Allingham,M.J., Samson,T., Meller,J., Boulter,E., Garcia-Mata,R., and Burridge,K. (2007a). RhoG regulates endothelial apical cup assembly downstream from ICAM1 engagement and is involved in leukocyte trans-endothelial migration. *J. Cell Biol.* **178,** 1279-1293.

van Buul,J.D. and Hordijk,P.L. (2009). Endothelial adapter proteins in leukocyte transmigration. *Thromb. Haemost.* **101,** 649-655.

van Buul,J.D., Kanters,E., and Hordijk,P.L. (2007b). Endothelial signaling by Ig-like cell adhesion molecules. *Arterioscler. Thromb. Vasc. Biol.* **27,** 1870-1876.

van Buul,J.D., van Rijssel,J., van Alphen,F.P., van Stalborch,A.M., Mul,E.P., and Hordijk,P.L. (2010). ICAM-1 clustering on endothelial cells recruits VCAM-1. *J. Biomed. Biotechnol.* **2010,** 120328.

van Wetering,S., van den,B.N., van Buul,J.D., Mul,F.P., Lommerse,I., Mous,R., ten Klooster,J.P., Zwaginga,J.J., and Hordijk,P.L. (2003). VCAM-1-mediated Rac signaling controls endothelial cell-cell contacts and leukocyte transmigration. *Am. J. Physiol Cell Physiol* **285,** C343-C352.

Verbeek,D.S., Goedhart,J., Bruinsma,L., Sinke,R.J., and Reits,E.A. (2008). PKC gamma mutations in spinocerebellar ataxia type 14 affect C1 domain accessibility and kinase activity leading to aberrant MAPK signaling. *J. Cell Sci.* **121,** 2339-2349.

Vestweber,D. (2007). Adhesion and signaling molecules controlling the transmigration of leukocytes through endothelium. *Immunol. Rev.* **218,** 178-196.

Voisin,M.B., Probstl,D., and Nourshargh,S. (2010). Venular basement membranes ubiquitously express matrix protein low-expression regions: characterization in multiple tissues and remodeling during inflammation. *Am. J. Pathol.* **176,** 482-495.

Wadham,C., Gamble,J.R., Vadas,M.A., and Khew-Goodall,Y. (2003). The protein tyrosine phosphatase Pez is a major phosphatase of adherens junctions and dephosphorylates beta-catenin. *Mol. Biol. Cell* **14,** 2520-2529.

Wakelin,M.W., Sanz,M.J., Dewar,A., Albelda,S.M., Larkin,S.W., Boughton-Smith,N., Williams,T.J., and Nourshargh,S. (1996). An anti-platelet-endothelial cell adhesion molecule-1 antibody inhibits leukocyte extravasation from mesenteric microvessels in vivo by blocking the passage through the basement membrane. *J. Exp. Med.* **184,** 229-239.

Wang,Q. and Doerschuk,C.M. (2001). The p38 mitogen-activated protein kinase mediates cytoskeletal remodeling in pulmonary microvascular endothelial cells upon intracellular adhesion molecule-1 ligation. *J. Immunol.* **166,** 6877-6884.

Wang,Q., Pfeiffer,G.R., and Gaarde,W.A. (2003). Activation of SRC tyrosine kinases in response to ICAM-1 ligation in pulmonary microvascular endothelial cells. *J. Biol. Chem.* **278,** 47731-47743.

Wang,S., Voisin,M.B., Larbi,K.Y., Dangerfield,J., Scheiermann,C., Tran,M., Maxwell,P.H., Sorokin,L., and Nourshargh,S. (2006). Venular basement membranes contain specific matrix protein low expression regions that act as exit points for emigrating neutrophils. *J. Exp. Med.* **203,** 1519-1532.

Ward,S.G. and Marelli-Berg,F.M. (2009). Mechanisms of chemokine and antigen-dependent T-lymphocyte navigation. *Biochem. J.* **418,** 13-27.

Way,K.J., Chou,E., and King,G.L. (2000). Identification of PKC-isoform-specific biological actions using pharmacological approaches. *Trends Pharmacol. Sci.* **21,** 181-187.

Webb,D.J., Donais,K., Whitmore,L.A., Thomas,S.M., Turner,C.E., Parsons,J.T., and Horwitz,A.F. (2004). FAK-Src signalling through paxillin, ERK and MLCK regulates adhesion disassembly. *Nat. Cell Biol.* **6,** 154-161.

Weed,S.A. and Parsons,J.T. (2001). Cortactin: coupling membrane dynamics to cortical actin assembly. *Oncogene* **20,** 6418-6434.

Wegmann,F., Petri,B., Khandoga,A.G., Moser,C., Khandoga,A., Volkery,S., Li,H., Nasdala,I., Brandau,O., Fassler,R. et al. (2006). ESAM supports neutrophil extravasation, activation of Rho, and VEGF-induced vascular permeability. *J. Exp. Med.* **203,** 1671-1677.

Williams,M.R. and Luscinskas,F.W. (2011). Leukocyte rolling and adhesion via ICAM-1 signals to endothelial permeability. *Am. J. Physiol Cell Physiol*.

Wittchen,E.S. (2009). Endothelial signaling in paracellular and transcellular leukocyte transmigration. *Front Biosci.* **14,** 2522-2545.

Wojciak-Stothard,B. and Ridley,A.J. (2002). Rho GTPases and the regulation of endothelial permeability. *Vascul. Pharmacol.* **39,** 187-199.

Wojciak-Stothard,B., Williams,L., and Ridley,A.J. (1999). Monocyte adhesion and spreading on human endothelial cells is dependent on Rho-regulated receptor clustering. *J. Cell Biol.* **145,** 1293-1307.

Wolburg,H. and Lippoldt,A. (2002). Tight junctions of the blood-brain barrier: development, composition and regulation. *Vascul. Pharmacol.* **38,** 323-337.

Wolburg,H., Wolburg-Buchholz,K., Kraus,J., Rascher-Eggstein,G., Liebner,S., Hamm,S., Duffner,F., Grote,E.H., Risau,W., and Engelhardt,B. (2003). Localization of claudin-3 in tight junctions of the blood-brain barrier is selectively lost during experimental autoimmune encephalomyelitis and human glioblastoma multiforme. *Acta Neuropathol.* **105,** 586-592.

Wong,D. and Dorovini-Zis,K. (1992). Upregulation of intercellular adhesion molecule-1 (ICAM-1) expression in primary cultures of human brain microvessel endothelial cells by cytokines and lipopolysaccharide. *J. Neuroimmunol.* **39,** 11-21.

Woodfin,A., Reichel,C.A., Khandoga,A., Corada,M., Voisin,M.B., Scheiermann,C., Haskard,D.O., Dejana,E., Krombach,F., and Nourshargh,S. (2007). JAM-A mediates neutrophil transmigration in a stimulus-specific manner in vivo: evidence for sequential roles for JAM-A and PECAM-1 in neutrophil transmigration. *Blood* **110,** 1848-1856.

Woodfin,A., Voisin,M.B., Beyrau,M., Colom,B., Caille,D., Diapouli,F.M., Nash,G.B., Chavakis,T., Albelda,S.M., Rainger,G.E. et al. (2011). The junctional adhesion molecule JAM-C regulates polarized transendothelial migration of neutrophils in vivo. *Nat. Immunol.*

Woodfin,A., Voisin,M.B., Imhof,B.A., Dejana,E., Engelhardt,B., and Nourshargh,S. (2009). Endothelial cell activation leads to neutrophil transmigration as supported by the sequential roles of ICAM-2, JAM-A, and PECAM-1. *Blood* **113,** 6246-6257.

Xia,Y. and Karin,M. (2004). The control of cell motility and epithelial morphogenesis by Jun kinases. *Trends Cell Biol.* **14,** 94-101.

Xiao,K., Allison,D.F., Buckley,K.M., Kottke,M.D., Vincent,P.A., Faundez,V., and Kowalczyk,A.P. (2003). Cellular levels of p120 catenin function as a set point for cadherin expression levels in microvascular endothelial cells. *J. Cell Biol.* **163,** 535-545.

Xiao,K., Garner,J., Buckley,K.M., Vincent,P.A., Chiasson,C.M., Dejana,E., Faundez,V., and Kowalczyk,A.P. (2005). p120-Catenin regulates clathrin-dependent endocytosis of VE-cadherin. *Mol. Biol. Cell* **16,** 5141-5151.

Yamauchi,J., Miyamoto,Y., Sanbe,A., and Tanoue,A. (2006). JNK phosphorylation of paxillin, acting through the Rac1 and Cdc42 signaling cascade, mediates neurite extension in N1E-115 cells. *Exp. Cell Res.* **312,** 2954-2961.

Yang,L., Kowalski,J.R., Yacono,P., Bajmoczi,M., Shaw,S.K., Froio,R.M., Golan,D.E., Thomas,S.M., and Luscinskas,F.W. (2006a). Endothelial cell cortactin coordinates intercellular adhesion molecule-1 clustering and actin cytoskeleton remodeling during polymorphonuclear leukocyte adhesion and transmigration. *J. Immunol.* **177,** 6440-6449.

Yang,L., Kowalski,J.R., Zhan,X., Thomas,S.M., and Luscinskas,F.W. (2006b). Endothelial cell cortactin phosphorylation by Src contributes to polymorphonuclear leukocyte transmigration in vitro. *Circ. Res.* **98,** 394-402.

Yao,Z., Diener,K., Wang,X.S., Zukowski,M., Matsumoto,G., Zhou,G., Mo,R., Sasaki,T., Nishina,H., Hui,C.C. et al. (1997). Activation of stress-activated protein kinases/c-Jun N-terminal protein kinases (SAPKs/JNKs) by a novel mitogen-activated protein kinase kinase. *J. Biol. Chem.* **272,** 32378-32383.

Yednock,T.A., Cannon,C., Fritz,L.C., Sanchez-Madrid,F., Steinman,L., and Karin,N. (1992). Prevention of experimental autoimmune encephalomyelitis by antibodies against alpha 4 beta 1 integrin. *Nature* **356,** 63-66.

Yokosuka,T., Kobayashi,W., Sakata-Sogawa,K., Takamatsu,M., Hashimoto-Tane,A., Dustin,M.L., Tokunaga,M., and Saito,T. (2008). Spatiotemporal regulation of T cell costimulation by TCR-CD28 microclusters and protein kinase C theta translocation. *Immunity.* **29,** 589-601.

Yokoyama,S., Tachibana,K., Nakanishi,H., Yamamoto,Y., Irie,K., Mandai,K., Nagafuchi,A., Monden,M., and Takai,Y. (2001). alpha-catenin-independent recruitment of ZO-1 to nectin-based cell-cell adhesion sites through afadin. *Mol. Biol. Cell* **12,** 1595-1609.

Yoshida,Y., Huang,F.L., Nakabayashi,H., and Huang,K.P. (1988). Tissue distribution and developmental expression of protein kinase C isozymes. *J. Biol. Chem.* **263,** 9868-9873.

Yuan,S.Y. (2002). Protein kinase signaling in the modulation of microvascular permeability. *Vascul. Pharmacol.* **39,** 213-223.

Zaidel-Bar,R., Milo,R., Kam,Z., and Geiger,B. (2007). A paxillin tyrosine phosphorylation switch regulates the assembly and form of cell-matrix adhesions. *J. Cell Sci.* **120,** 137-148.

Zhang,J., Betson,M., Erasmus,J., Zeikos,K., Bailly,M., Cramer,L.P., and Braga,V.M. (2005). Actin at cell-cell junctions is composed of two dynamic and functional populations. *J. Cell Sci.* **118,** 5549-5562.

Zlokovic,B.V. (2008). The blood-brain barrier in health and chronic neurodegenerative disorders. *Neuron* **57,** 178-201.